ESTIMATING THE EFFECT OF MID-FREQUENCY ACTIVE SONAR ON THE POPULATION HEALTH OF BLAINVILLE'S BEAKED WHALES (*MESOPLODON DENSIROSTRIS*) IN THE TONGUE OF THE OCEAN

David Moretti

A Thesis Submitted for the Degree of PhD
at the
University of St Andrews

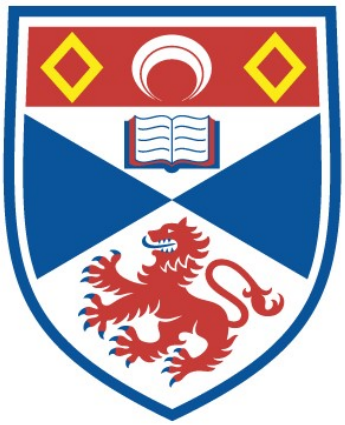

2019

Estimating the effect of mid-frequency active sonar on the population health of Blainville's beaked whales (*Mesoplodon densirostris*) in the Tongue of the Ocean

David Moretti

University of
St Andrews

This thesis is submitted in partial fulfilment for the degree of

Doctor of Philosophy (PhD)

at the University of St Andrews

March 2019

Abstract

Passive acoustic methods were used to study the effect of mid-frequency active sonar (MFAS) on a population of Blainville's beaked whales (*Mesoplodon densirostris, Md*) at the U.S. Navy Atlantic Undersea Test and Evaluation Centre (AUTEC), Bahamas. AUTEC contains an array of bottom-mounted hydrophones that can detect *Md* echolocation clicks. Methods to estimate abundance, the risk of behavioural disruption, and the population level effect of repeated MFAS exposure are presented. A passive acoustic abundance estimation method, a parametric equation that predicts the probability of foraging dive disruption as a function of MFAS received level and an *Md* bioenergetics model were developed. The effect of changes in energy flow on the demographic characteristics of an *Md* population were explored. Passive acoustic data from AUTEC were used to estimate the behavioural disturbance resulting from sonar operations; combined with the bioenergetic model, this suggested that the effect of sonar operations could cause an increase in a female's age at maturity, a longer inter-calf-interval, calf survival rate and probability of giving birth that could in turn result in a declining population. Model results were also compared to those from an expert elicitation study. A power analysis for predicting abundance via passive acoustic and visual monitoring were used to inform recommendations for a long-term monitoring plan that includes passive acoustic monitoring of *Md* abundance combined with a photo-identification study at both AUTEC and a reference site (Abaco) to improve demographic rate estimates.

Candidate's declaration

I, David Moretti, do hereby certify that this thesis, submitted for the degree of PhD, which is approximately 49,228 words in length, has been written by me, and that it is the record of work carried out by me, or principally by myself in collaboration with others as acknowledged, and that it has not been submitted in any previous application for any degree.

I was admitted as a research student at the University of St Andrews in September 2010.

I received funding from an organisation or institution and have acknowledged the funder(s) in the full text of my thesis.

30th August 2019

Date Signature of candidate

Supervisor's declaration

I hereby certify that the candidate has fulfilled the conditions of the Resolution and Regulations appropriate for the degree of PhD in the University of St Andrews and that the candidate is qualified to submit this thesis in application for that degree.

30th August 2019

Date Signature of supervisor

30th August 2019

Date Signature of supervisor

Permission for publication

In submitting this thesis to the University of St Andrews we understand that we are giving permission for it to be made available for use in accordance with the regulations of the University Library for the time being in force, subject to any copyright vested in the work not being affected thereby. We also understand, unless exempt by an award of an embargo as requested below, that the title and the abstract will be published, and that a copy of the work may be made and supplied to any bona fide library or research worker, that this thesis will be electronically accessible for personal or research use and that the library has the right to migrate this thesis into new electronic forms as required to ensure continued access to the thesis.

I, David Moretti, confirm that my thesis does not contain any third-party material that requires copyright clearance.

The following is an agreed request by candidate and supervisor regarding the publication of this thesis:

Printed copy

No embargo on print copy.

Electronic copy

No embargo on electronic copy.

30th August 2019

Date Signature of candidate

30th August 2019

Date Signature of supervisor

30th August 2019

Date Signature of supervisor

Underpinning Research Data or Digital Outputs

Candidate's declaration

I, David Moretti, hereby certify that no requirements to deposit original research data or digital outputs apply to this thesis and that, where appropriate, secondary data used have been referenced in the full text of my thesis.

30th August 2019

Date Signature of candidate

Table of Contents

List of Acronyms

AN/AQS	Joint Army-Navy nomenclature/aircraft (A), sonar (Q), detection, range, and bearing (S)
AUTEC	Atlantic Undersea Test and Evaluation Center
BRS	Behavioral Response Study
C/A ratio	Dependent calf to adult female ratio
CEE	Controlled exposure experiment
CI	Confidence interval
CS-SVM	Class specific support vector machine classifier
CTP	Click Train Processor
CV	Coefficient of variation
CW	Continuous wave
dB	Decibel
dBV_{rms}	Decibel re volts rms
DICASS	Directional Command-Activated Sonobuoy System
DTag	Digital recording tag
EE	Expert elicitation
EIS	Environmental Impact Statement
FFT	Fast Fourier Transform
GAM	Generalized additive model
GLM	Generalized linear model
GVP	Group Vocal Period

HPDI	Highest Posterior Density Interval
HRC	Hawaiian Range Complex
ICI	Inter-Click Interval
kHz	kilohertz
M3R	Marine Mammal Monitoring on Navy Ranges Program
Md	*Mesoplodon densirostris* (Blainville's beaked whale)
Me	*Mesoplodon europaeus* (Gervais' beaked whale)
MFAS	Mid-frequency active sonar
MMPA	Marine Mammal Protection Act
NAEMO	Navy Acoustic Effects Model
NAS	National Academy of Science
NDE	National Defense Exemption from Requirements of the MMPA
N	Nitrogen
nmi	Nautical miles
NWPC	Northwest Providence Channel
Pa	Pascal
PCAD	Population consequences of acoustic disturbance model
PCoD	Population consequences of disturbance model
PMRF	Pacific Missile Range Facility
P_{N_2}	Partial pressure of nitrogen
PTS	Permanent threshold shift
RF	Radio Frequency
RL_{rms}	Root mean squared receive level (of sound)

RMS	Root mean squared
SCC	Submarine Commander's Course
SEL	Sound exposure level
SCORE	Southern California Offshore Range
Sec	Seconds
Sonar	Sound navigation and ranging
Sp	Species
TDOA	Time Difference of Arrival
T&E	Test and evaluation
TOTO	Tongue of the Ocean
TTS	Temporary threshold shift
UDP	User datagram protocol
USWTR	Undersea Warfare Training Range
US	United States
Zc	*Ziphius cavirostris* (Cuvier's beaked whale)

Acknowledgements

I would especially like to acknowledge Len Thomas and John Harwood, who served as advisors on this research and endured hours of questions and discussions. Their unending patience and advice are much appreciated.

This thesis summarizes work that started in 1999 with the simple premise that passive acoustics could be applied to the study of cetaceans on the U.S. Navy Ranges beginning with AUTEC. A white paper by myself and Jessica Shaffer to Bob Gisiner at ONR resulted in a new project start: the Marine Mammal Monitoring on Navy Ranges (M3R) program. Bob ignored criticism that the density of animals at the Atlantic Undersea Test and Evaluation in the Tongue of the Ocean did not justify the effort. His words to me in that first year where to "Give it a try. Every time we look we seem to find something." Thanks Bob, your insight and willingness to take a chance got the ball rolling.

The early effort used hardware and software that had been developed by the Navy Range's signal processing team who continue to design and build the tracking signal processors for the Navy's undersea Ranges. They have been key to the development of algorithms, hardware, software and systems and that allow the Navy Ranges' infrastructure to be adapted to the study of cetaceans, including Ron Morrissey, Susan Jarvis, Nancy DiMarzio, and Jessica Shaffer, who have been there from the beginning. Over the years, multiple people made and continue to make key contributions including Stephanie Watwood, Ashley Dilley, Scott Fisher, Bert Neales, Karin Dolan, Sarah Blackstock, Thomas Fetherston, Peter Hulton, Mary Lou Hedberg, Anna Maria Izzi, and Ben Jones, along with multiple others who have made their way through the lab.

I have had the pleasure of working with some incredibly dedicated collaborators, but would especially like to thank Diane Claridge and Charlotte Dunn at the Bahamas Marine Mammal

Research Organization in the Bahamas, who have provided data, analysis, and advice that have found their way into this thesis. The number of collaborators has been large, so forgive me for thanking you in mass. A special thanks to the folks at the Centre for Research into Environmental and Ecological Model (CREEM) and the Sea Mammal Research Unit (SMRU) at St. Andrews, MarEcotel Research, and Cascadia Research. Thanks also to Cornell University, Oregon State University, the University of Southern California San Diego, San Diego State University, the Netherland's TNO, the University of Hawaii, the University of New Hampshire, Woods Hole Oceanographic Institution, the University of Massachusetts, Dartmouth, and the University of Rhode Island.

This research would not have been possible without the support of AUTEC, the Southern California Offshore Range (SCORE), and the Pacific Missile Range Facility (PMRF). We are the proverbial weird uncle who comes to Thanksgiving dinner for free food and drink. We work on a not-to-interfere basis, but that really means they have supported this research with little financial compensation in the midst of their primary mandate to conduct Fleet testing and training.

I would especially like to acknowledge our program sponsors including the Office of Naval Research (ONR), the Living Marine Resources (LMR) program, PACFleet, NAVSEA, Environmental Security Technology Certification Program (ESTCP), Advanced Instrumentation, Systems Technology (AIST), and NUWC's In-House Laboratory Independent Research (ILIR) Program.

Finally, thanks to my wife Jill and daughters Carolyn, Katelyn, and Vanesa who have put up with years of a "non-verbal me" sitting for hours with computer in my lap at home, in the car, in

Maine, on airplanes ……. Thank you for your unending patience and support. This is a purely selfish endeavor for which you got little personal return. I am extremely grateful!

Funding

This work was supported by the U.S. Navy

Chapter 1

Blainville's Beaked Whales and Sonar

1.1 Effect of Acoustic Disturbance on Individuals and Populations

Acoustic disturbance of marine mammals, including Blainville's beaked whales (*Mesoplodon densirostris*, hereafter *Md*), has become an area of concern within the U.S. Navy after several widely reported marine mammal stranding events that coincided with mid-frequency (2 to 10 kHz) active sonar (MFAS) Navy operations (D'Amico et al., 2009; Filadelfo et al., 2009). This thesis focuses on the development and application of methods to assess the effect of MFAS on individual behaviour and on the population health of animals repeatedly exposed to MFAS. It is particularly concerned with *Md* on the Atlantic Undersea Test and Evaluation Center (AUTEC) in the Tongue of the Ocean (TOTO) in the Bahamas, but the results are applicable to all the U.S. Navy's major range facilities including the Southern California Offshore Range (SCORE) off the coast of Southern California, the Pacific Missile Range Facility (PMRF) off the Island of Kauai, HI, and the Undersea Warfare Training Range (USWTR) that is scheduled to begin operations in late 2019.

The deleterious health effects of repeated sound exposure have been widely studied in humans (Ising and Kruppa, 2004). The problem has given rise to a broad body of research as evidenced by dedicated research journals such as *Noise and Health*. An estimated 120 million people suffer from direct auditory damage resulting in hearing loss (Chepesiuk, 2005). In addition, long-term noise exposure has been linked to physiological effects, including increased stress and elevated blood pressure (Basner et al., 2014; Münzel et al., 2014). For example, a meta-analysis of 14

studies concluded: “Road traffic noise is a significant risk factor for cardiovascular diseases” (Babisch, 2014).

Like sonar, airport noise is loud, intermittent, and most likely to occur between the hours of 0500 and 2400. In fact, concern over airport noise was addressed in the U.S. “Airport Noise and Capacity Act” which was passed in 1990 (Morrison et al., 1999). Such noise has been blamed for disruption of sleep, and an increase in depression (Franssen et al., 2004; Tarnopolsky et al., 1980). Chronic exposure to elevated airport noise has been shown to have a negative impact on reading comprehension and long-term memory in children (Lercher et al., 2003; Stansfeld and Matheson, 2003) though there is little evidence of increased morbidity in population areas directly within airport flight paths (Morrell et al., 2008).

The background noise level due to anthropogenic activity in over half of U.S. protected areas has more than doubled over the last century (Buxton et al., 2017). Several studies on the effects of noise on wild animal populations, in particular birds, have been undertaken (Shannon et al., 2016), though separating confounding factors, such as road deaths and habitat changes, is difficult (Reijnen et al., 1995). However, studies that use isolated populations exposed to anthropogenic noise have provided support for the hypothesis that chronic noise exposure can have a deleterious effect on bird population dynamics (Bayne et al., 2008; Francis et al., 2009; Habib et al., 2007; McClure et al., 2013). Senzaki et al. (2016) used simulated traffic noise and “prey rustling” sounds to quantify its effect of noise on short-eared owls (*Asio flammeus*) and long-eared owls (*Asio otus*) foraging efficiency. Even at low noise levels (40 dB(A)), the owls’ prey detection probability was ~17% lower. This effect extended out to at least 120 m from the source of the traffic noise.

Industrial noise from oil and gas drilling equipment in the boreal forest of Canada was shown to reduce the abundance of several species including white-throated sparrows (*Zonotrichia albicollis*), yellow-rumped warblers (*Dendroica coronata*), and red-eyed vireos (*Vireo olivaceus)* (Bayne et al., 2008). Francis et al. (2009) detected differences in the species mix of bird populations in northern New Mexico woodlands that were away from and near natural gas well noise-producing compressors suggesting a species-specific response. McClure et al. (2013) used an array of speakers to simulate passing vehicles in what was dubbed a "phantom road" along a migratory path in Idaho. They found a 25% reduction in bird abundance (59 species) during periods of "road noise". Some species totally avoided the periods of noise.

Several other avian studies have shown that anthropogenic disruption causes habitat displacement, negative changes in foraging behavioural, and a reduction in nesting success (Beale and Monaghan, 2004; Coleman et al., 2003; Fernández-Juricic and Tellería, 2000). However, context can mediate the response. In particular, displacement may not occur if the costs of moving are high (Gill et al., 2001). Beale and Monaghan (2004) compared the response to disturbance of ruddy turnstones (*Arenaria interpres*) that were provided with additional food to that of individuals who did not receive a food supplement. Those provided with additional food took flight at larger distances than those that were not supplemented, implying that birds in poorer condition are more tolerant to disturbance.

The complex effect of noise within an ecosystem can make an analysis of the long-term effect difficult. For instance, in the New Mexico woodland environment study, increased noise led to a reduction in abundance of nest-predator western scrub-jays (*Aphelocoma californica*), which in

turn led to an increase in the nesting success of song birds (Francis et al., 2009). Luo et al. (2015) found that traffic noise adversely affected the foraging success of Daubenton's bats (*Myotis* d*aubentonii),* even though the bat's echolocation frequency was well above the dominant noise, suggesting the effect was due to avoidance vice interference or a masking effect.

Shannon et al. (2016) reviewed 242 separate studies of the effects of noise on wildlife, spanning over 20 years. One study from 1990 on the effect of aircraft noise on sea birds was included (Brown, 1990). By 2013, 40 papers were included in the review, of which 17 were related to birds and 10 to aquatic mammals. They recommend future noise studies should "(1) expand geographic and taxonomic sampling, (2) explore interacting effects, (3) remove or reduce noise, (4) measure responses over a gradient of noise levels, (5) evaluate mitigation measures, and (6) improve reporting of acoustic metrics."

1.2 Marine Mammals and Noise

1.2.1 Commercial Sources

As with terrestrial animals, marine mammals are exposed to anthropogenic noise produced by both commercial and military activities (Slabbekoorn et al., 2010; Williams et al., 2015). There are many sources of anthropogenic noise (Hildebrand, 2009), though studies tend to be focused on the rise in the background ambient sound field primarily due to shipping, commercial echosounders, and impulsive sources, especially pile driving (National Academies of Sciences, Engineering, and Medicine, 2017).

1.2.1.1 Shipping Noise

Over the last century, a general rise in background noise has been postulated. Hildebrand (2009) estimated up to a potential 12 dB re μPa, (hereafter dB), rise in the ocean ambient over a 40-year

span by analysing Navy north-eastern Pacific surveillance array data (Andrew et al., 2002; McDonald et al., 2008, 2006). This rise coincided with an approximately 4.5 times increase in the total number of commercial ships (Hildebrand, 2009).

It should be noted, a signal's reported source and received levels are presented in units given by the referenced study. Generally, levels from sources such as a sonar are measured as a root-mean squared value (RMS) and if no other reference is given, a received level reported in dB is assumed to be in units of dB_{rms} re 1μPa and a source level in units of dB_{rms} re 1μPa @ 1m (Hildebrand, 2009).

Payne and Webb (1971) were among the first to suggest such an increase in ocean noise could hinder the communications of large baleen species such as fin whales (*Balaenoptera physalus*) via masking. Masking occurs when one signal reduces the signal to noise ratio (SNR) and hence the detectability (Clark et al., 2009) of another biologically more important signal. Hatch et al. (2008) measured the contribution of large ships to the noise background in the Stellwagen Bank National Marine Sanctuary and found that in areas of high ship traffic the acoustic power was double that of less trafficked areas. Parks et al. (2007) noted a reduction in the rate and an increase in the fundamental call frequency in North Atlantic (*Eubalaena glacialis*) and South Atlantic (*Eubalaena australis*) right whales in high noise conditions. Castellotte et al. (2012) used acoustic recordings to compare fin whale calls from areas of high and low ship traffic and found differences in the structure of 20 Hz song notes. In high noise conditions, the duration, centre frequency, bandwidth, and peak frequency all decreased potentially to compensate for the increased background noise.

In addition to the possible effect on animal communication, it has been theorized that the rise in shipping noise may have resulted in a chronic rise in stress (Wright et al., 2007). In the days immediately following the 911 terrorist attack in the U.S., shipping around the globe was severely curtailed. During this period, Rolland et al. (2012) measured a 6 dB decrease in level of ambient noise in the Bay of Fundy. Faecal hormones collected from North Atlantic right whales during this period had lower levels of stress hormones than those collected during periods of "normal" shipping both before and after the event.

1.2.1.2 Impulsive Sources

Pile Driving

The number of off-shore wind farms under construction is increasing as such sites offer strong, consistent winds (Perveen et al., 2014). Once these farms are in place, their contribution to ocean ambient noise is low. However, their construction often entails pile-driving, which produces loud impulsive noise (Madsen et al., 2006). While pile-driving is not unique to wind farm development, their proliferation has made them the focus of recent studies.

David (2006) noted the "likely sensitivity of bottlenose dolphins" to pile-driving. He suggested the potential for behavioural changes and the masking of vocalizations. Tougaard et al. (2009) measured a significant reduction in the number of passive acoustic detections of harbour porpoise (*Phocoena phocoena*) off the Danish coast during a four-month pile driving operation out to ~20 km at source levels of approximately 235 dB re $\mu Pa_{pp\ @}$ 1m. Brandt et al. (2011) also reported a reduction of harbour porpoise around pile driving in the Danish North Sea. They postulated that density was reduced out to a mean distance of 17.8 km, based on passive acoustic detection of echolocation clicks. Dähne et al. (2013) detected a similar change in density during pile driving off the coast of Germany using both visual aerial surveys and passive acoustics.

During pile driving operations, acoustic detections of animals decreased up to 10.8 km from the source, while detections between 25 and 50 km increased, suggesting animals moved away from the sound.

Explosives

Explosive devices produce loud impulsive signals and can be a significant source of noise in certain locations (Hildebrand, 2009). For instance, Debich et al. (2015) documented a proliferation of explosions, presumably from "seal bombs" at a site approximately 24 km west of Santa Barbara Island off the coast of Southern California., between June and October, 2013.

In addition to potential displacement, animals within the explosive blast zone are subject to effects ranging from a temporary threshold shift in hearing (TTS) to death (Ketten, 1995). Ketten et al. (1993) documented damage in all four ears from two humpback whales that died following an explosion in Trinity Bay, Newfoundland, Canada. Danil and St. Leger (2011) documented the death of three long-beaked common dolphins (*Delphinus capensis*) as well as 70 western grebes (*Aechmophorus occidentalis*) just off the coast of San Diego due to blast trauma from a Navy underwater explosive training event.

Seismic Airguns

Seismic airguns produce broadband impulsive sounds with maximum energy below 1,000 Hz and with source levels that can reach well above 220 dB (Duncan, 2017; Heath and Wyatt, 2014; Mattsson et al., 2012). It has been suggested that such activities could lead to the stranding of marine mammals (Castellote and Llorens, 2016). Malme et al. (1984) investigated the potential effect of oil industry activities on migrating grey whales and concluded there was "no long-term

relationship (between) growth rates in the grey whale population" and seismic activity off the coast of California. More recently, the Behavioural Response of Australian Humpback whales to Seismic Surveys study has investigated the effect of seismic airguns on the behaviour of humpback whales using both visual and passive acoustic methods (Cato et al., 2013). Dunlop et al. (2017a) reported minor changes in respiration, movement patterns, and breaching when animals were exposed to transmissions from a full airgun array, but concluded that these were unlikely to cause additional stress. Dunlop et al. (2017b) calculated a dose-response relationship for animal avoidance as a function of received level and distance from the source. They found animals were likely to avoid the source within a distance of 3 km at levels over 140 dB re 1 $\mu Pa^2\ s^{-1}$.

Castollete et al. (2012) monitored fin whale 20 Hz calls during a 10-day seismic survey using Navy surveillance arrays. A decrease in the number of calls was detected during the first three days of the survey, after which bearings to the animals suggested they were moving away from the source. Richardson et al. (1999) used aerial surveys to measure bowhead whale (*Balaena mysticetus*) distribution around seismic surveys and found a reduction in numbers within 20 km of operating airguns, while numbers at greater distances increased suggesting the animals avoid the airguns. Blackwell et al. (2013) measured a significant reduction in bowhead whale call localizations near seismic activity in the Beaufort Sea, though it was not possible to discern if the animals avoided the source, stopped calling or both. Harris et al. (2001) recorded the distances that seals were sighted from a seismic survey ship with no source emissions, one airgun, and a full array of airguns operating during a three-month survey off the north coast of Alaska. Seals were recorded at a greater distance from the ship during full airgun array operations, although they remained within 250m of the vessel.

Echosounders

Echosounders are used on numerous commercial vessels to locate fish, measure depth, and map the ocean floor. Lurton and DeRuiter (2011) reviewed the characteristics of various bottom-mapping echosounders and evaluated their potential effect on marine mammals using existing mitigation criteria. They concluded that the potential for physical damage to animals from these sources is low, because of the short pulse length and narrow beampattern, but they believed there may be a behavioural reaction. Vires (2011) measured the distribution of *Md* groups using click detection data collected on the Atlantic Undersea Test and Evaluation Center (AUTEC) hydrophones in the Bahamas before, during, and after a prey mapping test. A ship with a 38 kHz Simrad EK60 echosounder with a 1024 µs pulse width and 208 dB re Pa@1m source level (Demer et al., 2015). This source was directed to *Md* foraging groups based on passive acoustic detection of their clicks. No change in temporal or spatial distribution was found due to the presence of the echosounder. In contrast, Olesuik et al. (2002) measured harbour porpoise avoidance beyond 3.5 km to an acoustic harassment device designed to reduce seal predation of commercially raised and harvested fish. While not an true echosounder, the device produces similar pulsed sounds. The device cycled on for 2.3 s and off for 2.1 s, and produced 10 kHz, 1.8 ms pulses at a repetition rate of 40 ms and source level of 194 dB re μPa_{pp}^2@1m. Quick et al. (2016) measured the response of short-finned pilot whales (*Globicephala macrorhynchus*) to an EK60 echosounder. During exposures of five animals', their heading variance increased significantly as compared to four individuals that were not exposed.

Perhaps the most widely reported incident in which approximately 100 melon-headed whales (*Peponocephala electra*) stranded occurred in 2008 off the coast of Madagascar (Southall et al., 2013). The most likely cause of the stranding was deemed by an international review panel to be

the operation of a 12 kHz multi-beam, bottom-mapping echosounder with a source level of 240 dB approximately 65 km offshore of the stranding location (Southall et al. 2013).

1.2.2 Military Sources

The first evidence that military sonars could affect cetacean behaviour came from studies in the mid-1990s of the effect of the Surveillance Towed Array Sensor System-Low Frequency Active (SURTASS-LFA) sonar. Grey whales (*Eschrichtius robustus*) migrating off the coast of California were exposed to low frequency (160-330 Hz) sonars positioned both inshore and offshore (Buck and Tyack, 2000). A 50% avoidance of the inshore source at a received level of 141 dB was found, suggesting the context of the exposure was a significant factor. In a separate study, Hawaiian humpback whales were observed to produce longer songs after exposure to SURTASS-LFA (Fristrup et al., 2003).

To mitigate the potential effect of SURTASS-LFA on cetaceans, a high-frequency (30 kHz), active sonar system is used to monitor for the presence of marine mammals in the vicinity of U.S. Navy vessels when this sonar is broadcasting (Ellison and Stein, 1999). The system is used to ensure that no animals are exposed to a level greater than 180 dB, which corresponds to a distance of 0.75 and 1.0 km from the source, depending on sound propagation conditions.

Military sound sources and mass strandings

Mass strandings of marine mammals may have many causes other than sonar exposure. For example, around 335 BC Aristotle wrote this about marine mammal strandings in *Historia Animalium*,

> "It is not known why they sometimes run aground on the seashore, for it is asserted that this happens rather frequently when the fancy takes them and without any apparent reason." (Aristotle)

Nevertheless, it has become apparent over the last two decades that, under certain circumstances, anthropogenic sound, including MFAS, may play a role in cetacean strandings (Ketten, 2014, Filadelfo et al., 2009). The issue gained heightened attention when 14 Cuvier's beaked whales (*Ziphius cavirostris*, hereafter referred to as *Zc*) stranded coincident with a Navy test of MFAS signals in the Kyparissiakos Gulf, Greece in 1996 (D'Amico and Verboom, 1998). Table 1.1 summarises beaked whale stranding coincident with Navy operations that have occurred since 1985.

Table 1.1 Potential MFAS associated beaked whale strandings gleaned from news reports.

Date	Location	Beaked	Total
February 1985	Fuerteventura, Canary Islands	13	13
November 1988	Fuerteventura, Canary Islands	4	6
October 1989	Fuerteventura, Canary Islands	24	24
May, 1996	Kyparissiakos Gulf, Mediterranean Sea	12	12
October 1999	U.S. Virgin Islands	4	4
March 2000	Northwest Providence Channel, Bahamas	14	17
May 2000	Madeira Archipelago	4	4
September 2002	Fuerteventura, Canary Islands	18	18
July 2004	Fuerteventura, Canary Islands	3	3
January 2006	Mediterranean Sea coast, Spain	4	4
November, 2011	Peloponnesian Coast, Italy / Corfu, Greece	10	10
February 2011	Sicily	2	2
April, 2014	Crete	7	7
March 2015	Guam	3	3

Debate over the causal association between MFAS use and beaked whales strandings was heightened by a widely scrutinized event that occurred in March, 2000 in the Bahamas' Northwest Providence Channel (Figure 1.6). Five surface ships using MFAS moved through the Channel in a 2-1-2 pattern from East to West. Eleven *Zc*, three *Md* and two minke whales (*Balaenoptera acutorostrata*) were found stranded shortly after the exercise, and at least six animals died (Balcomb and Claridge, 2001; England et al., 2001). This event led to the initiation of a U.S. Navy research program on the effect of MFAS on marine mammals, including the research described in this thesis.

Several experiments have been conducted to investigate the individual- and population-level response of a number of whale species to sonar exposure. Passive acoustic monitoring of *Md* at AUTEC was used to document the displacement of animals from the range during multi-ship MFAS tests (McCarthy et al., 2011; Tyack et al., 2011). Controlled exposures of individual *Md*

to MFAS at AUTEC also provided evidence for the disruption of foraging, and movement of the animal away from the MFAS source (Tyack et al., 2011). A similar avoidance response was documented for an exposure of *Zc* to MFAS in Southern California (DeRuiter et al., 2013). Falcone et al. (2017) documented a change in *Zc* dive behaviour when exposed to tactical MFAS on or near SCORE using satellite tag data from 16 animals. An increase in the duration of deep foraging dives, shallow dives, and surface intervals was measured. These responses were more pronounced with mid-power sources closer to the animals. A bottlenose whale (*Hyperoodon ampullatus*) in the North Atlantic exposed to MFAS moved away from the source and executed the longest (94 min.) and deepest (2339 m) dive ever recorded for the species (Miller et al., 2015). In addition, controlled exposure experiments with a European towed military sonar documented behavioural changes (Southall et al., 2007) in killer whales *(Orcinus orca),* long-finned pilot whales *(Globicephala melas),* and sperm whales *(Physeter macrocephalus*) (Miller et al., 2012). Sonar in the 1-2 kHz range produced more pronounced changes than to higher frequency (6-8 kHz) signals. Goldbogen et al (2013) documented behavioural changes in blue whale (*Balaenoptera musculus*) feeding behaviour following exposure to sonar. The severity of the response depended on the animals' feeding state. Animals showed no response during shallow dives, but showed a pronounced response during deep-feeding dives.

The importance of context was illustrated by the response of a *Zc* to a nearby experimental sonar with a source level of 210 dB (Southall et al., 2012) and a military sonar with a source level of approximately 235 dB over 50 km away (DeRuiter et al., 2013). The two sources resulted in similar received levels but only the nearby source elicited a detectable response. It should be noted that, in addition to the large difference in source separation distances, the animal was followed by four surface craft in the period preceding playback from the smaller source. Falcone

et al. (2017) found that the same received level resulted in a longer interval between consecutive *Zc* foraging dives when the source was a smaller Navy sonar (e.g. helicopter deployed MFAS) than when it was a larger ship-mounted sonar (53C MFAS). This adds further support to the hypothesis that the distance and characteristics of the source may be contributory factors. A helicopter MFAS is deployed for tens of minutes at the same location, has a lower source level than ship-mounted sonars of approximately 217 dB (U.S. Fleet Forces Command, 2008) and may be repositioned in a pattern that is extremely difficult to predict. In contrast, ship-deployed sonar is generally broadcast for an extended time and the movement of the source ship is relatively predictable.

Signal structure has also been suggested as a potential factor. Predator avoidance behaviours in prey animals have been widely studied (Brodie Jr. et al., 1991; Frid and Dill, 2002; Howland, 1974) and suggest sounds that are associated with a predator may result in a more severe reaction, as was found in humpback whales (*Megaptera novaeangliae*) exposed to killer whale calls (Curé et al., 2015). If animals perceive MFAS as a threat, they may respond in a manner similar to that elicited by a predator (Harris et al., 2018). Therefore, understanding the anti-predator response may provide insight into the nature of the response and its potential risk. For example, sperm whales switched to a "non-foraging, non-resting state" when exposed to both low-frequency active sonar and killer whale calls (Curé et al., 2016; Sivle et al., 2012). In the 2007 Behavioural Response Study in the Bahamas, a tagged *Md* was exposed to both an MFAS signal and killer whale calls on successive foraging dives (Tyack et al., 2011). In response to the MFAS playback, the animal stopped foraging at a received level of ~140 dB and slowly moved away from the source ship at a shallow ascent angle. When exposed to killer whale calls two hours later, the animal stopped echolocating at a received level of 98 dB and moved slowly to the

surface away from the source ship but continued to move away at the surface in a straight line. The animal did not forage for another 10 hours. The response to the killer whale playback was more severe than to the MFAS playback, though the initial MFAS playback may have preconditioned the animal and contributed to the response to the killer whale playback.

Additional signal characteristics, such as the rise-time of the signal, may contribute to the severity of the response. Götz and Janik (2011) documented a pronounced startle response in grey seals (*Halichoerus grypus*) for signals with short (5 ms) versus long (100 ms) rise times. This could affect the response of whales to MFAS signals in the open ocean, because acoustic propagation effects are likely to reduce the rise-time of a signal over long distances. Such differences in rise-time could have contributed to the differential response of a *Zc* to near and far MFAS sources reported by (DeRuiter et al., 2013).

Considered together these studies strongly suggest that sonar exposure results in various behavioural responses (Harris et al., 2018), although the effects of contextual variables such as source type, distance, and rise-time need to be determined. However, little is known about the long-term, population effect of repeated MFAS exposure (Harris et al., 2018). This thesis explores methods for assessing the response to, and the effect of, such repeated exposure at AUTEC, where there is a well-documented *Md* population (Claridge, 2013, 2006). It describes methods for estimating population trends, for assessing the probability of behavioural disruption from sonar exposure, and models the potential population effect of repeated, long-term foraging disruption.

1.3 A Brief History of Sonar

The initial motivation to develop methods for detecting and locating submerged objects was the potential impact of icebergs on trans-Atlantic shipping as the volume of this traffic increased at the turn of the 20th century. The first patent for an active sonar system, which used a circular plate driven by an electromagnet to produce a 540 Hz signal, was granted to Reginald Fessenden in 1913 (Rolt, 1994). The advent of World War I and the expansion of submarine warfare focused attention on the development of systems capable of detecting these vessels. By the mid-1930s, piezoelectric transducers emerged as the technology of choice for producing underwater sound, and by World War II arrays of transducers were used to increase the source level and directionality. The term sonar (SOund Navigation And Ranging) does not appear until 1942. It is attributed to the then director of the Harvard Underwater Sound Laboratory, F.V. Ted Hunt (D'Amico et al., 2009; Warren, 1988).

The simplest form of sonar is passive sonar, which uses an underwater microphone (a hydrophone) to detect sound generated from a source of interest, such as a boat. However, passive sonar depends on a noisy source for its effectiveness. Submarines maintain a tactical advantage by staying submerged, out of sight and, most importantly, quiet. Modern diesel-electric submarines are powered by batteries when submerged, thus significantly reducing the number of moving parts and generated noise. To quote Paul Perkins, a former submariner, sonarman, and pioneer in the field of marine mammal acoustics, "*nothing runs quieter than a battery*."

Western global influence depends heavily on the projection of military force through the deployment of high-value carrier battle groups. The quiet diesel-electric submarine provides a means of asymmetric warfare for nations with limited financial and technical resources. For a

relatively low cost, a diesel-electric submarine could severely impact the operations of a naval battle group. Because they generate little noise when submerged, passive sonar is ineffective in detecting them, leaving active sonar as the only viable means of detection. Consequently, world navies have emphasised active sonar training and testing (Grace, 2008).

Active sonar uses a sound-producing device to transmit a known signal, and a hydrophone to detect the return echo from the target of interest. The distance from the target is derived by dividing the total round-trip transit time in half and multiplying it by the speed of sound in seawater (Urick, 1996). Since active sonar depends on the reflection of sound off the target, in general, the louder the transmission, the louder the echo, and the greater the detection range. Modern tactical sonar uses arrays of sound producing and receiving piezo-electric transducers to form a directed beam for both transmission and reception of sound, and to increase the power of the transmitter and the sensitivity of the receiver. By "steering" the beam, it is possible to focus energy transmissions on the target, reduce interfering noise while listening for the echo, and track the target based on the strength of the signal received in a particular beam (Ainslie, 2010; Urick, 1996).

Since their introduction in the early 1900s, active sonar systems have steadily evolved. In particular, active systems have advanced from using simple pulsed continuous wave (CW) to signals using a combination of signal types, including a frequency upsweep or downsweep (Figure 1.1). Frequency sweeps are particularly insensitive to Doppler shifts which occur when the transmitted signal from a moving ship reflects off a moving target.

For the U.S. Navy, testing of such systems and training sailors in their proper use, while at the same time minimizing the environmental impact of MFAS operations, is a continual area of concern.

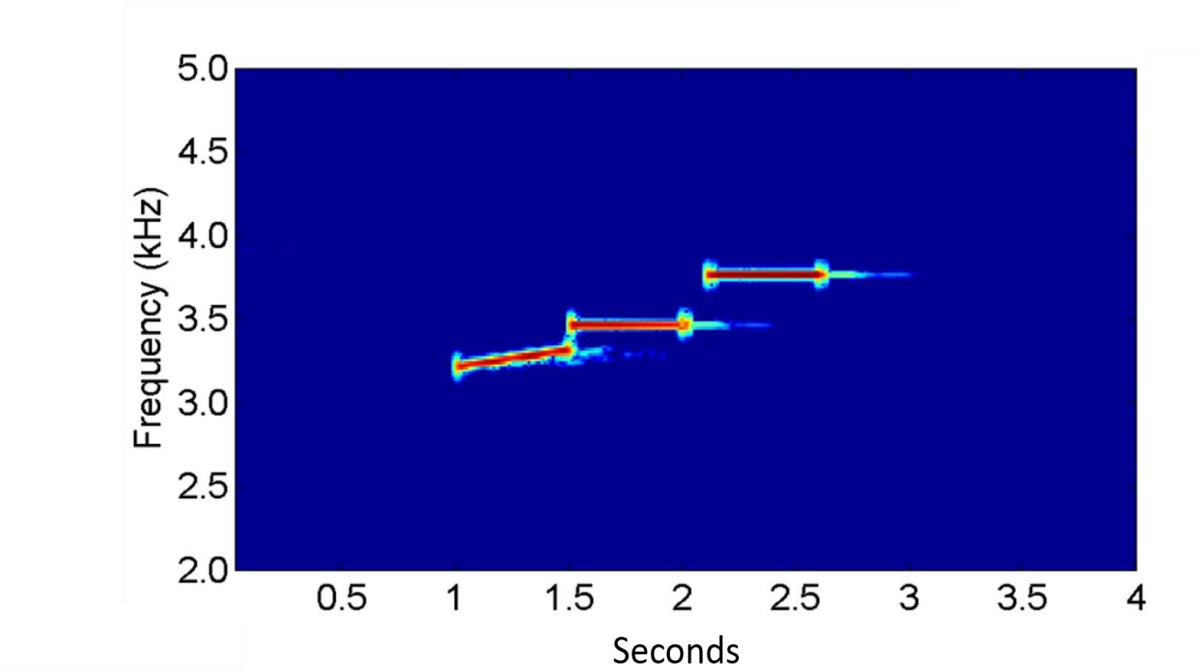

Figure 1.1 Spectrogram (time (s) vs frequency (kHz)); amplitude in color, blue=min, red=max) of a representative sonar signal used as part of the Behavioural Response Study, consisting of an upsweep, CW, CW combination (Southall et al., 2012).

1.4 Blainville's Beaked Whale

1.4.1 Overview

Beaked whales represent a guild of 22 known species in the Ziphiidae family. A new species (that is yet to be named) was discovered stranded on St. George Island in the Alaska Pribilof Islands as recently as 2014 (Welch, 2016). *Md* is the most widely distributed of 15 known mesoplodont species and inhabits deep-water canyon environments in tropical to temperate waters around the globe (Mead, 1989; Perrin et al., 2009).

Beaked whales spend little time on the surface and have a low surface profile, making them particularly hard to locate and identify (Baird et al., 2006; Johnson et al., 2008). For instance, Barlow (1999) estimated the probability of observing a mesoplodont species at the surface from a ship on the transit line during a marine mammal survey is only 0.23 (CV=0.35). Consequently, data on their behaviour, life-history, and demographics are sparse. The majority of information on beaked whales has been derived from long-term studies of *Md* in the Bahamas (Claridge, 2013, 2006) and Hawaii (Baird et al., 2008, 2006), *Zc* off the coast of California (Falcone et al., 2009; Schorr et al., 2014), *Md* and *Zc* in the Canary Islands (Carrillo et al., 2010), and northern bottlenose whales (*Hyperoodon ampullatus*) off the Atlantic coast of Canada (Gowans et al., 2000; Whitehead, 2013).

1.4.2 Physical Characteristics

The name "beaked" generally refers to their distinct rostrums. *Md* are named for the French zoologist Henri de Blainville, who in 1817 first documented the species based on a piece of jawbone. The extremely dense rostrum bone gave rise to the species name "*densirostris*" (Pitman, 2002; Stewart et al., 2002).

Md are moderate-sized, round-bodied animals. The maximum recorded length and weight of an adult are 4.7 m and 1,000 kg (Claridge, 2013; Mead, 1989). The animals' coloration can be dark grey to greyish brown or slightly blue (Ross et al., 1988). Their relatively small (in relation to their body) flippers fold into depressions on their sides. Their falcate dorsal fin is positioned roughly two-thirds of the way down the animal's back (Pitman, 2002; Stewart et al., 2002).

Of mesoplodonts, *Md* exhibits the greatest sexual dimorphism (Heyning, 1984; Mesnick and Ralls, 2018). Only adult males develop two erupted tusks from their lower jaw, which has an

accentuated mandibular ramus that curves dorsally (Heyning, 1984; McCann, 1963). The base of the mandible arches up over the upper mandible, with the tusks erupting on the apex of the arch. This mandibular arch is more pronounced in males. Distinct scarring patterns found on adult males suggesting the tusks are used in fights for females (Dalebout et al., 2008; Heyning, 1984; McCann, 1963). These patterns, along with cookiecutter shark (*Isistius sp*.) bite scars, are used to identify individuals via photo identification (Claridge, 2013).

1.4.3 Age Parameters (Gestation, Sexual Maturity, Life Expectancy)

To date, *Md's* life expectancy is unknown, but an examination of data from other beaked whale species suggests they are long-lived. Kasuya (1977) examined Baird's beaked whales (*Berardius bairdii*) tooth cementum and counted the growth layer groups with the assumption that each layer represents one year of growth. Of 20 Baird's beaked whales, five individuals were at least 50 years old. The oldest male was estimated to be 71 years old and the oldest female 39 years old. The age at maturity was estimated to be between 8 to 10 years of age.

Benjaminsen and Christensen (1979) found the oldest of 54 (27 females and 37 males) commercially harvested northern bottlenose whales from Norway and Iceland to be 37 years old. Sexual maturity was estimated to occur between 7 to 11 years of age based on the presence of sperm in the testes and *corpora lutea* in the ovaries. Perrin and Myrick (1980) estimated a Gervais' beaked whale (*Mesoplodon europaeus)* to be 27 years old.

Claridge (2013) recorded multiple sightings of an adult male *Md* in the Bahamas over a span of 14 years, suggesting a long life expectancy as was reported for other beaked whales. Based on sighting data and examination of morphological features (in particular, size, mandibular arch development, and the eruption of tusks) male sexual maturity was estimated to occur at 9 to 10

years of age. The youngest *Md* observed to give birth was 10 years, with the age at sexual maturity estimated to be 9 years, assuming a one-year gestational period (Claridge, 2013).

1.4.4 Social Behaviour

In the Bahamas and Canaries, *Md* associate in groups of 1 to 11 animals (Aguilar de Soto et al., 2012; Claridge, 2013; McSweeney et al., 2007) with median group size in the Bahamas of four (Claridge, 2006). The groups generally consist of loosely associated females with a single adult male in fission-fusion relationships and their young (Claridge, 2013, 2006; McSweeney et al., 2007). Like other beaked whale species, including *Zc* (McSweeney et al., 2007; Schorr et al., 2014), and northern bottlenose whales (Gowans et al., 2000), *Md* groups exhibit high site fidelity (Claridge, 2013). *Md* young are closely associated with their mothers for up to three years (Claridge 2013).

1.4.5 Dive Behaviour and Feeding.

Beaked whales, including *Md*, execute deep foraging dives, in which the group dives and surfaces together approximately every two hours, with a mean duration of approximately 60 minutes (Baird et al., 2006; Claridge, 2013; Johnson et al., 2006a). The deepest breath hold-dive, to approximately 3,000 m, and the longest (137 min) dive were both recorded on a tags placed on a *Zc* in the San Nicolas Basin near the Southern California Offshore Range (Schorr et al., 2014). Above 300 m, the animals are nearly silent, presumably to avoid predators (Johnson et al., 2008, 2006). *Md* at AUTEC routinely forage at depths between 700 and 1,000 m (Dolan et al., 2019).

Below 300m, they produce short (< 500 ms) echolocation clicks, presumably in search of prey (Johnson et al. 2006). Thus, detections of these periods of group clicking or group vocal periods,

can provide insight into the animals' spatial and temporal distribution, foraging behaviour, and abundance (Jones et al., 2008; Manzano-Roth et al., 2016; McCarthy et al., 2011; Moretti et al., 2010).

Beaked whales have a bilateral set of throat grooves that expand during suction feeding (Heyning, 1996). Based on stomach and faecal content analysis, *Md* feed on benthic fish and cephalopod species captured during deep foraging dives (MacLeod et al., 2003).

Between foraging dives the animals may execute a series of vocally quiet dives to an intermediate depth (< 300 m). These were referred to as "bounce dives" by Tyack et al. (2006), who suggested that they are required to handle blood-gas exchange, in particular, the nitrogen load after deep foraging dives. However, Baird et al. (2008) found a diel variation with a lack of bounce dives at night in tag data from six *Md* and two Zc in Hawaii and suggested this may be a predator avoidance behaviour. Also, Schorr et al. (2014) reported an "occasional" *Zc* making near back-to-back deep foraging dives.

1.4.6 Beaked Whale Acoustics

Beaked whales' physical and vocal behaviour are particularly suited for passive acoustic monitoring using bottom-mounted hydrophones, such as those found on U.S. Navy ranges. Their vocal behaviour has been documented using recording tags, some of which were applied at AUTEC (Johnson et al., 2006b, 2004; Tyack et al., 2011). The combination of beaked whales, MFAS operations, and an extensive hydrophone array at AUTEC, as described below, provides the opportunity to study beaked whale reaction to MFAS exposure *in situ*, and to use these data to study the aggregate effects of repeated exposure.

As noted above, data gleaned from tag recordings show that *Md* only vocalize during deep (>300m) foraging dives (Johnson et al., 2004). At AUTEC, *Md* are the most abundant beaked whale species, and on average, a group dives approximately 9.2 times per day (Moretti et al., 2010). They have been measured repeatedly foraging at ~1,000 m (Dolan et al., 2019).

The clicks as recorded on the AUTEC hydrophones (Figure 1.2) are composed of a ~300 µs upsweep (90% energy criteria) from approximately 25 to 45 kHz (upper hydrophone bandwidth) with a peak frequency of approximately 30 kHz (Figure 1.3).

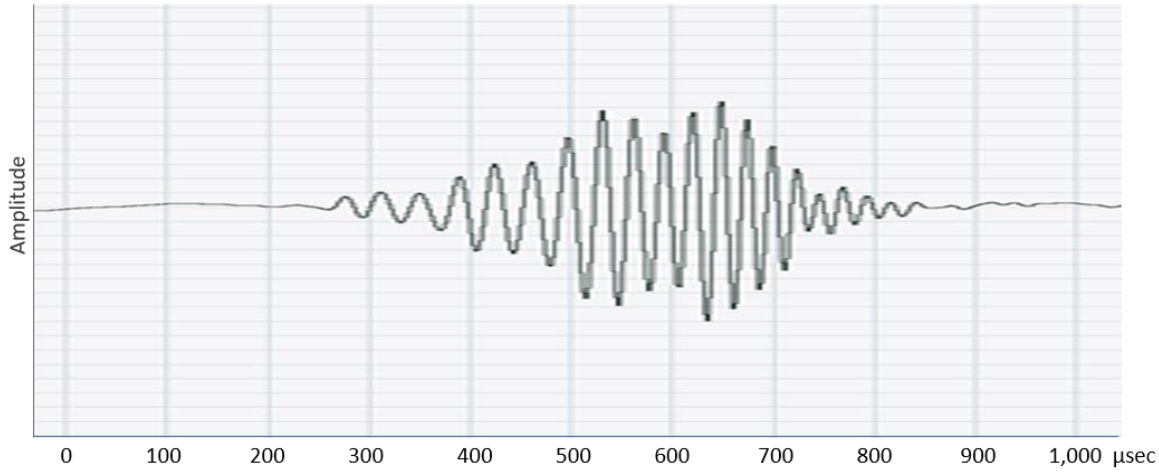

Figure 1.2 Time domain plot of an AUTEC Blainville's beaked whale echolocation click extracted from AUTEC hydrophone data.

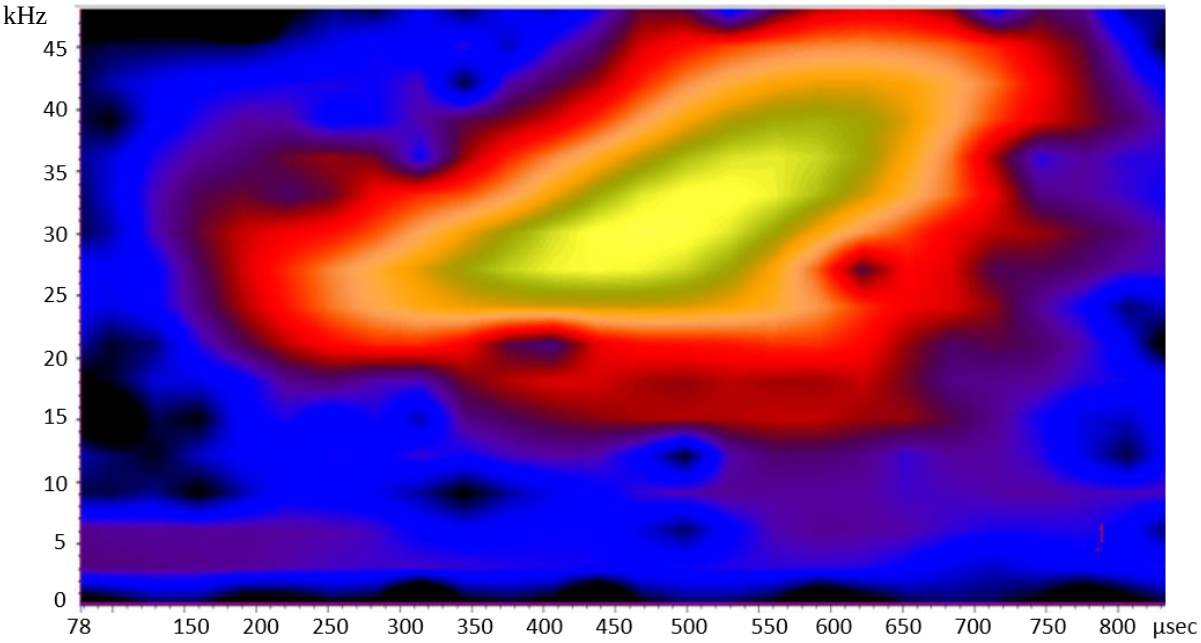

Figure 1.3 Spectrogram of an AUTEC Blainville's beaked whale echolocation click extracted from AUTEC hydrophone data with amplitude represented by the colour (yellow=max, black=min).

Shaffer et al. (2013) combined data from recording tags and the surrounding AUTEC hydrophones to estimate that the on-axis source level of an *Md* click is in excess of 200 dB, with a 3dB beam-width of ~6 degrees. These data suggest *Md* use the echoes from the loud frequency upsweeps they emit to illuminate their prey (Madsen et al., 2005).

The presence of *Md*, *Zc* and Gervais beaked whale (*Me*) at AUTEC has been visually verified (Claridge, 2006; Gillespie et al., 2009), but they can also be readily identified using passive acoustics. Both the frequency content of their echolocation clicks and the inter-click interval (ICI) provide features (Figure 1.4) that can be used to identify each species (Jarvis, 2012; Jarvis et al., 2008). At AUTEC, on average *Md* produce ~3.33 clicks per second (ICI = 0.303 s, 95% CI 0.297-0.310), ~*Zc* produce 1.92 clicks per second (mean ICI=0.54 95% CI 0.52-0.56), whereas *Me* produce ~3.57 clicks per second (mean ICI=0.28, 95% CI 0.277-0.281). *Md* click

energy spans the 25-50 kHz band with a peak at ~30 kHz. *Zc* click energy spans the 15-50 kHz frequency band with peak energy at ~38 kHz and frequency null at approximately 25 kHz. *Me* click energy spans the 20 to 50 kHz band with peak energy at 40 kHz. Note, the upper frequency is affected by the 48 kHz hydrophone bandwidth (Figure 1.4).

Md Inter-Click Interval

Average	0.303175
Max	0.4813
Min	0.1738
Standard deviation (N=256)	0.047

Zc Inter-Click-Interval

Average	0.543
Maximum	0.679
Minimum	0.392
Standard Deviation (n=47)	0.067

Me Inter-Click-Interval

Average	0.279
Maximum	0.379
Minimum	0.22
Standard Deviation	0.031

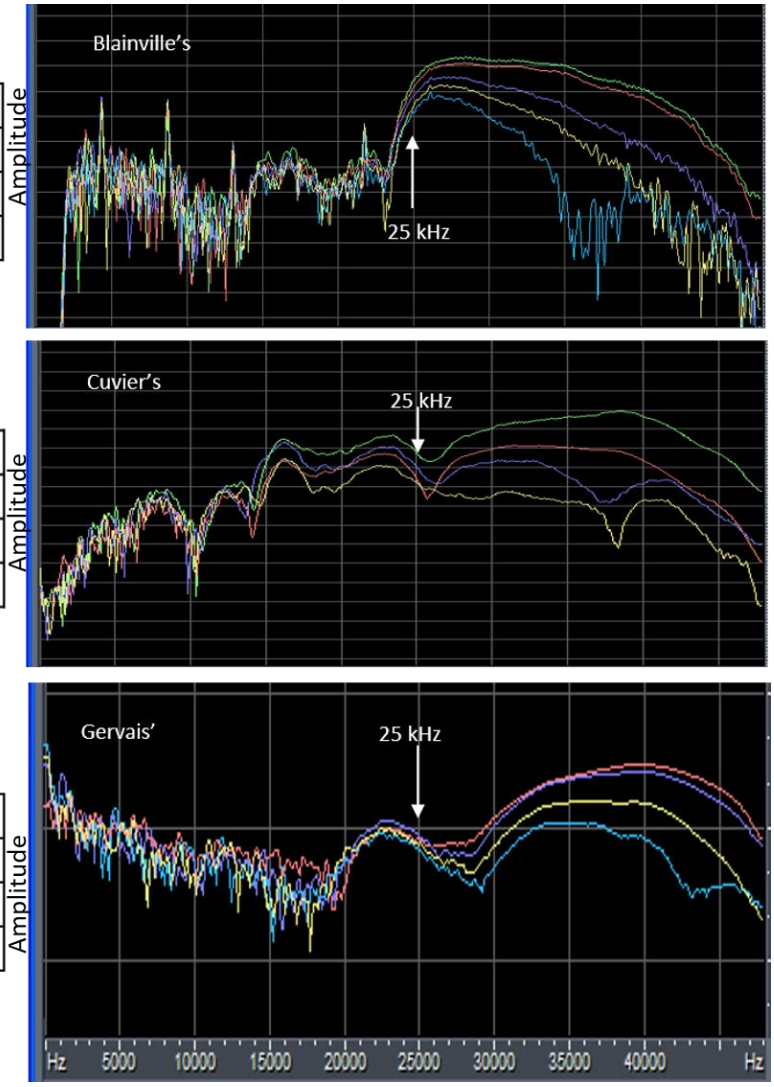

Figure 1.4 Frequency (Hz) vs. amplitude (dB) for successive clicks from an animal's beam moving across a hydrophone for Blainville's (top), Cuvier's (middle), and Gervais' (bottom) beaked whales recorded on the AUTEC Range. Each colour represents a separate click in a click train from highest (top) to lowest (bottom) amplitude.

During the vocal period of a foraging dive, which at AUTEC has a mean duration of ~30 minutes, as many as 5,000 clicks can be produced (Shaffer et al., 2013). From time to time, the rate of clicking increases rapidly into a buzz (Johnson et al., 2004); which is believed to be a prey capture attempt (Jones et al., 2008).

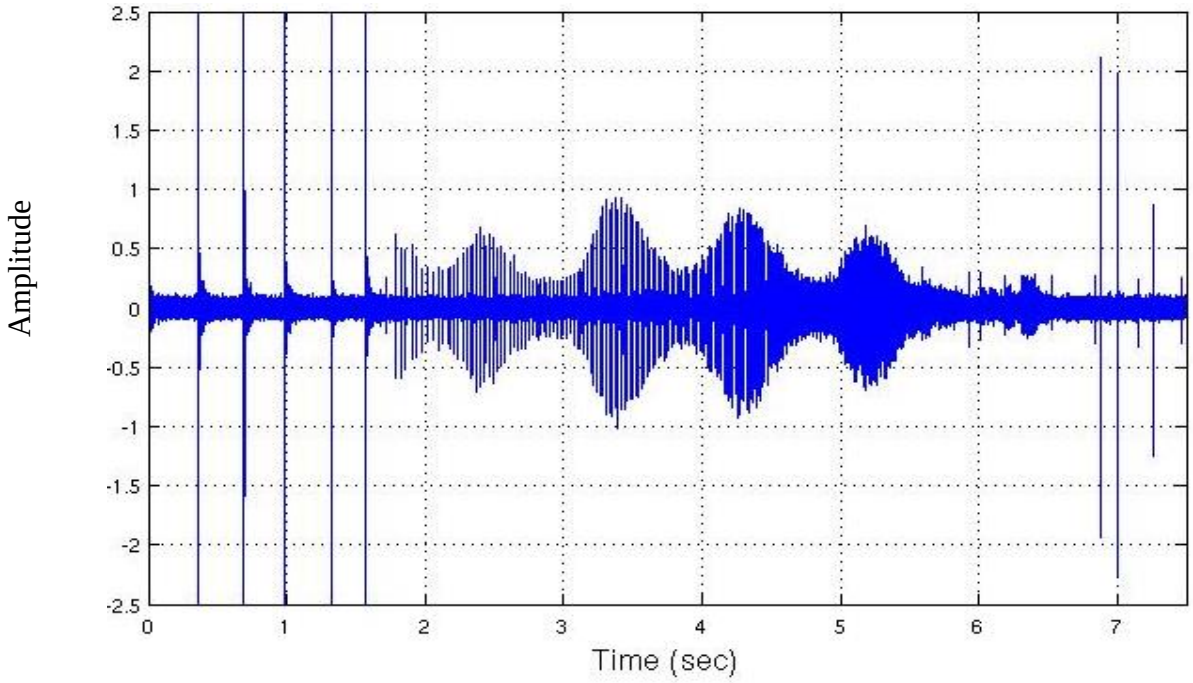

Figure 1.5 AUTEC Md echolocation clicks followed by a rapid series of buzz clicks.

The distinct timing and structure of the echolocation clicks associated with these dives make them particularly suited for passive acoustic monitoring. Dolphin clicks are impulsive with typically short duration (< 200 µs), and short and variable inter-click intervals (Au 2012). By comparison, *Md* echolocation clicks (Figure 1.5) typically are longer (>300 ms) and consist of a distinct upsweep (Johnson et al. 2006). Beaked whale echolocation click-trains are rhythmic with slower inter-click intervals as compared to most dolphin species. For example, *Md* at

AUTEC has a mean interval of approximately 0.3 s throughout a foraging dive, while dolphins tend to click at a more variable and rapid rate (<0.2 s interval) (Au, 1993; Au and Herzing, 2003). This near constant click rate, frequency structure, and click duration are used to distinguish beaked whale echolocation clicks from other small odontocetes.

1.5 Beaked Whale Stranding Theories

Several theories as to why beaked whales strand have been postulated. Because beaked whales dive repetitively to great depths, their blood likely saturates with nitrogen during these dives (Houser et al., 2008). Consequently, a number of studies have focused on a potential link between strandings and some form of decompression sickness (Fernández et al., 2005; Hooker et al., 2009; Rommel et al., 2005; Zimmer and Tyack, 2007).

Jepson et al. (2003) examined eight *Zc*, one *Md*, and one *Me* that stranded in the Canary Islands in September 2002 coincident with a Navy MFAS operation. Gas bubble formation, consistent with decompression sickness, was found in multiple organs, resulting in widespread microvascular haemorrhaging. Fernández et al. (2005) examined the bodies of fresh stranded *Zc* and found nitrogen bubbles in major organs. They speculated that sonar exposure during a foraging dive may cause the animals to surface quickly, causing decompression sickness (Fernández et al., 2005). Rommel et al. (2005) reviewed the physiology of beaked whales, bottlenose dolphins (*Tursiops truncatus*) and domestic dogs (*Canis familiaris*) to help fill knowledge gaps and illustrate physiological differences. They suggested multiple mechanisms that could explain the potential sensitivity of beaked whales to sonar. Included were sonar-mediated gas and/or fat emboli, acoustically mediated bubble growth, dysbaric osteotrauma (pressure changes resulting in disruption of oxygen or blood supply to the bone or marrow),

structural resonance that causes tissue damage, behavioural alterations that lead to gas emboli, or "diathetic fragility" in which structural or air-space resonance causes bleeding. Cox et al. (2006) suggest there may also be a "vestibular response" to sonar that affects the ability of beaked whales to navigate, and results in disoriented animals moving into unfamiliar shallow water.

Based on the findings from necropsies of stranded beaked whales, several studies investigated potential mechanisms for bubble formation. Zimmer & Tyack (2007) modelled gas bubble formation in various tissues. They speculated that the animals ascend and move away from the source rapidly at the surface, with successive limited shallow dives. Under such conditions, the model predicted bubble formation in brain tissue.

Hooker et al. (2009) constructed a gas exchange model, using data from *Md*, *Zc* and northern bottlenose whales. They compared the partial pressure of nitrogen (P_{N_2}) during the day, when animals alternate between mid-depth bounce dives and deep foraging dives, to night time behaviour, when the animals remain near the surface between deep foraging dives. The model predicted no measurable differences in P_{N_2} across the three species' dive behaviour. However, *Zc*, the species most associated with stranding incidents, with longer dives and shorter surface intervals appeared to be at a higher risk.

As discussed above, in the 2007 and 2008 controlled exposures at AUTEC, the tagged animals stopped foraging and moved slowly to the surface away from the source at a shallow angle in response to MFAS, killer whale, and pseudo-random noise playbacks (Tyack et al. 2011). A controlled exposure of a Cuvier's beaked whale to MFAS in Southern California (DeRuiter et al. 2013) found that the animals' foraging was disrupted, but, as with *Md* at AUTEC, it moved away from the source and ascended at a shallower angle and at a slower rate than dives with no

exposure. Such a slow ascent rate would lessen the chance that animals fail to handle the gas exchange and develop decompression sickness in contrast to the rapid movements assumed by Zimmer and Tyack (2007).

Houser et al. (2008) found that a bottlenose dolphin (*Tursiops truncatus*) trained to repetitively dive to depths sufficient to cause lung collapse recovered without injury despite an elevated nitrogen concentration in its blood. They state that their findings "do not support the proposition that repetitive breath-hold diving within the depths at which lung gas exchange occurs is sufficient to produce asymptomatic N_2 bubbles".

Beaked whales may be placed in situations where unusual diving behaviour is likely to occur if they are caught between a ship deploying sonar and the shore. In these circumstances, they may be "herded" ahead of the sonar into an unfamiliar shallow water environment. For example, in the mass stranding that occurred in the Kyparissiakos Gulf, Greece, the research vessel *Alliance*, moved away from the coast while broadcasting MFAS. It then turned and ran parallel to the shore in deeper water. Finally, it turned toward the shore before ending sonar transmissions; a run geometry that could potentially move beaked whales from deep to shallow waters (D'Amico and Verboom, 1998). Similar conditions also occurred in relation to the 2000 Bahamas strandings described in section 1.2.2. As was the case with the Greek stranding, this could have herded animals from deep to shallow water (Balcomb and Claridge, 2001; England et al., 2001).

Most recently, the conclusions of a 2017 beaked whale workshop were reported by Bernaldo de Quirós et al. (2019). The research to-date regarding beaked whale strandings was summarized. They suggested combined factors may play a role in sonar related strandings. They postulate a "fight or flight" response may contribute to the animals' inability to regulate their nitrogen load

which leads to decompression sickness similar to the theory presented by Zimmer and Tyack (2007). Based on the current knowledge base they recommend: (1) a moratorium on MFAS in those regions where atypical mass stranding events continue (e.g. regions of the Mediterranean Sea), (2) continued research in areas with MFAS to determine if sub-lethal impacts on individuals result in population-level impacts, (3) comparative studies on populations of beaked whales in the absence of MFAS, (4) determination of life-history parameters, (5) studies in anatomy, physiology, and pathophysiology to better understand the development of decompression-like sickness in whales, and (6) continued development of technologies to measure physiological responses of free-swimming beaked whales.

In response to this evidence of the potential association between MFAS use and beaked whale strandings, the U.S. Secretary of the Navy, in consultation with the Commerce Department, issued a "National Defense Exemption (NDE) from Requirements of the Marine Mammal Protection Act" in 2007. The NDE called for "increased vigilance" during major MFAS operations carried out in areas with what are commonly known as the five "Bahamas factors" (England, 2007).

1. The presence of beaked whales
2. A rapid change in bathymetry
3. Multiple ships or submarines (≥3)
4. An area surrounded by land masses, separated by less than 35 nautical miles and at 10 nautical miles in length or an embayment
5. A significant surface duct that traps sound at near the surface

1.6 The Atlantic Undersea Test and Evaluation Center (AUTEC)

1.6.1 Acoustic Range Layout

All of the "Bahamas factors" occur at AUTEC that lies ~130 km south of the Northwest Providence Channel (NWPC) in the Bahamas. AUTEC is situated in the Tongue of the Ocean (TOTO), which forms the southern branch of the Great Bahama Canyon. It is a deep (~2,000 m) canyon, approximately 30 x 100 km in size, surrounded by water less than 100 m deep, except for the canyon mouth, where it meets the NWPC. AUTEC is the U.S. Navy's principal undersea test and evaluation range, where MFAS is routinely used (McCarthy et al., 2011). AUTEC's location in the TOTO can be attributed to the quiet acoustic conditions afforded by its unique bathymetry. The TOTO is free of major shipping traffic and is protected from severe sea-state conditions (Figure 1.6).

The acoustic range is composed of an array of 91 widely-spaced (~4 km), bottom-mounted hydrophones designed to track sub-surface vehicles over an area of approximately 1200 km^2. The hydrophones are cabled to shore and monitored by a signal processor. The hydrophone array (Figure 1.7) is configured in offset rows that allow the formation of hexagonal sub-arrays (Figure 1.8). This array geometry provides favourable precision for determing the location in three dimensions of sub-surface vehicles within the array (Vincent, 2001). The array spacing is determined by a number of factors including the sensor depth, maximum target depth, source level, source beam pattern, and typical sound velocity profile. This layout is designed to optimize tracking of undersea vehicles.

Figure 1.6 AUTEC Range (white outline) with the path of Navy ships before the 2000 Bahamas stranding event. Beaked whale stranding locations are indicated by dots whose size (max=3, min=1) is proportional to the number of stranded animals (Cuvier's: red; Blainville's: yellow).

Typically, tracked vehicles are equipped with a "pinger" that emits a known signal at a known repetition rate. The array layout assures the detection of a ~37 kHz tracking ping with a source level of approximately 192 dB on at least four hydrophones. Pings are detected and precisely (<100 ms) time-tagged. The vehicle's position can then be determined by solving for the latitude, longitude, depth, and the time-of-emission (Vincent, 2001). *Md*, *Zc*, and *Me* echolocation clicks have on-axis source levels of at least 200 dB (Shaffer et al., 2013) and a centre frequency within

the bandwidth of the hydrophones, allowing the same technology to be used to detect and localize these species (Jarvis et al., 2014).

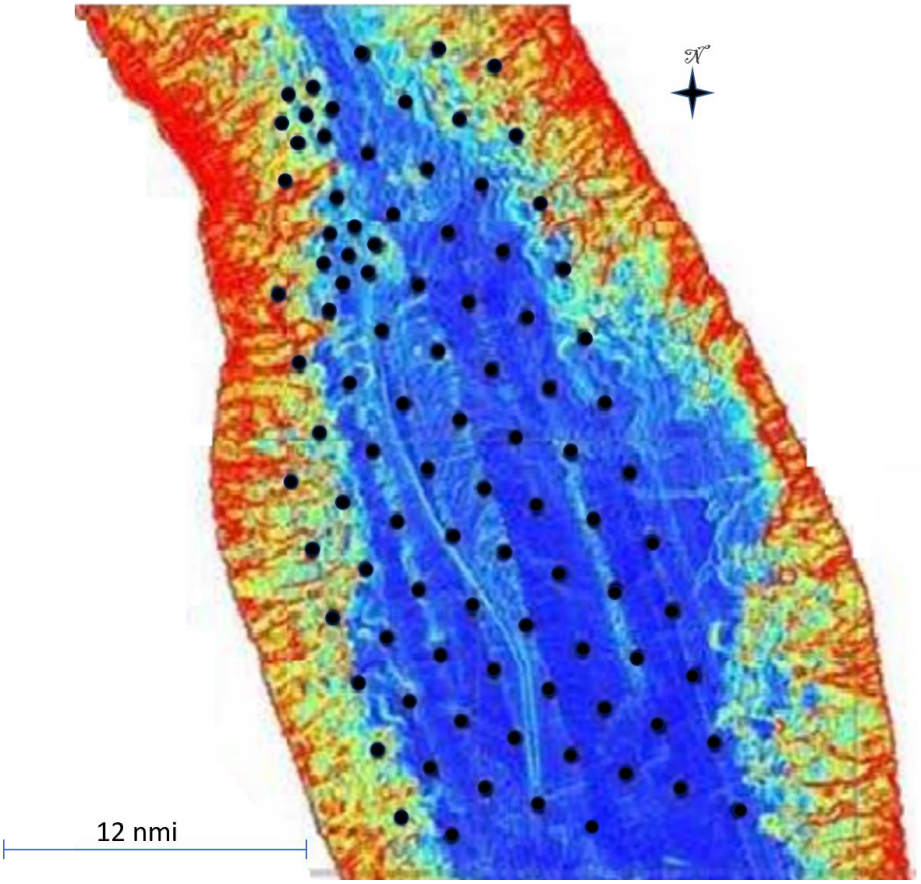

Figure 1.7 Approximate AUTEC hydrophone array (black dots) layout in the TOTO

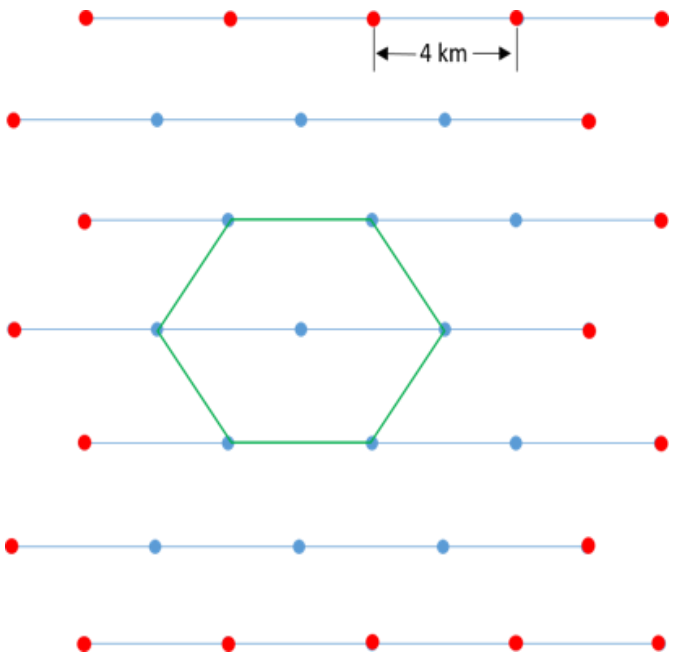

Figure 1.8 Idealized hydrophone array layout with hexagonal sub-array indicated

1.6.2 System Signal Processing Hardware and Software

The tracking signal processor currently used by all U.S. Navy ranges to detect and time-tag pings emitted from range pingers evolved from the signal processor developed as part of the Marine Mammal Monitoring on Navy Ranges (M3R) project (Jarvis et al., 2014). This has allowed integration of marine mammal passive acoustic monitoring into each of the Navy's undersea ranges including AUTEC, SCORE, and PMRF. It is scheduled for installation on USWTR, and the Canadian Nanoose range in 2019.

The processor architecture is based on a simple Linux cluster of commodity computer nodes (Jarvis et al., 2014). A processing node is configured with a set of analog-to-digital boards that digitize the incoming hydrophone signals at a sample rate of 96 kHz. At AUTEC, all 91 hydrophones are simultaneously sampled along with an Inter-Range Instrumentation Group B (IRIG-B) modulated time signal (Martin et al., 1998). Each digitized hydrophone signal is

packetized, time-tagged, and transmitted as a user datagram protocol (UDP) packet and multicast on a dedicated gigabit Ethernet. Down-stream processing nodes, including those that run beaked whale detection, classification, and localization algorithms, read and act on data from selected hydrophones Figure 1.9.

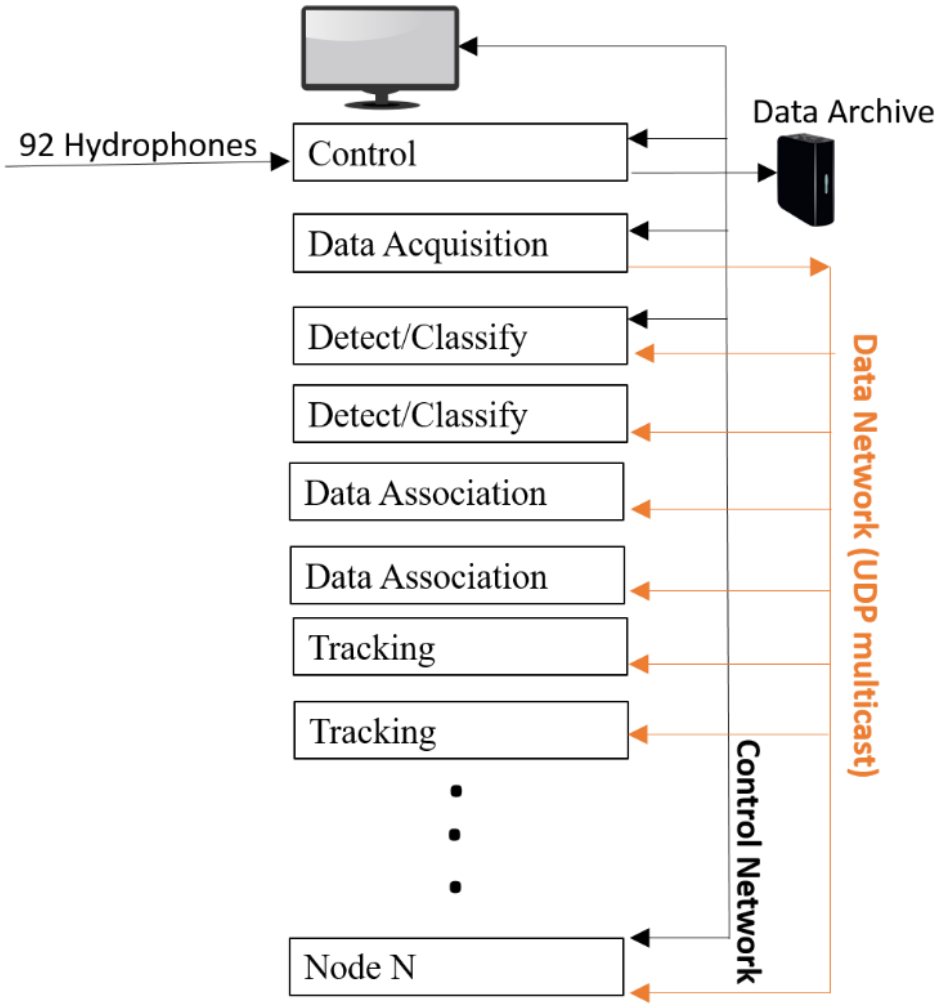

Figure 1.9 System hardware block diagram

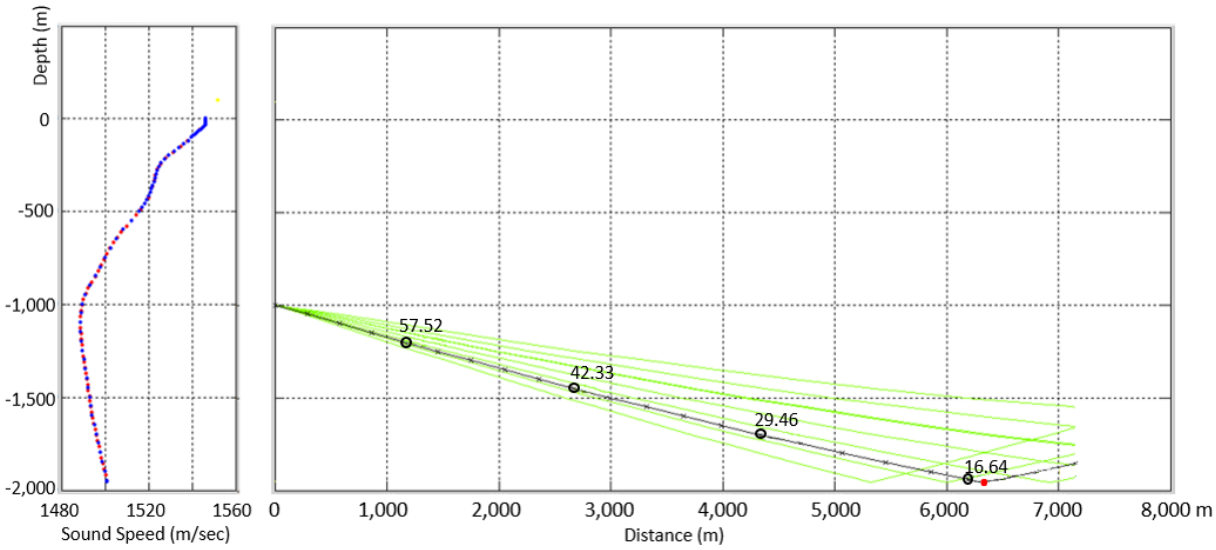

Figure 1.10. The sound velocity profile of a beaked whale click on AUTEC in August (left-hand panel). The blue dots are measured values, the red dots are interpolated values. The right-hand panel shows a ray trace for a 30 kHz source with a 6 degree beam and 200 dB re µPa @1m source level at a depth of 1000m. Signal strength relative to a 75 dB noise background is indicated.

The algorithm used to detect *Md* echolocation clicks is based on a hard-limited, 2048-point Fast Fourier Transform (FFT) with a 50% overlap. This provides a timing resolution of 10 ms. The energy in each bin of the FFT is compared to a noise-variable-threshold which consists of a simple exponential average computed over a 100 ms time period. Individual noise-variable thresholds are computed for each bin of the FFT. If the bin is over the threshold, the bin is set to one. Bins below the threshold are set to zero. For every FFT with at least one bin above the threshold, a detection report is generated. The report contains the hydrophone, time of detection, the bin with the maximum energy, the level in the maximum bin, and a binary mask that marks all bins above and below the individual bin threshold (Jarvis et al., 2014). By combining the hard-limited output of every FFT, a 2-dimensional spectrogram can be displayed for each hydrophone on demand.

The maximum on-axis detection range of a beaked whale on AUTEC using the generic FFT based transient detector has been estimated at 6.5 km (Shaffer et al., 2013). This is substantially greater than the spacing of the hydrophones (~4 km). During a foraging dive, an individual produces several thousand high amplitude echolocation clicks (Johnson et al., 2006b, 2004; Shaffer et al., 2013). Although the beam pattern is narrow (Shaffer et al., 2013; Zimmer et al., 2008), given the source level and the number of clicks produced, a deep diving animal within the array, surrounded by hydrophones, is certain to be detected on at least one sensor.

The detector is run on all range hydrophones. Their detection range is illustrated in Figure 1.10 using the sound velocity profile applied to a simple ray trace model for conditions on AUTEC in August. The animal is assumed to be vocalizing at a depth of 1,000 m with a downward directed echolocation click (6-degree beam width) and a source level of 200 dB. Using a conservative background noise level of 75 dB, the signal to noise ratio was estimated to be 16 dB (1 Hz noise bandwidth) at approximately 6 km.

Figure 1.11 shows a 30-second 2D spectrogram for AUTEC hydrophone 80. Both beaked whale echolocation clicks and MFAS are present. *Md* echolocation clicks appear as lines with energy above 24 kHz at a nearly constant ICI. MFAS sonar is evident in the middle of the display with a mean frequency of approximately 8 kHz. Signals at 8 kHz on the far left and right of the display are likely reverberations from the main sonar ping.

The system architecture is highly adaptable. Since digitized data from each hydrophone are cast as user datagram protocol packets onto a dedicated one-gigabyte data network in a separate time-tagged packet, any “down-stream” processing node can monitor the data stream for hydrophones of interest. To accommodate an increase in processing load, new nodes can be added and simply

connected to the system networks. The current data limit, based on a one-gigabyte network, is approximately 300 hydrophones at a sample rate of 96 kHz (Jarvis et al., 2014). Over time, the system has been expanded to include additional tools for passive acoustic analysis. Both a real-time sonar detector and a class-specific support vector machine (CS-SVM) classifier have been added, along with changes to the localization algorithm that incorporate the CS-SVM detection reports (Jarvis, 2012; Jarvis et al., 2008).

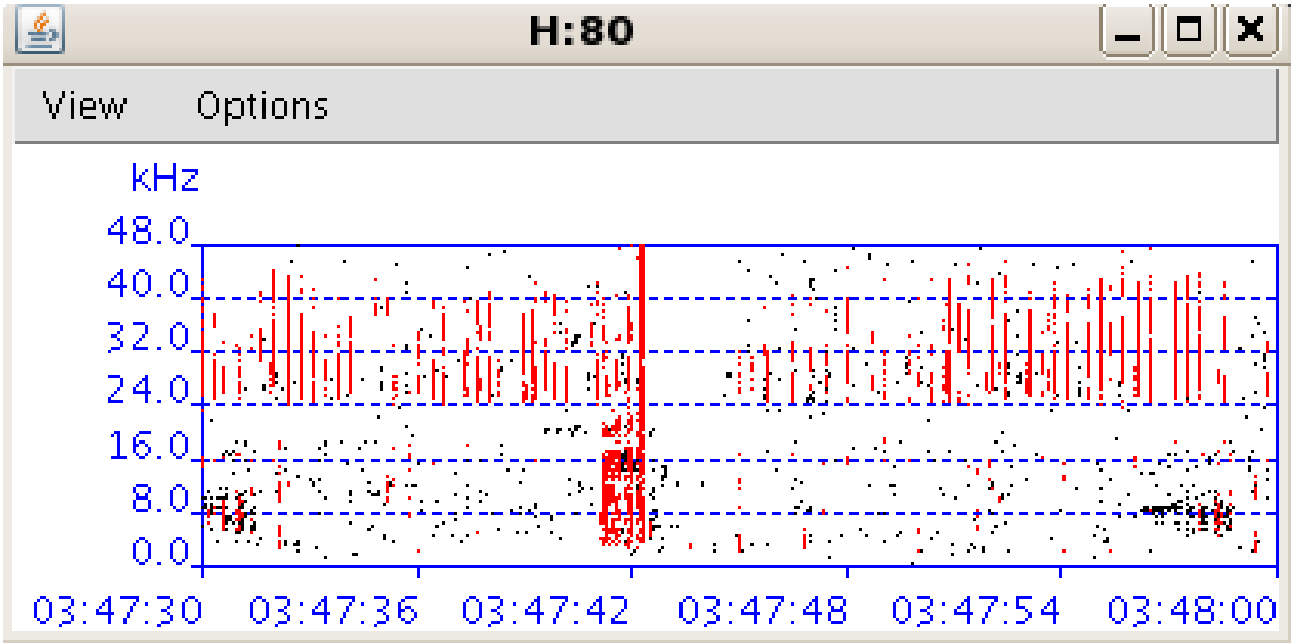

Figure 1.11 M3R 2D spectrogram with Md echolocation clicks (24-45 kHz) and MFAS pings at ~8 kHz

1.7 Passive Acoustic Abundance and Density Estimation

McDonald and Fox (1999) used passive acoustic data from a single hydrophone to estimate the minimum density of fin whales off the Hawaiian island of Oahu, although they acknowledged that the estimate required "multiple assumptions and caveats". Harris (2012) estimated the abundance of fin whales in the north-east Atlantic and blue whales in the northern Indian ocean

using data from sparse seismic arrays. In each case, the received level at the hydrophone was measured and the range to the animal was estimated based on an assumed source level and estimated propagation loss. Marques et al. (2013) provided a review of passive acoustic density estimation methods with a focus on those conducted from fixed, bottom-mounted sensors including examples from AUTEC.

One of the advantages of using data from instrumented Navy ranges is that the high density of hydrophones means that animals vocalizing within the array are highly likely to be detected. Because the structure of *Md* echolocation clicks was known, it was possible to develop appropriate detectors and classifiers at AUTEC (Jarvis, 2012; Jarvis et al., 2014, 2008). From recording tags, the dive rate and rate of click production per dive were determined (Johnson et al., 2006a; Shaffer et al., 2013). Sighting data provided a measure of the number of animals per group (Claridge 2013). These estimates could then be combined with the passive acoustic detection of echolocation clicks to estimate abundance and density (Marques et al. 2013).

Two passive acoustic density estimation methods have been developed for *Md* at AUTEC (Marques et al., 2013). Marques et al. (2009) were the first to apply click counting to obtain an estimate of *Md* abundance. Moretti et al. (2010) built on this study and applied dive starts rather than clicks as the cue that was counted. These methods have also been used for sperm whales (*Physeter macrocephalus*) at AUTEC (Ward et al., 2012), minke whales (*Balaenoptera acutorostrata*) at PMRF (Martin et al., 2013), and harbour porpoises in the Baltic (Kyhn et al., 2012).

As will be discussed, the dive counting method was expanded to support the dynamic monitoring of the *Md* population in the TOTO. The application of the method provides a potential means of

tracking the size of the population on a range of temporal scales (daily, weekly, monthly). Such monitoring is critical in evaluating the effect of anthropogenic activity on the population, including MFAS activity (National Academies of Sciences, Engineering, and Medicine, 2017). While traditional visual line-transect methods are available, the effort required to obtain adequate sample sizes for a cryptic species such as *Md* is substantial and is likely to require multiple years of data and provide estimates with a large level of uncertainty. Given the presence of the hydrophone array, passive acoustic monitoring offers a powerful method of monitoring the population and is a natural choice.

1.8 Thesis Structure

1.8.1 Background

The goal of this thesis is to develop and demonstrate passive acoustic methods to investigate the long-term effect of repeated MFAS exposure on cetaceans with a focus on "sonar sensitive" beaked whales. It is the author's hope that the described methods will be applied to long-term monitoring of beaked whale populations on U.S. Navy undersea ranges, and the information provided used to inform future environmental policy decisions.

The primary focus of previous studies of beaked whales and sonar has been on their acute response (DeRuiter et al., 2013; Tyack et al., 2011). However, beaked whales have been found on all the Navy ranges where MFAS is routinely used (Manzano-Roth et al., 2016; Schorr et al., 2014; Tyack et al., 2011). While no mass strandings have been reported, their presence provides an unprecedented opportunity to study their acoustic behaviour both with and without MFAS present over an extended time period. The *Md* and sonar detection data collected at AUTEC are combined in this thesis, which focuses on the development and application of passive acoustic

methods to measure the effect of long-term MFAS exposure on *Md* at AUTEC. These techniques are also being adapted for monitoring *Zc* at SCORE and *Md* at PMRF.

The body of the thesis is divided into the following major chapters:

Chapter 2. A passive acoustic dive counting method for monitoring Blainville's beaked whale density using a distributed hydrophone array

Chapter 3. Determining the risk of behavioural disturbance caused by military sonar

Chapter 4. A bioenergetics model for Blainville's beaked whales in the Bahamas

Chapter 5. Measuring beaked whale MFAS exposure and evaluating its population level effects using both bioenergetic and expert elicitation methods

Chapter 6. Towards integrated monitoring of the exposure of beaked whales to mid-frequency active sonar (MFAS) and its population consequences

1.8.2 Long-Term Monitoring of Abundance

Chapter 2 presents a method for semi-automated, monitoring of beaked whale density on AUTEC. This extends the method developed by Moretti et al. (2010).

Beaked whales associate in groups that forage synchronously and only vocalize during deep foraging dives. Detections of beaked whale echolocation clicks therefore indicate the presence of a group of animals defined as one or more geographically associated animals that execute a coordinated deep foraging dive (Claridge 2013). These are referred to as Group Vocal Periods (GVPs). Moretti et al. (2010) manually extracted GVPs from the detection data. These were combined with estimates of the number of GVPs per unit time, dive rate, and group size, determined via visual observations and data from recording tags, to produce an estimate of abundance over a one-week period around a multi-ship MFAS operation. Here, the method is

expanded with semi-automated extraction of GVPs and derivation of correction factors for false alarms and false negatives. Two years of data were analysed to illustrate its application.

1.8.3 Behavioural Risk Function

Chapter 3 describes the derivation of an *Md* behavioural risk function, published in Moretti et al. (2014). This function predicts how the probability of foraging dive disruption varies with MFAS received level.

GVP detection can be used as a proxy for foraging behaviour. The tools used to identify GVPs can also be used to detect transient signals such as MFAS. Together with information on operational schedules and ship tracks obtained from AUTEC, they provide a record of when whales were exposed to sonar transmissions along with an estimate of their exposure levels.

GVPs were detected ahead of and during a multi-ship MFAS operation. Data were divided into 30-minute periods, the approximate length of a GVP. The probability of a dive start with no sonar on a range hydrophone was calculated and considered a baseline value. Sonar pings were detected on the hydrophones during the operation and the root mean squared received level on each range hydrophone was estimated using an acoustic propagation model. The probability of a dive start as a function of RL was estimated and compared to the baseline probability to produce a parametric risk function that presents the probability of foraging dive disruption as a function of sonar RL.

1.8.4 A Bioenergetics Model for *Md*

Chapter 4 documents the development and application of a beaked whale bioenergetics model. A model developed for long-finned pilot whale (*Globicephala melas*) was adapted for *Md* (Hin et al., in press). The model is used to investigate the effect of changes in resource density has on

the body condition of *Md* females and their calves. *Md* adult females are followed through their life histories from weaning to death. The population growth rate, reproductive success, age at sexual maturity, the proportion of females that calve, and the ratio of calves to adult female ratio are reported. Case histories for three females and their calves at three levels of resource density are presented to illustrate the effect of changes in energy intake on individual female life histories with a focus on the calving cycle.

1.8.5 Predicting the Effect of MFAS Disruption via a Bioenergetics Model and Expert Elicitation

MFAS disruption on the AUTEC range was measured using passive acoustic methods for data collected in 2012. More than seven months of data combined with AUTEC operational logs were used to identify days during the year when MFAS operations occurred. For those days with passive acoustic data, the start and stop time of the event was precisely measured based on the detection of MFAS pings. The time before the MFAS event was compared to the time during as a measure of dive disruption. The results were used to estimate the probability of behavioural disruption on each day with MFAS and its subsequent effect on energy intake for each of 1,000 female from weaning to death. The bioenergetics model was then used to investigate the effect of measured MFAS behavioural disruption on the AUTEC *Md* population.

Booth et al. (2015) used expert elicitation to investigate the potential effect of repeated MFAS exposure on *Md* at AUTEC. The experts were asked to predict the effect of behavioural disruption on calf survival and the probability of giving birth. Chapter 5 compares the expert elicitation results with predictions from the bioenergetics model using the same assumptions as the experts.

1.8.6 Summary of Results and Future Studies

Chapter 6 presents a summary of results along with a review of the research required to apply the passive acoustic methods described herein. It provides a power analysis to determine the level of both visual and passive acoustic monitoring required to detect changes in abundance at AUTEC. This analysis is used to provide recommendations for a monitoring plan that could be used on all the Navy's undersea ranges, especially AUTEC, SCORE, and PMRF were there are documented beaked whale populations (Claridge, 2013; Falcone et al., 2009; Manzano-Roth et al., 2016). The methods are particularly suited for detecting trends of abundance. However, to truly understand the effect of repeated disruption, a better understanding of the population is required. This includes the population's range and demographics, the movement of individuals, feeding behaviour during disruption, life histories, and temporal and spatial prey distribution. Thus, the recommendations include coordinated passive acoustic monitoring and a continuation of both tag and observational studies.

Clearly, the research described here required the integration of data from passive acoustics, recording tags, satellite tags, visual observations, and biological sampling. If these methods are to be further refined and expanded to other species and sites, it is vitally important to understand the steps required to develop methods described in this thesis.

Chapter 2

A Passive Acoustic Dive Counting Method for Monitoring Blainville's Beaked Whale Abundance Using a Distributed Hydrophone Array

2.1 Introduction

The focus of this thesis is the development of passive acoustic methods to evaluate the potential effect of repeated exposure of beaked whale populations to MFAS using Atlantic Undersea Test and Evaluation Centre (AUTEC) data as a test case. To understand these effects, one of the first steps is to determine whether there are any trends in abundance. Traditionally, visual methods such as line transect surveys (Jewell et al., 2012) and capture-recapture of photo-identified individuals (Barlow et al., 2011; Gormley et al., 2005) have been used to estimate marine mammal abundance. However, such methods can be challenging for deep diving species including beaked whales, since observation of these species at the surface is difficult (Kaschner et al., 2012). For example, Barlow (1999) estimated that the probability of detecting *Mesoplodon* spp. on the track line during a line transect survey was only 0.23 (CV=0.35). Claridge (2013) needed to pool data across six years to obtain sufficient sightings to derive an estimate of beaked whale abundance at AUTEC in the Bahamas. Passive acoustic methods provide an alternative approach for estimating density and abundance (Marques et al., 2013).

In this Chapter, methods that could potentially be used to monitor beaked whale abundance on AUTEC are reviewed. A semi-automated version of the dive-counting method developed by Moretti et al. (2010) is then used to estimate changes in the density of Blainville's beaked whales (*Mesoplodon densirostris*, henceforth *Md*) over a two-year period to demonstrate its potential for monitoring. This method was developed in parallel with the development of the Marine

Mammal Monitoring on Naval Ranges (M3R) program; a multi-year, multi-faceted research effort that used data collected opportunistically from the extensive U.S. Navy hydrophone array at AUTEC.

2.1.1 Passive Acoustic Density Estimation of Beaked Whales

Passive acoustic methods have been used for decades to provide indices of abundance for terrestrial animals, in particular, forest birds (Ralph and Scott, 1981). When appropriate additional information is collected beyond just a count, for example distances to detected birds, it is possible to estimate absolute density and abundance (Buckland, 2006). Equivalent methods, reviewed by Marques et al. (2013), have been developed to estimate cetacean density and abundance. However, their application to beaked whales presents challenges which are described in this section.

2.1.1.1 Counting Clicks and Other Cues

As the name implies, click counting, which was developed by Marques et al. (2009, 2013), uses the detection and counting of echolocation clicks in a point transect framework to estimate whale density (*D*) from Equation 2.1.

$$\widehat{D} = \frac{n(1-\hat{c})}{K\pi w^2 \hat{P} T \hat{r}_c} \qquad \text{Equation 2.1}$$

where

n = total number of echolocation clicks detected in time period *T,*

c = proportion of false positives,

K = number of sensors,

w = maximum detection range of sensors,

P = average click detection probability within range w, and

r_c = click production rate.

Click detection probability, the proportion of false positives and detection range are likely site-specific parameters (Marques et al., 2009). The detection range is dependent on the signal to noise ratio at the receiver that is a function of multiple parameters including the average source level, beam pattern, and orientation (Ainslie, 2010). It is also influenced by the local bathymetry and sound velocity profile, and the noise background (Urick, 1996). The probability of detection and the proportion of false positives are heavily influenced by the local soundscape, especially interference from other sound producing organisms, such as small odontocetes.

Marques et al (2009) used data from recording tags attached to five *Md* on AUTEC that performed a total of 21 foraging dives to estimate some of these parameters. The tags provided an estimate of the number of clicks produced during a single animal per foraging dive, along with the mean number of dives per day. Detection range and click detection probability were determined by calculating the position of each tagged animal at the time each click was emitted. This was accomplished by first producing a "pseudo-track" of the tagged animal using dead reckoning based on the accelerometer, heading and depth data recorded on the tag. The tags also provided a precise, relative time-record of the echolocation clicks produced by each animal. These records were compared with the clicks detected on surrounding hydrophones. The interval between clicks recorded on the tag varied slightly with time. It was assumed the resulting pattern was unique and could be used to identify a particular click train when it was detected on a hydrophone. This approach was used to correlate click trains produced by a tagged animal with click trains detected on surrounding hydrophones, and to calculate the time difference of arrivals

(TDOAs) between the clicks recorded on the tag and those detected on the hydrophones. The TDOAs were used to estimate precise locations for tagged animals, which in-turn were used to correct the pseudo-track calculated via dead reckoning (Shaffer et al., 2013). In its simplest form the click detection probability can be estimated by comparing the number of clicks emitted by the animal to the corresponding clicks detected on the surrounding hydrophones and detection range can be estimated by comparing the distance of the animal at the time of emission to the receiving hydrophone for each detected click associate with the animal. However, the probability of detection is dependent on the animal's orientation to the hydrophone as well as its distance. This is a particular problem for *Md* because the half-power beam width of their clicks has been estimated at less than 10 degrees (Shaffer et al. 2013; Zimmer et al. 2005). To estimate the probability of detection, a binary regression was used which treated each click emitted from the tagged animals as a trial for each nearby hydrophone, with a success being that the click was detected on that hydrophone and a failure that it was not. The binary regression yielded a detection function, and this in turn, was used to estimate the average detection probability for whales within the maximum detection range of a sensor (see Marques et al. 2009 for details).

In order to estimate the proportion of false positives, random one-hour periods were selected from the detection archives. Two-dimensional spectrograms were examined to determine the number of beaked whale clicks within this period. These manually-extracted results were then compared to the clicks detected using the M3R click detection algorithm (Jarvis et al., 2014).

Marques et al. (2009) calculated a CV of 19.6% for their estimates of *Md* density on AUTEC using equations 2.2 and 2.3, which are based on the delta method (Powell, 2007).

$$var(\widehat{D}) \approx \widehat{D}^2\sqrt{CV(\hat{n}^2) + CV(\hat{r}^2) + CV(\hat{c}^2) + CV(\widehat{P}^2)} \qquad \text{Equation 2.2}$$

where

$$CV(\hat{x}) = SE(\hat{x})/\hat{x} \qquad \text{Equation 2.3}$$

Marques et al. (2011) extended their approach to other calls rather than clicks using acoustic data from three bottom-mounted recording buoys in the Bering Sea to estimate the abundance of North Pacific right whales (*Eubalaena japonica*). The detection probability was estimated from the observed distances to detected calls. Detection distances were estimated for a bandlimited right whale upsweep using a propagation model based on mode propagation (six modes) in a shallow waveguide as described by Wiggens et al. (2004). The cue production rate was obtained from contemporaneous recordings and visual sightings from ship-based surveys.

Küsel et al. (2011) investigated the extension of click counting to a single hydrophone in the AUTEC array to estimate *Md* density. The mean detection probability was estimated by making assumptions about the distribution of source level, using a propagation model and a characterization of detector performance within a Monte Carlo framework. Six days of data were analysed and resulted in an estimate that was higher to those reported by Marques et al. (2009) using all AUTEC hydrophones.

Harris (2012) used bottom-mounted seismometers to detect blue whales (*Balaenoptera musculus*) calls in the Indian Ocean and fin whale (*Balaenoptera physalus*) calls in the northeast Atlantic. Similar to Marques et al. (2009), these were used as cues to estimate call densities. Call source levels were estimated based on the literature and the detection ranges to the calling animals calculated using a propagation model. The actual animal density could not be estimated as no estimates of call rate were available.

2.1.1.2. Dive Counting

Observational (Claridge, 2013) and tag data (Tyack et al., 2006) have shown that *Md* typically associate in groups of 2 to 11 individuals and that these groups dive synchronously and forage at depth (usually below 300m) (Dolan et al., 2019; Shaffer et al., 2015). Loud (>200 dB on-axis) echolocation clicks (Shaffer et al., 2013) are only produced during these deep foraging dives (Johnson et al., 2006b, 2004). Moretti et al. (2010) developed a dive counting method for estimating local abundance and density of beaked whale based on the detection of the start of the vocalizations produced by a group of *Md* during these foraging dives rather than individual clicks, where a "group" is defined as one or more animals. The period during which an animal produce echolocation clicks during deep, foraging dives is termed a group vocal period (GVP). At AUTEC, GVPs last approximately 30 min (Moretti et al., 2010). The detection of sustained echolocation clicks on multiple hydrophones is, therefore, a strong indicator of a GVP.

The density of animals within the hydrophone field can be estimated using Equation 2.4:

$$\widehat{D} = \frac{n_d \hat{s}(1-\hat{c})}{\hat{r}_d T \hat{P} A} \qquad \text{Equation 2.4}$$

where

n_d = total number of GVP starts detected in time period T,
s = mean group size,
r_d = dive rate (number of GVP starts/unit time),
c = proportion of false positives,
P = probability of detecting a GVP within the hydrophone field, and
A = coverage area of the hydrophone array.

The mean group size for animals in the Bahamas was estimated to be 4.1 animals (CV= 46%) from visual observations (Claridge 2006). It is assumed that group size as estimated from visual

observations is an accurate estimate of the size of a group detected acoustically. From the visual observations and more recent passive acoustic tracking of animals on the AUTEC hydrophones (Dolan et al., 2019; Shaffer et al., 2015), group associated animals have been documented diving together (Claridge, 2013). During tests at AUTEC echolocation clicks have been repeatedly detected on the hydrophones surrounding on-water observers after they have reported a group's coordinate dive start. All 21 recorded foraging dives at AUTEC recorded on tags were detected on the surrounding hydrophones (Shaffer et al., 2013).

The rate at which *Md* undertake deep foraging dives was estimated from these recording tag data. Moretti et al. (2010) estimated that *Md* on AUTEC undertake 0.36 dives/hour (CV=10.6%). Moretti et al. (2010) assumed $P = 1$, and $c = 0$ (i.e. all GVP starts were detected and there were no false positives) because two-dimensional spectrograms associated with each dive record were always inspected by an analyst to ensure they were *Md* vocalizations (Figure 2.1).

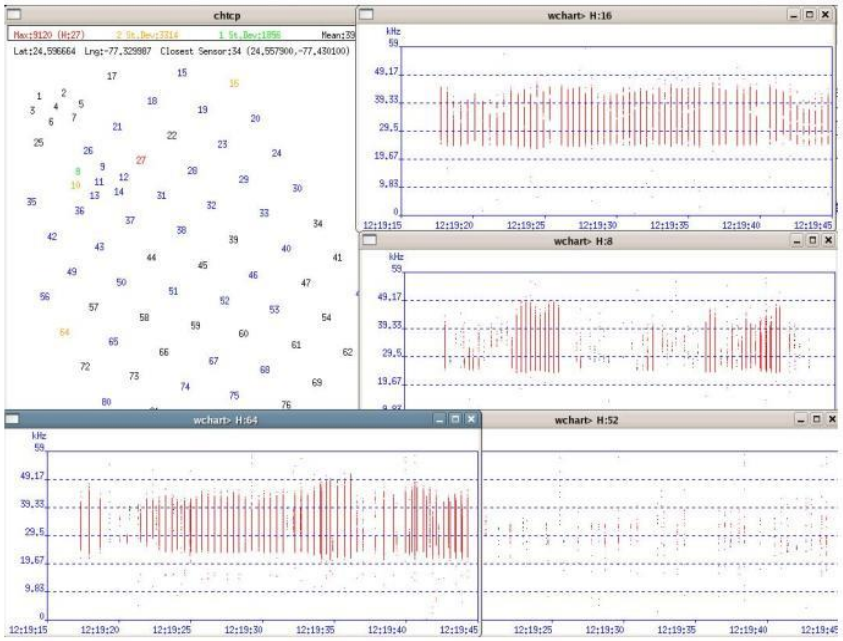

Figure 2.1 Range display (upper-left), i.e. map showing hydrophone locations and numbers, with the level of hydrophone activity indicated by colour. The other panels show two-dimensional spectrograms for selected hydrophones with *Md* click trains in red.

The maximum on-axis source level of *Md* vocalisations is approximately 210 dB (Shaffer et al., 2013; Zimmer et al., 2005); and animals typically produce more than 4,000 clicks per foraging dive (Shaffer et al., 2013; Zimmer et al., 2005). Given the hydrophone spacing on AUTEC (approximately 4 km), it is reasonable to assume a high proportion of the emitted clicks in the hydrophone field will be detected and identified on more than one hydrophone. However, the number of hydrophones on which echolocation clicks are detected strongly depends on the orientation of the animal relative to the hydrophones. For groups outside the hydrophone array but moving towards it, there is a high probability that a hydrophone will come within the main axis of an animal's narrow beam. For groups moving away from the array, the main beam axis will be pointing away from the hydrophones, making detection of echolocation clicks less likely. It is assumed that all groups within the hydrophone array are counted while those outside the array are discarded. To reduce bias, only groups detected on at least one hydrophone inside the array were considered; groups that were only detected on edge hydrophones were also discarded from the analysis.

Detection and classification algorithms vary widely (Yack et al., 2010). For example, the M3R system supports three algorithms that are based on a support vector machine (Jarvis, 2012), a Fast Fourier Transform, and a linear matched filter (Jarvis et al., 2014). Detecting GVPs is less dependent on the click detection-classification algorithm and associated detection statistics than simply detecting clicks. In a Gaussian noise background, click counting is clearly straight-forward. However, in real-world environments, especially those with many, potential time-varying, interfering sounds, click counting can be challenging. For instance, the presence of large groups of other odontocete species will increase the proportion of false positives, resulting in temporal and spatial variation in the value of this parameter. As discussed in Chapter 1, *Md*

produce sustained clicks trains with a distinctive mean inter-click interval (ICI) (Johnson et al. 2006; Madsen et al. 2005). These characteristics can be used to distinguish *Md* GVPs from other interfering species, making the dive counting approach more tolerant of challenging acoustic environments. This is especially important in environments where Risso's dolphins (*Grampus griseus*) occur because this species can produce click trains that mimic beaked whale calls (Madsen, Kerrc, and Payne 2004). There is more variability in a Risso's dolphin ICI, which typically results in the misclassification of short (<5 s) click trains. However, these can be rejected based on click-train length.

The identification of individual GVPs can be challenging if several groups are diving simultaneously in close proximity. The method described by Moretti et al. (2010) required labour intensive manual extraction of dives from *Md* detection archives. Decisions as to what constituted a GVP and its start were dependent on direct inspection by an analyst and therefore subject to individual biases. The Methods section describes an extension of the dive counting method to semi-automate this process so that it can be used to analyse data collected over multiple years. However, the extended semi-automated methods must account for false negative and false positive detections.

To date, the original method described by Moretti et al. (2010) has been applied to *Md* at AUTEC and on the hydrophone array on the Pacific Missile Range Facility (PMRF) off Kauai, HI (Manzano-Roth et al.; 2016). The latter authors used the method to investigate change in *Md* abundance around multi-ship sonar operations. On-going studies at AUTEC, the Southern California Range, and PMRF have begun applying the method described in this Chapter.

2.1.1.3 Other Passive Acoustic Methods

Ward et al. (2012), analysed 42 days of AUTEC hydrophone data for the presence of sperm whale (*Physeter macrocephalus*) echolocation clicks. Because of the loud click source level and broad beam pattern (Møhl et al., 2000), it was assumed a sperm whale within the field of hydrophones would be detected. Clicks were associated into trains and assigned to an individual using methods developed by Baggenstoss (2011a, 2011b, 2008). Data from tags were used to estimate the proportion of time animals spend clicking. Fifty 10-minute samples were taken over a six-week period and the number of vocalizing individuals in each period counted. The number of animals counted over all periods was adjusted by the "tag-derived" proportion of time animals spend vocalizing to estimate the abundance.

Kyhn et al. (2012) used data from logging devices for estimating harbour porpoise (*Phocoena phocoena*) density in the Baltic. Effective detection ranges of 22 to 104 m, depending on the device used, were estimated by matching visual and acoustic detections. A snap-shot method was applied in which the detection of clicks was used to mark the presence or absence of animals. This method was also used as part of the Static Acoustic Monitoring of the Baltic Sea Harbor Porpoise project, in which acoustic data were collected for two years on 304 data loggers (Koblitz et al., 2014). Harbour porpoise population density was measured for the entire area during the winter, and in the summer season for the northeast and southwest areas.

Mellinger et al. (2014) estimated the density of calling fin whales (*Balaenoptera physalus*) by measuring the total energy in the 15 to 25 Hz band that encompasses the frequency range of the low frequency down-swept calls typically produced by the animals. The method was applied to an array of 24 seismometers off the coast of Portugal. It assumes that the total energy in the band is proportionate to the number of calling animals within a calculated hearing radius. An

estimated source level of 179dB re μPa_{p-p} @ 1m was used (Charif et al., 2002; Payne and Webb, 1971). Calls were modelled as 0.270 s equal amplitude signals at a pulse period of 22.6 s (Watkins et al., 1987). A Monte Carlo model using the Range Dependent Acoustic Model (RAM) (Collins, 1993a, 1993b, 1992, 1989) was constructed to predicted the in-band energy at each hydrophone as a function of the number of surrounding animals. A density map for the sensor field was produced.

2.1.2 Visual Estimation of Beaked Whale Density

As noted above, estimating beaked whale density and abundance using visual sightings is challenging because the animals spend little time at the surface, are hard to detect and the observers' ability to spot animals is highly dependent on sea-state. For example, Whitehead (2013) fit 23 years of data on sightings of beaked whales on the Scotian Shelf off the east coast of Canada to a Poisson model to estimate an annual rate of increase of 23% in Sowerby's beaked whale (*Mesoplodon bidens*) abundance. Over the entire period, 115 sightings were obtained. At his main study site, the sightings rate was one animal for every 37 hours of observation. These data could only be collected during summer months because adverse sea-state conditions obviated data collection from the small vessel that was used outside this period. They suggested the observed increase could have been due to a reduction in acoustic disturbance, in particular the reduction in ground fisheries due to a moratorium implemented in 1993, a total moratorium on fishing in 2004, and the declaration of the Gully as an "pilot" Marine Protected Area in 1998 and a fully protected area in 2004.

Barlow et al. (2005) reviewed the use of visual line transect survey methods for estimating beaked whale density and, as noted above, estimated that the probability of sighting a beaked whale on the track-line was only 0.23, a low value for a cetacean species. For surveys conducted

off the coast of California by a team of three observers, the sighting rate in Beaufort sea state 0/1 was ~10 animals per 1,000 km of survey distance; this rate dropped to ~10 per 1500 km of survey distance in sea state 4 (Barlow and Gisiner, 2006).

Moore and Barlow (2013) fitted a Bayesian hidden-process model to sightings of beaked whales on the U.S. west coast to estimate population trends. They concluded that there had been an overall population decline and suggested that passive acoustic methods, based on data from the hydrophone array on the Southern California Anti-Submarine Warfare Range, could be used to test their conclusions.

Both Whitehead et al. (1997) and Gowans et al. (2000) used capture-recapture techniques to estimate the abundance of bottlenose whales (*Hyperoodon ampullatus*) on the Scotian Shelf using photo identification. A total of 1701 hours of effort from 1988 to 1999 yielded 851 sightings, or one sighting every 2 h. However, Gowans et al. (2000) estimated that only 29% of animals were reliably marked. This led to an estimate of 223 (95% CI: 166-308) individuals from right photographs and 242 (95% CI: 172-361) from left side photographs. Claridge (2013) used Bayesian capture-recapture methods to estimate the abundance of *Md* using photographs collected on AUTEC and at a similar sized site off the southern tip of Abaco, 150 km to the north. A total of 235 vessel surveys at Abaco resulted in the identification of 73 unique individuals. At AUTEC unique 34 individuals were identified during 102 surveys. The median estimate of abundance at AUTEC was 42 whales (75% highest posterior density interval (HPDI) = 32-55) and at Abaco it was 80 whales (75% HPDI = 63-99). At both sites, a large amount of field time, conducted over multiple years, was required to obtain these estimates. This methodology is unlikely to detect a population decline on the time scale necessary to inform management decisions on AUTEC.

2.1.3 A Comparison of AUTEC Passive Acoustic Density Estimates

The multiple studies at AUTEC provide the opportunity to compare the results from different beaked whale estimation methods. Data from the Marques et al. (2009) click-counting study produced an estimated density of 25.3 (95% CI 17.3–36.9) or 22.5 (95% CI 15.4–32.9) animals/1,000 km^2, depending on assumptions about false positive detections. Küsel et al. (2011) focused on the same data but from a single hydrophone and produced a density estimate of 69.60 animals/1,000 km^2(95% CI 50.86–95.25). For the single hydrophone analysis, data from the literature were used to inform the model whereas Marques et al. (2009) used data from tagged animals at AUTEC. This resulted in a cue rate (0.649 clicks/s) that was 1.595 higher than the rate measured locally, though the AUTEC tag derived probability of detection (0.032) was 2.30 times higher. However, Marques et al. (2009) analysed data from 82 AUTEC hydrophones rather than a single hydrophone. This comparison highlights two significant factors. First, cue rates and critical parameters derived from alternate sites may not match those measured on site. Second, local variation may lead to significant differences when compared to a larger area. Both spatial and temporal variation must be considered.

The results from click and dive counting can also be compared. Moretti et al. (2010) used dive counting to estimate a density with no disturbance of 16.99 animals/1,000 km^2 (95% CI 13.47–21.43) during a 65 hour period in May 2008. Marques et al. (2009) used click counting to estimate a density of 19.23 animals/1,000 km^2 (95% CI 12.69–29.13). Both methods depend on cue rates (dives or clicks) and similar multipliers to account for estimation error. For this exercise, dive starts were verified by an analyst and it was assumed that any dive within the hydrophone field would be detected. Therefore, the only multipliers were for group size and dive rate. This led to a CV of 11.89%. By comparison, click counting required multipliers for the probability of detection, the false

positive rate, and the click production rate, with their associated uncertainties. This led to an overall CV of 21.43%. Determining which method is preferred will depend heavily on the site and on data available. As illustrated by Küsel et al. (2011), applying data from the literature derived from different sites can lead to significant error. While the AUTEC click and dive counting examples used locally derived visual and tag data, obtaining such data is time consuming and costly.

The preferred density estimation method will depend heavily on-site conditions. The probability of detection and false positive rate are both a function of the acoustic environment. For instance, AUTEC has a relatively low density of all cetacean species, as compared to SCORE, where many odontocete species are in abundance and whose clicks can lead to a significantly higher false positive rate and lower the overall probability of detection. For dive counting at AUTEC data were manually verified, but such analysis is costly and quickly becomes impractical if the time over which data are collected and analysed is expanded. This chapter describes a method to semi-automate the dive counting process, but the uncertainty in the estimate does increase. Also, cue stability over time must be considered. For click counting it is assumed that the cue rate as well as the multipliers remain constant over time. However, changes in both beaked whale behaviour and the surrounding soundscape may affect this. When choosing an appropriate method, it is therefore important to consider the site-specific temporal and spatial uncertainty in these estimates. This is especially true when applying these estimation methods to a Navy range where the soundscape is influenced by sonar operations, as has been illustrated by a number of studies (Falcone et al., 2017; Manzano-Roth et al., 2016; McCarthy et al., 2011; Moretti et al., 2010, 2014). Thus, any passive acoustic method that is chosen should include a measure of MFAS activity.

2.2 Methods

The dive counting method described in Moretti et al. (2010) was extended to allow multiple years of data to be analysed. Abundance was estimated over time scales of a year, a month, and a day. Because it was impractical to detect GVPs manually on all these time scales, software tools to identify GVPs using click detections were developed as part of the M3R program. For this analysis, click detection reports from an FFT-based detector were used (Jarvis et al., 2014). Potential *Md* click detections were then analysed using a click train processor (Section 2.5.1) which combined sequences of clicks recorded on individual hydrophones into click trains. A collection of temporally and spatially bounded click trains could represent one or more groups of foraging animals echolocating on prey during a deep foraging dive. Collectively, an attempt is made to take all detected *Md* clicks and associate them into click trains for each hydrophone. These click trains were then associated using an "auto-grouper" program (Section 2.5.2) into GVPs using a set of heuristic rules based on detection ranges between trains and their start and stop time, where each GVP represents a group of foraging animals associated together over the vocal part of a synchronous dive.

Within the hydrophone array, the hydrophone with the greatest number of clicks was designated as the centre hydrophone. All click trains detected within the maximum measured detection range of 6.5 km (Shaffer et al., 2013) of this hydrophone were associated as a GVP. The time of detection of the first click in the initial click train was designated as the GVP start for that hydrophone. The stop time of the GVP was assigned when no click had been detected for three minutes (Tyack et al., 2011). The GVP start and stop times, and the number of clicks detected were then determined for all the hydrophones on which this GVP was detected. The duration of the GVP was calculated as the difference between the earliest recorded start time and last

recorded stop time. The total number of clicks recorded on all hydrophones was then calculated. The inter-click interval (ICI) for each hydrophone was calculated as the total GVP duration for that hydrophone divided by the total number of detected clicks.

The raw GVP data were then filtered to reduce false positives by examining the number of hydrophones on which the GVP was recorded. Given the maximum detection range of 6.5 km (Shaffer et al., 2013), an *Md* group whose individual members are separated by 1 km (Shaffer et al., 2015) and is at the centre of the array could, at most, ensonify the seven nearest hydrophones and the six surrounding hydrophones (Figure 2..2). Therefore, any GVP that was detected on more than 13 hydrophones was eliminated from the record as infeasible.

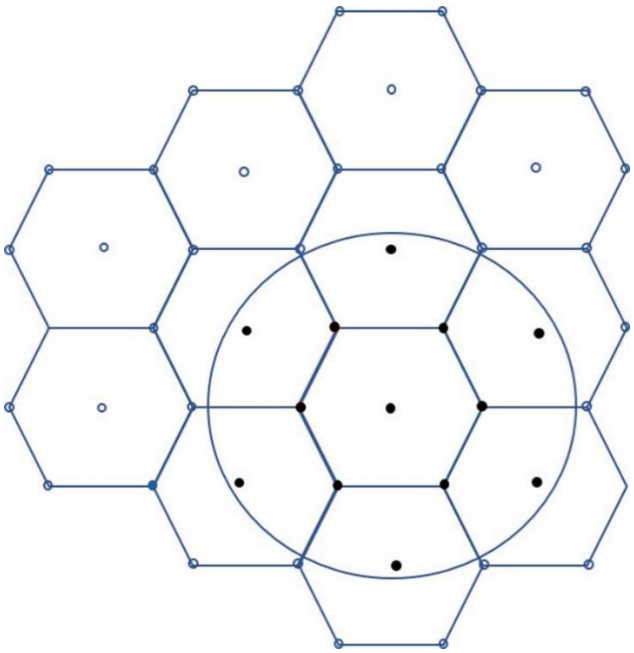

Figure 2.2 Idealized view of a hydrophone array with 4km spacing. The circle represents the extent of an *Md* group with individuals separated by 1 km and a maximum detection radius of 7.5km (6.5km + 1 km) from the group centre to the hydrophones. The black dots represent hydrophones potentially ensonified by the group.

The mean distance between hydrophones (~4 km; Jarvis et al. (2014)) is substantially less than their 6.5 km detection range. Therefore, an *Md* group clicking within the hydrophone array should ensonify at least two hydrophones for some portion of the GVP (Shaffer et al., 2013). GVPs that were only detected on a single hydrophone were eliminated from the record.

Only GVPs that included at least 500 detected clicks summed over all group-associated hydrophones were retained. The threshold was chosen to reduce false alarms from ancillary dolphin species while limiting the number of missed groups based on AUTEC tag data reported by Shaffer et al. (2013) from 13 GVPs recorded from four animals across four different groups. The mean ICI was 0.33 s (95% CI 0.32-0.35). The mean number of click per dive was 5075 clicks (95% CI 4393-5757). The 500 click threshold is less than one tenth the mean number of clicks per GVP produced by a single animal.

The data for all GVPs in a particular year were consolidated into a single data file for analysis. Table 2.1 illustrates the format of this file for four GVP records.

Table 2.1 An example of the consolidated GVP data format.

GVP number	Duration (min)	Total number of clicks	Edge group	Number of Hydrophones	Centre hydrophone ID	Centre hydrophone click count	Maximum ICI (s)	start (Linux days)
2	67.45	13172	0	5	68	4508	0.379	15340.02
3	34.78	1243	0	3	83	820	0.362	15340.03
6	16.23	904	0	2	75	848	0.375	15340.06
7	39.032	3871	0	7	36	1570	0.380	15340.06

Dive counting assumes that at least 501 clicks produced during any GVP that starts within the hydrophone field will be detected on the surrounding hydrophones and identified as part of a GVP. The AUTEC hydrophone array was designed so that a 37 kHz ping with a source level of 192 dB emitted over the array is certain to be detected on at least four hydrophones. All 26 dives

recorded on DTags attached to *Md* during the 2007 and 2008 Behavioural Response Studies (Tyack et al., 2011) were manually detected on AUTEC hydrophones. Therefore, it was assumed that *P* (detection probability) and *c* (proportion of false positives) for the software tools could be estimated from the number of GVPs detected automatically compared to the number detected manually in samples from the archives.

Forty random one-hour samples were extracted from the archives. An independent analyst examined 2-dimensional spectrograms from all hydrophones for the presence of *Md* clicks. Detected clicks were assigned to a GVP and the GVP start and stop times for each hydrophone recorded. These results were compared to the filtered auto-grouper outputs to estimate *P* and *c*. A nonparametric bootstrap, sampling one-hour samples with replacement, (1,000 iterations) was run to estimate variance.

Approximately four months of archive data were available from 2011 and seven months from 2012. Contiguous data blocks, defined as those periods in which there were no gaps greater than 24 h in GVP detections were then identified. In total, five data blocks representing a total of 330 days (Figure 2.3) were used in the analysis.

A yearly and monthly estimate of density was produced. Daily density estimates for January 2012 and the surrounding months were compared to the corresponding monthly estimate to investigate if a lower January estimate was reflected in daily estimates. It should be noted that the estimates use the same values of *c*, *P*, and *s* (i.e., they assume these values are constant).

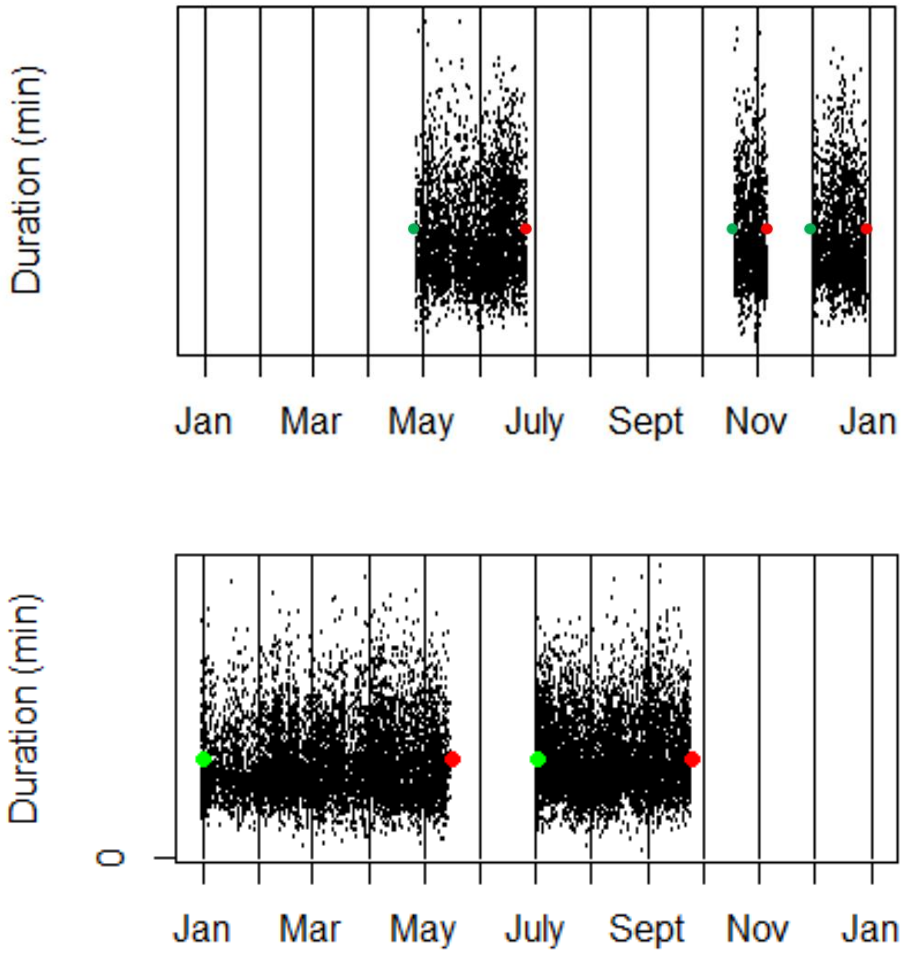

Figure 2.3 Data from the 2011 (upper panel) and 2012 (lower panel) archives presented as time vs. GVP duration. The start of each data block is marked with a green dot and the end by a red dot.

2.3 Results

Of the GVPs identified by the auto-grouper program, 50% were considered to be false positives and removed from the database (Figure 2.4).

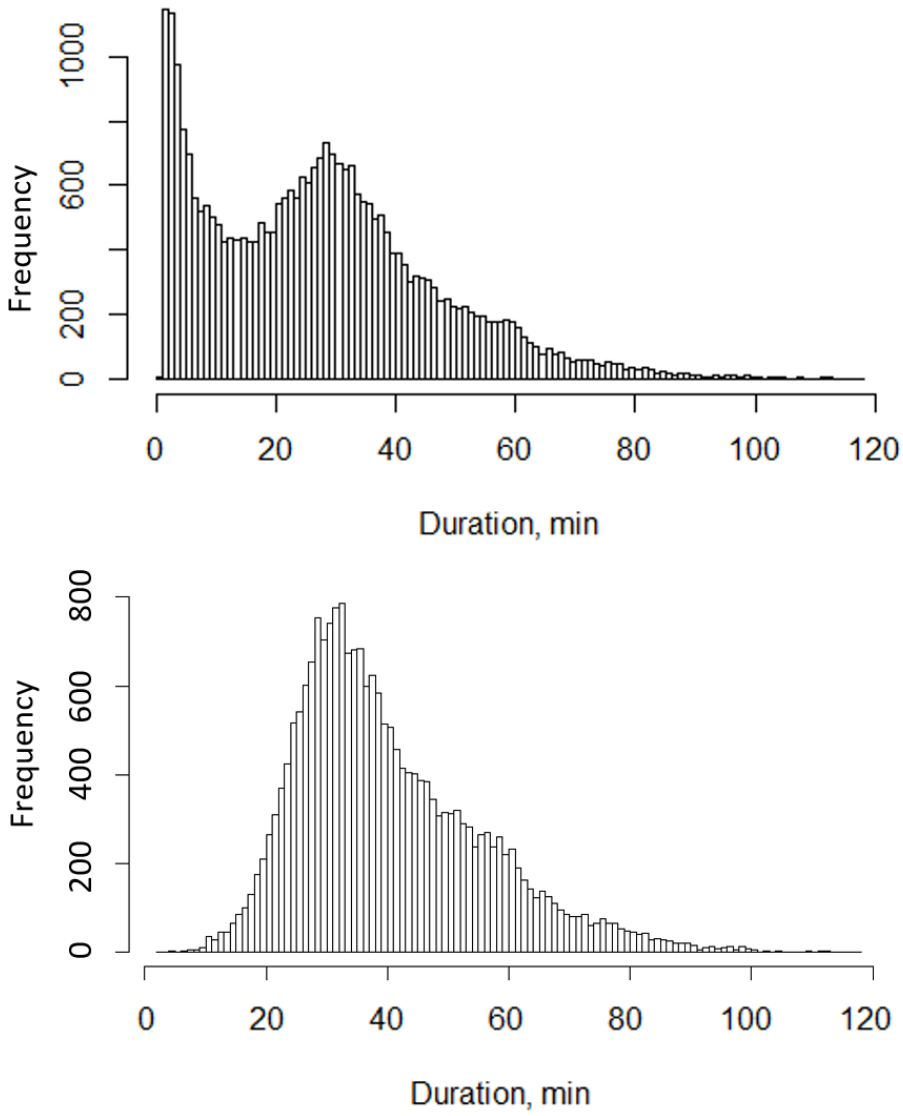

Figure 2.4 Unfiltered histogram of raw auto-grouper GVP durations (upper panel), and the same data with probable false positives removed (lower panel).

Table 2.2 Md detection statistics for 40 one-hour random samples (AUTEC 2011-2012).

Sample #	Total # Manual Dive Starts	Total # Auto Dive Starts	# Exact Matches	# Confused Matches			# Dive Starts Manual Only (FN)	# Dive Starts Auto Only (FP)
				# Manual Dive Starts	# Auto Dive Starts	Confused vs. Auto		
1	6	6	6	0	0	0	0	0
2	1	3	1	0	0	0	0	2
3	6	4	3	2	1	1	2	0
4	5	5	5	0	0	0	0	0
5	4	3	3	0	0	0	1	0
6	6	6	4	1	2	1	1	1
7	6	7	4	1	2	1	1	2
8	8	8	7	0	0	0	1	1
9	2	3	1	1	2	1	0	1
10	8	5	4	3	1	1	3	0
11	5	6	4	0	0	0	1	2
12	10	10	9	0	0	0	1	1
13	5	5	5	0	0	0	0	0
14	7	7	5	1	2	1	1	1
15	4	5	3	1	2	1	0	1
16	7	7	7	0	0	0	0	0
17	6	9	4	2	4	2	0	3
18	5	5	5	0	0	0	0	0
19	0	3	0	0	0	0	0	3
20	5	3	2	0	0	0	3	1
21	2	1	1	0	0	0	1	0
22	9	9	9	0	0	0	0	0
23	8	7	6	2	1	1	1	0
24	5	5	5	0	0	0	0	0
25	7	5	5	0	0	0	2	0
26	7	9	5	2	4	2	0	2
27	6	8	4	2	4	2	0	2
28	5	4	4	0	0	0	1	0
29	7	7	7	0	0	0	0	0
30	5	4	4	0	0	0	1	0
31	1	1	1	0	0	0	0	0
32	5	6	5	0	0	0	0	1
33	6	5	5	0	0	0	1	0
34	5	4	3	0	0	0	2	1
35	7	6	4	1	2	1	2	1
36	8	12	5	2	4	2	1	5
37	8	8	6	1	2	1	1	1
38	4	9	4	0	0	0	0	5
39	4	3	2	0	0	0	2	1
40	7	7	6	0	0	0	1	1
Total	**222**	**230**	**173**	**22**	**33**	**18**	**31**	**39**

Table 2.2 shows the results from the 40 one-hour random sample periods that were examined by an independent analyst. For 78% (173/222) of the GVPs reported, the auto-grouper output exactly matched that of the analyst with no GVP confusion. Cases where there was a mismatch between the analyst's opinion and the auto-grouper output were marked as "confused" and likely represent situations where at least two *Md* GVPs overlapped in time and space so that clicks from more than one group were detected on the same hydrophones.

For "confused" groups the analyst estimate was assumed to be correct. The auto-grouper output was compared to the analyst's and the number of groups correctly predicted by the auto-grouper was calculated (Confused vs. Auto, Table 2.2). Assuming the analyst identified all GVP starts correctly, the *P* was estimated to be 0.86 with CV=2.7%, which represents the exact matches plus "confused" auto-grouper matches, divided by the total number of GVPS identified by the analyst ((173+18)/222); *c* was estimated to be 0.17 (39/230), with a CV=22.3%.

Moretti et al. (2010) used an estimated mean group size of 2.62 animals, based on sightings data collected by D. Claridge through 2010. For the extended data analysis, an updated mean group size of 2.34 animals (n= 73, CV=5.5%) based on data collected from 2005 to 2016 was used (Claridge and Dunn 2017). The coverage area (1200 km^2) presented in Moretti et al. (2010) was used to calculate monthly and daily estimates of density.

Moretti et al. (2010) used the delta method (Equations 2.2 & 2.3) to calculate the CVs of their estimates. For the estimates reported here, the CVs for $\hat{P}$ (0.027) and $\hat{c}$ (0.223) were calculated using a bootstrap of the 40 sampled values with replacement across 1,000 replicates. These were combined with CVs for the dive rate $\hat{r}_d$ (0.055), and group size $\hat{s}$ (0.106), reported in Moretti et

al (2010) (Equation 2.5). This resulted in a CV of 25%, compared with the CV of 11 % reported by Moretti et al. (2010).

$$var(\widehat{D}) \approx \widehat{D}^2 \sqrt{CV(\hat{r}_d^2) + CV(\hat{s}^2) + CV(\hat{c}^2) + CV(\widehat{P}^2)} \qquad \text{Equation 2.5}$$

Figure 2.5 shows the mean estimated density of *Md* on the AUTEC hydrophone array in every month of 2011 and 2012 for which data were available. Figure 2.6 shows daily estimates of density for the period 22 November 2011 to 1 April 2012; the mean density for this period was 29.8 *Md* per 1,000 km^2 (95% CI 26.8-32.7) with a minimum density of 17.4 *Md* per 1,000 km^2 (95% CI 13.0-21.8) and a maximum of 36.6 *Md* per 1,000 km^2 (95% CI 27.4- 45.9).

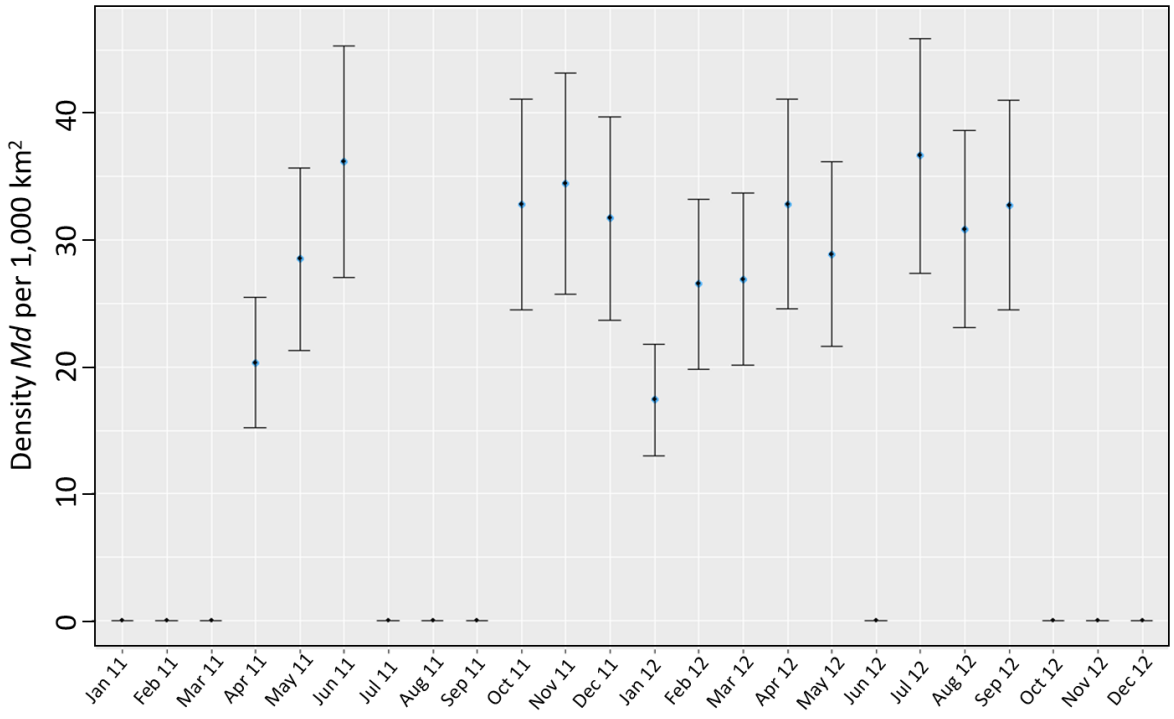

Figure 2.5 Estimated density of *Md*/1,000 km^2 for all months in 2011 and 2012 when detection data were available (blue dots). Months with no archive data are indicated with a small black line at 0. Vertical lines indicate 95% CI on estimates calculated via the Delta method.

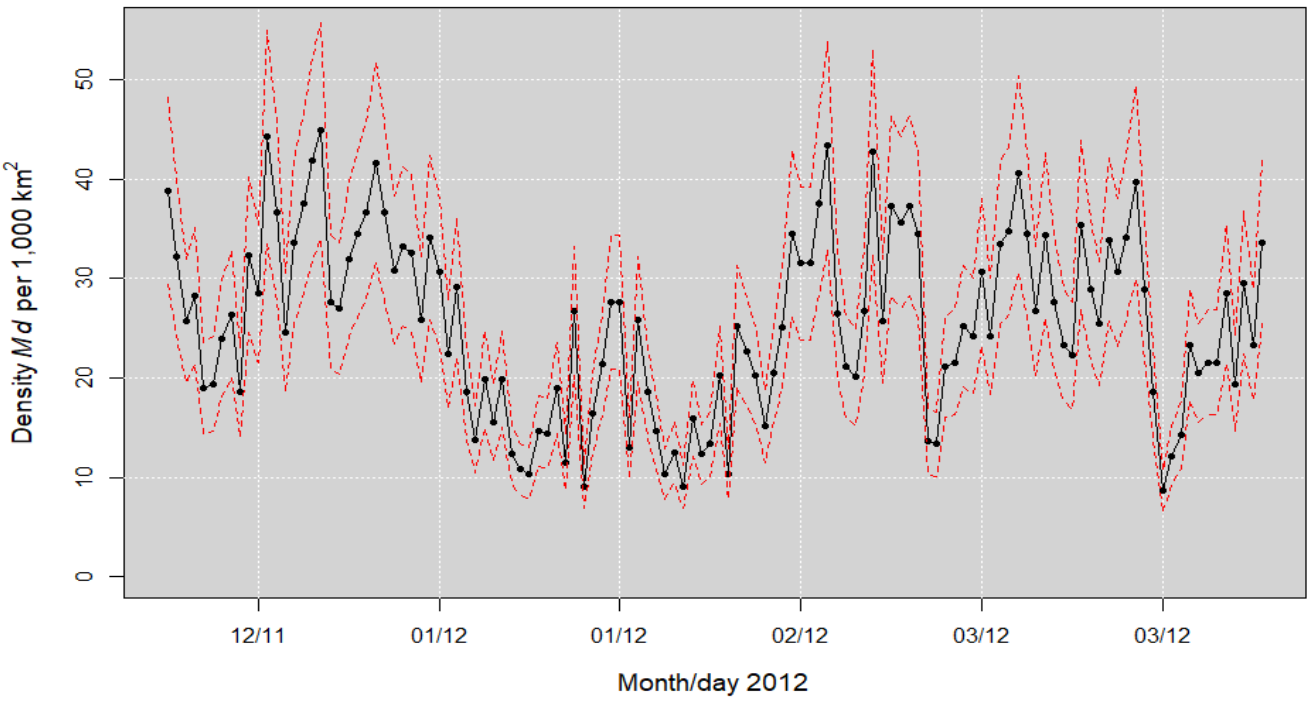

Figure 2.6 Daily estimates of *Md* density per 1,000 km^2 for 22 November 2011 to 1 April 2012. The 95% CIs are shown in red.

Figure 2.6 shows a steady decline in density from approximately 25 December 2011 to 1 January 2012 (95% CI in red). The level remains low throughout the month and begins a steady increase on approximately 5 February 2012. Figure 2.6 suggests the January decline shown in the monthly plot (Figure 2.5) is real and not a measurement error or anomaly. The plot also provides insight into the daily fluctuations in dives detected which presumably are due to *Md* groups moving onto and off the hydrophone array.

2.4 Discussion

Moretti et al. (2010) estimated a density of 17.0 *Md* per 1,000 km^2 (95% CI 13.47-21.43) on AUTEC in the 65 h period before a military operation while applying click counting to the same

data resulted in an estimate of 19.23 *Md* per 1,000 km^2 (95% CI 12.69-29.13) which was higher but comparable. However, the estimates are highly correlated as they use the same click detection data.

Marques et al. (2009), estimated that the density in 2008 was 22.5 or 25.3 *Md* per 1,000 km^2 (95% CIs 15.4-32.9, and 17.3-36.9 respectively), depending on the assumption used for the level of false positives. The mean monthly density derived from 14 months of data collected over a two-year period analysed in this Chapter produced an estimate of 29.8 *Md* per 1,000 km^2 (95% CI 26.8-32.7), with a range from 17.4 *Md* per 1,000 km^2 to 36.6 *Md* per 1,000 km^2.

The only other estimate of *Md* abundance at AUTEC comes from a study by Claridge (2013), who used a Bayesian framework to fit a capture-recapture model to photo-identification data from AUTEC and estimated a median abundance of 42 animals (75% HPDI = 32-55). If all these animals are present on the range at the same time, this equates to a density of 35 *Md* per 1,000 km^2. This is very close to the maximum density estimate (36.6 *Md* per 1,000 km^2 with 95% CI 27.4- 45.9) obtained here.

This comparison illustrates the utility of passive acoustics for monitoring density and abundance. This capture-recapture estimate required 102 vessel surveys and yielded only 20 encounters with groups of *Md*. However, these visual data did provide the estimate of group size that was used in the passive acoustic density estimate, and the demographic data used for the population modelling presented in Chapter 4.

Dive counting provides a means of obtaining repeated estimates of whale density in a cost-effective manner, provided the infrastructure to support the method exist. This is true for U.S. Navy ranges where existing hydrophone arrays can be used to collect data, but the application of

passive acoustic methods to other locations is more problematic. In addition, obtaining estimates of dive rates, group sizes, and vocal behaviour for populations at other locations requires extensive investments.

Once appropriate sensors are in place, whether fixed hydrophones or recording buoys, passive acoustic data can be collected on a nearly continuous basis. Because these data can be processed using semi-automated methods, analytical costs are reduced, and the results do not depend on human judgment.

By contrast, visual surveys and capture-recapture methods require repeated vessel surveys, with significant personnel and ship costs. Analysis of photographs requires visual inspection by a trained analyst. However, information collected as part of visual surveys can be used to provide estimates of population stage structure, and survival, birth and migration rates that are important indicators of population health. In addition, on-water observers who are in close proximity to animals can collect biopsy and faecal samples, which can be used for health assessment. They can also attach recording and tracking tags to animals used extensively to measure cue rates and associated multipliers.

2.4.1 Click vs. Dive Counting

Hildebrand et al. (2015) estimated densities of Cuvier's and Gervais' beaked whale (*Ziphius cavirostris* and *Mesoplodon europaeus*) at weekly intervals by applying both click- and dive-counting methods to data collected at three sites in the Gulf of Mexico using recording buoys with a single hydrophone. A simulation model was used to estimate the relationship between detection probability and range. Beaked whale detections required a minimum of 75 s of clicks

with no more than 1 h between click trains. The two methods showed similar trends in density, with a maximum difference of 40% and a minimum of 8%.

Click and dive counting methods requires estimates of the cue rate (*r*), *P* and *c*. Both methods assume that the values of these parameters remain constant over time unless they can be measured repeatedly which is quite possible for *P* and *c* which are derived from passive acoustic detection data but is difficult for *r* that requires tag data. Any bias in the parameter estimates will result in a consistent bias in the associated density estimate but an unbiased trend estimate. Random variation in these parameters should also cause no bias in the trend estimate; however, a systematic trend in any one will bias the estimated population trend.

For both methods, *P* and *c* are likely to be dependent on the hydrophone array geometry and the sound propagation characteristics of the study site. For example, there are significant differences in spacing, bathymetry, and ambient noise among the three major U.S. Navy Ranges and the new Undersea Warfare Training Range (USWTR) off the coast of Jacksonville, FL. The implementation of passive acoustic methods at these sites comes with considerable challenges because the basic parameters must be estimated for each new installation. For example, Schorr et al. (2014) noted that the dive rate of Cuvier's beaked whales at SCORE (~7 per day) differs from the rates reported for Liguria (11-12 per day), and Hawaii (~10 per day). The dive rate can be derived from satellite tags whereas, click counting depends on measuring clicks emitted by the animals with recording tags. Satellite tags (Schorr et al., 2014) typically have a significantly longer deployment duration as compared to recording tags (weeks to months vs. days) (Johnson and Tyack, 2003; Southall et al., 2012) though the technology is rapidly changing. Dive counting also requires a group size estimate that is typically derived with sighting data by the on-water team coincident with tag deployment.

2.4.2 Further Applications of Passive Acoustic Monitoring

The methods for estimating *Md* density using passive acoustic data described in this Chapter were developed as part of an on-going, multi-faceted effort which combined long-term visual observation, development of detection and classification algorithms, along with the use of both short-term recording tags and mid-term satellite tags. These passive acoustic methods require infrastructure in the form of hydrophone arrays or portable acoustic devices. Therefore, at this point in time, they are only readily applicable in areas with existing military or scientific hydrophone arrays, such as those found on the U.S. Navy undersea ranges, where beaked whales are present and repetitively exposed to MFAS.

Monitoring beaked whale populations exposed to MFAS has been court-mandated in Southern California and Hawaii (Buzzas, 2016); therefore, the design of an appropriate monitoring methodology is an important consideration. Fleishman et al. (2016) suggest that there are four basic steps that should be followed in establishing a program for monitoring the effects of disturbance:

1. develop an appropriate theory of change;
2. define a biologically meaningful effect size;
3. select the response variable for monitoring; and
4. specify the temporal sequence for monitoring.

One "theory of change" is that repetitive MFAS exposure causes disruption and potential displacement of animals from preferred foraging habitat leading to reduced energy intake. These changes in energy intake may lower birth rate and calf survival, thus reducing individual fitness and population density.

Claridge (2013) suggested that the lower density of *Md* at AUTEC as compared to Abaco may be the result of MFAS exposure. Moore and Barlow (2013) suggested that MFAS exposure may be associated with a decline in beaked whale populations in Southern California, and recommended passive acoustic monitoring as an appropriate methodology for investigating this. Hence, animal density is likely to be a suitable response variable for the monitoring of beaked whale populations. Passive acoustic monitoring provides a highly scalable temporal sequence of density estimates and provides a powerful means of assessing change over periods of days, months, seasons, or years.

The development of the methods for estimating *Md* density on AUTEC using dive counting illustrates the steps that would be required to extend these methods to additional species. They are as follows.

1. Investigate the species' acoustic behaviour.
2. Determine the relationship between acoustic signals and actual behaviour patterns.
3. Identify a suitable acoustic cue for monitoring.
4. Measure the cue production rate.
5. Implement an efficient cue detector.
6. Estimate the cue detection parameters (P and c) and multipliers (s).

The nature of *Md* call behaviour was poorly understood before the development and attachment of recording tags (Johnson and Tyack, 2003). These tags revealed the structure of *Md* calls: echolocation clicks were only produced when animals were below 200 m during deep foraging dives; they were produced at a reasonably constant rate both day and night; they had a characteristic mean repetition rate (Johnson et al., 2004; Zimmer et al., 2005) and a high source

level (Shaffer et al., 2013; Zimmer et al., 2008). This information confirmed that echolocation clicks provided an acoustic cue that could be associated with a known behaviour (foraging) and which was produced at a measurable rate (Johnson et al., 2006b, 2004). In addition, *Md* clicks have a distinct structure with strong features that supported the design of a suitable detector/classifier (Baumann-Pickering et al., 2014, 2013; Jarvis, 2012).

The passive acoustic methods presented here provide a first step in establishing a means of long-term estimates in beaked whale density on the U.S. Navy undersea ranges including AUTEC, by leveraging information that is collected routinely on widely-spaced, bottom-mounted hydrophones. These assets have been used to study *Md in situ* and complete the steps necessary to develop a prototype system to measure density. The AUTEC systems are beginning to be used to study the long-term effect of MFAS exposure on *Md*. They are also being applied to Cuvier's beaked whales at SCORE (DiMarzio et al., 2018) and *Md* at PMRF (Manzano-Roth et al., 2016). Coordinated passive acoustic, visual, tag, biopsy, photo-identification, and ship track data are being collected, that over time should provide a means of better understanding the reaction of *Md* to sonar and its long-term effect on the population. While the focus of this study is passive acoustic monitoring, data from multiple modalities have been used to inform the development of these techniques. A monitoring plan for AUTEC and other ranges is being developed, following the approach advocated by Fleishman et al. (2016), with the aim of identifying any long-term effects of MFAS exposure on beaked whale populations.

2.5 Appendices

2.5.1 Click Train Processor

A Click Train Processor (CTP) program, written in Java by Ronald Morrissey, inputs M3R detection archives and produces click trains from detection reports for a particular algorithm type on a hydrophone by hydrophone basis. Each detection report includes an entry for the hydrophone number, algorithm type, time-of detection and class type which defines the detector/classifier used.

For each hydrophone, detection reports for a particular algorithm and class type are examined and buffered. Detection reports for the algorithm and class of interest are extracted (e.g. algorithm: Class Specific Support Vector Machine (CSSVM); class of interest: *Md*). With the receipt of a click, the click training processing begins. If the number of clicks exceeds the "Click Threshold" within a 5 s window, with no time between clicks exceeding the "Maximum Difference" a train is established. With each successive ping, the chain is maintained, provided a new ping is received within a specified "Time-Out" period after the most recent click. If no ping is received within the Time-Out period, the click train is closed. The ICI is also reported as the mean value calculated over a 0.5 s moving average filter where the time window is defined by a user-defined "Time Constant". The time of the first and last ping detection times in the chain are noted and a report is generated. The program parameters and default setting are given as follows.

Click Threshold <5 clicks>
Time-Out <180 s>
FFT Click Threshold (Hz) <468.75Hz> (FFT-based detector only)
Time Constant <0.5 s>
Maximum Difference <1.0 s>

For each FFT detection report, a decision is made as to whether the FFT output constitutes a click. Each report provides a binary bit-map representing each FFT bin where those bins with sufficient energy above a noise-variable adaptive threshold are set to one. The number of bins and associated bandwidth resolution vary depending on the sample rate of the FFT (Jarvis et al., 2014). For example, the standard "high frequency" FFT detector executes a 2048-point FFT at a sample rate of 96 kHz. This results in 1024 reported bins each with a bandwidth resolution of 46.89 Hz. The "low frequency" detector runs an FFT size of 4096 samples with a bin resolution of 1.46 Hz. For the FFT-based detector, a click is declared if the number of bins in which energy is reported reaches the minimum specified "FFT Click Threshold". The threshold is specified in Hertz and is calculated for each detection report by multiplying the number of bins reported above the noise-variable threshold times the bin width in Hertz. For example, the default "FFT Click Threshold" for the high-frequency FFT-based detector is 468.75 Hz which represents 10 bins, each at a bin resolution of 46.875 Hz (96,000 sample rate). For algorithms such as the class-specific support vector machine (CS-SVM), the detection reports are used directly and the bin-threshold is ignored and reported as "-1".

The CTP algorithm tracks the ICI with either a first-difference method or a multi-difference histogram (referred to in the CTP data as "cepstrum,") that simulates the output of a cepstrum process. The multiple differences from "cepstrum" or first differences are summed into a running histogram using an exponential average (Equation 2.6) where time bins are computed from 0-1 s in 0.1 s increments and from 1-10 s in 1s increments (Figure 2.7)

$$avg\_bin = 0.5*avg\_bin+0.5*new\_bin \qquad \text{Equation 2.6}$$

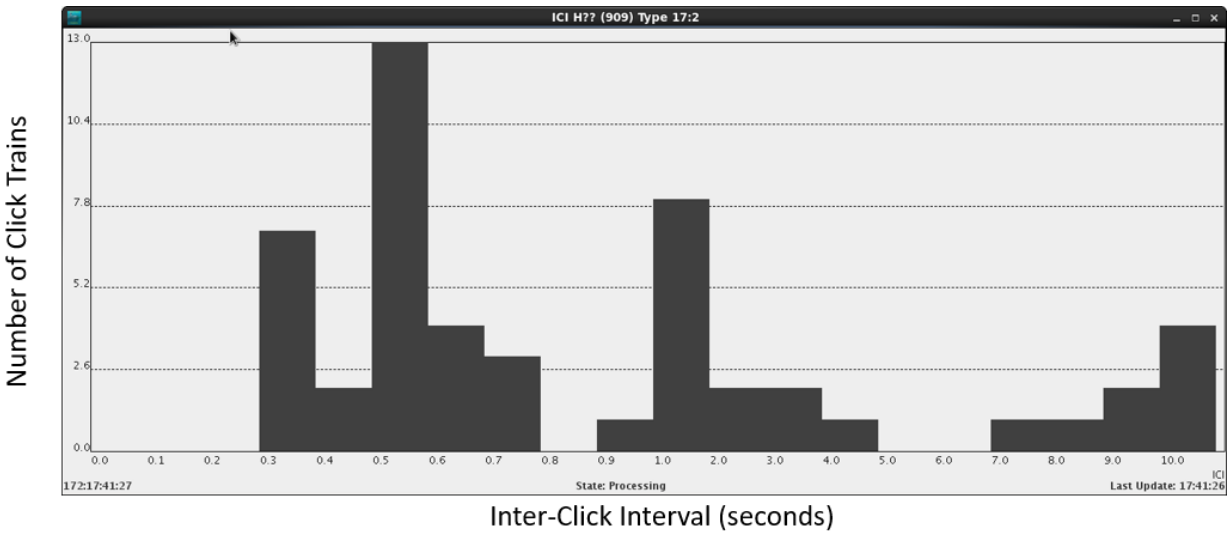

Figure 2.7 Click Train Processor histogram output for Cuvier's beaked whale group with reported ICI of .55.

Table 2.3 provides an example output using the CS-SVM classifier and consequently does not use a bin threshold to determine if a click is present. Therefore, the return threshold field (TH) is set to -1. The hydrophone (HYD) which generated the report and the classifier output type (TYP) are listed where the first TYP number is assigned to the algorithm and the second number the class type. For example, TYP 12:01 represents a CS-SVM detection (12) of class *Md* (01). A minimum of 5 clicks is required to begin a click train (RQ=5). If no clicks are received for 180 s, the click training times out (TMO) and the click train is ended. For each hydrophone (HYD), the total number of clicks in the reported click train is provided (CNT), along with the start and stop times and dates (START, STOP), the click train duration in seconds (DT), and the ICI, also in seconds.

Table 2.3 Click train processor output file for CS-SVM detection reports indicating the hydrophone(HYD), Algorithm and subclass (TYP), click threshold (TH), number of clicks required to initiate click train (RQ), time-out period in seconds (TMO), count of clicks in chain (CNT), start (START) and stop time (STOP) of click chain, click train duration in seconds (DT), inter-click interval in seconds (ICI).

HYD	TYP	TH	RQ	TMO	CNT	START		STOP		DT	ICI
804	12:02	-1	5	180	7	2015	212:16:05:18.57	2015	212:16:05:27.70	9.130667	0.104000251
605	12:00	-1	5	180	7	2015	212:16:05:28.42	2015	212:16:05:42.42	13.99466	0.00800025
605	12:04	-1	5	180	7	2015	212:16:05:28.42	2015	212:16:05:42.42	13.99466	0.00800025
87	12:03	-1	5	180	24	2015	212:16:05:35.15	2015	212:16:05:54.14	18.99748	0.990422685
87	12:05	-1	5	180	51	2015	212:16:05:33.14	2015	212:16:05:54.15	21.01350	0.988826761
87	12:01	-1	5	180	24	2015	212:16:05:32.41	2015	212:16:05:54.13	21.72817	0.026714231
804	12:01	-1	5	180	6	2015	212:16:05:19.52	2015	212:16:06:15.39	55.872	0.08
38	12:00	-1	5	180	7	2015	212:16:05:46.80	2015	212:16:06:41.57	54.76312	0.744007476

2.5.2 Auto-Grouper Program

The M3R program developed a Matlab-based program (auto-grouper) to associate beaked whale click trains produced by the Click Train Processor into individual GVPs (Figure 2.8). For each group hydrophone, the program outputs the start and stop time and the number of clicks detected.

The program is based on a heuristic set of rules developed by analysts with extensive experience visually detecting and classifying *Md* GVPs via spectrogram analysis. The program exploits the known *Md* deep foraging dive characteristics and knowledge of the click structure within the AUTEC hydrophone array to detect and classify *Md* GVPs. Based on visual observations, it is known that animals at AUTEC associate in small groups with a mean group size of 2.34 animals/group as described above (Claridge, 2013). The animals dive as a group when executing deep foraging dives, at AUTEC, approximately 9.2 dives/day (Moretti et al., 2010). GVP echolocation clicks begin below 200 m and the mean GVP duration is 33 min (Shaffer et al.,

2013). Based on recording tag and hydrophone measurements, the on-axis click source level is above 200 dB (Shaffer et al., 2013; Zimmer et al., 2008). The maximum on-axis detection range at AUTEC is approximately 6.5km (Shaffer et al., 2013). With a hydrophone baseline of approximately 4 km, this means a click could be detected just over 1.5 times the hydrophone baseline if the animals were optimally located within the hydrophone field and the animal moved such that an on-axis click was directed at each surrounding hydrophone. The number can potentially expand to up to 19 hydrophones if GVPs from 2 different groups overlap in space and time. However, in practice detections of clicks are detected on 3.5 hydrophones on average (SD =1.5 hydrophones, n=1559 GVPs).

To begin the process, the click train output file is filtered for class type depending on the algorithm of interest. Currently, both the CS-SVM and the FFT-based classifiers can be used for beaked whale analysis (Jarvis et al., 2014). Only, click trains on designated hydrophones of interest are accepted. Each click train stop and start time is checked for valid times and dates. Click trains with an ICI between 0.23 s and 0.4 s and a duration between 1-60 min are selected. The lower ICI limit was chosen to reduce conflict with various species of dolphins. The upper limit was chosen to reduce confusion with Cuvier's beaked whales at AUTEC with a measured mean ICI of 0.54s (95% CI 0.51-0.57). The data are processed in one-day blocks that are sorted by click density (clicks/min) from maximum to minimum.

To begin the process the first buffered click train (max click density) is used to establish a group. Initially, the hydrophone associated with the click train is used as the group centre and the surrounding six hexagonal array hydrophones associated with the centre hydrophone are identified. As click trains are added, the geometric mean between phones is assigned the group centre and adjacent hydrophones are identified for the group inclusive of any additional

hydrophones. The next click train in the buffer is examined. If it is on a hydrophone within or adjacent to the group hydrophones, it is examined for time. If the start or stop of the new click train is not within 10 minutes of the group start or stop, the group is not added to the current group and the process repeats if there are other available groups to check for membership. If there are no additional groups, a new group is established and the process is repeated with the next click train. If there are no additional click trains, the process advances to the next one-day data buffer. If there are no additional data, the data for each group are written to a file.

If a click train is detected on an existing or adjacent hydrophone of an existing group and less than 10 minutes has elapsed, the hydrophone distance from the group centre is examined. If it is less than 1.5 times the baseline, it is added to the current group, new group metrics are calculated, and the process repeats with the next click train. If the distance exceeds the threshold and the click density is less than 12 clicks/second or the click train duration is less than 10 minutes, the click train start and stop time is compared to the current group. If the click train falls within the group start and stop, it is added to the group, else it is compared to the next group if available or if no additional groups exist, it is used to establish a new group. This process repeats until all click trains have been examined. For each group, the hydrophones, clicks per hydrophone, and each hydrophone stop and start time are reported.

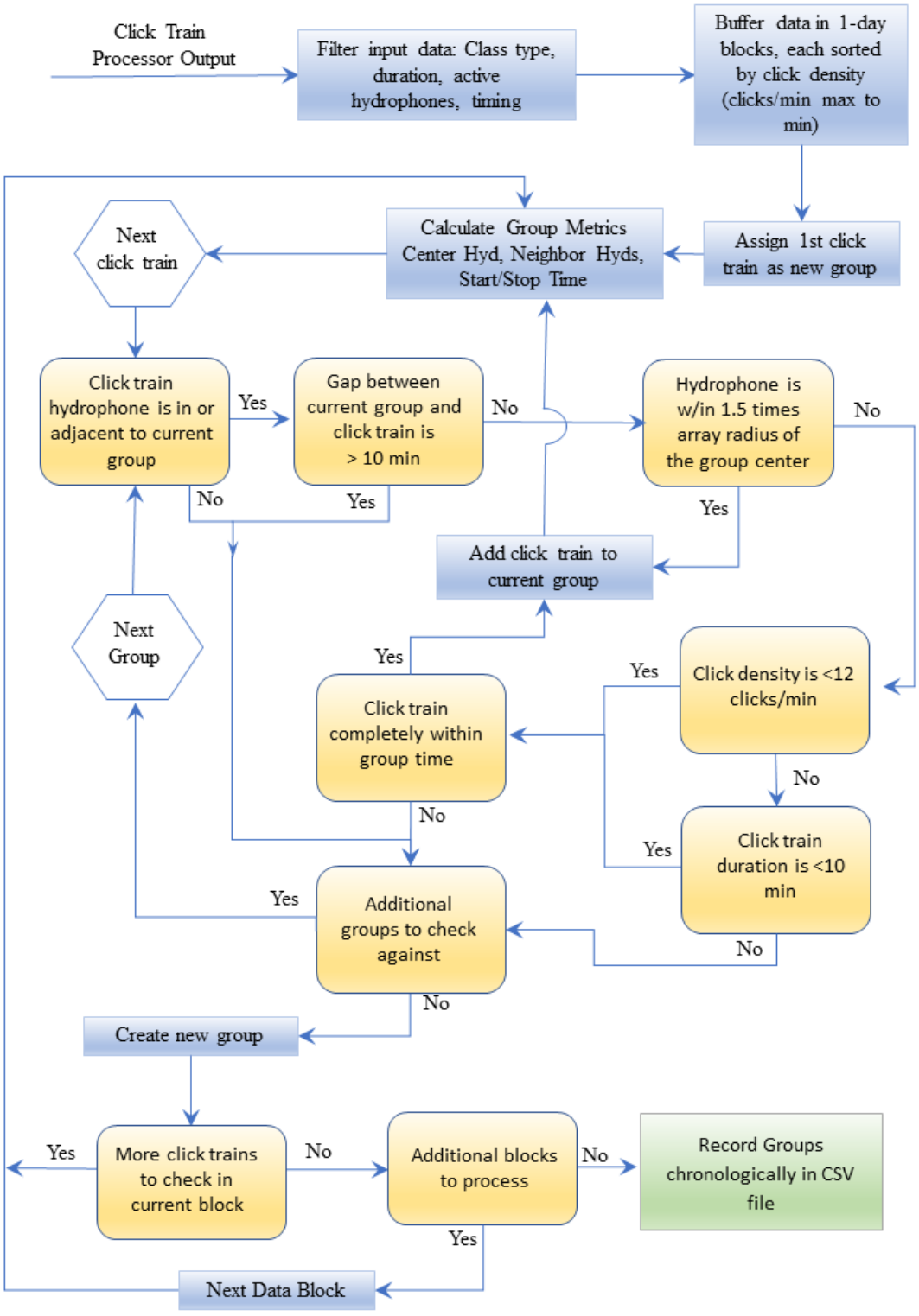

Figure 2.8 Click train processor block diagram (Karin Dolan, pers. comm.)

2.6 Contributions

The dive counting algorithm was developed by the author in collaboration with the M3R team and Len Thomas and Tiago Marques from the University of St Andrews. The published paper was drafted by the author with edits and advice by the contributing authors. In particular, Tiago Marques provided input into using the delta method to calculate the coefficient of variation. The isolation of GVPs around operations was performed by analysts at NUWC under the direction of the author. The author developed the R code and performed the analysis of the data to obtain the final estimates of abundance and density.

Analysis of GVPs from 2011 and 2012 data at AUTEC was performed by the author who also designed the sampling plan to determine false positives and developed the required R-code. The manual visual verification of GVPs from the M3R detection records was performed by an independent NUWC analyst, Jessica Fothergill.

The software used to generate unfiltered GVPs was developed over a number of years out of the M3R program for which the author is the Principal. Investigator Ron Morrissey developed display and system tools, and Susan Jarvis worked extensively on the Class Specific Support Vector Classifier (CS-SVM) that is used to detect beaked whales. Karin Dolan developed the original auto-grouper Matlab code and Figure 2.8.

Chapter 3

Determining the Risk of Behavioural Disturbance Caused by Military Sonar

3.1 Introduction

The principal legislation relating to marine mammals in the U.S. is the 1972 Marine Mammal Protection Act (MMPA), which was amended in 2007. Its primary objective is to "maintain the health and stability of the marine ecosystem", with the goal being to "obtain an optimum sustainable population (for each species) keeping in mind the carrying capacity of the habitat." An optimum sustainable population is defined as "the number of animals which will result in the maximum productivity of the population or the species, keeping in mind the carrying capacity of the habitat and the health of the ecosystem of which they form a constituent element."

The Act allows incidental "taking" of marine mammals for up to a five-year period, provided there is a "negligible impact on such species or stock". Negligible impact is defined as "an impact resulting from the specified activity that cannot be reasonably expected to, and is not reasonably likely to, adversely affect the species or stock through effects on annual rates of recruitment or survival." There are three kinds of takes: level A, level B, and behavioural. A level A take is based on a permanent threshold shift (PTS) in hearing; in other words, permanent hearing damage. Level B type takes are based on levels that are likely to cause a temporary threshold shift (TTS) in hearing. Behavioural (level B type II) takes are the result of "harassment". Harassment is defined as

> "any act that disturbs or is likely to disturb a marine mammal or marine mammal stock in the wild by causing disruption of natural behavioural patterns, including, but not limited to, migration, surfacing, nursing, breeding, feeding, or sheltering, to a point where such behavioural patterns are abandoned or significantly altered."

The MMPA provides special consideration for military operations.

> "For a military readiness activity (as defined in section 315(f) of Public Law 107–314; 16 U.S.C. 703 note), a determination of "least practicable adverse impact on such species or stock" under clause (i)(II)(aa) shall include consideration of personnel safety, practicality of implementation, and impact on the effectiveness of the military readiness activity. Before making the required determination, the Secretary shall consult with the Department of Defense regarding personnel safety, practicality of implementation, and impact on the effectiveness of the military readiness activity."

To meet the requirement of the MMPA within U.S. waters, the U.S. Navy prepares Environmental Impact Statements (EISs) on a regular basis for the broad areas where it conducts testing and training. The effects of these activities on marine mammals are modelled using the Navy Acoustic Effects Model (NAEMO) (Blackstock et al., 2018). NAEMO estimates the number of level A, level B, and behavioural "takes" likely to be associated with mid-frequency active sonar (MFAS) exercises. Level A and level B takes are determined by estimating the number of animals that are exposed to a sound exposure level (SEL) in units of dB re 1µPa^{2}·sec measured over 24 h or a received level (RL) in units of dB re 1µPa (hereafter dB) over a specified threshold level. SEL and received level (RL) criteria for PTS and TTS are based on experiments with captive animals (Finneran et al., 2005; Finneran and Schlundt, 2010; Schlundt

et al., 2000). They take the form of step functions based on the dual SEL-RL criteria, under the theory that exposure to repetitive noise (SEL) or a single loud noise (RL) above the thresholds will cause physical damage. Therefore, animals that are exposed above the specified SEL *or* RL threshold are assumed to be affected (taken) while those below are unaffected. By contrast, behavioural take criteria are based on RLs, and have typically taken the form of probabilistic dose-response functions.

A dose-response function (also called a risk function) gives the probability of a negative outcome (in this case behavioural response) as a function of a given level of exposure to a stressor (in this case sonar RL). The application of such analysis has traditionally been used to estimate the effect of chemicals on human health, to the point where standardized modelling principles have been developed (EPA Risk Assessment Forum, 2012; International Program on Chemical Safety (IPCS), 2009). A dose-response framework may be justified in the context of cetacean behavioural response on the basis of strong variation both among individuals or within individuals over time. As a result, some individuals within a population may respond at relatively low RLs and others only at higher levels (Ellison et al., 2012; Harris et al., 2018).

Dose-response functions have been developed for a number of cetacean species using experimental exposures for both free-ranging and captive animals. For example, Miller et al. (2014) placed tags on eight killer whales (*Orcinus orca*) in the wild and exposed them to escalating levels of MFAS by moving the ship closer to the whales. The response data were then used to develop a behavioural risk function that predicts the probability of avoidance to MFAS as a function of RL and sensation level (RL minus hearing threshold). They reported a 0.5 probability of reaction at an RL of 142 dB. Antunes et al. (2014) used data from similar experiments to study the reaction of long-finned pilot whales (*Globicephala melas*) to tactical

sonar. The resulting risk function predicted that 50% of the population would respond at an RL of 170 dB.

U.S. Navy captive bottlenose dolphins *(Tursiops truncatus*) have been used to develop both hearing thresholds and dose-response functions. Houser et al. (2013) exposed 30 captive dolphins to MFAS. A 0.5 probability of response, defined as a change in respiration rate, was measured at 145 dB. At levels greater than 175 dB, animals refused to participate in the experiment. The hearing sensitivity as a function of frequency (Finneran and Houser, 2006; Houser and Finneran, 2006) of these dolphins was measured via both behavioural (Finneran et al., 2005; Finneran and Schlundt, 2010) and evoked potential measurements (Houser and Finneran, 2006). The onset of TTS when exposed to escalating levels of sound was also measured (Finneran et al., 2005; Schlundt et al., 2000). Kastelein et al. (2012) used a similar methodology to measure the hearing sensitivity of captive harbour porpoises (*Phocoena phocoena*), and their TTS level and recovery when exposed to a 4 kHz signal.

The dose-response functions used by the U.S. Navy have been informed by these studies. Initially, it took the form of a Feller function (Equation 3.1; Figure 3.1), with a 0.5 probability of disturbance at a RL of 165 dB (U.S. Fleet Forces Command, 2008):

$$P_r(L) = \frac{1}{\left(1+\frac{45}{L-120}\right)^{10}} \qquad \text{Equation 3.1}$$

where L = root mean squared RL.

This was derived from studies of captive animals (Finneran et al., 2005; Schlundt et al., 2000), controlled exposure experiments (CEEs) on right whales (Nowacek et al., 2004), and an analysis of the exposure levels associated with an incident in the Haro Straits in Washington State, in which killer whales and harbour porpoise were exposed to MFAS transmissions from the USS Shoup (Commander U. S. Pacific Fleet, 2003). Following an analysis of results from studies at Atlantic Underwater Test and Evaluation Center (AUTEC), (McCarthy et al., 2011; Moretti et al., 2010);(Tyack et al., 2011), this risk function was replaced by one with a step (Figure 3.1) at 140 dB (Finneran and Jenkins, 2012).

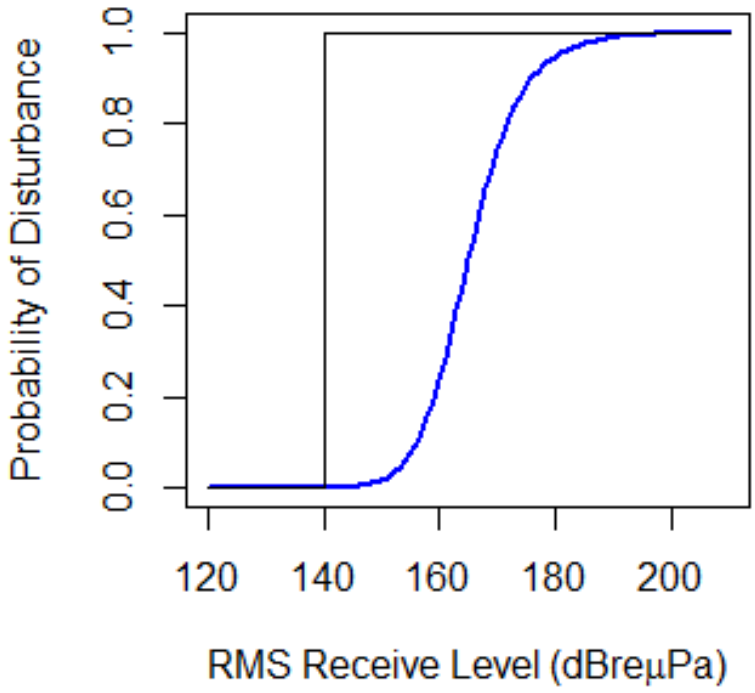

Figure 3.1 The functions used by the U.S. Navy to estimate the probability of a behavioural disturbance as a function of RMS received level until 2015. The blue line represents the Feller function defined by Equation 3.1. The black line represents a step function at 140 dB.

Many of the data for these dose-response functions comes from CEEs (see Harris et al. 2018 for a review). Typically, a CEE involves a progressive escalation of the output level of the source (Southall et al., 2012) up to its maximum, or a change in the position of the source relative to the animals being exposed (Miller et al., 2011). This "dose escalation" approach provides an estimate of the minimum RL that results in the onset of a behavioural change. The portable sources used in these experiments usually have a maximum output level that is significantly lower than that of a navy ship sonar (Southall et al., 2012; Tyack et al., 2011). Therefore, to a achieve a given RL, the source must be much closer to the animal than a navy ship would be. For instance, for an RL of 140 dB, a portable source with an output level of 210 dB must be positioned at a distance of approximately 3 km from the animal. By comparison, a 53C sonar, with a reported output level of 235 dB, would generate the same RL at a distance of well over 30 km. It is likely that animals, such as beaked whales, that have evolved to use acoustics to hunt prey, can distinguish between close and distant sources, and this is likely to affect their responses to theses source.

DeRuiter et al. (2013) exposed a tagged Cuvier's beaked (*Ziphius cavirostris*) whale to the same portable sound source during a deep foraging dive at a distance of less than 4 km. Although the animal reacted to the portable source at a low RL, as with the CEE on *Md* in the Bahamas (Tyack et al., 2011), the tag recording also revealed that it had been exposed to an MFAS signal from a distant Navy vessel at approximately the same RL. However, the animal did not react to this distant source, implying its reaction may have depended on the distance to the source as well as the RL. This suggests that small portable sources may not give a realistic dose-response function to navy sonars. To avoid these issues, some CEEs have been carried out with the source of interest. These include the use of a seismic airgun in a study of humpback whales (*Megaptera*

novaeangliae) in Australia (Cato et al., 2013; Dunlop et al., 2017a, 2017b) and the use of a tactical MFAS in a study of multiple species, including killer whales, sperm whales (*Physeter macrocephlus*), and long-finned pilot whales, in the North Atlantic (Miller et al., 2011).

An additional problem with a typical CEE is that the tagged animal is often followed by multiple vessels. The engine noise from the following vessels is certainly audible to the animal and could also elicit a reaction. As an extreme example, an AUTEC Range support craft was directed at top speed towards a group of *Md* that had been tagged as part of a 2007 study of behavioural responses to sonar (Tyack et al., 2011). This vessel was extremely noisy due to mismatched propellers, and therefore created loud cavitation noise directly above the animals. Echolocation clicks detected on surrounding hydrophones indicated a general coordinated change in movement of these foraging animals when the support craft was in close proximity (Pirotta et al., 2012).

One way to avoid the problems associated with CEEs is to use opportunistic data obtained from *in situ* observations of the reaction of animals to actual sound sources. Williams et al. (2014) observed the reaction of Northeast Pacific killer whales to passing ships and used these data to derive a dose-response function for RLs below 150 dB. They reported "subtle" behavioural changes at an RL of 130 dB. Lusseau and Higham (2004) documented the effects of whale watching vessels on a bottlenose dolphin community in Doubtful Sound, New Zealand. The results of this study led to environmental management recommendations in regards to marine sanctuaries. Falcone et al. (2017) investigated the response of Cuvier's beaked whales in Southern California to MFAs. In this case, observations were made by combining data from satellite telemetry tags with passive acoustics data and U.S. Navy records of MFAS use. There

was an overall increase in the interval between deep dives when the animals were exposed to MFAS.

This chapter describes a method for deriving a risk function for behavioural takes (level B, type II) using data collected opportunistically on the hydrophones at the AUTEC Range before and during a three-day multi-ship MFAS operation. *Md* and sonar detection archives were combined with AUTEC ship track data and acoustic propagation models to estimate the risk of a behavioural disturbance, defined as the disruption of a foraging dive, as a function of estimated RL during the MFAS operation. This effort utilized detection of echolocation clicks and mid-frequency active sonar (MFAS) from actual Navy operations on AUTEC hydrophones and is therefore not subject to the issues associated with CEEs described above. The research presented here is based on a study undertaken by Moretti et al. (2014), although here a longer period (72 rather than 19 h) was used to verify the pre-exposure probability of detecting *Md*.

RL was used to describe the level of exposure as opposed to SEL. SEL is a measure of the cumulative energy received over some time period. For actual, repeated U.S. Navy MFAS operations, the determination of the time period is arbitrary. For example, NAEMO calculates SEL over a 24-hour period. The stop and start of MFAS and the time between measured bouts were uncontrolled making the selection of the SEL time criteria difficult. Also, passive acoustic methods were used to detect *Md* GVPs as a proxy for foraging dives. Over a given period, it is not possible to track a single individual or group making estimation of SEL extremely difficult, especially if the animals avoid MFAS exposure. Consequently, RL was used to describe the level of exposure. This was relatively straight forward to estimate and is repeatable. In addition, for U.S. environmental permitting, behavioural takes are calculated using an estimate of RL

instead of SEL (Finneran and Jenkins, 2012). Therefore, for this analysis, the dose-response curve was calculated as a function of RL.

The term MFAS is used to describe tactical sonar, but multiple types of devices are used throughout the military. AUTEC is the site of repeated navy operations that involve the use of a variety of different MFAS. While the source signals are similar, the output level of these sources and deployment techniques vary widely. MFAS sources include loud (235 dB) surface ship sonar but also smaller devices such as sonobuoy and helicopter deployed sonar. A preliminary investigation of the effect of these different source types was also conducted to determine if further investigation was warranted. The techniques used to derive the *Md* behavioural risk function presented in this chapter were applied to data from both single surface ship operations and smaller MFAS sources.

3.2 Methods

3.2.1 Data Sets

Hydrophone data

The Marine Mammal Monitoring on Navy Ranges (M3R) system digitizes data from the 91 AUTEC hydrophones at a sample rate of 96 kHz and provides a measurement bandwidth of approximately 48 kHz. Signals above 45 kHz are attenuated by an anti-aliasing filter. These data were used to detect MFAS pings between approximately 2.5 and 4.5 kHz, and *Md* echolocation clicks between approximately 20 and 45 kHz.

Multi-ship anti-submarine warfare (ASW) exercise data

During ASW exercises, ships typically assemble on either the north or south side of the AUTEC range which contains the hydrophone array. They actively search with MFAS for a target

positioned somewhere within the range. Each ship transmitted an MFAS signal within an assigned frequency band at a "range-rate" (inter-ping interval) appropriate for the operational area. The chosen range-rate allows for a ping to travel to the edge of the range and for its reflection to return to the ship before the next ping is emitted. For example, a range-rate of 25 s allows the transmission of sonar pings and receipt of their reflection out to approximately 18 km without overlap with the next outgoing ping.

For the operation studied, the search scenario was repeated a total of six times over the course of approximately three days with a mean duration of 8.61 h (minimum = 6.73 h, maximum = 9.83 h). Each scenario was separated by a quiet period, with a mean duration of 4.26 h (minimum = 3.65 h, maximum = 6.62 h) during which the participating vessels repositioned and no MFAS was transmitted. The exercise took place in May 2009 (Table 3.1) and spanned almost exactly 72 h.

Table 3.1. Summary of sonar activity during the 2009 multi-ship MFAS exercise.

Period	**Start Date**	**Time MFA Active (h:min)**	**Duration (h)**
Pre-Test	13-May		19.58
Scenario 1	14-May	10:47-19:56	9.15
Gap 1			4.35
Scenario 2	15-May	00:17-09:35	9.30
Gap 2			2.62
Scenario 3	15-May	12:12-21:02	9.83
Gap 3			3.65
Scenario 4	16-May	00:41-07:25	6.73
Gap 4			6.62
Scenario 5	16-May	14:02-21:57	7.92
Gap 5			4.05
Scenario 6	17-May	02:00-10:44	8.73
Post-test			12.57

3.2.2 Detection of *Md* Groups

As described in Chapter 2, *Md* click detections were used to identify the start of GVPs. For this analysis, GVPs were detected by an analyst who examined the M3R Range displays and 2D spectrograms. Data were divided into 30 min periods, which is approximately the duration of an *Md* GVP, and each GVP start was assigned to its appropriate 30 min interval. The centre of the group was calculated as the mean centre of all hydrophones associated with the group, weighted by the number of clicks detected on each hydrophone. The hydrophone closest to the calculated position was designated the centre hydrophone.

3.2.3 Detection of MFAS Pings

For periods of active MFAS operations, sonar pings from various surface combatants detected on the hydrophones surrounding the surface ship were noted in the archives by the analyst. The location of the ping emission was calculated with the assumption that the pings were transmitted from one of three surface ships taking part in the operation. The ship closest to the first hydrophone on which the MFAS ping was detected was assumed to be the source of the transmission.

3.2.4 Ship Tracks

Surface combatants were precisely tracked by large area tracking range (LATR) pods. These rely on GPS to determine each ship's position, which is transmitted to a shore-based receiver via a radio frequency link. These data were provided by AUTEC and used in the subsequent analysis.

3.2.5 Estimating RL

Direct recording of hydrophone outputs during U.S. Navy operations was not authorized. Therefore, the time-varying sound field was estimated by combining the MFAS ping detection data with the AUTEC surface ship track data. One of the prime considerations in this calculation

is the distance of the source from the animal. The estimates of RL used here were based on the precisely known position, output level, and beam patterns of the sonars being used. These data provide input to a modified version of NAEMO, which uses the Comprehensive Acoustic Simulation System, Gaussian Ray Bundle (CASS/GRAB) model to estimate propagation loss (Weinberg and Keenan, 1996). The Oceanographic and Atmospheric Master Library, was used to estimate the site bathymetry, sound speed profile, bottom loss, and wind speed (Giddings, 2008). A 3-dimensional, seasonal, sound speed profile with 0.25 degree resolution and seasonal wind speed with one degree resolution were used. The modelling was done to a horizontal resolution of 50 m and a depth resolution of 25 m.

Propagation loss values were recalculated along 20-degree radials for each of 18 analysis points (Figure 3.2). These points were equally divided across the range into six rows, each with three columns. The *RL* for every emitted ping detected on the GVP centre hydrophone was estimated based on the closest point on the closest radial to the hydrophone.

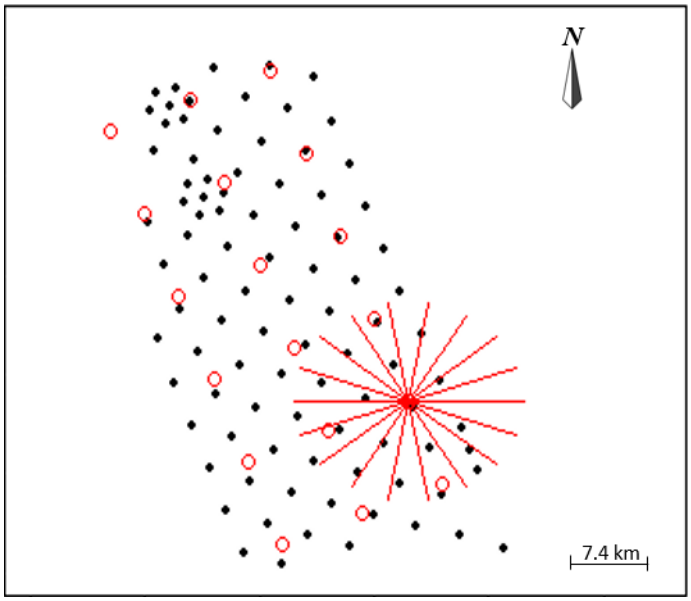

Figure 3.29 Calculation of propagation loss at 18 positions along each 20 degree radial, an example of which is indicated by the red lines. The black dots show the location of the AUTEC hydrophones which are arranged on an approximately 4 km grid.

3.2.6 Pre-exposure Probability of *Md* Detection

Data during a 72-hour period before the first MFAS-active operation were analysed to estimate the pre-exposure probability of detecting a GVP. In this period, no MFAS was transmitted on the range, but the three ships that would take part in the MFAS exercise carried out operations that did not involve the use of sonar. Thus, examination of this period served to deconflict the effect of sonar from the effect of the ships participating in the exercise.

Dives outside the range were excluded as only GVPs on inner hydrophones were considered. Edge-phone only groups were removed. The pre-exposure probability ($\hat{P}_B$) of the start of a deep foraging dive being detected on a hydrophone in a given 30 min period was calculated by taking the global mean of all GVP detections during the 72-hr period. Specifically, the total number of GVP starts (*S)* detected on all hydrophones and assigned to a centre hydrophone was divided by the total number of hydrophones (82) times the total number of periods (*T*):

$$\hat{P}_B = S/82T \qquad \text{Equation 3.4}$$

where S is given by

$$S = \sum_{i=1}^{K} \sum_{j=1}^{T} w_{ij} \qquad \text{Equation 5.3}$$

and where w_{ij}=1 indicates a GVP start occurred in a given period (*j=1,2,…,39*) on any hydrophone (*i*) (w_{ij}=0 otherwise). This assumes a maximum of one GVP on any hydrophone in a 30-minute period which was true for all but two cases.

Though no MFAS was used during the period, any response from animals during the subsequent MFAS operations may have been preconditioned by the vessel operations that occurred during this period. As noted above, Pirotta et al. (2012) detected a change in the direction of travel for of *Md* groups during deep foraging dives at AUTEC in response to ship-generated noise. However, the Pirotta et al. (2012) vessel was extremely noisy and was directed towards animals that were foraging, whereas navy ships are designed to be acoustically quiet.

3.2.7 Overall change during a multi-ship exercise

A simple metric of the overall change in detections of dive starts during the multi-ship MFAS exercise period is given by the ratio of the average probability of detecting a dive start (per hydrophone and 30 min period) in the 72-hour pre-exposure period ($\hat{P}_B$) to the average probability of detecting a dive start in the 72-hour exercise period (denoted $\hat{P}_{MFAS}$):

$$\Delta = \frac{\hat{P}_B}{\hat{P}_{MFAS}} \qquad \text{Equation 3.4}$$

If the exercise is associated with a decrease in detection of dive starts, this ratio will be less than 1. This quantity was calculated, together with a confidence interval from a nonparametric bootstrap (see Section 3.2.10).

Only a single multi-ship MFAS exercise period is analysed in this chapter, raising the question of how the change in detections observed here compared with that in other pairs of 72-hr periods with no sonar activity in the second period. To address this, data from approximately 7 months in 2012 with no sonar activity, previously used in Chapter 2 were examined. Data from two periods of 136 and 86 days respectively (1/1-5/16; 7/2-9/24) were divided into 72-hour blocks, and the ratio Δ calculated for each successive pair of blocks. The distribution of these were compared with the Δ estimated during a 2009 ASW exercise.

3.2.8 Probability of Behavioural Disturbance as a function of RL

For each 30 min period, the presence or absence of a GVP start centred on the hydrophone was noted along with the maximum RL. Although it was possible for more than one dive to start in a 30 min period, this happened only twice, and dive starts were modelled as a Bernoulli process. A generalized additive model (GAM) with a binomial response distribution and logit link function was used to estimate the probability of a dive starting as a function of RL with the software R (version 2.15.2) and the mgcv package (version 1.7-22; Wood 2017). The default thin plate regression spline smooth function was used as the results did not vary with smooth function. Spatial and temporal residuals were checked and no significant autocorrelation was found.

The probability of detecting a GVP start at a particular RL ($\hat{P}_{rms}$) was then compared to the pre-exposure probability of detecting a dive start (P_B) to calculate the probability of disturbance, $\hat{P}_{d(rms)}$:

$$\hat{P}_{d(rms)} = \frac{min\,(0,\hat{P}_B - \hat{P}_{rms})}{\hat{P}_B} \qquad \text{Equation 3.5}$$

The minimum operator was used to ensure that $0 \leq \hat{P}_{d(rms)} \leq 1$. In practice, $\hat{P}_B$ was always greater than $\hat{P}_{rms}$, suggesting MFAS has a consistent negative affect on *Md* dive behaviour.

3.2.9 Parametric Approximation

Although the GAM represents a flexible approach to characterizing the risk function, the results are not readily represented as a single equation. Hence, a parametric approximation was also calculated. A generalized linear model (GLM) with a probit link function was used to model the relationship between the probability of behavioural disturbance (a GVP not starting in a 30-minute time period) and RL.

3.2.10 Uncertainty quantification

A bootstrap procedure was used to provide a measure of uncertainty for the pre-exposure probability $\hat{P}_B$, for the overall change Δ and for the probability of a dive as a function of MFAS RL $\hat{P}_{rms}$. Ten thousand random realizations of $\hat{P}_B$ were generated by resampling with replacement from the 144 30-min segments before MFAS operations began. For quantifying uncertainty in Δ, 10,000 random realizations of $\hat{P}_{ASW}$ were similarly generated by resampling with replacement from the 144 30-min segments during the ASW exercise. Each of the before and during bootstraps were paired, and a value of Δ generated. A 95% confidence interval was generated by taking the 2.5th and 95.7th quantile of these values (the "percentile method").

For the behavioural disturbance function, a parametric bootstrap was used to obtain 10,000 random realizations of $\hat{P}_{rms}$ by simulating new parameter estimates for the smooth basis function

in the GAM assuming the parameters followed a multivariate normal distribution with mean equal to the estimated values and covariance equal to the estimated covariance matrix (Wood, 2017). These were then combined to provide 10,000 resampled estimates of the probability of disturbance as a function of RL ($\hat{P}_{d(rms)}$) with 95% confidence intervals computed by taking the 2.5th and 97.5th percentile of the resulting distribution.

3.2.11 Effect of Source Type

Differences in the reaction of beaked whales to sources with lower output levels than 53C sonar have been seen in both CEEs (DeRuiter et al., 2013) and in opportunistic studies (Falcone et al., 2017). During 2012, a number of unit level tests were conducted. These consisted of helicopter-deployed sonar, Directional Command Active Sonobuoy Systems (DICASS), or single surface ship operations which extended for less than a day. Information from these tests were used for a preliminary investigation of the response to different source types.

Data from a total of 14 dipping sonars and DICASS sonars were combined. Three separate unit-level events involving a 53 sonar were considered. Unlike the multi-ship biannual tests, the 53C events typically included one ship participating in a single-day operation that lasted four to five hours. Unlike other U.S. Navy Ranges, AUTEC is located in an enclosed basin precluding the possibility that distant sonar from ancillary operations could be simultaneously detected and confound the results. Also, AUTEC controls the water space which significantly reduces the chance of unknown vessels or acoustic sources being present.

The GVP data from the 24 hours directly ahead of the operations were combined to calculate a pre-exposure probability of response. The RL of sonar on each hydrophone was estimated using CASS/GRAB model (Weinberg and Keenan, 1996) combined with the vessel tracking data

provided by AUTEC. The RL at the assigned *Md* group centred hydrophone was used in the calculation. For this analysis, the position uncertainty for the group is approximately half the hydrophone baseline (2,000 m). For a small source within this distance, the RL for an animal at a depth of 100 m could range between ~177 dB for a source directly overhead to ~150 dB for a source at 2 km. However, the maximum RL within the dataset was 151 dB, placing the source just outside this distance. The RL reduces logarithmically with distance. For sources at a distance between 2 km to 4 km, the RL uncertainty is reduced to 6 dB (150 dB to 144 dB).

Pre-exposure GVP start data were gathered from the day ahead of the operation, divided into 30 min periods, and pooled to estimate $\hat{P}_B$. Sonar ping data were extracted from the detection archives and combined with vessel track data obtained from AUTEC. These were used to estimate the sound field for each operation. GVP starts were also extracted from the archives. The GVP starts and sonar were also divided into 30 min periods and a GAM was used to estimate the probability of a dive being detected as a function of RL ($\hat{P}_{rms}$). Finally, the probability of disturbance ($\hat{P}_{D(rms)}$) was calculated. A GLM was then fit to the estimated function.

3.3 Results

3.3.1 Multi-Ship MFAS Analysis

During the 72 h ahead of the MFAS operations, GVPs were recorded in 353 30-minute periods over the 82 hydrophones, giving a probability of a GVP being detected of $\hat{P}_B$ =0.030 (95% CI 0.026-0.034). In the subsequent 72 h during MFAS operations and gaps, GVPs were detected in 162 GVP 30-minute periods, giving a probability of a GVP detection of $\hat{P}_{MFAS}$ =0.014 (95% CI

0.012-0.016). This represents an overall decline in detections of over 50%, with Δ=0.47, and is statistically different from no change because confidence intervals on Δ do not include 1.0 (95% CI 0.38-0.58).

The 7-month baseline data from 2012 yielded 36 paired 72-hour comparisons. The mean value of Δ from these was 1.03, with values ranging from 0.51 to 1.88 (standard deviation 0.31). Hence the value observed for the multi-ship MFAS exercise was outside the range observed in the baseline dataset.

The probability of a GVP start as a function of RL is shown in Figure 3.3, which presents the probabilities on both a logit and linear scale. Estimated RLs ranged from 110 dB, with a $\hat{P}_{rms}$ of 0.0238 to 180 dB, with a $\hat{P}_{rms}$ of 0.0019. There was only one 30 min period with an RL above 170 dB, and only four with an RL below 135 dB. Estimated RLs in the 30 min periods when GVP starts were detected ranged from 125 dB to ~174 dB, and 97% of the RLs were above 135dB.

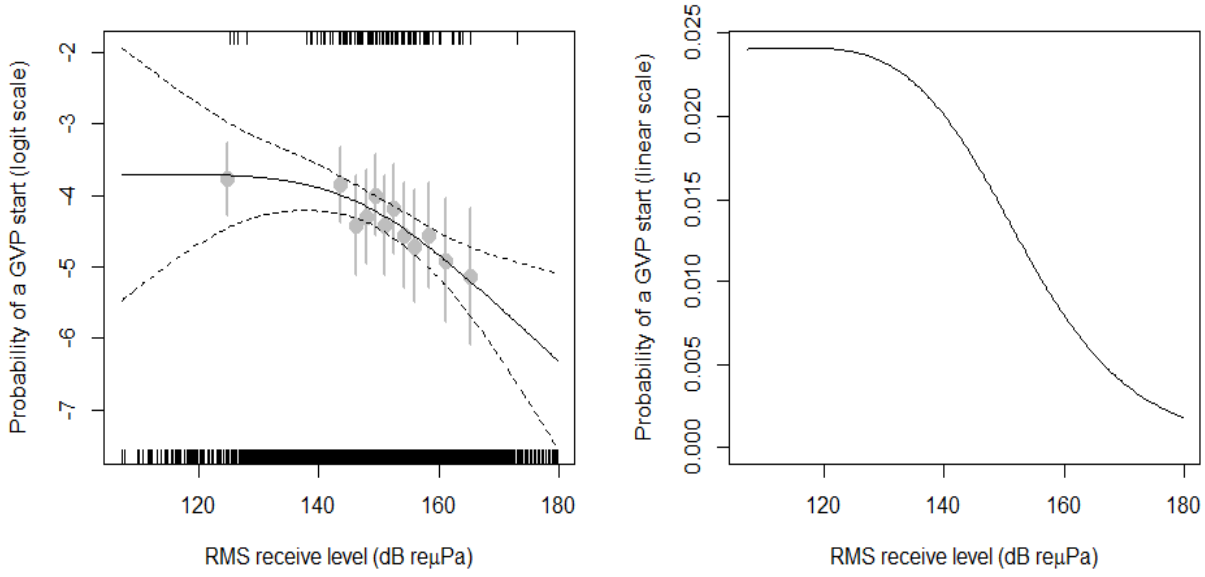

Figure 3.3 Estimated probability of detecting a GVP start as a function of maximum RL on a given hydrophone in a 30 min period plotted on a logit scale (left-hand plot) and a linear scale (right-hand plot). Dashed lines on the left plot indicate pointwise 95% confidence limits on the fitted relationship. Short vertical lines at the top of the lef-hand plot indicate the maximum RL during 30 min periods when GVP starts were detected, those at the bottom indicate the maximum RL in 30 min periods when GVP starts were not detected. The grey dots represent the proportion of 30 min periods during which a GVP start was detected, calculated using approximately 1/12th of the data going from lowest to highest RL. Grey vertical lines indicate 95% binomial confidence intervals on these proportions.

The fitted relationship between the probability of disruption of a GVP and RL is shown in Figure 3.4 (Moretti et al. 2014). There is a 50% probability of dive disruption at an RL of 149.8 dB and a probability of 0.2 at 130 dB. The confidence region becomes very wide for RL values below 130 dB.

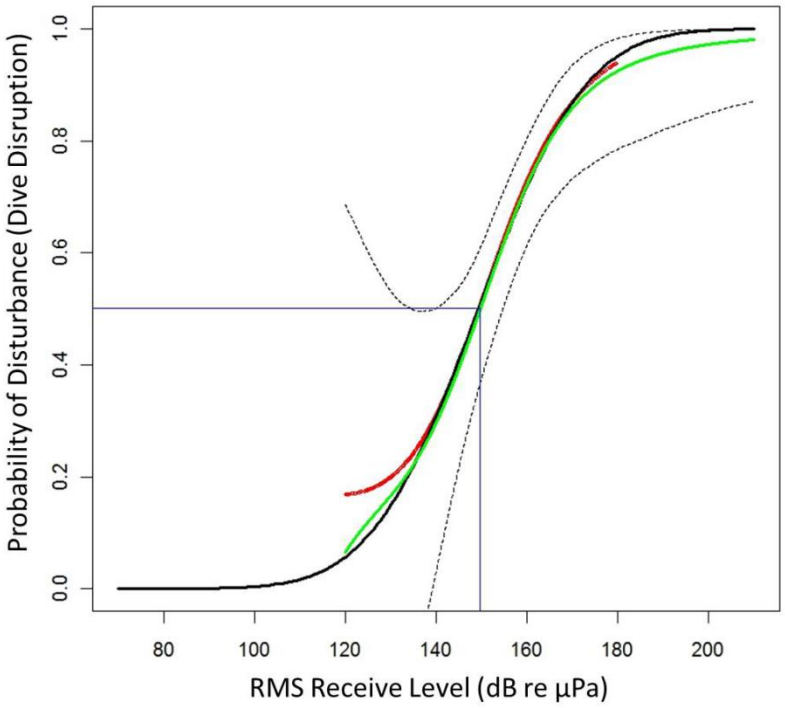

Figure 3.4 The probability of dive disruption as a function of estimated RL. The estimate from the GAM is shown in red, and the bootstrap mean is shown by the green line. Point-wise 95% confidence limits from the bootstrap are indicated by black dotted lines. The parametric GLM approximation is shown in black. The RL associated with a 0.5 probability of dive disruption (149.8 dB) is indicated in blue.

The parametric equation derived from the GLM closely approximated the GAM-based risk function. The function is given as

$$P[disturbance] = F(-8.073 + 0.05407RL_{rms}) \qquad \text{Equation 3.6}$$

where *F(z)* is the cumulative normal distribution function

$$F(z) = \int_{-\infty}^{z} \frac{1}{\sqrt{2\pi}} exp\left[-\frac{y^2}{2}\right] dy \qquad \text{Equation 3.7}$$

3.3.2 Effect of Source Type

The maximum estimated RL during operations with small source sonars was 152 dB, which equates to a source distance of approximately 2.1 km. No GVPs were detected during this time. In addition, no GVPs were detected when the source was within 2 km suggesting the probability of animals executing a deep foraging dives in these circumstances is low. In the 2007 playback at AUTEC in which the source vessel was positioned directly above, the animal stopped foraging at an RL of approximately 136 dB (Tyack et al., 2011).

The risk function obtained from observations made when a single ship was operating a 53C MFAS (Figure 3.5) is similar to the one derived from the multi-surface ship MFAS operation, with the 0.5 probability of disturbance occurring at an RL of ~150 dB. However, the data from operations that used dipping sonars and DICASS sonars indicate a 0.5 probability of disturbance at an RL of ~139 dB.

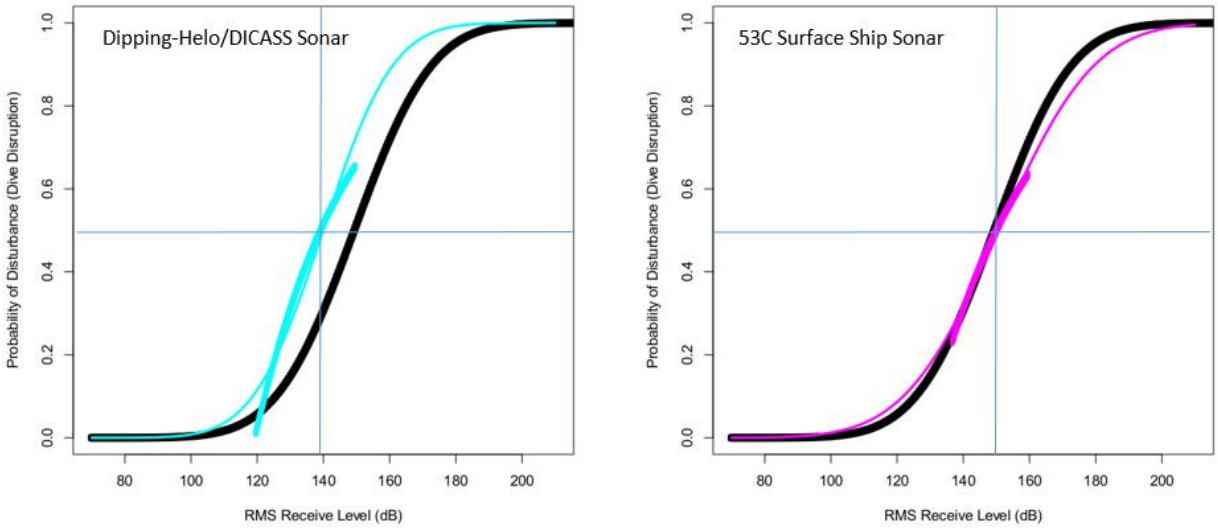

Figure 3.5 The probability of a behavioural disruption as a function of sonar RL obtained from operations involving small sonar sources (left) and from single-ship MFAS operations (right) is given by the thick blue and purple lines. A parametric GLM approximation for each is shown by the thin blue and purple lines. The risk function obtained from the multi-ship operation is shown in black.

3.4 Discussion

To meet required environmental compliance mandates, the US Navy calculates the number of behavioural takes for broad operational areas using NAEMO. In this model, simulated animals are uniformly distributed across the prescribed area, based on the best available density estimates, and sonar sources are moved through the area carrying out typical operational scenarios (U.S. Fleet Forces Command, 2008), and the associated source transmissions are modelled. The time-varying sound field is estimated using a propagation model (Weinberg and Keenan 1996) and the RL for each MFAS transmission at each simulated animal is calculated. A risk function is then used to determine whether there is a behavioural take for each ping exposure based on the estimated RL.

Figure 3.6 compares the *Md* risk function derived in this Chapter to the historic risk functions used by the U.S Navy. To investigate the effect of using these different risk functions, NAEMO was run for a typical multi-ship MFAS operation at the Pacific Missile Range Facility with a standard run geometry and 53C sonar settings. The step function shown in Figure 3.6 produced a greater number of behavioural takes than the risk function developed in this Chapter, while the Feller function produced a smaller number.

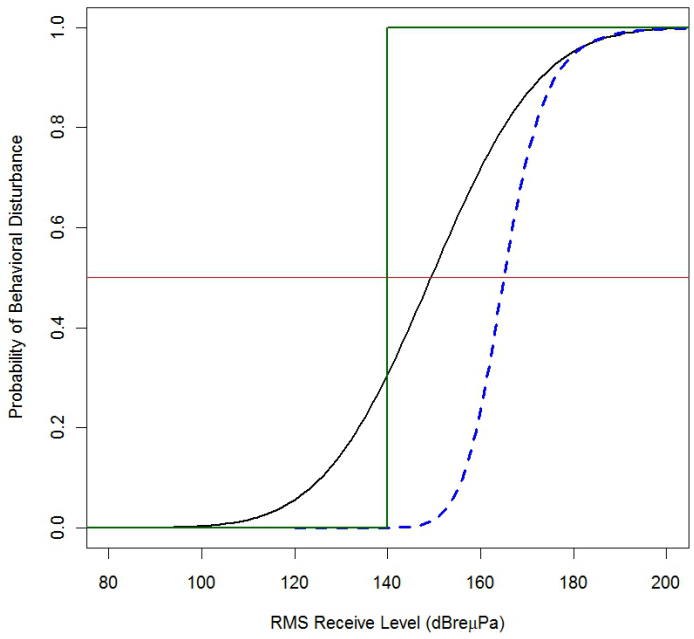

Figure 3.6 A comparison of risk functions relating the probability of behavioural disturbance to RL from sonar signals. The step function used by the U.S. Navy is shown by a green line and the historical function by a blue-dashed line. The empirical function developed in this paper is shown by a solid black line. The solid red line indicates the 0.5 probability of disturbance.

Differences in GVP detection rates observed before and after the multi-ship MFAS operation in 2009 where higher than those reported here. This could be the result of natural variation in the density of beaked whales on the AUTEC Range. Certainly, the number of GVPs detected per day before the 2009 multi-ship MFAS operation (128) is much higher than the mean values for 2011 and 2012 (68 GVPs/day) reported in Chapter 2. However, the 2009 data were extracted by manual analysis, whereas the 2011 and 2012 data were extracted using automated methods, and hence contain false positives; this may at least partly account for the difference. Nevertheless, the check that was performed on variation in count over successive 72-hour periods showed that the decline in detections associated with the sonar exercise in 2009 was outside the range observed during baseline conditions in the 2012 dataset. Future work could use the same

methods described here to analyse additional multi-ship MFAS exercises to check for consistency in response between exercises.

The *Md* risk function presented here is based on data from a multi-ship MFAS operation that took place over a five-day period and included three surface ships, dipping sonars and DICASS sonars. However, the sample of RLs was dominated by transmissions from 53C sonars. The published source level of the 53C sonar is 235 dB, while the source level of dipping sonar is approximately 220 dB and for the DICASS sonar it is 215 d B (U.S. Fleet Forces Command, 2008). Propagation modelling based on sound velocity profile on AUTEC in August, suggests that the RL for an *Md* group 20 km from a 53C sonar and at 100m depth would be approximately 143 dB. To experience the same RL from a dipping sonar, an animal would have to be within 6 km of the source. The risk curve derived from the analysis of small source operations (Figure 3.5) indicates that animals actually respond to these sources at a lower RL than for surface ship sonar. The animals may be responding to the proximity of the small source as well as the RL, echoing the results obtained with Cuvier's beaked whale (DeRuiter et al., 2013).

There are additional contextual differences that should also be considered. Typically, surface ship sonar is enabled and used over a period of several hours, and the near constant nature of the 53C transmissions over this period would provide *Md* with the opportunity to evaluate the movement of the source. By contrast, a helicopter deploying a dipping sonar will choose a spot, lower the transducer and transmit a signal for tens of minutes before moving to a different spot and repeating the procedure. This may also have contributed to the observed difference in Cuvier's beaked whale response to the two sonar types observed by (Falcone et al., 2017). DICASS sonars are deployed from an aircraft and transmit for a number of hours. They drift

with the current so that their position changes relatively slowly. It is not clear if this affects how beaked whales respond to these transmissions.

Ultimately, the use of a single risk function for all sonar types may prove too simplistic to reasonably assess the probability of behavioural disruption. Source types, operational differences, and behavioural context may all contribute to the effect of MFAS exposure. However, the *Md* behavioural risk function initially derived by Moretti et al. (2014), and updated here, is the first that describes the responses of multiple animals to an actual Navy operation. It therefore provides a more reliable basis for risk analysis and future research than functions based on the responses of small numbers of animals to small portable sources.

3.5 Contributions

The method used in this analysis was designed by the author after much discussion with the other authors of Moretti et al. (2014), in particular, Tiago Marques and Len Thomas. Data analysis contained in this chapter was conducted by the author. The R-code was written by the author with advice from Len Thomas and Tiago Marques.

MFAS start and stop times were extracted from FFT-based detection archives by Ashley Dilley. The RL values used in the analysis were estimated using a variant of the NAEMO model provided by Bert Neales. Small source data were isolated in M3R archives by Mary Lou Hedberg and run through code provided by the author. Statistical advice was provided by Len Thomas and Tiago Marques. Len Thomas was particularly helpful with the derivation of measures of uncertainty for the risk function and analysis of residuals. The criteria analysis was completed by the NAEMO modelling group using the behavioural risk function provided by the author.

Chapter 4

A Bioenergetics Model for Blainville's Beaked Whales in the Bahamas

4.1 Introduction

Since the late 1960s, Mid-Frequency Active Sonar (MFAS) operations have been conducted at the Atlantic Undersea Test and Evaluation Center (AUTEC) in the Bahamas. As documented in the preceding chapters, this area includes a small population of Blainville's beaked whale (*Mesoplodon densirostris* hereafter *Md*). For at least the last three decades, operations with surface ship sonar, helicopter-deployed sonar, and various portable devices have been undertaken multiple times per year. Past studies suggest exposure to MFAS displaces animals and disrupts foraging (Falcone et al., 2017; Manzano-Roth et al., 2016; McCarthy et al., 2011; Moretti et al., 2010; Tyack et al., 2011). This may restrict their energy intake, leading to a reduction in energy reserves, which are a convenient measure of individual health. (Fleishman et al., 2016; King et al., 2015; New et al., 2013). Disturbances that result in behavioural or physiological changes of the kind observed at AUTEC may affect vital rates (such as mother and/or calf survival and the probability of giving birth) directly, or indirectly via a change in health, as shown in Figure 4.1. Changes in health may lead to a reduction in birth rate and calf survival resulting in reduced reproductive success. As a result, repeated exposure to MFAS could affect the size and status of the local *Md* population. Understanding how changes in health, as measured by the size of an individual female's energy reserves, affect an individual's reproductive cycle and life-history is an essential step in assessing the population consequences of disturbance (PCoD).

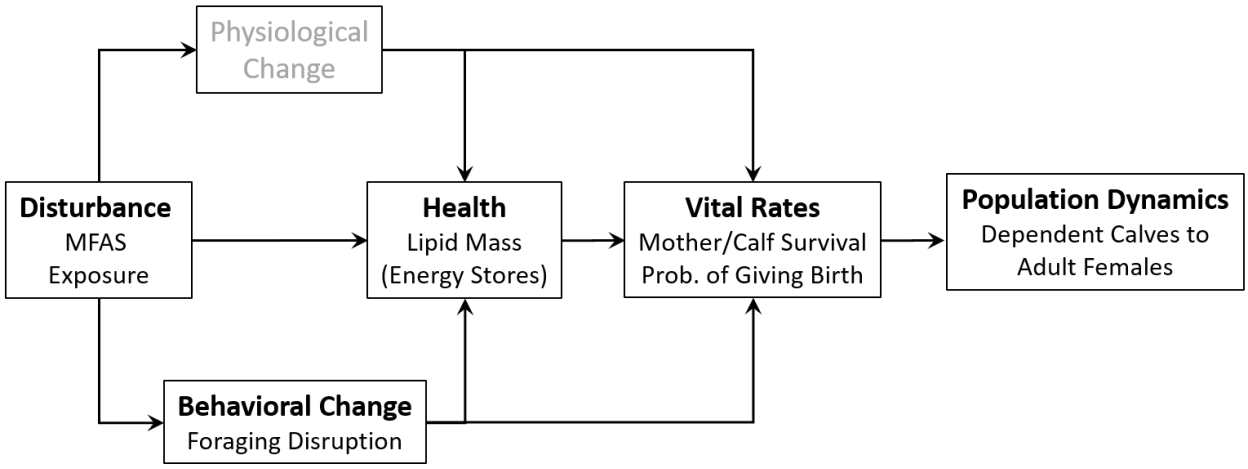

Figure 4.1 The Population Consequences of Disturbance (PCoD) framework described in Fleishman et al. (2016), adapted to illustrate the potential effects of disturbance caused by MFAS exposure on beaked whale population dynamics.

Pirotta et al. (2018) provided a decision tree for identifying the most appropriate structure for modelling PCoD. The first decision point is to determine if basic demographic rates for the population are available. *Md* in the Bahamas have been monitored for more than two decades, provided data regarding basic life history parameters (Claridge, 2013, 2006). In addition, field studies of other beaked whale species in the Ligurian Sea (D'Amico et al., 2003), Hawaii (Baird et al., 2008, 2006), the Scotian Shelf in Canada (Gowans et al., 2001; Whitehead et al., 1997) and the Canary Islands (Aguilar de Soto et al., 2012) have added to the available data, as have studies on harvested animals (Benjaminsen and Christensen, 1979; Kasuya, 1997, 1977).

The next step is to assess the availability of information on the relationship between a measure of health and individual fitness. Although studies to measure the body condition of medium-sized cetaceans as a measure of health using photographs from aerial drones (J. W. Durban et al., 2015) have commenced, no results for *Md* are currently available. In situations like these, where

there are no data on the direct effects of disturbance on individual health, Pirotta et al. (2017) recommend building a simple bioenergetics model for the population. Such models can be used to infer the potential effect on *Md* vital rates resulting from the loss of foraging dives in response to MFAS exposure. Such loss has been documented (Moretti et al., 2010) using passive acoustic methods (Jarvis et al. 2014). Model predictions can then be compared with estimates of vital rates from the local population.

Bioenergetics models have been traditionally used on terrestrial populations. For example, de Roos & Galic (2009) developed a dynamic energy model to investigate population changes in ungulates. The model suggested a pronounced effect on the survival of young animals during times of resource scarcity. More recently, bioenergetic models have been widely used to investigate the potential effects of disturbance on marine mammals (Pirotta *et al.*, 2017). Nabe-Nielsen et al. (2014) applied a bioenergetics model to a population of harbour porpoises (*Phocoena phocoena*) that inhabit inshore Danish waters to study the effect of noise, food, displacement and bycatch under multiple scenarios. New et al. (2014) investigated the population level effect of behavioural shifts in elephant seals (*Mirounga angustirostris*) driven by environmental changes using a model informed by tag data. They predicted a potential reduction in population size in the case of long-term (30 years), persistent disruption. Baleen whales have been the focus of a number of studies. Villegas-Amtmann et al. (2015) developed a bioenergetics model for grey whales (*Eschrichtius robustus*), that have a two-year reproductive cycle and used it to investigate the effect of disturbance on population dynamics. A 37% reduction in energy intake in the year in which a female gave birth resulted in the weaning of a calf at a lower mass and a delay in pregnancy. Further loss of 30-35% of energy intake in the subsequent year led to the inability of the female to become pregnant, and a 40-42% reduction

led to the death of the female. Pirotta et al. (2017) developed a stochastic dynamic state variable model to study the effect of disturbance on blue whales (*Balaenoptera musculus*). The model was used to investigate the interplay between behavioural decisions driven by changes in the environment and reproduction. The authors suggested that long-term disruption potentially driven by climate change could have a greater impact on reproduction than periodic disturbance caused by anthropogenic events. McHuron et al. (2017) articulated a PCoD framework for assessing the effect of disturbance on pinnipeds, which was then used to inform the development of a California sea lion (*Zalophus californianus*) bioenergetics model (McHuron et al., 2018). The model results suggested repetitive disturbance could negatively affect population growth, with the largest effect on pup survival. Farmer et al. (2018) developed a bioenergetics model for sperm whales (*Physeter macrocephalus*) in the Gulf of Mexico also built around the PCoD framework. They noted that studies have postulated that sperm whale foraging may be disrupted by acoustic disturbance (Curé et al., 2016; Miller et al., 2011, 2012), including seismic airguns (Miller et al., 2009) that are used extensively in the Gulf of Mexico. The model suggested the effect of disturbance is greatest for smaller females, particularly during pregnancy and lactation

Most recently, Hin et al. (in press) developed a continuous time, bioenergetics model for the effects of disturbance on North Atlantic long-finned pilot whales (*Globicephala melas*) using the Dynamic Energy Budget approach pioneered by Kooijman (2010). This uses a standard set of equations to model the energetic requirements of different life history stages that can be parameterised using information from the literature. In this Chapter, that model is modified to operate in discrete time and adapted for *Md*. In Chapter 5 this adapted model is used to examine the potential effect of disturbance associated with exposure to MFAS.

4.2 Methods

The model developed by Hin et al. (in press) tracks the way in which individual female marine mammals assimilate energy over the course of their lives from weaning to death, and how this energy is allocated to field metabolism, growth, foetal development, and lactation. Excess energy is stored in a reserve compartment (Kooijman, 2010; de Roos & Galic, 2009) primarily as fat tissue around internal organs and as blubber. The model also tracks these energy fluxes up to the age at weaning for every calf that a female produces. In this way, it is possible to examine the population consequences of different environmental conditions (including the effects of disturbance) using the expected lifetime reproductive output of each simulated female. The original model was cast as a set of differential equations and operates in continuous time. To speed calculation and more easily account for the effects of disturbance associated with MFAS use, which tends to occur on a daily scale, the model was recast as a set of difference equations with a time step of one day.

The model was parameterized with values drawn from the literature for *Md*, or an appropriate surrogate species (Table 4.1). If no suitable value from the literature was available, values from the long-finned pilot whale model were used.

Table 4.1 Summary of model parameter values and their sources

Symbol	Units	Value	Definition	Source
T_p	days	365	Duration of pregnancy	Mead 1984
T_L	days	986	Age at weaning	Claridge 2013
T_n	days	365	Calf age at which female begins to reduce milk supply	Hin et al. (in press)
T_D	days	445	Mean waiting period before onset of pregnancy	Martin & Rothery 1993
L_0	cm	189	Length at birth	New et al. 2013
L_∞	cm	450	Maximum length	Mead 1984
k	$cm.day^{-1}$	0.00045	Von Bertalanffy growth rate	Bloch et al. 1993
	$kg \cdot cm^{-1}$	$6.339x10^{-6}$	Structural mass-length scaling constant	New et al. 2013
	–	3.081	Structural mass-length scaling exponent	New et al. 2013
ω_M	–	0.2	Relative metabolic cost of reserves	Hin et al. (in press)
ρ	–	0.3	Target body condition	Lockyer (1993)
ρ_S	–	0.15	Starvation threshold	Lockyer 1993
μ_S	-	0.2	Starvation mortality scalar	Hin et al. (in press)
φ_L	-	2.7	Lactation scalar	Lockyer 1993
η	–	15	Steepness of assimilation response around target body condition	Hin et al. (in press)
γ	–	2	Shape parameter for relationship between resource assimilation and age	Hin et al. (in press)
T_R	days	500	Age at which calf's foraging efficiency is 50%	Hin et al. (in press)
ξ_M	–	–2	Shape parameter for relationship between milk provisioning and female body condition	Hin et al. (in press)
ξ_C	–	0.25	Shape parameter for relationship between milk assimilation and calf age	Hin et al. (in press)
σ_M	-	0.75	Field metabolic rate scalar, equivalent to 2.5x Basal Metabolic Rate according to Kleiber's 1975 equation	New et al. 2013
σ_G	$MJ \cdot kg^{-1}$	30	Energy costs per unit structural mass	Hin et al. (in press)
σ_L	–	0.86	Lactation efficiency	Lockyer 1993
ε^+	$MJ \cdot kg^{-1}$	55	Anabolic reserves conversion efficiency	Hin et al. (in press)
ε^-	$MJ \cdot kg^{-1}$	35	Catabolic reserves conversion efficiency	Hin et al. (in press)

4.2.1 Resource characterisation

Energy flux depends on resource density (R in MJ.m^{-3}) and the state of the individual. To avoid having to account for differences in energy density, catchability, and digestibility among prey, and differences among individual whales in their ability to assimilate energy from these prey, the resource is characterised in terms of the amount of assimilated energy it can provide to a female. Although it would be impossible to measure resource density defined in this way, it provides a useful qualitative measure of environmental quality, with high resource density indicating high quality environments, and low resource density associated with poor environments. The amount of energy assimilated per day will depend on the volume searched by an animal each day. For simplicity, we assume this is constant over time.

4.2.2 States

Individual females are characterised by their age (t in days), structural size (length, L_t and core body mass S_t), reserve mass (F_t), total mass ($W_t = S_t + F_t$), maintenance mass ($S_t + \omega_M F_t$, which accounts for the different costs of maintaining core tissue and reserves), and reproductive state. Relative body condition (ρ_t) is defined as reserve mass/total body mass (F_t / W_t). Females can be in one of five states:

- 'resting' (i.e. neither pregnant nor lactating, this includes the juvenile period from weaning to first conception),
- 'waiting' (females that are able to become pregnant but have not yet ovulated),
- 'pregnant',
- 'lactating', and
- 'waiting & lactating'.

4.2.3 Survival and Life Expectancy

Hin et al. (in press) used detailed information from (Bloch, 1993) on the age-structure of the Northeast Atlantic long-finned pilot whale population to calculate an age-dependent mortality schedule (Figure 4.2), and a matching cumulative survival curve (Figure 4.3). This curve matches well with the survival rates for juvenile and adult *Md* estimated by Claridge (2013) and is used here. It is composed of background mortality that is constant with age, elevated juvenile mortality that decreases with age, and senescence mortality that increases with age. Thus, mortality is high during the animal's early years, reaches a minimum as a young adult, and increases with age (Figure 4.2).

As discussed in Chapter 1, few data exist on life expectancy in beaked whales. Benjaminsen and Christensen documented a 37-year-old northern bottlenose whale (*Hyperoodon ampullatus*) among 54 animals examined, and Kasuya (1977) reported a maximum age of 50 years for Baird's beaked whale (*Berardius bairdii*). On this basis, it was assumed that no *Md* would survive beyond its 50^{th} birthday.

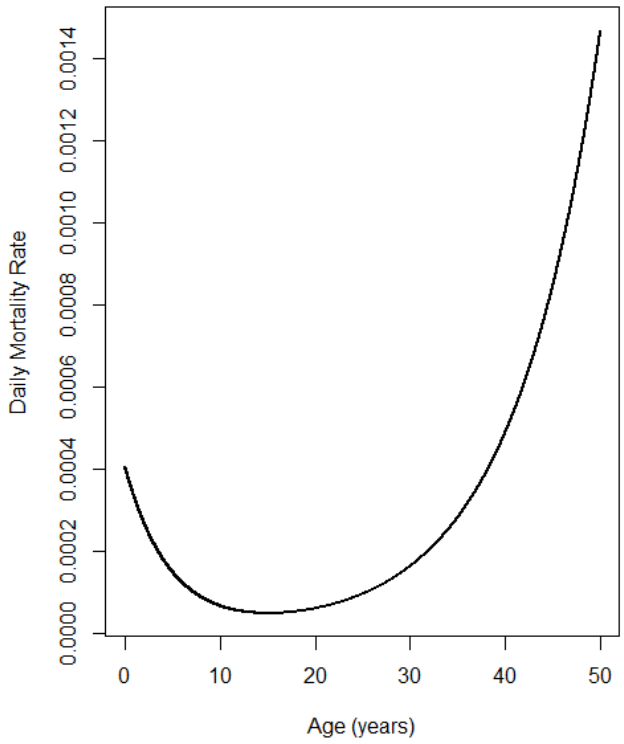

Figure 4.210 Age-dependent mortality schedule for Northeast Atlantic long-finned pilot whales (data from Bloch 1993), used here for Blainville's beaked whale.

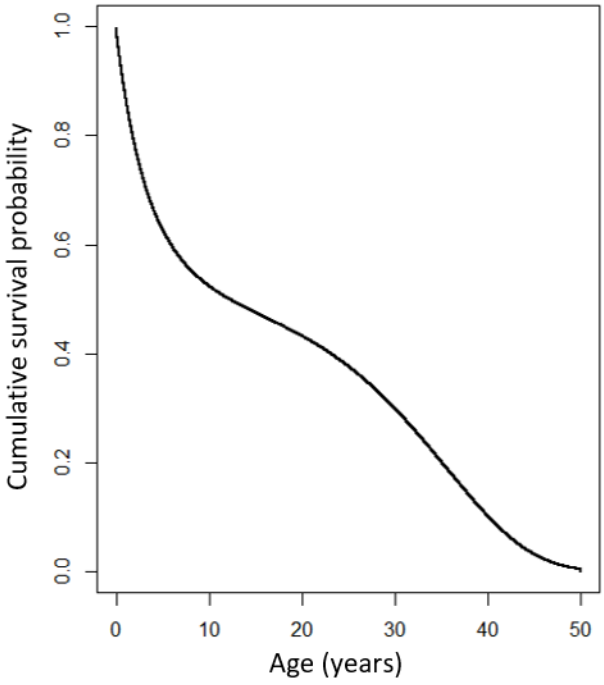

Figure 4.3 Cumulative survival probability for Northeast Atlantic long-finned pilot whales (data from Bloch 1993), used here for Blainville's beaked whale.

The life expectancy of each simulated individual is set by drawing a random number between 0 and 1. Death is presumed to occur at the age when the cumulative survival probability shown in Figure 4.3 falls below this value. This process ensures that the simulated individuals represent a random sample of all possible female life histories, and so their mean reproductive success can be used as an estimate of the population growth rate.

In addition to background mortality, simulated females and calves suffer from an increased risk of mortality if their relative body condition falls below a pre-defined starvation threshold (ρ_s, set at 0.15, based on the lowest values observed in long-finned pilot whales, (Lockyer 1993). Survival on each day that ρ_t is below this threshold is determined by conducting a binomial trial with the probability, ϕ_t, defined by Equation 4.1.

$$\phi_t = e^{-\mu_s(\frac{\rho_S}{\rho_t}-1)} \qquad \text{Equation 4.1}$$

where

ρ_S = starvation threshold,

ρ_t = relative body condition on day *t*, and

μ_s = strength of starvation parameter.

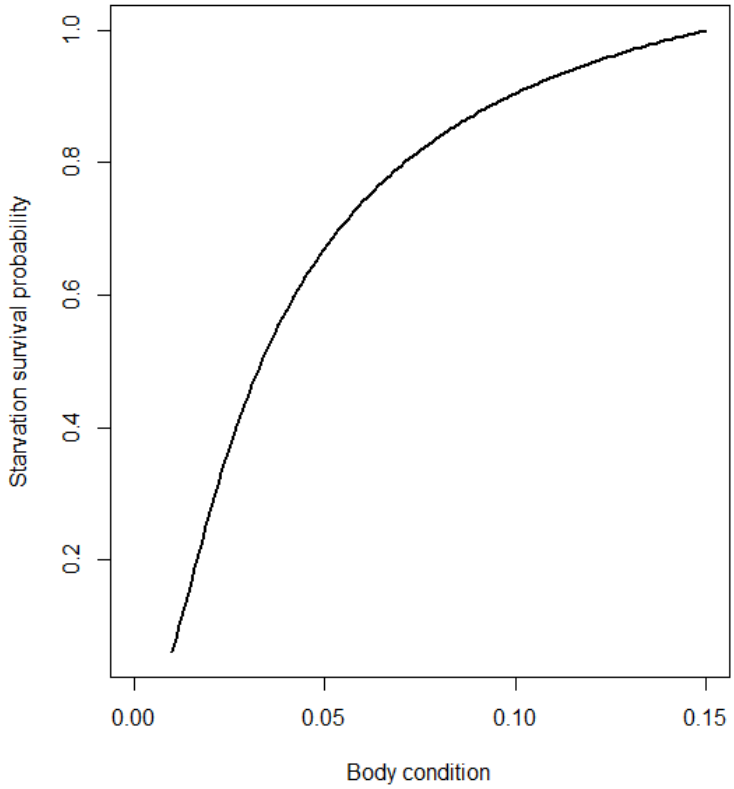

Figure 4.4 Assumed relationship between body condition and the probability of survival

The daily survival rate for *Md* foetuses was assumed to be constant at 0.9994 over the course of pregnancy, equivalent to a 20% mortality overall. This was based on a report of a 17% failure rate for pregnant bottlenose dolphins (*Tursiops truncatus*) in Sarasota Bay, Florida (Wells et al. 2014).

4.2.4 Growth

Following Hin et al. (in press), growth is modelled using the von Bertalanffy growth curve:

$$L_t = L_\infty - (L_\infty - L_0).e^{-kt} \qquad \text{Equation 4.2}$$

where L_t is the length at age t (in days). The maximum length (L_∞) of 471 cm for *Md* was taken from Mead (1984). This is 51 cm larger than the longest of seven animals recorded by the

Smithsonian Museum of Natural History (Table 4.2). The length at birth (L_0) was taken from New et al. (2013) and is calculated as 0.42 x L_∞. A growth rate (k) of 0.000327, as estimated for long-finned pilot whales by Bloch et al. (1993), was used. The resulting growth curve is shown in Figure 4..

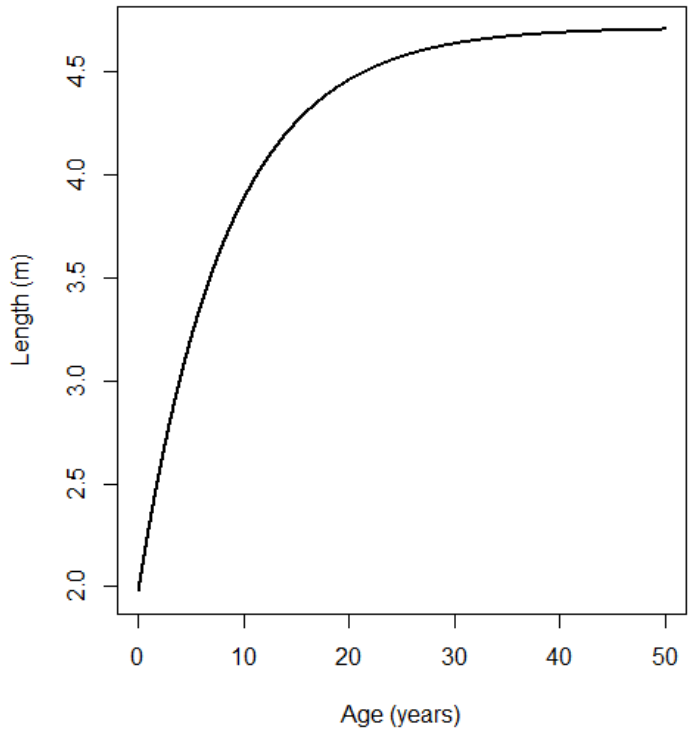

Figure 4.5 Von Bertalanffy growth curve for Blainville's beaked whales.

Structural mass (S_t) at age was estimated using the relationship

$$S_t = (6.339 \times 10^{-6}) L_t^{3.081} \qquad \text{Equation 4.3}$$

where L_t is the length at age t, and the mass-length scaling constant and exponent for Baird's beaked whale were applied (New et al. 2013). This gave predicted masses at length for females similar to those reported for *Md* (Table 4.2).

Table 4.2. Length and weight measurements for seven live stranded Blainville's beaked whales courtesy of the Smithsonian Museum of Natural History

Date Collected	Ocean	Location	Sex	Length (cm)	Weight (kg)	Predicted Weight (kg)
3/4/1975	North Atlantic	North Carolina	Female	397	850	644
9/21/2001	North Atlantic	North Carolina	Female	196	86	73
5/16/1986	North Pacific	Okinawa	Male	369	646	514
2/14/1986	North Atlantic	New York	Male	420	781	766
7/13/1984	North Atlantic	North Carolina	Female	411	670	717
10/17/1997	North Atlantic	Florida	Male	403	1210	674
4/20/1998	North Atlantic	New Jersey	Female	361	545	481

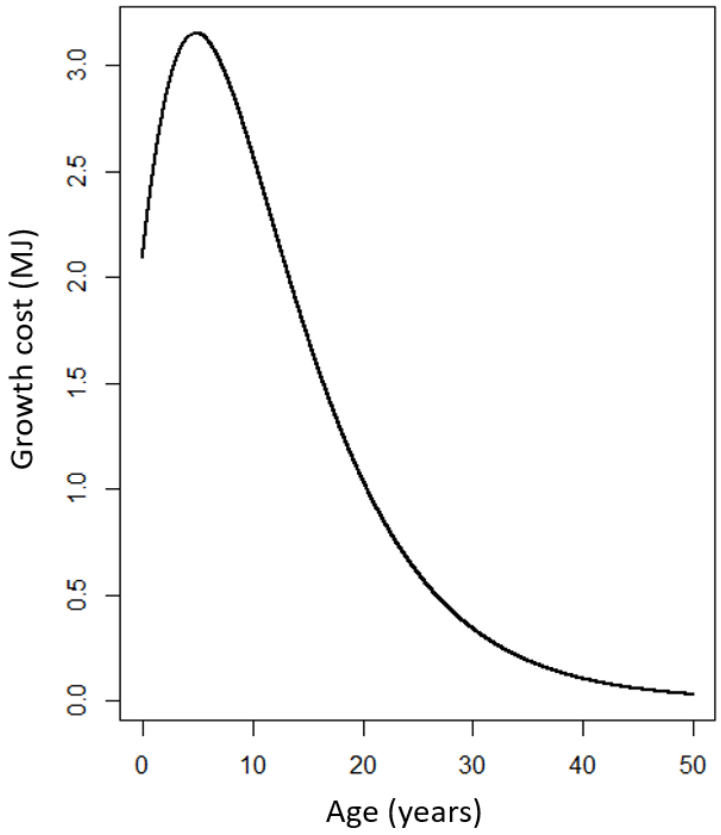

Figure 4.6 Daily cost of structural growth in MJ from birth to maximum life expectancy.

Growth in foetal length is assumed to be linear so that the foetus grows at a constant rate from length 0 cm at conception to L_0 at the end of the gestation period (T_p = 365 days). The structural mass of the foetus is estimated using the same mass-length relationship as that was used for females. As a result, the structural mass of the foetus increases exponentially over the course of pregnancy.

The daily cost of growth is calculated as the difference in structural mass between consecutive days multiplied by the energy cost per unit of structural growth (σ_G = 30 MJ.kg^{-1}). Figure 4.6 shows the daily cost of growth over the lifetime of a female, and Figure 4.7 shows the same costs for the foetus.

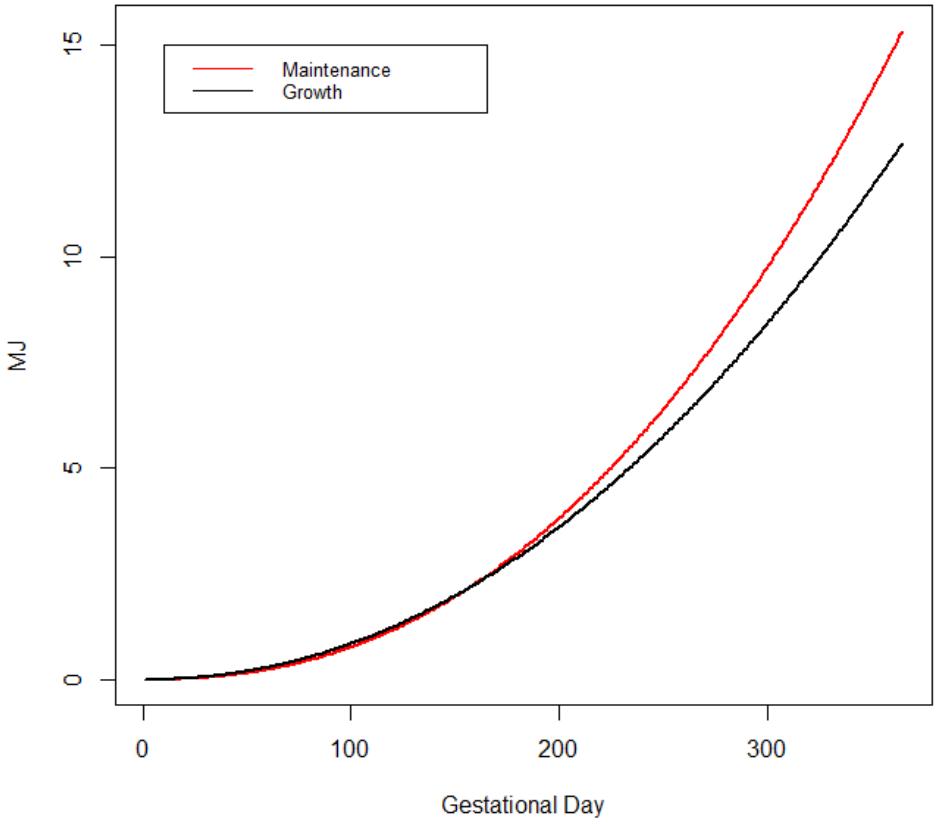

Figure 4.7 Daily cost of foetal growth (black) and maintenance (red) in MJ.

4.2.5 Maintenance

Daily field metabolic costs (FM_t) are assumed to be a multiple (σ_M) of the animal's maintenance mass to the power ¾, following Kleiber (1975):

$$FM_t = \sigma_M .(S_t + \omega_M F_t)^{3/4} \qquad \text{Equation 4.4}$$

Following New et al. (2013), σ_M is assumed to be 0.75, equivalent to 2.5 x Basic Metabolic Rate. For pregnant females, the mass of the foetus is included in the maintenance mass, so the cost of foetal maintenance (Figure 4.8) is included in her maintenance costs.

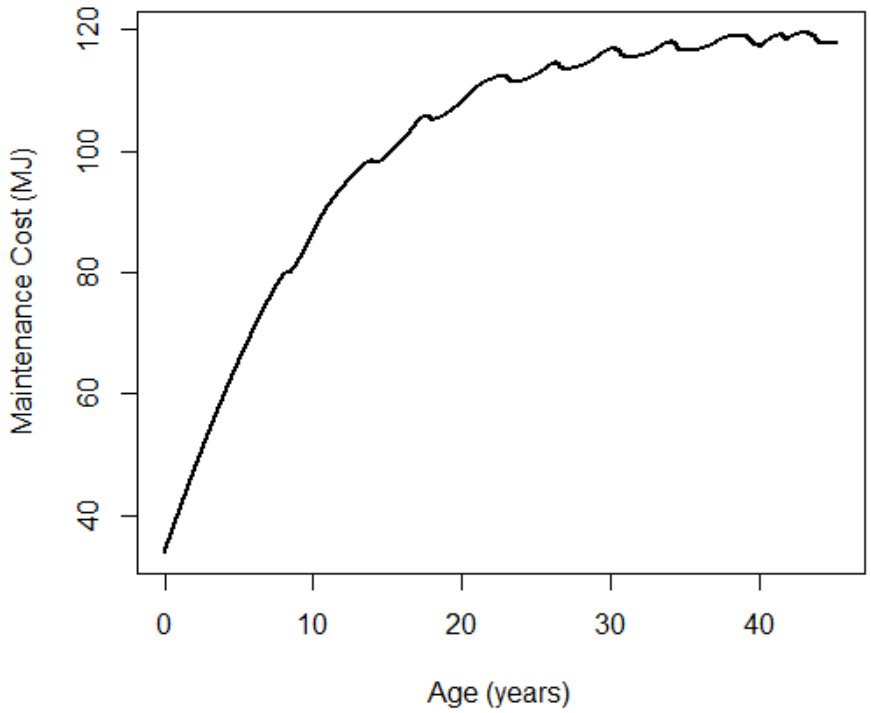

Figure 4.8 The daily cost of maintenance in MJ over a female's lifetime. The "ripples" correspond to pregnancies, which increase a female's effective maintenance mass.

4.2.6 Resource Feeding

The amount of assimilated energy obtained from feeding each day depends on the resource density (*R*), which is assumed to be constant over time, the structural size of the animal to the power 2/3 (i.e. $S_t^{2/3}$, following Kooijman 2010), and the individual's body condition (ρ_t). Individuals are assumed to assimilate energy at the maximum possible rate when their body condition is close to the threshold for starvation (ρ_s), and reduce their intake as their body condition approaches a maximum threshold (ρ = 0.3, based on data from pilot whales, and the assumption that deep-diving *Md* should, like pilot whales, aim to be slightly negatively buoyant - Aoki et al. 2018). This relationship also allows animals to compensate for the effect of lost foraging opportunities on their relative body condition by increasing energy assimilation on subsequent days, provided sufficient resources are available. Energy assimilation on day *t* (I_t) is therefore described by following equation.

$$I_t = \frac{R \cdot S_t^{2/3}}{1 + e^{-\eta_f \cdot \left(\frac{\rho}{\rho_t} - 1\right)}} \qquad \text{Equation 4.5}$$

where

η_f = shape parameter,

ρ = target condition index, and

ρ_t = body condition on day *t*.

Figure 4.9 shows the assumed relationship between relative body condition and energy assimilation.

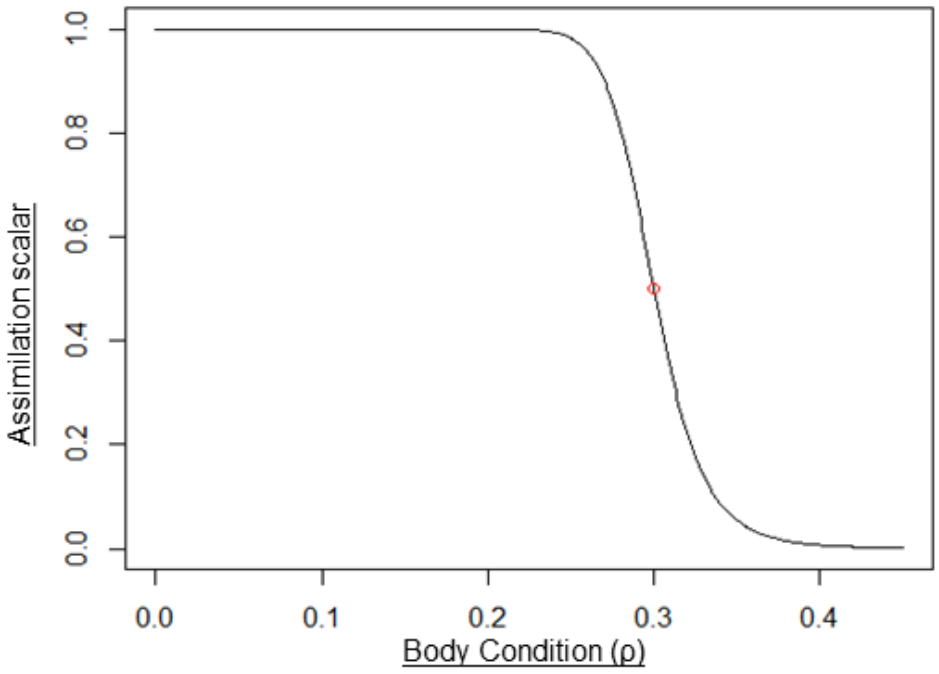

Figure 4.9 The assumed effect of relative body condition on energy assimilation

It is assumed that calves have poor foraging skills at birth but that these increase with age until they reach an asymptote. This is modelled with the function:

$$\zeta_t = t^{\gamma/(T_R^{\gamma}+t^{\gamma})} \qquad \text{Equation 4.6}$$

where ζ_t is foraging efficiency on day t, γ is a shape parameter (arbitrarily set to 2), and T_R is the age at which the calf achieves a foraging efficiency that is 50% of an adult's. Figure 4.10 shows the function while Figure 4.11 illustrates the change over time in the calf's energy assimilation from its own foraging.

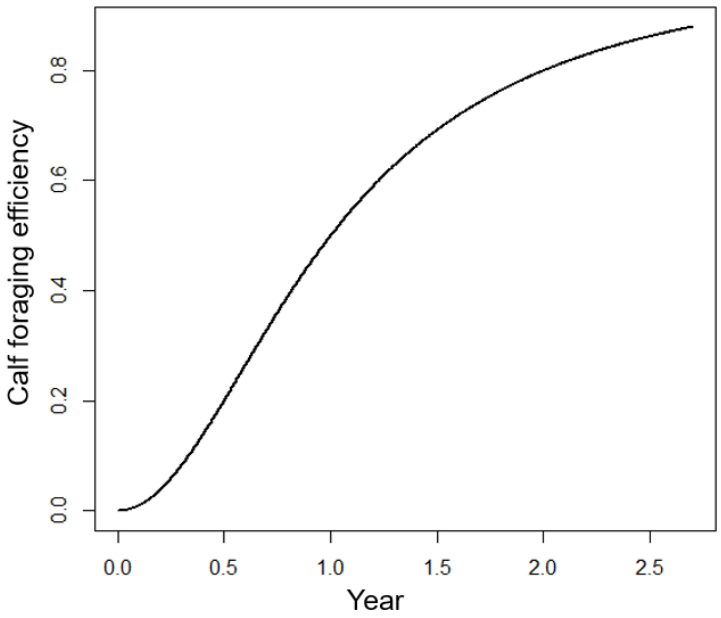

Figure 4.10 Assumed changes in a calf's foraging efficiency from birth to weaning. The calf is assumed to attains 50% foraging efficiency when it is one year old.

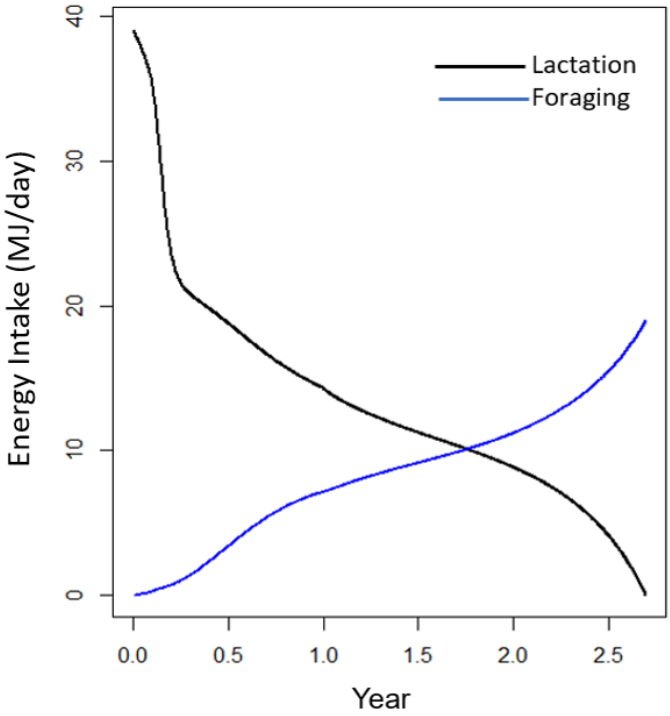

Figure 4.11 Daily assimilation of energy via milk (black line) and via foraging (blue) for a calf from birth to weaning. Energy assimilation from milk is also reflected in the energetic costs of lactation for the calf's mother.

4.2.7 Milk Consumption

The amount of energy obtained by the calf from milk is determined by its structural size to the power 2/3 (as is the case with the energy it obtains through foraging) multiplied by a scalar (φ_L) that reflects the energy density of milk, and by its body condition (using the same function - Equation 4.2 - as for resource intake). Provided the female is in good body condition (i.e. $\rho_t \simeq 0.3$), she provides all of the calf's requirements during the first 12 months of its life. After this time, the proportion of the calf's requirement provided by the female falls monotonically to zero at weaning (Figure 4.12).

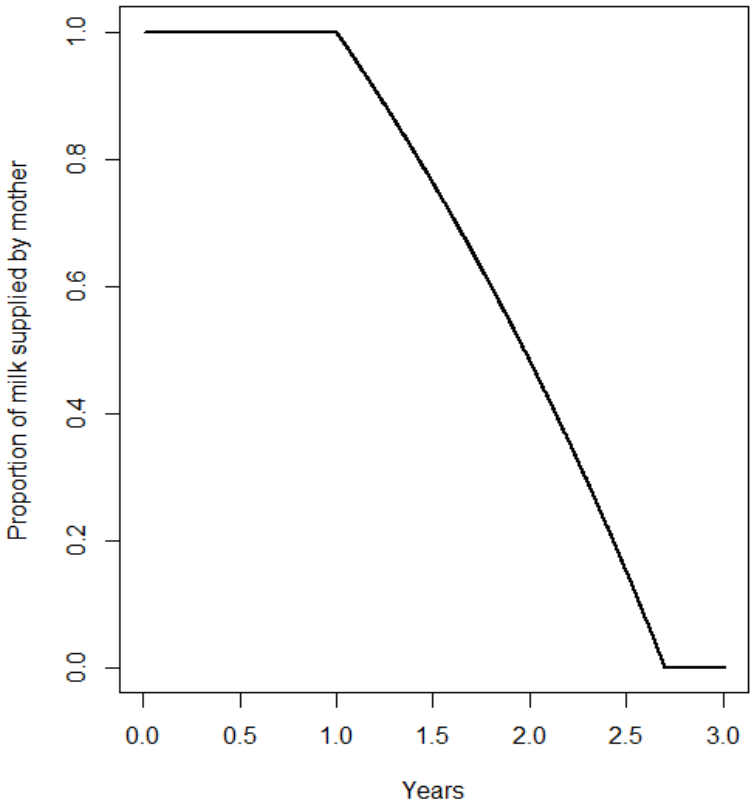

Figure 4.12 Variation in the proportion of the calf's milk requirement supplied by its mother over the course of lactation.

At any time during lactation, the female may reduce the amount of milk she supplies to her calf if her body condition has fallen below ρ. This is determined by Equation 4.7 and illustrated in Figure 4.13.

$$\eta_t = (1 - \xi_m)(\rho_t - \rho_s)/((\rho - \rho_s) - \xi_m(\rho_t - \rho_s)) \qquad \text{Equation 4.7}$$

where η_t is the milk supply on day t and ξ_m is a shape parameter. As a result, females that are in poor condition may cease to provide any milk for their calves before they reach the age of weaning (T_L).

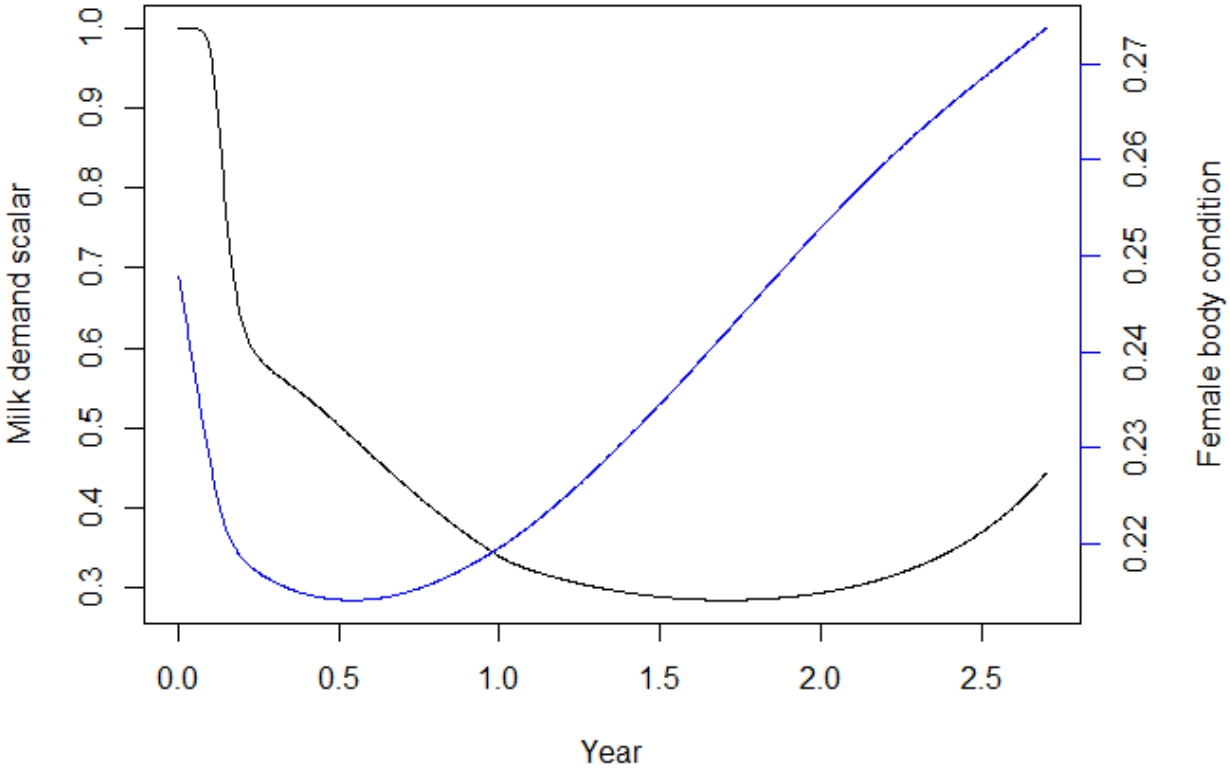

Figure 4.13 Variation in the proportion of calf's demand for milk (black) that is supplied by its mother as a function of her relative body condition (blue) from birth to weaning.

An efficiency parameter (σ_L) is used to take account of the fact that the energetic cost to the female of supplying milk must include the efficiency with which she can create milk (assumed to be 0.9 by Hin et al., in press), and the efficiency with which her calf can assimilate energy from milk (assumed to be 0.95 by Hin et al., in press).

4.2.8 Reserve Mass Dynamics

The energy reserves of the female and her calves function as a buffer for incoming and outgoing energy flows (De Roos and Galic, 2009). If assimilated energy on a particular day exceeds energy expenditure, the surplus energy can be converted to reserves, the parameter ε^+ takes account of the costs of creating reserve tissue and its energy density. If energy expenditure exceeds energy assimilation, the balance is provided by catabolizing reserve tissue, with each kg of tissue providing ε^- MJ.

4.2.9 Reproduction

A female is assumed to be capable of becoming pregnant if her reserve mass is sufficient to cover the energetic costs of foetal growth and maintenance, and to avoid any starvation mortality. Females are not allowed to become pregnant before the age of four years since this has never been observed in *Md*. Similarly, females are not allowed to become pregnant early in lactation to avoid the possibility that a female may give birth to a calf while she is still lactating.

In order to become pregnant, a female must also ovulate successfully and this ovum must be fertilized. No data on the ovulation rate for beaked whales are available. However,(Martin and Rothery, 1993) found that long-finned pilot whales only ovulate, on average, once per year and that each ovulation has a 0.82 probability of being successfully fertilized. These data were used to model the onset of pregnancy as a stochastic process with a daily probability of 0.82/365. This

resulted in a mean waiting time between the day on which a female's reserve mass crossed the threshold for pregnancy and the onset of pregnancy of 405 days and a 95% CI of 25-1211 days,

During pregnancy, females must cover the costs of foetal growth and foetal maintenance, as described in sections 4.2.4 and 4.2.5. In addition, females are assumed to transfer energy to their foetus to allow it to build up sufficient reserves so that its relative body condition is at the threshold for starvation mortality (ρ_s) at parturition.

The energetic costs of lactation are determined by the demands of the calf and the body condition of the female. They are particularly high during the first year (Figure 4.12) as the female is providing all of the energy the calf needs for maintenance and growth, plus sufficient energy for the calf to increase its reserves so that its body condition approaches the maximum permitted value (Figure 4.14).

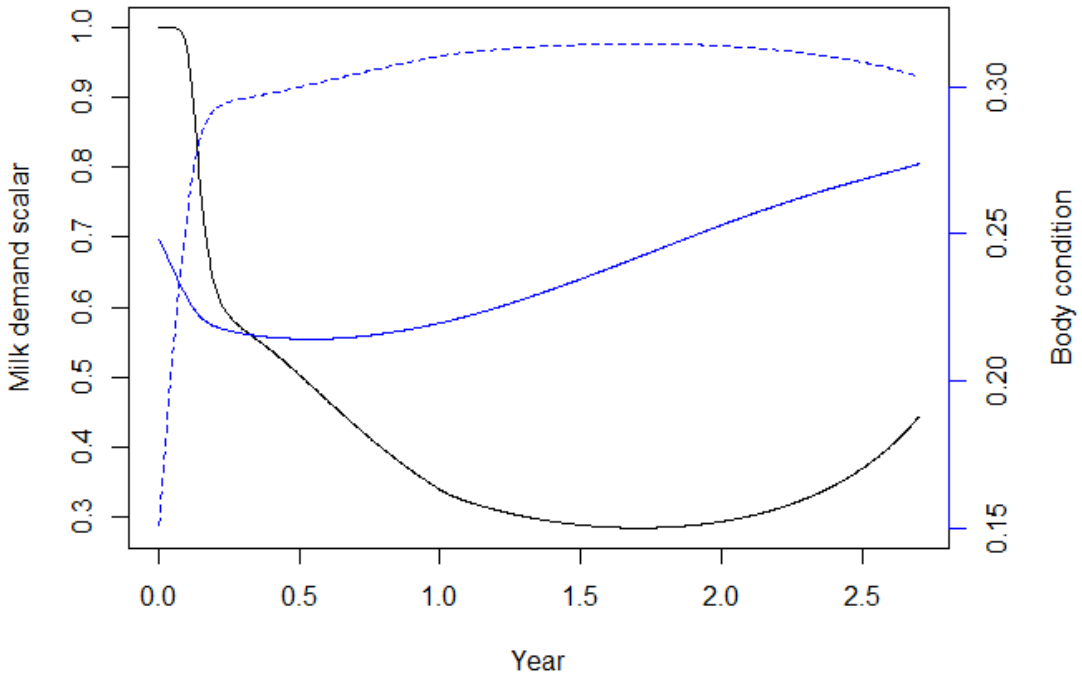

Figure 4.14 Predicted changes in the relative body condition of a calf (dashed blue line) and its mother (solid blue line) from birth through weaning. The calf's milk demand from birth to weaning is shown by the black line.

4.2.10 Model outputs

The *Md* bioenergetics model was used to identify those periods during the lives of a female and her calves when energy requirements are likely to be particularly high, and therefore they are likely to be most vulnerable to disturbance that disrupts foraging. In addition, it was used to determine the effects of different resource densities on a set of population characteristics that could also be measured from free-ranging animals.

Reproductive success

Reproductive success (*Sr*) was defined as the number of female offspring (assuming a 50:50 sex ratio) that were raised to weaning age by each simulated female during her lifetime.

Population growth rate

The annual growth rate (λ) of a population composed of females with the life histories in a particular simulation scenario can be estimated as

$$\lambda = S_r^{1/\bar{E}} \qquad \text{Equation 4.8}$$

where *E* is mean life expectancy in years.

Calf to adult (CA) ratio

Information on the ratio of calves to adult females is available from the *Md* population at AUTEC and from an MFAS undisturbed population off Abaco in the Grand Bahamas (Claridge, 2013). Claridge (2013) defined adult females as those animals that were at least 9 years old, and this definition was used to calculate the CA ratio for the simulated populations. A sample of 10 females (the average number of adult females observed each year by Claridge (2013)) was drawn from all the simulated females that were predicted to survive until age 9 years. A random day between each animal's 9th birthday and its death was selected and the simulation was checked for

the presence of a calf on that day. This was repeated 1,000 times to estimate the sampling variance.

Mean age at maturity

The age at which each simulated female gave birth to her first calf was identified, and her age at maturity estimated by subtracting the duration of gestation (assumed to be 365 days) from this value, thus mimicking the approach used by Claridge (2013).

The effects of resource density on population characteristics were evaluated by simulating 1,000 females for each resource scenario. Although 95% confidence intervals were calculated for most of these outputs, they are (with the exception of CA ratio which takes account of observational sample size) unrealistically narrow because all simulated females followed identical growth curves and encountered exactly the same resource density each day. In reality, there would be much more variation than this.

4.3 Results

The life histories of three females that reached the maximum life expectancy of 50 years at three different resource densities are shown in Figure 4.15. At the highest resource density (1.4 $MJ \cdot m^{-3}$), nine calves were successfully weaned and two died as a result of background mortality. The fate of the final calf is unknown as the female died when reaching her maximum life expectancy (50 years). Female body condition declined slightly during each pregnancy, and markedly during the first year of lactation. The mean value of the minimum female body condition for each calving cycle is 0.24 (95% CI 0.23-0.25) with the lowest value (0.20) reached during the first calving cycle (Figure 4.15A). Maternal body condition then recovers as the calf becomes less dependent on its mother, but the time taken to recover to the maximum observed

body condition of 0.28 was longer for the first two calves. The mean ICI is 3.06 years (95% CI 2.53-3.54) with a minimum of 1.69 years between pregnancies.

Figure 4.15 A: $\bar{R}$ =1.4 MJ·m^{-3}

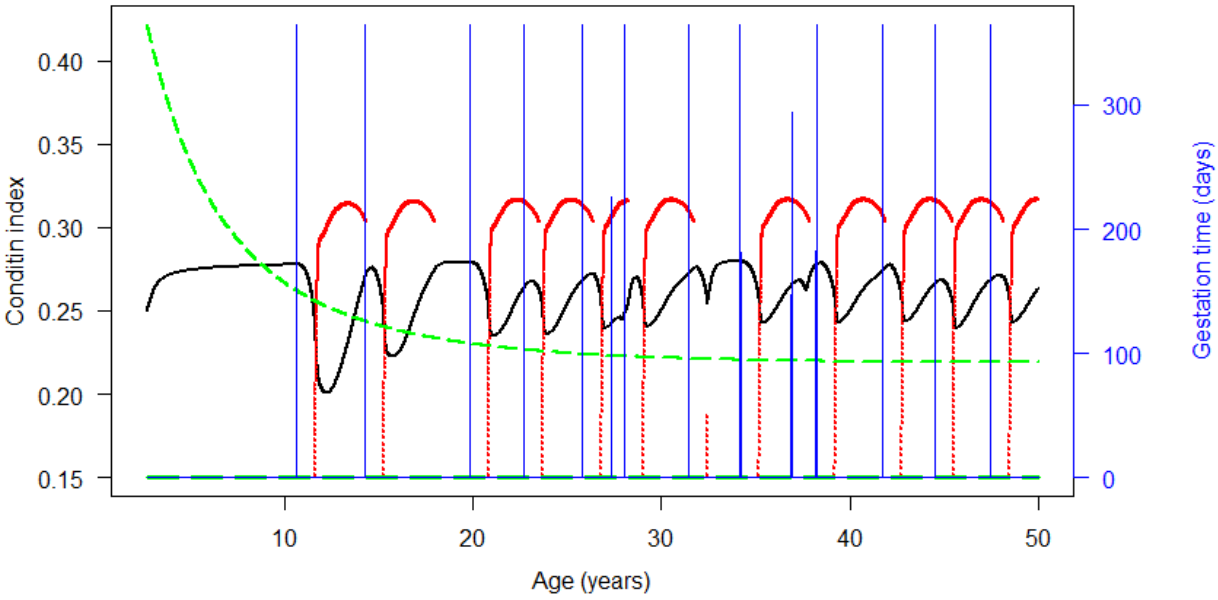

Figure 4.15 B. $\bar{R}$ =1.3 MJ·m^{-3}

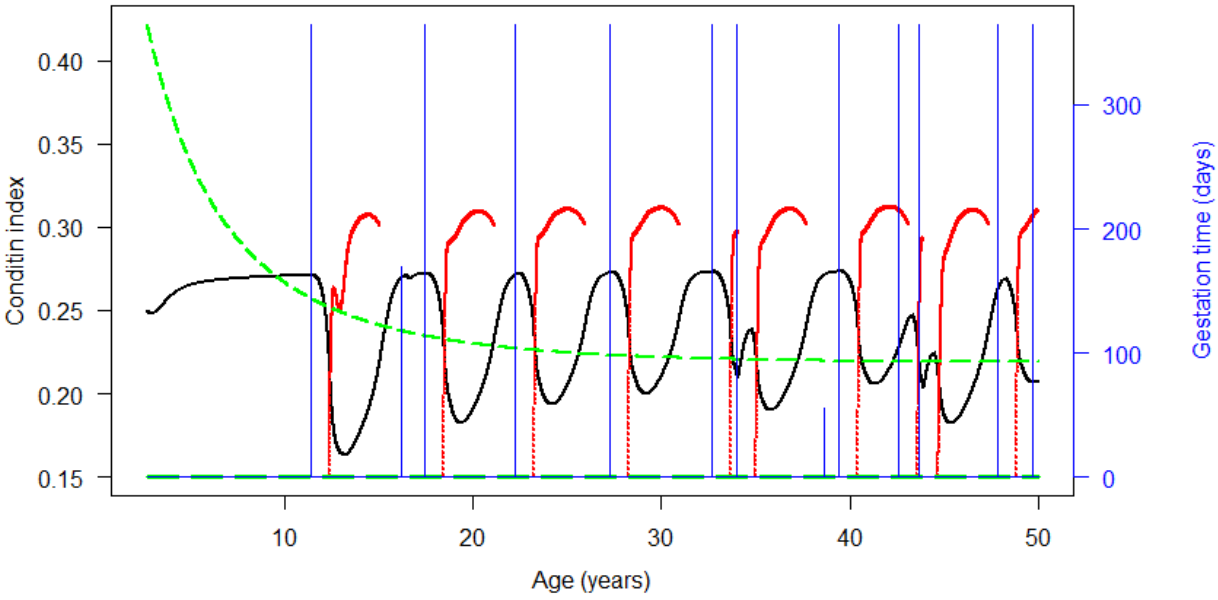

Figure 4.15 C: $\overline{R}$ = 1.2 MJ·m^{-3}

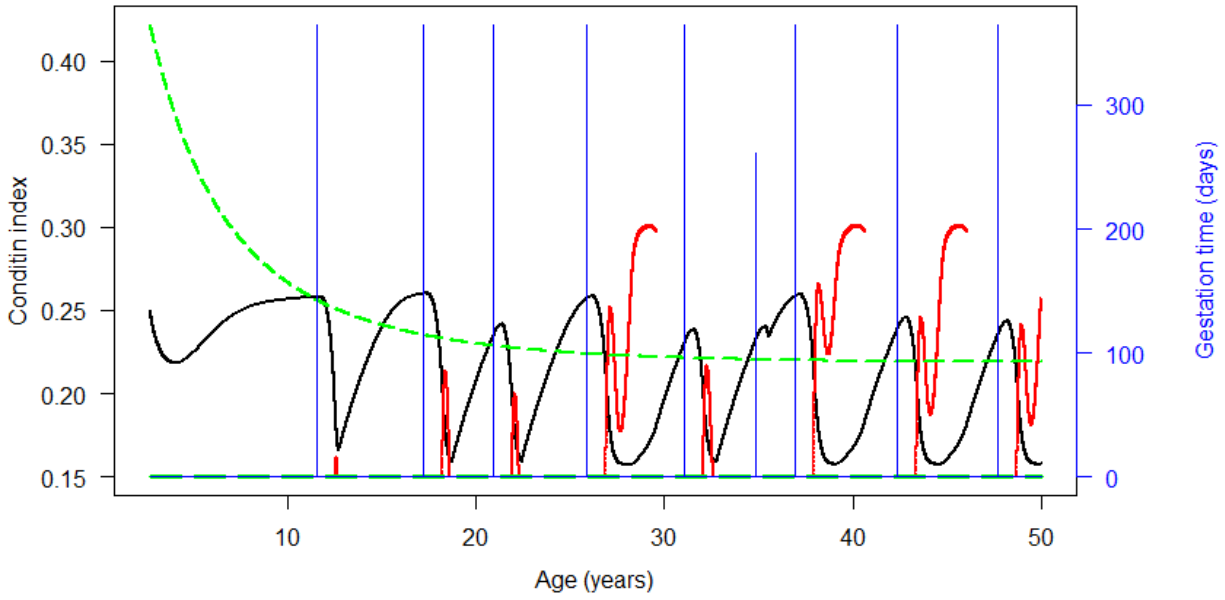

Figure 4.15 A-C. Life histories of a female that survives to age 50 at three different resource densities. The relative body condition of the female is shown in black and the body condition of each calf is shown in red. The threshold for pregnancy is given by the light green dashed line. The starvation threshold is shown by the dashed, dark green line. The days on which a foetus was conceived are shown by vertical blue lines whose height is equal to the number of days that the foetus survived

At an intermediate resource density of 1.3 MJ·m^{-3} (Figure 4.15B), the mean minimum body condition for each calving cycle was 0.172 (95% CI 0.155-0.190), and the lowest value of 0.157 was recorded again during the first lactation period. Nine calves were born of which seven calves were raised to weaning. The female was still nursing a calf when she reached her maximum life expectancy, so the calf's fate was undetermined. The female's recovery time increased, which resulted in a longer ICI equal to 4.06 years (95% CI 2.94-5.17).

At the lowest resource density of 1.2 MJ·m^{-3} (Figure 4.15C) eight calves were born of which three survived to weaning. The mean minimum female body condition in each calving cycle was 0.159 (95% CI 0.156-0.162), just above the starvation threshold of 0.15, with an absolute

minimum body condition of 0.157. The body condition of the three calves that survived lactation showed a marked dip when the female's condition was at its lowest. However, in each case, the calf survived to an age at which it was able to obtain sufficient energy from foraging to build its reserves. The lowest $\bar{R}$ gave rise to to the longest ICI of 5.3 years (95% CI 4.67-5.94)

The change in the minimum body condition through each calving cycle is illustrated in Figure 4.16. With $\bar{R}$ =1.20 MJ·m^{-3}, at each calving cycle the female's minimum body condition dips to just above the starvation threshold which results in a reduction in milk production, a prolonged recovery and an increased ICI.

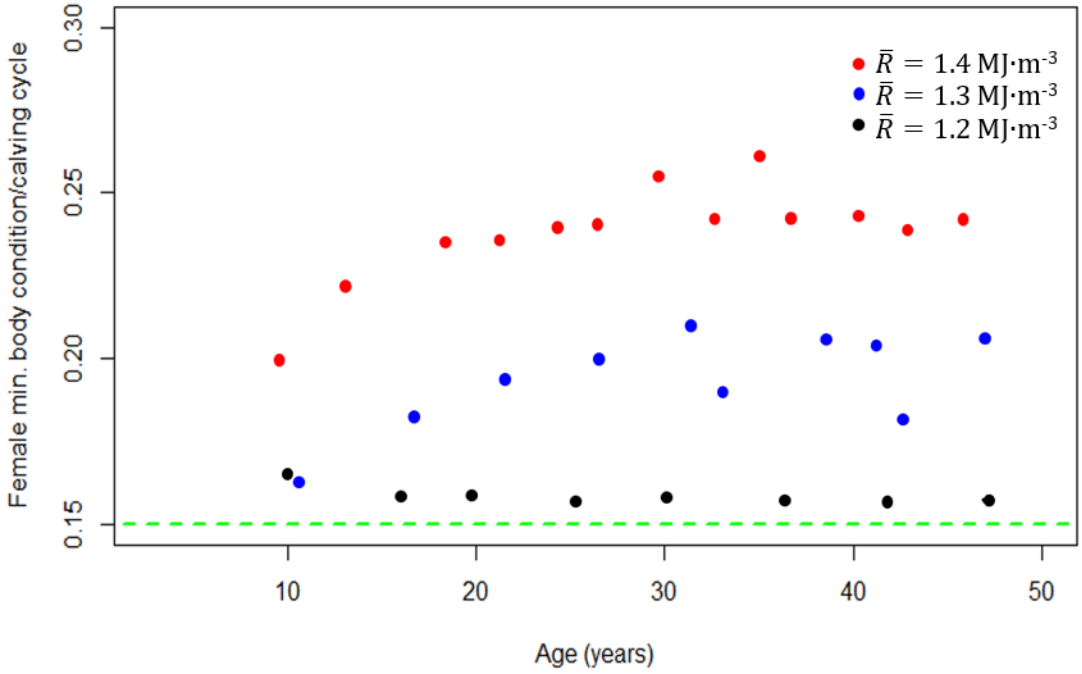

Figure 4.16 Minimum body condition during each calving cycle for a female that reached maximum life expectancy (50 years) at three different resource densities ($\bar{R}$). The starvation threshold is given by the green dashed line. Each dot represents one cycle.

Table 4.2 Model outputs as a function of Resource Density. provides a summary of the relationship between resource density and various population characteristics. With $\bar{R}$ equal to

1.32 MJ·m^{-3}, S_r = 1.033 (95% CI 0.97-1.10) and λ =1.001., i.e. there is near zero growth in the population size over time. At this value, the mean age at maturity is 11.0 years and the CA ratio is 0.46 (95% CI 0.46-0.47).

Table 4.2 Model outputs as a function of Resource Density ($\bar{R}$)

Resource Density (MJ·m^{-3})	Mean reproductive success	Annual growth rate	Mean age at sexual maturity	ICI	CA ratio	Proportion of females that calve
1.45	1.281	1.010	10.137	4.089	0.543	0.652
1.40	1.216	1.008	10.397	4.082	0.526	0.634
1.38	1.215	1.008	10.495	4.173	0.516	0.643
1.35	1.174	1.007	10.621	4.277	0.504	0.639
1.32	1.033	1.001	10.950	4.563	0.466	0.630
1.30	0.967	0.999	11.054	4.794	0.439	0.624
1.28	0.910	0.999	11.410	5.019	0.387	0.620
1.25	0.705	0.985	11.857	5.069	0.331	0.568
1.20	0.218	0.937	12.843	5.119	0.152	0.317
1.19	0.061	0.887	13.257	5.138	0.087	0.107

Increasing $\bar{R}$ to 1.4 MJ·m^{-3}, increases S_r by approximately 18% to a mean value of 1.22 (95% CI 1.14-1.29) and λ increases to 1.01. This results in a population that doubles approximately every 70 years. The mean age at sexual maturity is 10.4 years (95% CI 10.30-10.50) and the CA ratio is 0.52 ((95% CI 0.51-0.53).

Reducing $\bar{R}$ to 1.20, results in a decrease of 79% in $\bar{R}_S$ to 0.22 (95% CI 0.20-0.24) with a λ equal to 0.94 (95% CI 0.93-0.94). This would result in a population decline of approximately 50% over 12 years. The mean age at maturity is 13 years. Figure 4.17 - 4.20 illustrate the relationship between resource density and these population characteristics in more detail.

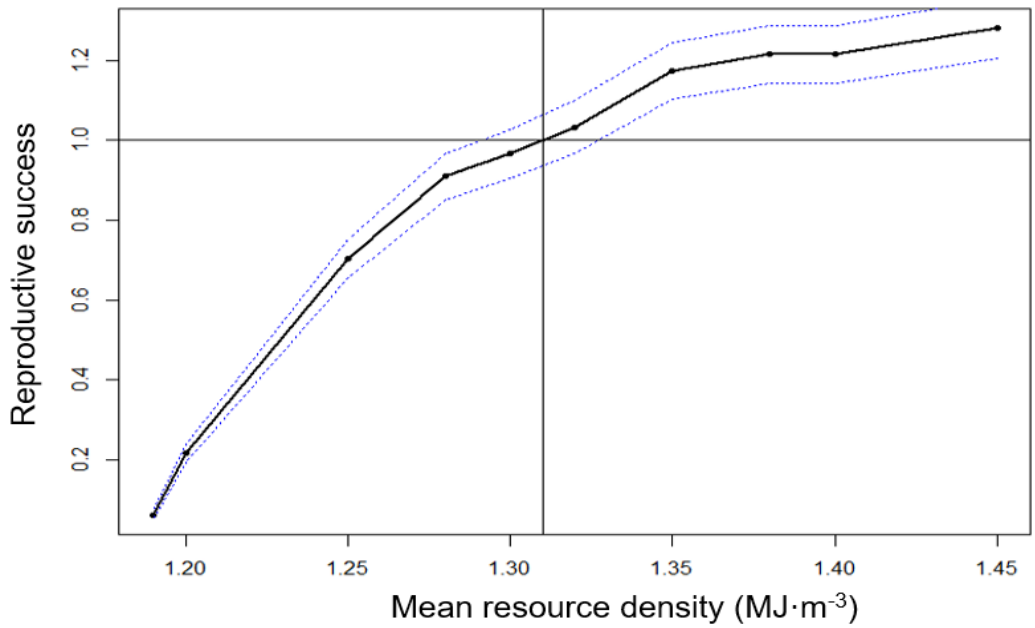

Figure 4.17 The relationship between mean reproductive success and resource density. The dashed lines show the upper and lower 95% confidence limits. The black lines reference the resource density at which reproductive success equals 1.

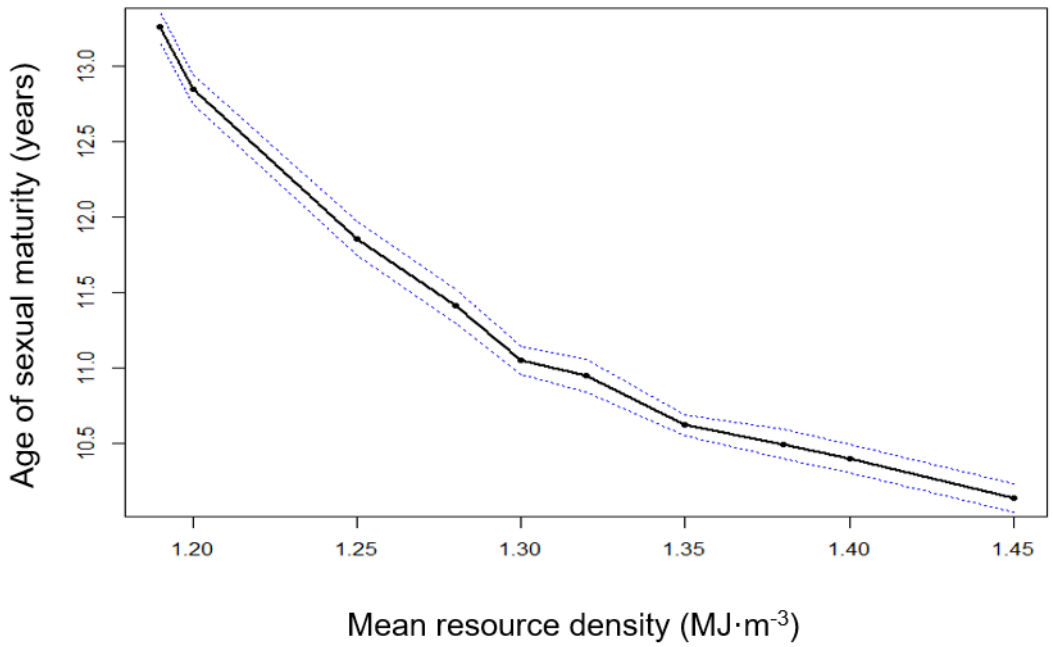

Figure 4.18 The relationship between mean age at sexual maturity and resource density with 95% confidence intervals in blue.

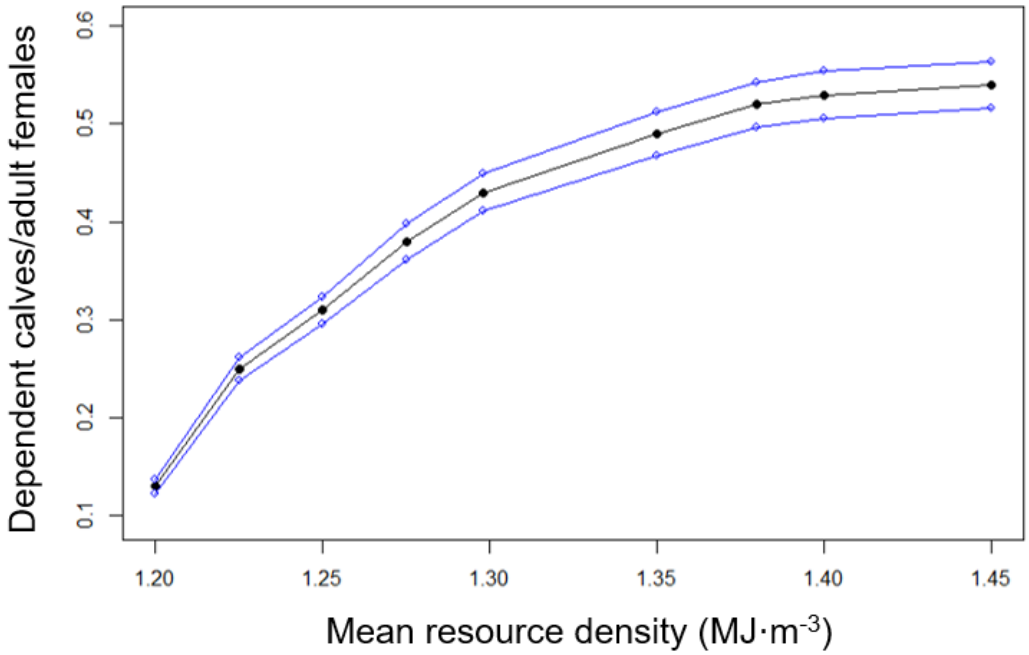

Figure 4.19 The relationship between the calf to adult ratio in the population and resource density with 95% confidence intervals shown by the blue lines.

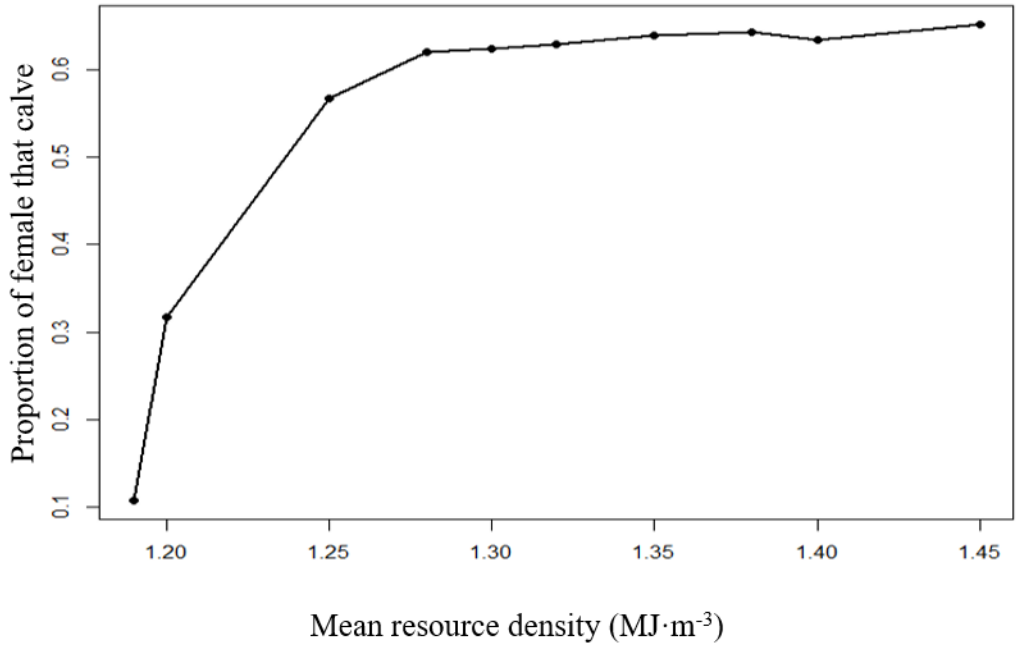

Figure 4.20 The proportion of females out of 1,000 simulations that calved successfully as a function of the mean resource density.

4.4 Discussion

The bioenergetics model described in this chapter provides a tool to investigate the effect of changes in energy flow on the demographic characteristics of an *Md* population. The model demonstrates how *Md* population dynamics are in a large part driven by resource density and the ability of animals to capitalize on local resources. A reduction in energy intake, whether due to reduced resource levels or disruption of foraging, has a clear effect on population characteristics. It can start a cascade of events that leads to a reduction in overall population growth rate. The magnitude of this effect is not uniform throughout an animal's life history. Disturbance is particularly problematic for young animals and a female's ability to successfully raise a calf.

Body size and reserves can have a significant impact on how individuals are affected by changes in resources. Consequently, the model accounts for changes in body size throughout an individual's life history and dynamically tracks the energy required for both growth and maintenance. Body condition is calculated as the ratio of reserves to total body size, so the absolute size of an animal's reserves is dependent on its body size, and therefore its age. While growth continues throughout an animal's life, it reaches 80% of its maximum length at 10 years of age (Figure 4.5). Consequently, young animals are expending more energy on growth than older adults but they have smaller absolute reserves. In addition, newly weaned animals are assumed to be less efficient at foraging than older animals and are therefore at greater risk from changes in the rate of energy assimilation.

The energetic demands on the female are particularly high during late pregnancy and lactation. As in domestic cattle (Fields and Sand, 1993), these demands reach a peak in the period of lactation. During its first year of life, the calf is assumed to be totally dependent on the female for its energy requirements. Consequently, regardless of resource density, the greatest reduction

in body condition during lactation is seen in young females, and especially during the initial calving cycle. As resource density drops, the time taken to recover from the effects of lactation increases. and this results in a higher ICI. For example, ICI increases from approximately 4.1 years at an $\bar{R}$ of 1.4 MJ·m^{-3} to 5.1 years at an $\bar{R}$ of 1.2 MJ·m^{-3}. Because the female's average body condition is reduced at low resource densities, her ability to raise a calf successfully is affected. This is reflected in a 50% decline in the proportion of females that are successful (0.634 to 0.317).

This sensitivity of population characteristics to changes in $\bar{R}$ is also reflected in the annual growth rate. A stable population is reached at an $\bar{R}$ of approximately 1.31 MJ·m^{-3}. A less than 5% reduction in resource density to 1.25 MJ·m^{-3} produces an annual growth rate of 0.985 which would lead to a declining population that would halve in size in under 45 years. Conversely, the population growth rate is less sensitive to an increase in resource density (Figure 4.16). A 10% rise in resource density to 1.45 MJ·m^{-3} results in a growth rate of 1.01, which would lead to the population doubling in approximately 70 years.

The model encompasses numerous assumptions as described above. However, demographic data collected at Abaco and AUTEC, provide an opportunity to compare the outputs to real-world data. The CA ratio of 0.52 observed at Abaco (Claridge, 2013) can be matched exactly with a resource density of 1.38 MJ·m^{-3}. This implies an annual growth rate of 1.008, which is too low to be detected using the monitoring techniques deployed at Abaco. The observed CA ratio at AUTEC can be matched by outputs from a model with a resource density of 1.22 MJ·m^{-3} (Figure 4.19). This results in an annual growth rate of 0.969 that would lead to a decline by approximately 1/3 over a 15-year period. *Md* have been routinely detected at AUTEC via passive acoustics and visual means since 2003, but more systematic data may be required to

detect changes in population size. Also, there are insufficient data at both sites to quantify the actual resource densities. Some species such as pilot whales are subject to seasonal resource variations in resource densities. However, the local *Md* populations at both Abaco and AUTEC in the Bahamas are less likely to be subjected to strong changes due to seasonality (Claridge, 2013), though relevant data on benthic prey in the Bahamas, especially long-term temporal data, are sparse (Hazen et al., 2011).

One major site difference between Abaco and AUTEC is the routine use of MFAS at AUTEC. Although MFAS events are transient and intermittent, they could have an impact if they fall during sensitive times in the reproductive cycle (Farmer et al., 2018), particularly for younger females. The model can be applied to such scenarios if both the disturbance and effect are reasonably well quantified. In Chapter 6, passive acoustic data will be used to quantify both the frequency and duration of MFAS events at AUTEC and the number of *Md* foraging dives around these operations.

The bioenergetics model presented is a step in the evolution of such models. Parameter values were gleaned from a variety of sources, including proxy species, where no data were available for *Md*. The collection of species-specific data on these parameters would certainly enhance the model's credibility. A better understanding of the animal's foraging behaviour, especially the variation in foraging success is critical. Though these animals forage at great depth, it may be possible to use passive acoustic detection of terminal "buzz" clicks as a measure of foraging success (Johnson et al., 2006a, 2004). Buzzes can be recorded on tags and also can be detected on the AUTEC hydrophones (Jarvis, in preparation). Such data may provide insight into the variation in foraging behaviour and foraging success.

The current model makes broad generalizations regarding individual animals and the environment. For example, all individuals are assumed to follow exactly the same growth curve which is unlikely to be true and might affect the model's output. While the model accounts for foetal mortality and females must attain a minimum body condition to become pregnant and carry a pregnancy to term, it does not include a general term for the rate of female rate infertility. Its addition would proportionately reduce the number of females that became pregnant that would lower the overall birth rate. As such data become available, they could be added to the model.

Resource density is used as a measure of the maximum energy an animal can assimilate from the environment. It accounts for multiple factors including prey density, different assimilation values between prey, the animals nutritional state, foraging efficiency etc. Understanding and incorporating the underlying variability would improve the model. For example, the prey field is assumed to be spatially and temporally constant. Limited data from AUTEC (Hazen et al., 2011) and the Southern California Offshore Range (Southall et al., 2019) showed spatial variation in the density of potential prey for beaked whales that was correlated with their foraging distribution. Incorporating the effect of spatial and temporal variation in prey fields within the model would be a logical next step. It is also unknown if animals adapt their behaviour in different prey fields to enhance capture probabilities. Understanding behaviours under different environmental conditions and disturbances would assure the model assumptions reasonably reflect an animal's behaviour and the consequences of their behaviour in terms of foraging success. However, this chapter demonstrates that relatively small changes in resource density may have a large effect on population characteristics and that the differences in population structure observed between Abaco and AUTEC may be explained, at least in part, by differences

in resource density. Understanding real-world variation and incorporating would improve modelled outputs.

4.5 Contributions

The basic model concept is documented in New et al. 2014 and example code was provided by Lelsie New and was modified and rewritten and used in the initial phase of this investigation. An updated version of the Hin et al. (in press) model originally used for pilot whales was provided by J. Harwood and was modified for *Md*, the results of which are included here.

Advice relating to the analysis of data and statistics and review of the results and manuscript was provided by J. Harwood and L. Thomas.

Chapter 5

Measuring Beaked Whale MFAS Exposure and Evaluating its Population-Level Effects using both Bioenergetic and Expert Elicitation Methods

5.1 Introduction

The objective of this chapter is to use the bioenergetics model for Blainville's beaked whales (*Mesoplodon densirotris* - hereafter *Md*) developed in Chapter 4 to assess the potential effects on population dynamics of the behavioural responses to mid-frequency active sonar (MFAS) observed at the Atlantic Undersea Test and Evaluation Center (AUTEC). These assessments are compared with observations of the demographic characteristics of this population and a neighbouring undisturbed population (Claridge, 2013) and results from an independent expert elicitation exercise (Booth et al., 2015).

Expert elicitation is a formalized, multi-disciplinary process used to make informed decisions when few direct analytic data are available (O'Hagan et al., 2006). It provides a quantified response from a group of experts, along with a measure of the uncertainty associated with this response (Clemen and Winkler, 1999). The expert elicitation process can provide a means of highlighting both the current state of knowledge and the data gaps. Expert elicitation is not intended to replace basic scientific research. However, if the underlying science does not yet exist, it can provide transparent, structured, and quantifiable inputs to a decision-making process when hard data are limited. Although a number of different approaches have been developed, they typically strive to combine probability distributions from multiple experts, where each

expert is asked to quantify the distribution of a given parameter or risk (Clemen and Winkler, 1999; Knol et al., 2010; O'Hagan et al., 2006).

Data from two study sites, Abaco and AUTEC, in the Bahamas (Figure 5.1) were used in the analysis reported here. While Abaco cannot be considered as a true "control" site for evaluating the effects of MFAS disturbance at AUTEC, it does serve as a comparative site. AUTEC is located in the Tongue of the Ocean (TOTO), a deep (~ 1,000m-1800m) enclosed ocean canyon surrounded by islands, or very shallow (<10m) water (Figure 5.1). The only means of entry and egress is through the Northwest Providence Channel. The TOTO was chosen as the site for a U.S. Navy test and evaluation range because of these bathymetric features, which result in a quiet acoustic environment with low ambient noise. By comparison, the Abaco site is near the mouth of the Northwest Providence Channel, with open ocean access on either side.

Figure 5.1 A Google Maps view of the Great Bahama Canyon. The Northwest Providence Channel stretches from east to west in the upper part of the image. The Tongue of the Ocean extends to the south of this Channel, ending in a circular cul-de-sac. The Abaco study site is indicated in yellow and the AUTEC range in red.

These sites are believed to contain discrete *Md* populations because no AUTEC animals have been sighted at both locations. However, one animal that was tagged in AUTEC did move to the Northwest Providence Channel (J. Durban unpublished data). There are also differences in population structure between the two sites. Based on 12 years of sighting data, Claridge (2013 and unpublished data) estimated that the ratio of calves to adult females (CA ratio) at Abaco was 0.52. By comparison, the CA ratio at AUTEC was estimated to be 0.21. As noted in Chapter 4, these differences in CA ratio may be the result of differences in resource density. Recent acoustic surveys found differences in prey size and distribution between the sites (K. Benoit-Bird personal communication). However, Claridge (2013) suggested that the difference in CA ratios may be the result of disturbance associated with MFAS use at AUTEC. Passive acoustic data (McCarthy et al., 2011; Moretti et al., 2010, 2014; Tyack et al., 2011) indicate that *Md* move off the AUTEC range when exposed to sonar. Joyce et al. (in press) analysed data from satellite tags placed on animals at AUTEC that were tracked before, during, and after MFAS events. The animals appeared to reduce the time spent foraging during the initial movement off-range, though the total percentage of time spent diving during MFAS transmissions was not lower than in the period before or after the exposure period. Manzano-Roth et al. (2016) documented a reduction in *Md* detections on the Pacific Missile Range Facility off the island of Kauai during MFAS operations there. DeRuiter et al. (2013) observed the disruption of a Cuvier's beaked whale (*Ziphius cavirostris*) foraging dive when exposed to an MFAS signal from an experimental source, and Stimpert et al. (2014) documented a similar reaction by a Baird's beaked whale (*Berardius bairdii*). Falcone et al. (2017) detected an increase in the interval between foraging dives for Cuvier's beaked whales fitted with satellite tags that were exposed to

MFAS in Southern California. Miller et al. (2015) used a recording tag to measure the reaction of a northern bottlenose whale (*Hyperoodon ampullatus*) in the North Atlantic to MFAS exposure. The animal executed the longest and deepest dive ever recorded for that species, then made a prolonged movement away from the source.

Together, these studies strongly suggest that exposure to MFAS disrupts beaked whale foraging. In this Chapter, the bioenergetics model developed in Chapter 4 is used to investigate the potential effect of such repeated foraging disruption on the structure and dynamics of an *Md* population.

5.2 Methods

5.2.1 Quantifying exposure to MFAS

Periods of MFAS use and *Md* group vocalization periods (GVPs) during 2012 were identified using passive acoustic detection archives from AUTEC. The start of a GVP was used as a proxy for the start of a foraging dive. MFAS pings were detected by an analyst using the Marine Mammal on Navy Ranges Program (M3R) 2-dimensional spectrogram displays (Jarvis et al., 2014). The times of these pings were used to identify the start and end of MFAS operations. AUTEC operational logs were used to confirm the presence and type of MFAS source.

MFAS operations either lasted a short duration (involving a single ship, sonobuoy, or helicopter) of less than one day or were large three-day, multi-ship events, which were conducted twice per year. During helicopter events, a helicopter flew to a location, hovered, and lowered a transducer into the water. MFAS pings were transmitted at a nominal repetition rate of 25 s and source level of 217 dB, for approximately 10 minutes in an attempt to locate a submerged target (U.S. Fleet Forces Command, 2008). Typically, these events lasted about 3 hours and were

generally repeated at a rate of approximately two per day. The multi-ship operations typically included two or three surface ships with MFAS. The ships are equipped with an AN/SQS-53C (hereafter 53C) sonar that transmits at a published source level of 235dB and is in use for up to 9 hours per day (McCarthy et al., 2011; Moretti et al., 2010, 2014).

A period of 72 hours without MFAS transmissions was required before a new MFAS operation was considered to start. This 72-hour period was based on data in McCarthy et al. (2011) which suggest that the number of *Md* groups on AUTEC return to the pre-exposure level within three days of the completion of a multi-ship MFAS operation. While dive rates generally returned to pre-operation levels in less than 24 hours after short duration operations, the 72-hour period was still used to assure clear separation between the effects of different operations.

GVPs were detected using the methods described in Chapter 2 and the outputs visually confirmed by an analyst. The number of GVPs detected during the MFAS period and a 24-hour post-exercise period was compared to the number detected in a seven-day time window directly ahead of the operation. If there were less than seven days between operations, the period from the start of the operation to the end of the previous operation was used. These ratios were then used to estimate the probability that an animal would remain on the range, or its reduced energy intake. Each ratio was entered into the appropriate element, corresponding to the day of sonar operation, of a time vector covering the whole of 2012. For those operational days with no GVP data, the mean ratio measured over all operation days with GVP data was used. For the two, three-day multi-ship operations, the data reported in Moretti *et al*. (2010) were used to determine the disturbance ratio.

5.2.2 Quantifying the effect of MFAS exposure on energy assimilation

The bioenergetics model described in Chapter 4 was used to investigate the potential effect of the MFAS operations detected in 2012 on the life histories of 1,000 simulated females using a range of values for resource density. The life expectancy of each female was determined by a random draw from a cumulative survival curve for the population (Figure 4.3), as in Chapter 4.

The disturbance time vector was replicated multiple times so that it covered the entire lifetime of any simulated individual. For each simulated individual, a binomial trial was conducted on each day when MFAS operation was predicted to occur using the disturbance probability for that day. This resulted in a vector of actual disturbance events. The effect of this disturbance on foraging was simulated by multiplying the resource density on each disturbance day by a "disturbance effect". Disturbance effects from 0.75 to 0.25 were modelled, where, for example, a value of 0.25 resulted in a 75% reduction in resource density on that day.

As described in Chapter 4 (Section 4.2.10) the model outputs for *reproductive success*, *population growth rate*, *calf to adult (CA) ratio*, and *mean age at maturity* were examined along with the following:

Probability of giving birth

The probability of giving birth for each simulated female was calculated as the ratio of the number of calves produced by that female divided by the number of years she spent as an adult (i.e. her life expectancy in years - 9).

Inter-calf Interval (ICI)

ICI could only be estimated for simulated females that produced at least two calves. It was calculated as the mean interval between the births of consecutive calves over the lifetime of these females.

Calf survival

Calf survival could only be calculated for a simulated female that actually gave birth to a calf. For these females, it was calculated as the number of calves that survived to weaning (age 2.7 years) divided by the number of calves produced by that female in her lifetime.

As in discussed in Chapter 4 (Section 4.2.10), while the 95% confidence intervals are calculated, in reality uncertainty would be considerably with the exception of CA ratio.

5.2.3 Expert Elicitation

Booth et al. (2015) used expert elicitation to predict the potential effects of disturbance associated with mid-frequency MFAS exposure on the survival and reproductive success of the *Md* population at AUTEC. They began the process by forming a Steering Committee with representatives from the U.S. Navy, the National Oceanographic and Atmospheric Administration, and the U.S. Marine Mammal Commission. The Steering Committee nominated a panel of experts who in the previous 5 years had published on the population biology of beaked whales, on the impacts of noise on the hearing of beaked whales, or on the effects of disturbance on beaked whales. Members of this panel were invited to attend a workshop. The 22 experts who actually took part in the workshop were provided with extensive background information on beaked whale ecology, and the available literature on the effects of noise on marine mammal behaviour. The actual elicitation used the 4-step interval approach developed by Spiers-Bridge

et al. (2010) in which experts were invited to give their best estimates of a quantity, the lowest and highest plausible values, and an estimate of the confidence they attached to the interval they created.

The experts were asked a series of questions designed to quantify their opinions on the likely effect of the disturbance responses that have observed in response to MFAS on calf survival and the probability of giving birth (fertility) over a 365-day period. They were first asked about the effect of a severe behavioural response (e.g. prolonged separation of mother and calf or long-term avoidance of an area, equivalent to a severity score of 8 or 9 in Southall et al. (2007). These were:

- the minimum number of days on which at least one severe behavioural response occurs that a mother-calf pair or a pregnant female could tolerate before it has any effect on calf survival or fertility (vertical line A Figure 5.2);
- the largest plausible reduction in calf survival (horizontal line B in the upper panel of Figure 5.2) that could be caused by many days of severe behaviour response to disturbance; and
- the number days of severe behavioural response to disturbance that would be required to cause this reduction in calf survival (vertical line C in the upper panel of Figure 5.2).

Most experts were willing to assume that the largest plausible reduction in the probability of giving birth caused by repeated behavioural responses was 100% (lower panel in Figure 5.2).

Next they were asked a series of questions based on a moderate behavioural response (e.g. change in direction of swimming or moderate avoidance of the sound source, equivalent to a severity score of 5 or 6 in Southall et al., 2007). They were asked to provide:

- the maximum number of days on which at least one moderate behavioural response occurs that a mother-calf pair or pregnant female could tolerate before it had any effect on calf survival or fertility (vertical line D in the upper panel of Figure 5.2, and vertical line C in the lower panel);
- the smallest plausible reduction in calf survival that could be caused by moderate behavioural responses to disturbance that occurred throughout the year (horizontal line E in the upper panel of Figure 5.2); and
- the number of days of moderate behavioural response to disturbance required to cause this reduction (vertical line F in Figure 5.2).

Finally, the experts were asked a series of question relating to the behavioural response to disturbance that they thought was most likely to occur to be caused by activity on US Navy testing ranges. These were their best estimates of:

- the number of days on which at least one of the most likely behavioural responses to disturbance occurs that a mother-calf pair or pregnant female can tolerate before these responses have any effect on calf survival or the probability of giving birth (vertical line G in the upper panel of Figure 5.2, and vertical line E in the lower panel);
- the percentage reduction in calf survival that could be caused by the most likely behavioural responses to disturbance, if they occurred throughout the year (horizontal line H in the upper panel of Figure 5.2): and
- the number of days of the most likely behavioural response required to cause this reduction in calf survival (vertical line I in the upper panel of Figure 5.2).

They were also asked to quantify their confidence in each of these responses, on a scale of 1 (no confidence) to 100 (complete confidence).

This information was used to generate a multivariate probability density function for the key parameters in Figure 5.2 (G, H and I in the upper panel, E and F in the lower panel) using the methods described in Donovan et al. (2016). These probability density functions were then represented as heat maps (Figure 5.3). As can be seen, experts differed widely in the values they provided for all of the parameters. However, the range of values for the parameter relating to the number of days of disturbance that a mother-calf pair can tolerate before there is any effect on calf survival was narrower than the range for the equivalent parameter for the effects of disturbance on the probability of giving birth.

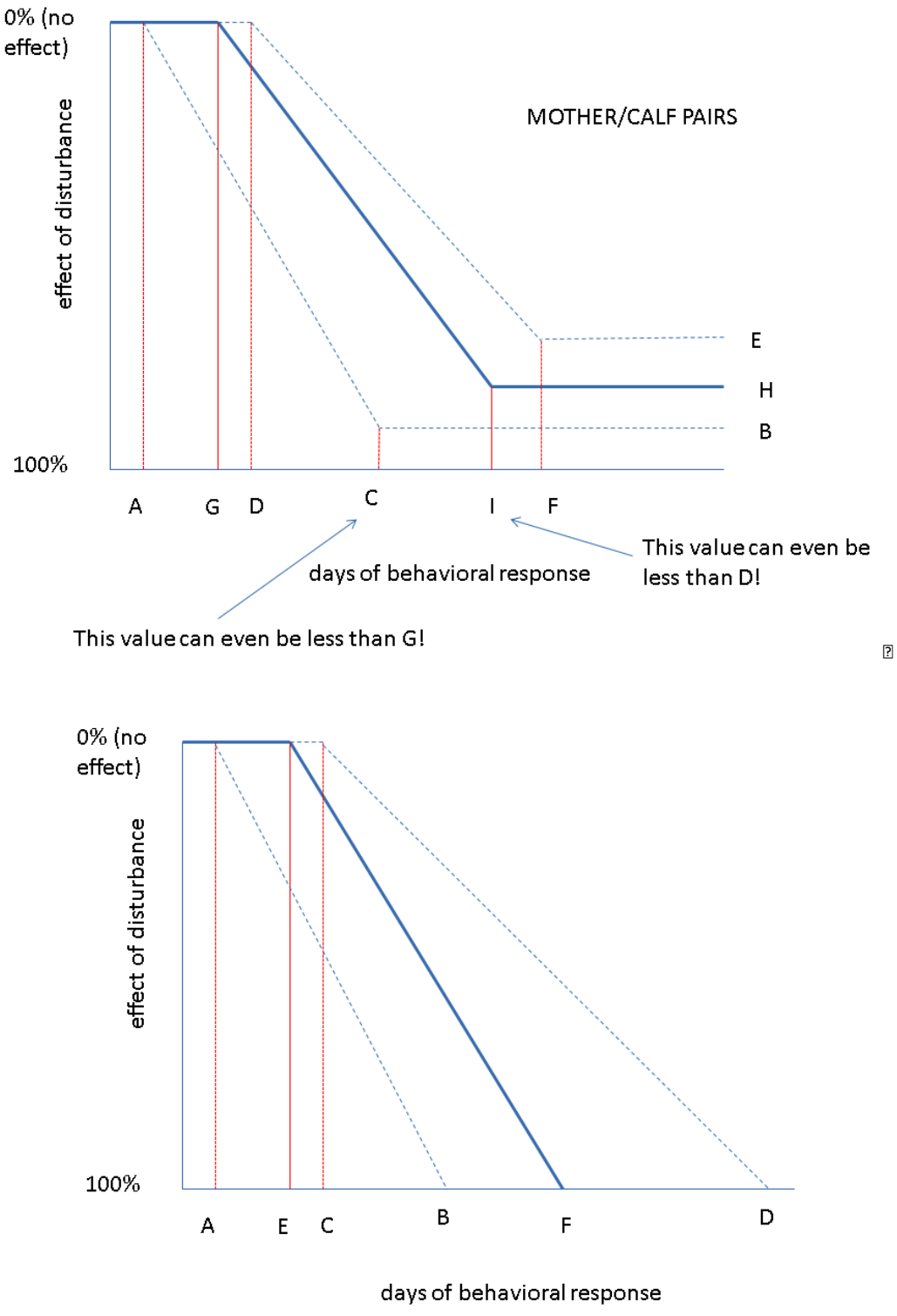

Figure 5.2 The hypothetical relationships between *Md* vital rates and the number of days of behavioural response used in the expert elicitation conducted by (Booth et al., 2015). Upper panel: effect of a behavioural response on calf survival. Lower panel: effect of a behavioural response on the probability of giving birth.

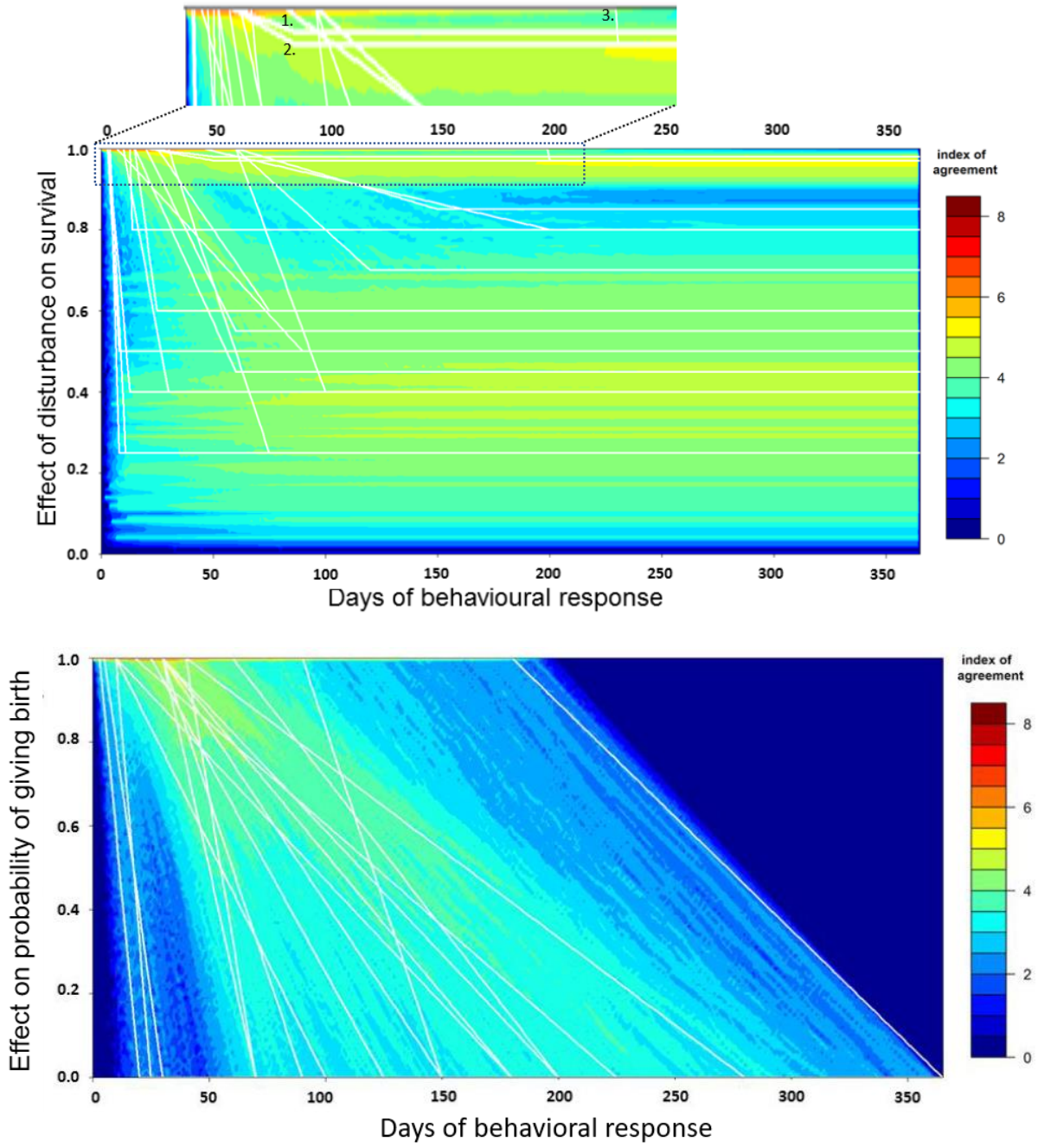

Figure 5.3 Heat maps showing the combined results from all experts for the relationship between the number of days of behavioural response by an *Md* on AUTEC and the effect on calf survival (upper panel) and the probability of giving birth (lower panel). The actual rate for an individual whale is estimated by multiplying the baseline population rate by the "effect" value given on the vertical axis. White lines show the relationship predicted by each expert. Hot colours indicate combinations of values for which there was strong support among experts; cool colours indicate combinations that had little support. Figures reproduced from Booth et al. (2015). A zoom of the upper segment of the top panel is provided. The three expert responses which predicted the least effect on survival (labelled 1-3 in the inset) are indicated.

5.2.4 Generating predictions from the bioenergetics model for comparison with the expert elicitation results

Runs of the bioenergetics model for comparison with the expert elicitation results were conducted using the resource density (R) of 1.32 $MJ.m^{-3}$ that yielded a CA ratio matching the one reported by Claridge (2013) for Abaco, as described in Chapter 4. This is referred to as an equilibrium environment, because each female is, on average, only able to raise one female calf to weaning in her lifetime. In effect, the population is at the carrying capacity of the environment and it is neither increasing nor decreasing in size, in the absence of disturbance. The model was also run with a resource density of 1.45 $MJ.m^{-3}$. This is referred to as a favourable environment, because each female is, on average, able to raise 1.28 female calves to weaning in her lifetime. In these circumstances, the population is expected to increase in size by 1% per annum.

The disturbance time vector for a specified number of days of disturbance was generated by randomly choosing the required number of days from the integers between 1 and 365, without replacement. This vector was then repeated to create a vector of disturbance events over the maximum lifetime of any simulated animal. This vector was used for each of the 1,000 simulated animals. On each disturbance day, resource density was set to zero, mimicking the effect of a severe behavioural response, as used in the elicitation process.

5.3 Results

5.3.1 Observed responses to MFAS

Nineteen MFAS operations were identified in 2012 (Figure 5.11). There were 154 days with GVP detections but no MFAS operations in 2012. A total of 10,447 GVPs, each of which represents a single dive by a group of animals (1 or more), were detected on these days, providing a mean daily detection rate of 67.2 GVPs (95% CI 56.2-78.3). A total of 4,702 GVPs were detected on the 73.73 days before MFAS operations, providing a mean daily detection rate of 61.8 GVPs (95% CI 51.4-72.2). There were 66 days when both GVPs and MFAS were detected. The mean daily detection rate on these days was 29.2 GVPs (95% CI 19.3-39.0), significantly lower (t-test d=19.87, t= -3.29, p-value = 0.03) than the detection rate on the preceding days.

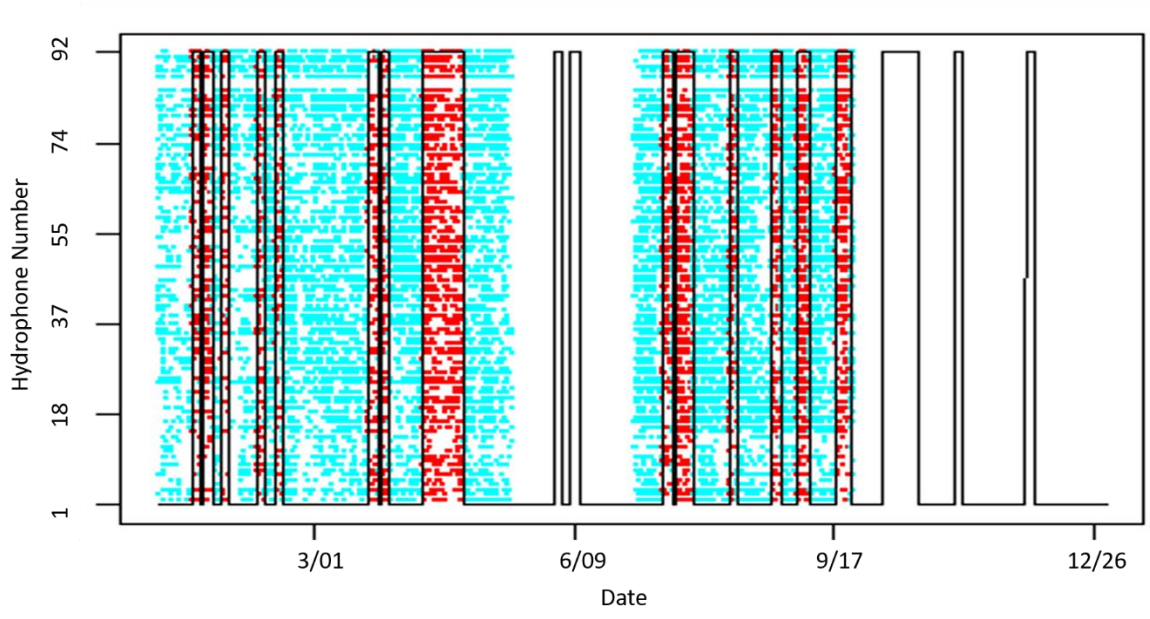

Figure 5.11 The distribution of GVPs and MFAS operations identified during 2012. Each cyan dot represents a GVP and the range hydrophone on which it is centred. They are used here to identify periods with GVP detection but no MFAS operations. Red dots show periods with GVP and MFAS detections. The black lines outline the durations of the 19 MFAS operations.

Figure 5.5 shows the ratio of the two GVP detection rates for each MFAS event. The mean value was 0.46 (95% CI 0.41-0.51, range 0.20-0.82).

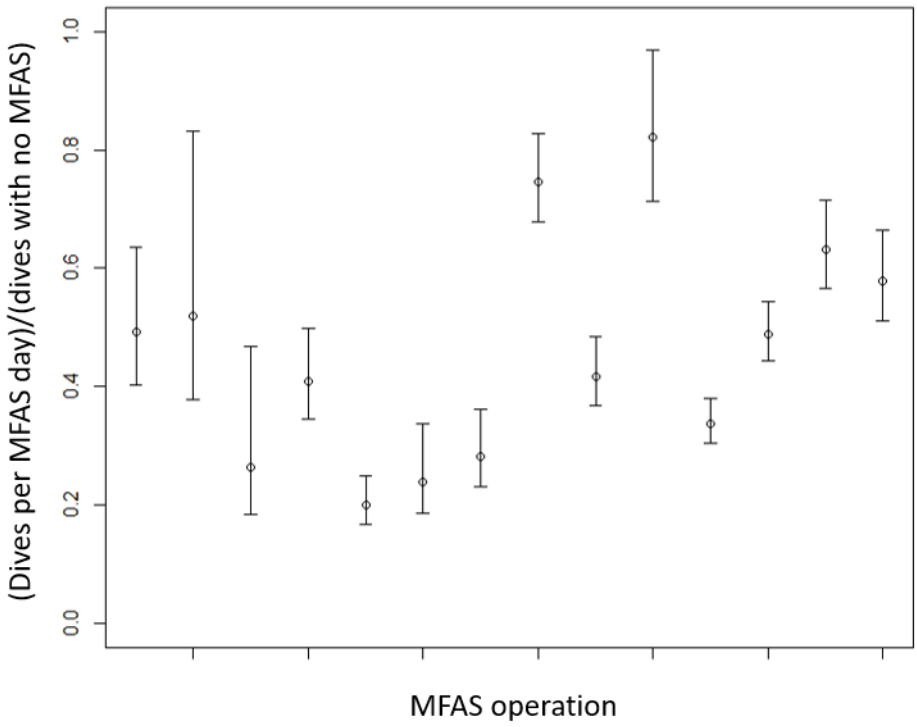

Figure 5.5 The probability of remaining on AUTEC during each of the MFAS operations detected in 2012. The 95% confidence intervals based on daily variability of GVP estimates around the operations are given as error bars.

The probability of remaining on the range during the biannual multi-ship operations was taken from Moretti *et al*. (2010). The mean daily detection rate for the 65-hour period ahead of one of these operations was 71.6 GVPs (95% CI 63.1-80.1), and the mean daily detection rate during the operation was 20.1 GVPs (95% CI 17.7-22.5). Therefore, the estimated probability of remaining on the AUTEC range is 0.28 (95% CI 0.23- 0.33).

5.3.2 Effects of MFAS exposure on bioenergetics

Figure 5.6 shows the effects of resource density on the CA ratio for an undisturbed population and for a population subject to the MFAS disturbance regime observed at AUTEC in 2012. The disturbance effect was set at 0.5, because telemetry data from animals disturbed on AUTEC in November 2015 (Joyce et al., in press) indicated that they began deep-diving within 12 hours of being exposed to MFAS. This suggests that energy acquisition may only be reduced by 50% on the day when an animal is disturbed. Results with other values for the disturbance effect are shown in the Appendix. The relationship between resource density and the CA ratio is approximately linear. A resource density of 1.32 $MJ \cdot m^{-3}$ produced a CA ratio for the undisturbed population of 0.47 (95% CI 0.33-0.55), slightly lower than the mean value observed at Abaco (0.52; 95% CI 0.35-0.69) by Claridge (unpublished data). At the same resource density, the CA ratio for the disturbed population was 0.27 (95% CI 0.20-0.34), slightly higher than the mean value observed at AUTEC (0.21 with 95% CI 0.08-0.35).

With a resource density of 1.32 $MJ \cdot m^{-3}$, the mean age at maturity for the undisturbed population was 10.95 years (95% CI 10.84-11.06), and for the disturbed population it was 12.30 years (95% CI 12.20-12.41). Claridge (2013) estimated that the age at sexual maturity at Abaco was 9 to 10 years, but this was based on sighting histories of only three females. The mean ICI for the undisturbed population was 4.56 years (95% CI 4.49-4.64), for the disturbed population it was 5.38 years (95% CI 5.31-5.45).

The mean probability of giving birth in the undisturbed population was 0.206 (95% CI 0.193-0.218) and 0.157 (95% CI 0.154-0.161) in the disturbed population. Disturbance reduced calf survival from 0.667 (95% CI 0.626-0.708) to 0.482 (95% CI 0.469-0.492). In combination, these

disturbance-induced changes in demographic characteristics reduced the predicted annual growth rate of the population from 1.00 to 0.98

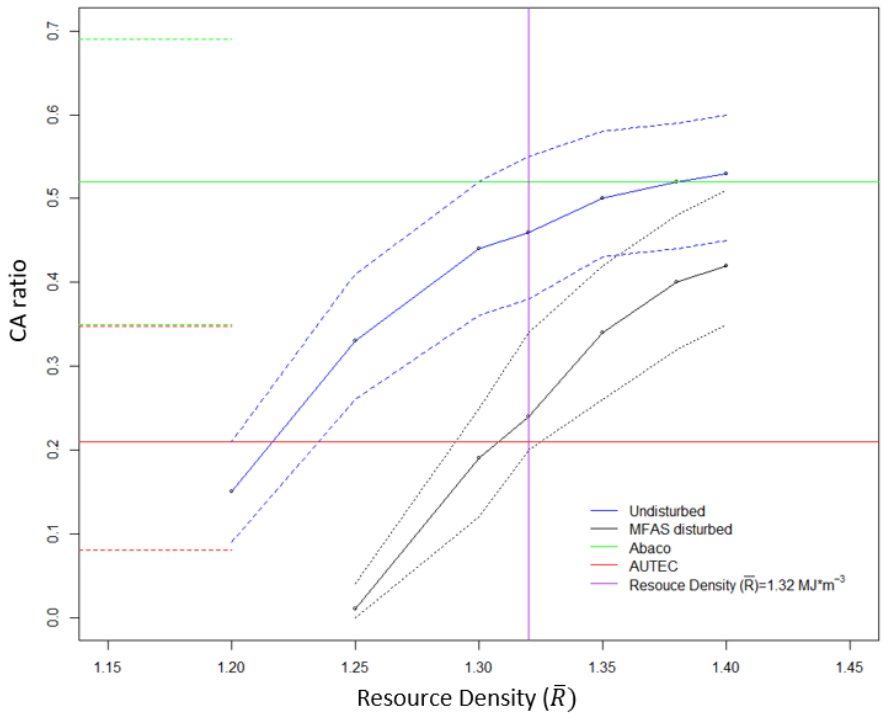

Figure 5.6 The median ratio of calves to adult females (CA ratio) as a function of resource density for an undisturbed population (blue), and for a population subject to the pattern of MFAS disturbance observed at AUTEC in 2012 (black). The 0.05 and 0.95 quantiles are shown as dotted lines. The mean CA ratio observed at Abaco is indicated by the green line. The mean CA ratio observed at AUTEC and its 95% confidence interval is shown in red.

5.3.3 Comparison with expert elicitation results

The effect of the number of days of disturbances on model predictions of the probability of giving birth and calf survival in an equilibrium environment (i.e. with R = 1.32 MJ·m^{-3}) and a favourable environment (i.e. R = 1.45 MJ·m^{-3}) are compared in Figures 5.7 and 5.8. In the equilibrium environment, most females are unable to raise a calf successfully if they are disturbed on more than 30 days per year (Figure 5.). However, in a favourable environment,

females can continue to raise calves when they experience up to 60 days of disturbance (Figure 5.). The effect of resource density on calf survival is similar (Figure 5.8).

In an equilibrium environment, the probability of giving birth was 0.206 (95% CI 0.164-0.247), if there was no disturbance. This value was reduced by 50% with 32 days of disturbance and to zero with ~40 days of disturbance (Figure 5.7). In a favourable environment, the maximum value for the probability of giving birth was 0.245 (95% CI 0.240-0.250). This value dropped by 50% with 50 days of disturbance and to zero with ~60 days (Figure 5.7).

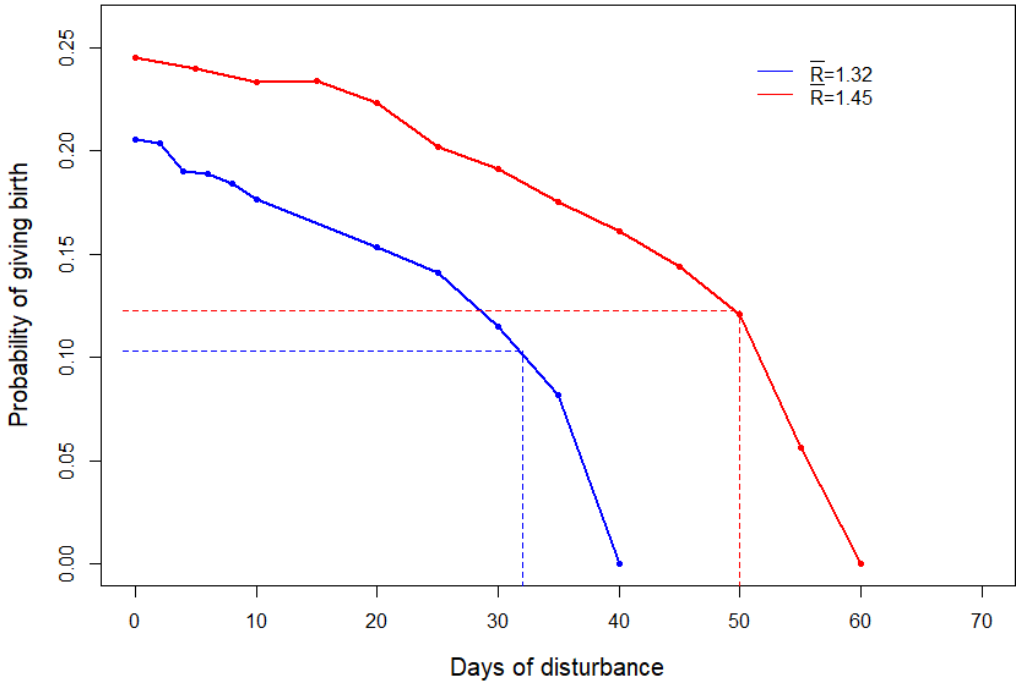

Figure 5.7 The probability of giving birth as a function of days of disturbance. The blue line shows the relationship in an equilibrium environment (resource density R =1.32 MJ·m^{-3}) and the red line shows it for a favourable environment (R = 1.45 MJ·m^{-3}). The number of days at which the probability of giving birth is 50% of its maximum value is indicated by the dashed lines.

Calf survival in the absence of disturbance was 0.66 (95% CI 0.64-0.65) . In an equilibrium environment it declined by 50% after 27 days of disturbance and to zero after 35 days. In a

favourable environment, calf survival declined by 50% after 49 days of disturbance and to zero after 55 days.

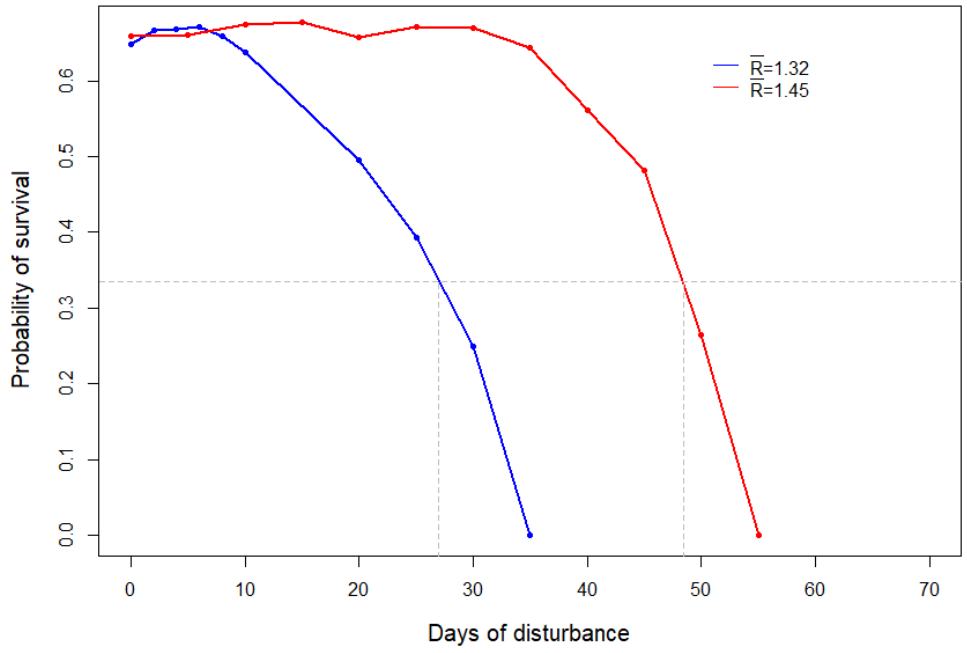

Figure 5.8 Calf survival as a function of days of disturbance in an equilibrium environment (blue line) and favourable environment (red line). The number of days of disturbance required to reduce survival to 50% of its maximum value is indicated by the dashed lines.

Figure 5.9 shows the medians, quartiles and 5th and 95th percentiles based on 10,000 random draws from the probability distribution shown in the lower panel of Figure 5.3, for the relationship between the number of days of behavioural response to disturbance and the probability of giving birth, together with the matching predictions from the bioenergetics model. The median number of days of behavioural response required to cause a 50% decline in the probability of giving birth is 80 days. Figure 5.10 is an enlarged version of Figure 5.9, showing the predicted effects of 0-125 days of disturbance response, and the number of days of disturbance response required to reduce the probability of giving birth by 20%.

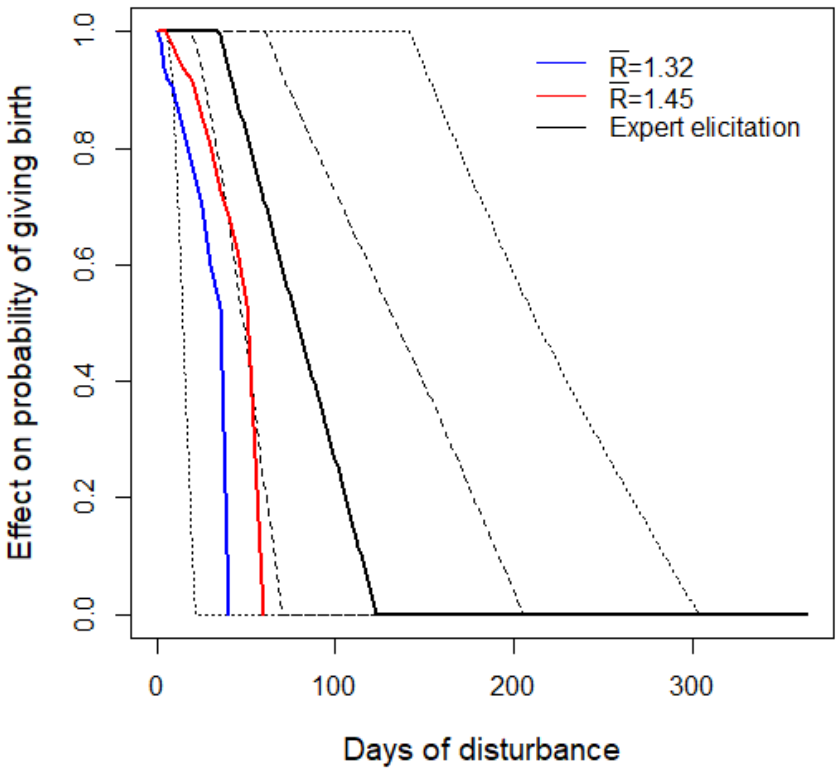

Figure 5.9 The effect of the number of days of disturbance on the probability of giving birth based on10,000 samples from the probability density function generated by the expert elicitation. The median value is shown in black. The heavy dotted lines represent the upper and lower quartiles, and the lightly dotted lines encompass 95% of the values. The effect of the same number of days of disturbance predicted by the bioenergetics model for an equilibrium environment is shown in blue and for a favourable environment in red.

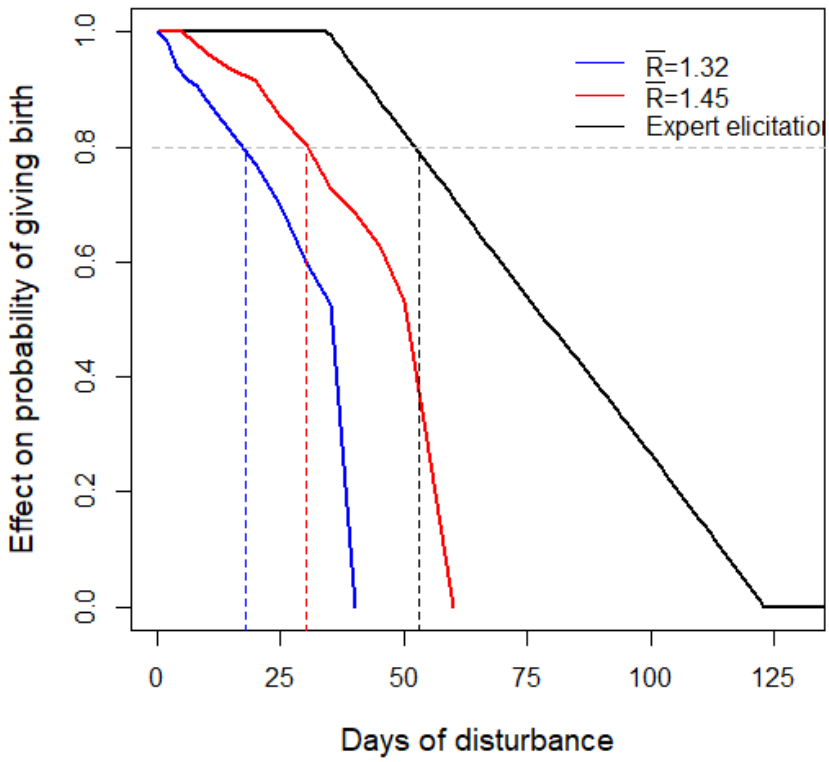

Figure 5.10 The effects of 0 to 125 days of disturbance on the probability of giving birth as predicted via expert elicitation (black). The effect of the same number of days of disturbance predicted by the bioenergetics model for an equilibrium environment is shown in blue and for a favourable environment in red. The vertical dashed lines indicate the number of days required for a 20% reduction for each trial case.

The calf survival value derived from the bioenergetics model covers the period from birth to weaning, which occurs at age 2.7 years. For comparison with the expert elicitation results, this was converted to an annual survival rate. Figure 5.11 shows the medians, quartiles and 5th and 95th percentiles based on 10,000 random draws from the probability distribution shown in the lower panel of Figure 5.3, for the relationship between the number of days of behavioural response to disturbance and calf survival, together with the equivalent predictions from the bioenergetics model. The rapid decline in calf survival predicted by the bioenergetics model with 30 days of disturbance (in an equilibrium environment) and 50 days (in a favourable

environment) is because the model predicts that no calves are born when there is this much disturbance, and therefore calf survival cannot be calculated. The median value from the expert elicitation suggests that at least 20 days of disturbance response is required to have any effect on calf survival. The equivalent predictions from the bioenergetics model were 10 and 30 days for low and high resource densities, respectively.

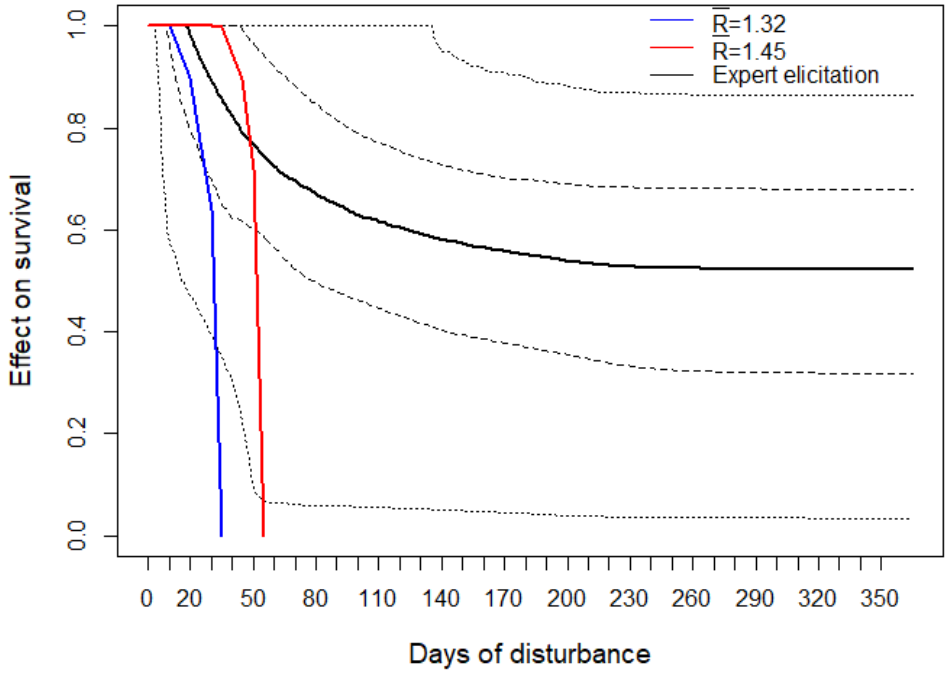

Figure 5.11 The effect of the number of days of disturbance on calf survival based on 10,000 samples from the probability density function generated by the expert elicitation. The median value is shown in black. The heavy dotted lines represent the upper and lower quartiles, and the lightly dotted lines encompass 95% of the values. The effect of the same number of days of disturbance predicted by the bioenergetics model for an equilibrium environment is shown in blue and for a favourable environment in red.

The bioenergetics model predicted a 20% decline in calf survival with 26 days of disturbance in an equilibrium environment and with 48 days in a favourable environment (Figure 5.12). The expert elicitation process predicted a 20% decline with 44 days of disturbance response.

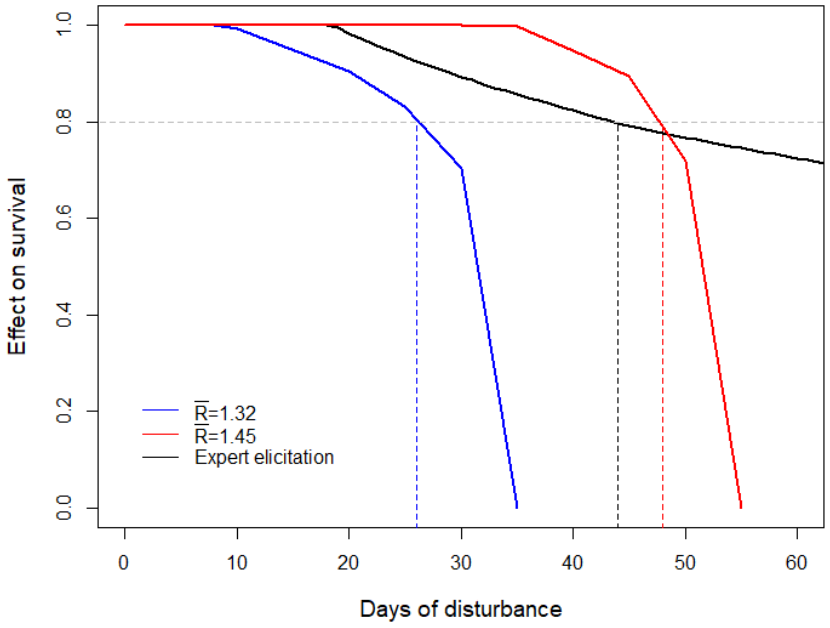

Figure 5.12 The effect of 0-60 days of disturbance on calf survival based on 10,000 samples from the probability density function generated by the expert elicitation. The median value is shown in black. The effect of the same number of days of disturbance predicted by the bioenergetics model in an equilibrium environment is shown in blue and in a favourable environment in red. The vertical dashed lines indicate the number of days required for a 20% reduction in calf survival.

5.4 Discussion

The outputs from the bioenergetic model suggest that the changes in behaviour in response to MFAS exposure observed on AUTEC could lead to an increase in a female's age at maturity, a longer ICI, a lower calf survival rate and a reduced probability of giving birth. If the resource density at AUTEC is 1.32 $MJ.m^{-3}$, and disruption to foraging results in a 50% reduction in energy assimilation, the predicted CA ratio was similar to that observed at AUTEC by Claridge (2013). As noted in Chapter 4, this CA ratio can also be duplicated by setting the resource density at AUTEC at 1.22 $MJ.m^{-3}$, even if behavioural disruption has no effect on the population. In both cases the population is predicted to decline by 50% over a 20-30 year period. However,

although *Md* have been routinely detected at AUTEC via passive acoustics and visual means since 2003.

Although the predictions of the effects of disturbance at AUTEC on population characteristics depend to some extent on the value used for resource density, they are not particularly sensitive to this choice. As Figure 5.6 illustrates, the difference between the CA ratio for a disturbed and an undisturbed population is not greatly affected by resource density, although - as might be expected – the difference decreases with increasing resource density. The effect of resource density on the other model outputs is similar. However, the value chosen for the effect of disturbance on daily energy assimilation (the disturbance effect) is critically important. Changing the value of this parameter from 0.5 to 0.25 results in a 50% decrease in the amount of energy a female can assimilate on a day when there is a disturbance. Similarly, increasing this parameter to 0.75 results in a 50% increase in assimilated energy.

Disruption to *Md* foraging in response to MFAS exposure has been well documented at AUTEC (Joyce et al., in press; McCarthy et al., 2011; Moretti et al., 2010, 2014; Tyack et al., 2011), but it is currently impossible to translate this disruption into an effect on energy intake. Although Joyce et al. (in press) documented a relatively rapid resumption in time spent at foraging depth by tagged animals displaced by an MFAS operation, there are no data on their foraging success. It is therefore important to obtain a better understanding of the foraging success of *Md* when they are on and off the range. Hazen et al. (2011) noted a correlation between the density of foraging *Md* and the occurrence of deep prey fields in the TOTO. Southall et al. (2019) found a similar correlation between Cuvier's beaked whales and prey density on the Southern California Offshore Range, and suggested that displacement from the range may affect the animals' ability to obtain sufficient energy intake. The development of techniques to quantify prey capture

attempts using buzzes as a proxy for foraging success (Johnson et al., 2004) and to monitor beaked whale movements and behaviour over extended time periods (weeks rather than days), together with improved measurements of benthic prey fields, should provide a better understanding of the consequences of displacement from AUTEC.

The results from the bioenergetics model indicate that young females are more vulnerable to the effects of disturbance than older animals, because the absolute size of their energy reserves is less and the cost of growth is higher. A young lactating female must supply the same volume of milk as a larger, older female from smaller reserves. All females are particularly vulnerable to disturbance during the first year of lactation when the calf is assumed to be totally dependent on its mother for its energy needs. Disruption of young females during this stage of lactation can, therefore, lead to the death of the calf and potentially of the mother.

The predictions from the bioenergetics model for the effects of disturbance on the probability of giving birth match quite closely with the lower quartile values from the expert elicitation (Figure 5.9). This was expected, because the assumption in the bioenergetics model that a disturbance response resulted in the complete loss of one day of foraging probably corresponds more closely to the severe behavioural response that the experts were asked to consider than the "most likely" response indicated by the median value. The predictions of the effects of disturbance on calf survival for the two different environments span the median values from the expert elicitation for disturbances ranging from 1 to 50 days. Beyond this level of disturbance the bioenergetics model predicts a much larger effect. This is a consequence of the interaction between the effects of disturbance on the probability of giving birth and calf survival in the bioenergetics model, and the fact that the model considers the effects of disturbance over multiple years.

The large divergence in opinion among experts depends on what mechanisms they considered to be important in translating behavioural responses into an effect on vital rates. They may have assumed that animals that were displaced as a result of disturbance continued to forage with little energy loss, or that the animals' dives were disrupted for the duration of the operations, or that animals were displaced to an area of poor habitat quality which led to a significant loss in energy.

It is also likely that some experts believed animals could compensate for lost foraging opportunities, even at high levels of disturbance, by increasing their foraging dive rate and/or duration on subsequent days. The bioenergetics model does allow females to compensate in this way if sufficient resources are available. Females that are resting (neither pregnant nor lactating) or waiting (able to become pregnant but have not yet ovulated) can probably compensate in this way under most environmental conditions. However, the bioenergetic model suggests that females in the third trimester of pregnancy and the first year of lactation are already feeding at the maximum possible rate, in order to cover the additional costs of gestation or milk production. This sets an upper limit on the number of days of disturbance days the female can compensate for, although this limit depends on resource density.

Some experts may have believed that beaked whales are primarily capital breeders and that a female can cover almost all of the costs of lactation from her energy reserves. This would allow some calves to survive, even at high levels of disturbance. The bioenergetics model assumes that there is a ceiling on the reserve mass that a female can accumulate, which is set by her need to remain neutrally buoyant and therefore forage effectively during lactation. This maximum reserve is insufficient to cover all of the energy costs of lactation.

The experts considered the effect of disturbance on calf survival and the probability of giving birth independently, whereas the bioenergetics model provided insight into the interaction between the two. For example, in the bioenergetics model, disturbance reduces the probability of giving birth because it increases the length of time that a female requires to build up sufficient reserve mass (as reflected by her relative body condition) to initiate a pregnancy. These effects accumulate over a number of years, but experts were only asked to consider the effects of disturbance over a single year. This is illustrated in Figure 5.13, which shows the effect of 30 days of disturbance per year over the lifetime of a female who survives to age 38 in an equilibrium environment. Without disturbance, the female is able to increase her body condition from weaning to approximately 5 years of age, despite the high costs of growth during these years (see Figure 4.6) and the fact that her feeding efficiency is less than 100%, as shown in the central panel of Figure 4.15. However, she is unable to do so when disturbed on a regular basis, and her body condition declines steadily over this time period (Figure 5.13). From age 5, her body condition improves, though more slowly than an undisturbed female, and she is unable to reproduce until she is approximately 14 years of age (compared to the mean age at maturity of 10.95 years for undisturbed females). When she finally gives birth to her first calf, her reserves are rapidly depleted during the latter stage of gestation and early lactation. As a result, she ceases to feed her calf and it dies. It then takes the female 5 years to recover her body condition to the point that she can become pregnant, and the cycle is repeated with the death of the second calf. Only when the female is 31 years of age she is able to raise a calf successfully, and even then, both the calf and the female risk death from starvation over an extended period.

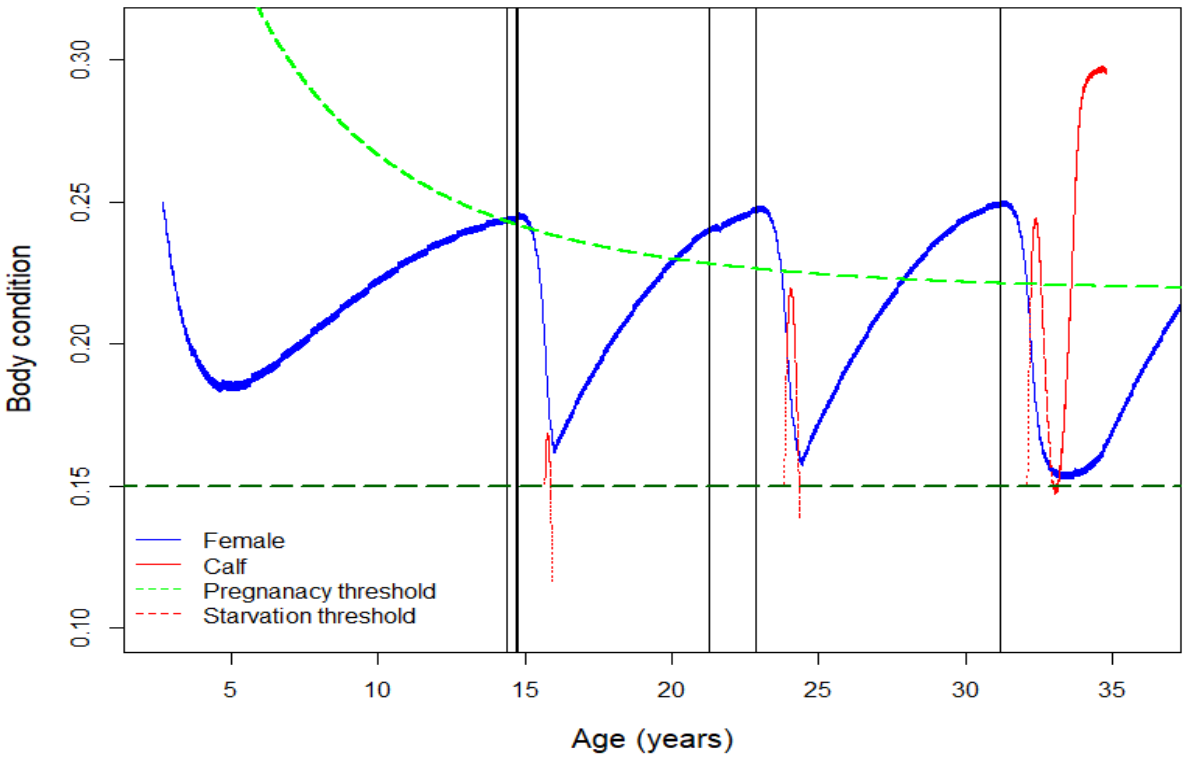

Figure 5.13 Predicted changes in the relative body condition (blue) of a female with 30 days of disturbance over her post-weaning lifetime. The day of conception for each pregnancy is marked by the vertical black lines. Changes in the relative body condition of each calf are shown in red. The pregnancy threshold is marked by the light green dashed line and the starvation threshold by the dark green line.

The bioenergetics model involves many assumptions about when females become pregnant, about the pattern of milk supply during lactation and the effect of body condition on this, about how quickly calves become proficient at feeding, and about the effect of body condition on survival. These assumptions were based on the best available data, but those data are very limited. In the elicitation process, experts were asked to construct their own mental models based on their experience and the information provided at the elicitation. It is unlikely that the assumptions underlying these mental models were identical to those used in the bioenergetics model. Consequently, it is not surprising that there is a wide spread in the values provided by the

experts and that these are different from those provided by the bioenergetics model. However, the bioenergetics model can be modified relatively simply in order to test the feasibility of these alternative mental models and the sensitivity of its own predictions to its underlying assumptions. Used in this way, it can provide a powerful tool for reducing variation among experts, and for avoiding unreasonably pessimistic or optimistic mental models. This approach was used in a recent repeat of the expert elicitation described in Donovan et al. (2016), and resulted in much less variability in expert opinion (J. Harwood, personal communication). In addition, the bioenergetics model can be used to identify those life history stages that are likely to be most sensitive to the effects of behavioural responses to disturbance. Experts can then be asked to focus on the relationship between disturbance and the relevant vital rates for those life history stages, rather than treating all adult females as identically susceptible to disturbance. Hopefully, a better-informed expert elicitation process will lead to more biologically reasonable results and foster the development of more accurate and insightful tools that can be used to guide the decision-making process.

5.5 Contributions

The analysis reported herein was conducted by the author. The recasting of the output from Hin et al (in press) model to allow comparison with the expert elicitation was carried out with help from J. Harwood, who also provided the results from the expert elicitation project.

The author provided the analysis of sonar data from AUTEC and developed the methods for approximating the dives lost from sonar via the use of passive acoustics. He also conducted the data analysis for the effect of disturbance via the extended model.

Archives that contained raw *Md* GVP data and sonar data during the time periods of interest were identified and the required data extracted from the M3R detection archives by colleagues at NUWC including Ashley Dilley and Karin Dolan who then ran these data through existing software to detect potential *Md* groups and sonar pings. These data were then processed by the author to determine the number of *Md* groups present with and without sonar, the results of which were used to estimate "dives lost" due to MFAS exposure.

5.6 Appendix: Tabular Summary of Bioenergetics Model Output

The tables below provide a summary of the results of the bioenergetics model outputs used for the analysis of MFAS operations at AUTEC and the comparison to expert elicitation. There are two major sections. The top panel shows the results from the expert elicitation study with increasing days of MFAS disturbance at a resource density of 1.32 $MJ \cdot m^{-3}$ (upper/tan) and 1.45 $MJ \cdot m^{-3}$ (bottom/blue).

The lower panel shows mix of results with and without measured AUTEC MFAS disturbance. The middle-green section shows the effect of changes in resource density with no MFAS disturbance (Note *Effect on Intake*=1.0). The bottom-grey section shows the effect of MFAS disturbance with changes in resource density. The upper-grey section shows the effect of MFAS disturbance at a resource density of 1.32 $MJ \cdot m^{-3}$. The yellow highlighted lines show the results at a resource density of 1.32 $MJ \cdot m^{-3}$ that produced results that approached those reported by Claridge (2013).

The mean outputs values were derived from 1,000 simulated individuals and are followed by the standard deviation (SD). Column definitions as follows:

1. *Rmean*: resource density ($MJ \cdot m^{-3}$)
2. *Days Disturb*: days of MFAS for expert elicitation.
3. *Disturb effect*: effect of disturbance on energy intake (0.0 to 1.0) for measured MFAS disturbance where 1.0 represents no effect.
4. *Effect on Intake*: the mean ratio of energy intake with disturbance to intake with no disturbance
5. *Life Expectancy*: mean life expectancy (years).

6. *Repro success*: the mean probability of females successfully weaning a calf over their lifetimes.
7. A*nnual Growth:* mean annual growth rate
8. *Birth Rate*: mean births per year per female
9. *First Born*: mean age (years) when females first give birth.
10. *ICI*: inter-calf interval (years).
11. *Calf Survival*: mean probability of calf survival
12. *Female Mortality:* number of female starvation deaths out of 1,000 individuals
13. *CA ratio*: mean dependent calf to adult female ratio across all 1,000 simulated animals.
14. *Breeders*: number of animals (out of 1,000) that successfully wean a calf.

Expert Elicitation

Rmean	Days Disturb	Effect on Intake	SD	Life Expectancy	SD	Repro Success	SD	Annual Growth
1.32	0	1.000	0.000	23.22	14.46	1.05	1.09	1.002
1.32	2	0.995	0.001	23.88	14.05	1.08	1.03	1.002
1.32	4	0.989	0.003	24.02	14.30	1.02	1.02	1.001
1.32	6	0.984	0.002	23.65	14.30	1.00	0.97	1.000
1.32	8	0.978	0.005	23.75	14.30	0.97	0.96	0.999
1.32	10	0.973	0.003	23.94	14.16	0.91	0.90	0.996
1.32	20	0.946	0.006	23.16	14.29	0.57	0.65	0.976
1.32	25	0.932	0.006	23.75	14.34	0.35	0.48	0.956
1.32	30	0.918	0.009	23.71	14.42	0.01	0.07	0.816
1.32	35	0.902	0.017	8.50	6.02	0.00	0.00	0.000
1.32	40	0.887	0.014	4.26	0.41	0.00	0.00	0.000
1.45	0	1.000	0.000	22.85	14.37	1.21	1.19	1.008
1.45	5	0.986	0.003	23.17	14.49	1.22	1.21	1.009
1.45	10	0.973	0.005	23.06	14.31	1.20	1.17	1.008
1.45	15	0.959	0.005	24.03	14.07	1.26	1.18	1.010
1.45	20	0.945	0.005	23.58	14.79	1.16	1.16	1.006
1.45	25	0.932	0.006	22.87	14.35	1.03	1.04	1.001
1.45	30	0.918	0.009	23.49	14.23	1.00	0.96	1.000
1.45	35	0.904	0.007	23.70	14.46	0.87	0.89	0.994
1.45	40	0.890	0.008	23.39	14.36	0.69	0.76	0.984
1.45	45	0.877	0.005	23.07	14.11	0.48	0.48	0.969
1.45	50	0.863	0.008	23.01	13.70	0.04	0.14	0.870
1.45	55	0.846	0.012	11.13	11.72	0.00	0.00	0.000

MFAS in grey, No MFAS in green

Rmean	Disturb Effect	Effect on Intake	SD	Life Expectancy	SD	Repro Success	SD	Annual Growth
1.32	1.0000	1.000	0.000	23.22	14.46	1.05	1.09	1.002
1.32	0.7500	0.971	0.004	23.34	14.29	0.88	0.91	0.995
1.32	0.5000	0.940	0.015	23.72	14.40	0.58	0.67	0.977
1.32	0.4000	0.929	0.007	24.02	14.30	0.30	0.44	0.952
1.32	0.3500	0.923	0.009	23.47	14.06	0.13	0.28	0.917
1.32	0.2500	0.911	0.012	21.93	14.17	0.00	0.05	0.782
1.40	0.5000	1.000	0.000	23.50	14.59	1.22	1.15	1.008
1.38	0.5000	1.000	0.000	23.70	14.35	1.21	1.16	1.008
1.35	0.5000	1.000	0.000	23.48	14.01	1.17	1.14	1.007
1.32	0.5000	1.000	0.000	22.65	14.51	1.03	1.08	1.001
1.30	0.5000	1.000	0.000	23.59	14.43	0.97	0.97	0.999
1.28	0.5000	1.000	0.000	23.47	14.58	0.91	0.93	0.996
1.25	0.5000	1.000	0.000	22.95	14.07	0.70	0.78	0.985
1.20	0.5000	1.000	0.000	23.41	14.29	0.22	0.36	0.937
1.19	0.5000	1.000	0.000	23.37	14.22	0.06	0.19	0.887
1.40	0.5000	0.941	0.009	22.36	14.09	0.92	0.95	0.996
1.38	0.5000	0.941	0.007	23.41	13.92	0.91	0.87	0.996
1.35	0.5000	0.941	0.006	23.62	14.54	0.76	0.80	0.989
1.32	0.5000	0.940	0.015	23.72	14.40	0.58	0.67	0.977
1.30	0.5000	0.941	0.005	23.16	14.09	0.32	0.46	0.952
1.25	0.5000	0.941	0.005	23.19	14.20	0.00	0.00	0.000

Expert Elicitation

Rmean	Days Disturb	Effect on Intake	Birth Rate	SD	First Born	SD	ICI	SD
1.32	***0***	1.000	0.206	0.666	11.837	1.531	4.565	0.994
1.32	***2***	0.995	0.204	0.068	11.890	1.544	4.652	1.050
1.32	***4***	0.989	0.190	0.074	12.259	1.818	4.772	1.056
1.32	***6***	0.984	0.189	0.065	12.084	1.494	4.870	0.987
1.32	***8***	0.978	0.184	0.064	12.093	1.503	5.058	1.080
1.32	***10***	0.973	0.177	0.066	12.395	1.721	5.099	1.032
1.32	***20***	0.946	0.153	0.062	13.123	1.610	5.470	1.078
1.32	***25***	0.932	0.141	0.054	14.000	1.629	5.805	1.233
1.32	***30***	0.918	0.115	0.052	16.270	1.699	6.225	1.159
1.32	***35***	0.902	0.082	0.064	17.043	1.901	6.218	1.387
1.32	***40***	0.887	0.000	0.000	0.000	0.000	0.000	0.000
1.45	***0***	1.000	0.245	0.076	11.142	1.644	3.944	0.944
1.45	***5***	0.986	0.240	0.081	11.162	1.520	4.051	1.006
1.45	***10***	0.973	0.233	0.086	11.261	1.459	4.187	1.087
1.45	***15***	0.959	0.234	0.074	11.510	1.577	4.248	1.136
1.45	***20***	0.945	0.223	0.079	11.669	1.526	4.333	1.029
1.45	***25***	0.932	0.202	0.076	11.858	1.521	4.641	1.034
1.45	***30***	0.918	0.191	0.061	11.848	1.511	5.011	1.172
1.45	***35***	0.904	0.175	0.065	12.333	1.672	5.130	1.156
1.45	***40***	0.890	0.161	0.062	12.768	1.437	5.442	1.082
1.45	***45***	0.877	0.144	0.057	13.733	1.632	5.743	1.080
1.45	***50***	0.863	0.121	0.051	15.688	1.906	6.173	1.291
1.45	***55***	0.846	0.056	0.039	22.062	1.893	8.255	1.543

MFAS in grey, No MFAS in green

Rmean	Disturb Effect	Effect on Intake	Birth Rate	SD	First Born	SD	ICI	SD
1.32	***1.00***	1.000	0.206	0.666	11.837	1.531	4.565	0.994
1.32	***0.75***	0.971	0.178	0.066	12.470	1.555	5.042	1.214
1.32	**0.50**	0.940	0.157	0.061	13.304	1.648	5.378	1.147
1.32	**0.40**	0.929	0.144	0.055	14.025	1.617	5.699	1.269
1.32	**0.35**	0.923	0.130	0.055	14.911	1.728	5.892	1.268
1.32	***0.25***	0.911	0.090	0.046	18.202	2.418	7.050	1.666
1.45	0.50	1.000	0.254	0.092	11.137	1.535	3.924	1.038
1.40	0.50	1.000	0.237	0.078	11.397	1.538	4.082	0.970
1.38	0.50	1.000	0.230	0.092	11.495	1.598	4.173	0.921
1.35	0.50	1.000	0.222	0.077	11.621	1.082	4.277	0.956
1.32	0.50	1.000	0.206	0.072	11.950	1.772	4.563	1.164
1.30	0.50	1.000	0.195	0.070	12.054	1.514	4.794	1.029
1.28	0.50	1.000	0.179	0.067	12.410	1.802	5.019	1.141
1.25	0.50	1.000	0.169	0.066	12.857	12.857	5.069	1.063
1.20	0.50	1.000	0.155	0.064	13.843	1.596	5.119	1.105
1.19	0.50	1.000	0.154	0.060	14.257	1.650	5.138	1.073
1.40	0.50	0.941	0.187	0.070	12.097	1.614	4.864	1.003
1.38	0.50	0.941	0.183	0.062	12.394	1.756	5.114	1.066
1.35	0.50	0.941	0.169	0.060	12.784	1.737	5.284	1.198
1.32	0.50	0.940	0.157	0.061	13.304	1.648	5.378	1.147
1.30	0.50	0.941	0.144	0.058	13.982	1.717	5.645	1.312
1.25	0.50	0.941	0.068	0.040	20.594	2.146	7.925	1.571

Expert Elicitation

Rmean	Days Disturb	Effect on Intake	Calf Survival	SD	Female Mortality	CA Ratio	SD	Breeders
1.32	***0***	1.000	0.649	0.198	0.000	0.468	0.051	619
1.32	***2***	0.995	0.667	0.208	0.000	0.455	0.048	647
1.32	***4***	0.989	0.669	0.207	0.000	0.439	0.050	624
1.32	***6***	0.984	0.672	0.213	0.000	0.425	0.050	629
1.32	***8***	0.978	0.659	0.214	2.000	0.415	0.049	632
1.32	***10***	0.973	0.638	0.217	1.000	0.391	0.049	623
1.32	***20***	0.946	0.495	0.187	7.000	0.276	0.045	531
1.32	***25***	0.932	0.394	0.165	4.000	0.188	0.039	418
1.32	***30***	0.918	0.250	0.096	14.000	0.054	0.022	14
1.32	***35***	0.902	0.000	0.000	745.000	0.003	0.006	0
1.32	***40***	0.887	0.000	0.000	887.000	0.003	0.006	0
1.45	***0***	1.000	0.659	0.183	0.000	0.546	0.048	622
1.45	***5***	0.986	0.661	0.187	0.000	0.533	0.050	627
1.45	***10***	0.973	0.334	0.200	0.000	0.527	0.049	635
1.45	***15***	0.959	0.678	0.190	0.000	0.515	0.050	658
1.45	***20***	0.945	0.658	0.185	0.000	0.501	0.052	612
1.45	***25***	0.932	0.671	0.204	0.000	0.463	0.049	619
1.45	***30***	0.918	0.670	0.214	0.000	0.427	0.050	643
1.45	***35***	0.904	0.644	0.216	2.000	0.377	0.048	613
1.45	***40***	0.890	0.562	0.214	7.000	0.310	0.046	567
1.45	***45***	0.877	0.482	0.178	28.000	0.245	0.044	472
1.45	***50***	0.863	0.265	0.086	37.000	0.080	0.027	80
1.45	***55***	0.846	0.000		566.000	0.011	0.010	0

MFAS in grey, No MFAS in green

Rmean	Disturb Effect	Effect on Intake	Calf Survival	SD	Female Mortality	CA Ratio	SD	Breeders
1.32	***1.00***	1.000	0.649	0.198	0.000	0.468	0.051	619
1.32	***0.75***	0.971	0.642	0.221	0.000	0.393	0.047	600
1.32	**0.50**	0.940	0.481	0.186	4.000	0.271	0.044	538
1.32	**0.40**	0.929	0.359	0.147	19.000	0.175	0.040	385
1.32	**0.35**	0.923	0.299	0.122	31.000	0.114	0.031	212
1.32	***0.25***	0.911	0.300	0.089	65.000	0.031	0.018	9
1.45	0.50	1.000	0.648	0.092	0.000			
1.40	0.50	1.000	0.655	0.185	0.000	0.526	0.049	634
1.38	0.50	1.000	0.671	0.193	0.000	0.516	0.048	643
1.35	0.50	1.000	0.672	0.197	0.000	0.504	0.048	639
1.32	0.50	1.000	0.667	0.202	0.000	0.466	0.049	603
1.30	0.50	1.000	0.642	0.203	0.000	0.439	0.048	624
1.28	0.50	1.000	0.619	0.215	0.000	0.387	0.049	620
1.25	0.50	1.000	0.550	0.204	0.000	0.331	0.047	568
1.20	0.50	1.000	0.276	0.106	0.000	0.152	0.036	317
1.19	0.50	1.000	0.213	0.070	0.000	0.087	0.029	107
1.40	0.50	0.941	0.662	0.196	0.000	0.425	0.049	600
1.38	0.50	0.941	0.657	0.224	1.000	0.399	0.047	640
1.35	0.50	0.941	0.586	0.213	3.000	0.337	0.049	577
1.32	0.50	0.940	0.481	0.186	4.000	0.271	0.044	538
1.30	0.50	0.941	0.382	0.167	7.000	0.186	0.038	395
1.25	0.50	0.941	0.000	0.000	19.000	0.015	0.013	258

Chapter 6

Towards Integrated Monitoring of the Exposure of Beaked Whales to Mid-Frequency Active Sonar (MFAS) and its Population Consequences

6.1 Overview

Current U.S. Navy marine mammal research, partly due to legal mandates (Buzzas, 2016), focuses on the effect of repeated long-term exposure to mid-frequency active sonar (MFAS) on beaked whale populations. This has become increasingly important as environmental permitting in the U.S. is ultimately driven by a determination of "negligible impact" as specified by the Marine Mammal Protection Act (MMPA). However, making this determination for beaked whales is exceedingly challenging. The research presented here examines this question and provides tools to help answer it and hopefully inform the decision-making process.

The author developed and applied passive acoustic methods to a population of Blainville's beaked whales (*Mesoplodon densirostris, Md*) at the Atlantic Undersea Test and Evaluation Center (AUTEC) to:

1) estimate *Md* density and abundance,

2) assess behavioural risk from MFAS exposure,

3) model the effects of MFAS-induced behavioural change on vital rates using a bioenergetics-based model, and

4) compare the output from the bioenergetics model with observations at AUTEC and predictions from an expert elicitation.

This chapter presents a short summary of the history of investigations relating to *Md* at AUTEC as an example of the research necessary to estimate the effect of MFAS disturbance. It summarizes the findings from this research and explores how this work could fit into an integrated monitoring programme. This programme is specifically tailored for AUTEC, but it could also be used on other Navy ranges. Programmes of this kind must occur in parallel with Navy operations with minimal interference, and be maintained by Navy range personnel. This is particularly important in training exercises, where the U.S. Navy goal is to "train as you fight". The aim of the programme is to monitor population abundance on Navy ranges, but also to illuminate any changes in demographic characteristics and rates that may occur and their population consequences. The proposed programme would use passive acoustics to monitor trends in population size and the coincident level of sonar use. This would be supported by supplementary monitoring using visual observational methods, and potentially the remote measurement of body condition. Results from combined passive acoustic and visual monitoring could be used in conjunction with a bioenergetic model to predict and monitor for potential adverse population level changes.

6.2 Beaked Whales and Navy Ranges

The U.S. Navy's undersea acoustic ranges are designed to precisely track undersea vehicles (Vincent, 2001). Currently, there are three major undersea ranges in operations. They are the Southern California Offshore Range (SCORE) off the coast of Southern California, the Pacific Missile Range Facility (PMRF) off the coast of Kauai, HI (Figure 6.1) that includes the Barking

Sands Tactical Underwater Range (BARSTUR) and the adjacent Barking Sands Underwater Range Expansion (BSURE). The third, the Atlantic Undersea Test and Evaluation Center (AUTEC) in the Bahamas, provided the data for this study. A new range, the Undersea Warfare Training Range (USWTR), off the coast of Jacksonville, FL, is scheduled to begin operation in late 2019 (Figure 6.2). Each facility includes a large array of bottom-mounted hydrophones similar to that described in Chapter 1. Cuvier's beaked whales (*Ziphius cavirostris, Zc*) have been detected at SCORE (Falcone et al., 2009) and *Md* have been detected at both PMRF (Manzano-Roth et al., 2016) and AUTEC (McCarthy et al., 2011; Moretti et al., 2010).

The hydrophones at AUTEC, SCORE, and PMRF lie in deep water (1,000 m) adjacent to steep canyon walls (AUTEC, SCORE) or a steep slope gradient (PMRF), features that are generally associated with beaked whale habitat (Mead, 1989; Pitman, 2008). USWTR lies on the Eastern U.S. Atlantic Ocean shelf-break, in water depths of roughly 50 m to 300 m. To date, the presence of beaked whales has not been documented there. However, the site lies to the east of critical habitat for the North Atlantic right whale (*Eubalaena glacialis*), where calving occurs during the winter months (Keller et al., 2012). While the USWTR hydrophones are outside this critical habitat, they could be used to monitor right whale calls within and around the range boundary using techniques similar to those developed for beaked whales. Right whales are far less, vocal so the efficacy of passive acoustic monitor of this species at USWTR should be evaluated (Parks et al., 2011). However, passive acoustic monitoring would also provide a precise record of MFAS transmissions in close proximity to the critical habitat. A Marine Monitoring on Navy Ranges (M3R) system similar to that used to gather passive acoustic data for this study is already installed on the three deep-water ranges and is scheduled for installation on USWTR and also the Canadian Nanoose range in 2019.

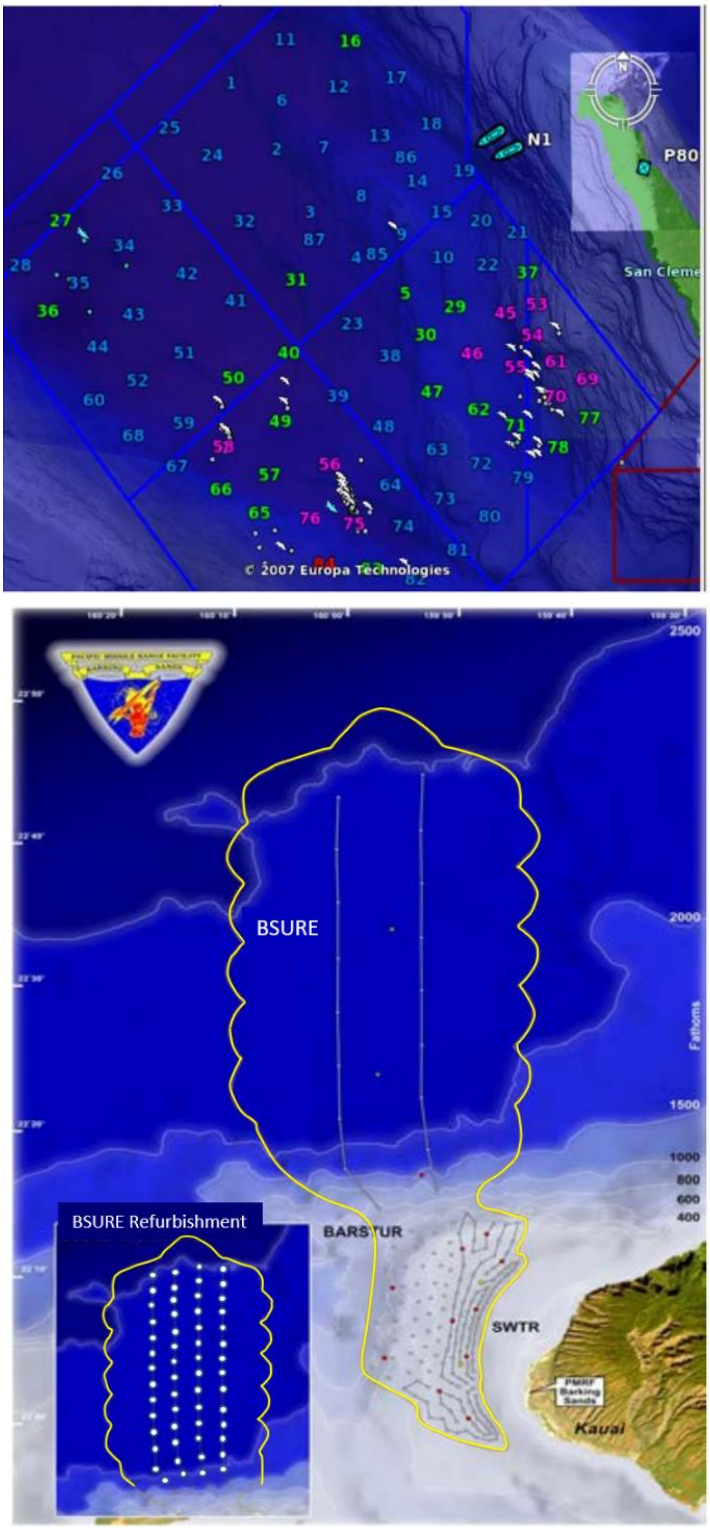

Figure 6.1 A Marine Mammal Monitoring on Navy Ranges (M3R) display of the SCORE hydrophone array in the San Nicolas Basin west of San Clemente Island with dolphin and ship positions (upper) and the PMRF hydrophone array off the island of Kauai (lower) with the BSURE replacement hydrophone array shown by the inset in the lower left.

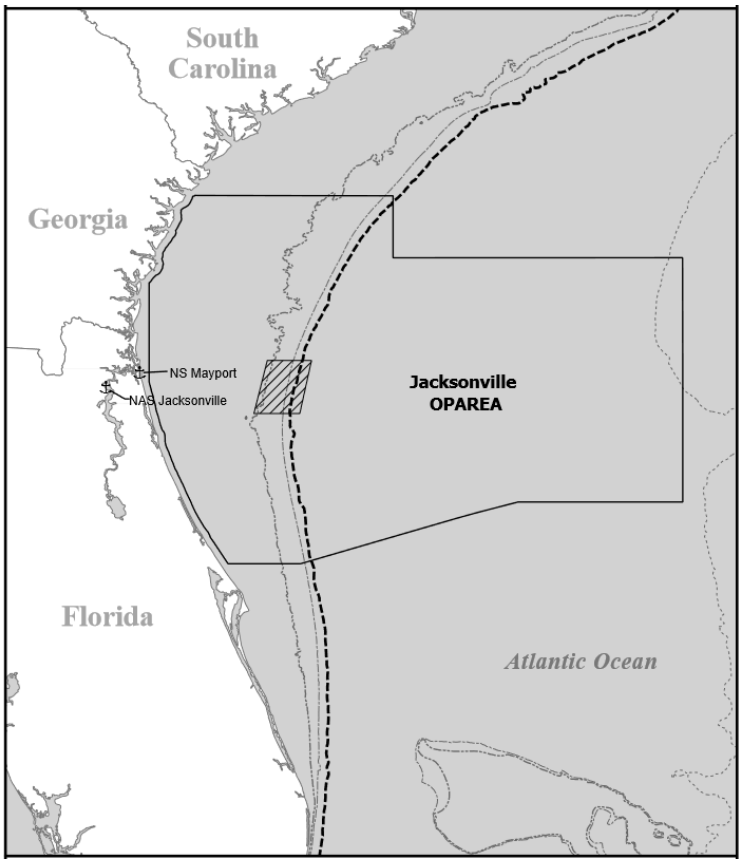

Figure 6.2 The USWTR (striped area), shown within the Jacksonville Operations Area (OPAREA) off Jacksonville, FL. The shelf break is marked by the heavy dashed line ("Atlantic Fleet Training and Testing Final Environmental Impact Statement/Overseas Environmental Impact Statement," 2013).

As illustrated in the previous chapters, these same technologies can also be used to study beaked whales *in situ* over broad temporal scales. Analytical tools have been developed for use with these hydrophone arrays (Jarvis et al., 2014). These tools can be used for passive acoustic monitoring systems, and to understand the acoustic and physical behaviour of these cryptic, "sonar sensitive" species and their reaction to MFAS exposure. The ultimate goal is to use the

derived data to determine the long-term effect on beaked whales of repeated MFAS exposure on the U.S. Navy undersea ranges.

Passive acoustic methods were not developed independently of other study modalities. The hydrophone array provides a means of extended listening to cetacean vocalizations. Making sense of the acoustic information requires an understanding of both the sound source and the context in which vocalizations are produced. This understanding grew out of a mix of studies that included visual observations, photo-identification (photo-ID) (Claridge, 2013, 2006), the use of recording and satellite tags (Baird et al., 2006; Johnson and Tyack, 2003; Joyce et al., in press; Schorr et al., 2014), and analysis of biopsy and faecal samples (Hooker et al., 2001). These studies revealed that beaked whales, including *Md*, are particularly suited for passive acoustic monitoring using deep, bottom-mounted hydrophone arrays. Their loud clicks (>200 dB) are produced at depth (>200 m) with a centre frequency (~30 kHz) that is well within the bandwidth of the hydrophones, making consistent detection of foraging animals likely (Johnson et al., 2006a; Shaffer et al., 2013). The whales' near silence when they are within 200 m of the surface, and the fact that echolocation clicks are only produced during deep foraging dives means that these clicks provide unambiguous information on the animals' spatial distribution while foraging (Arranz et al., 2011; Johnson et al., 2006a, 2004). Thus, passive acoustic methods should be a fundamental component of a long-term Navy range monitoring programme, because they can document behavioural changes that may result in population effects and help develop management strategies to minimize such effects.

A causal link between MFAS exposure and beaked whale strandings has been widely acknowledged (D'Amico et al., 2009; England et al., 2001). While the exact mechanism that leads to these strandings remains elusive (Bernaldo de Quirós et al., 2019), animals' reaction to

MFAS exposure has been documented by controlled exposure experiments (DeRuiter et al., 2013; Miller et al., 2012; Tyack et al., 2011), passive acoustic studies (Manzano-Roth et al., 2016; McCarthy et al., 2011; Moretti et al., 2010), and the use of satellite tags (Falcone et al., 2017; Joyce et al., in press). The best-documented event is the mass stranding of beaked whales in the Northwest Providence Channel, Bahamas in 2000, in which Navy MFAS operations were directly implicated (England et al., 2001). As with many other strandings, *Zc* and *Md* composed the majority (15 of the 17) of stranded animals (Balcomb and Claridge, 2001; England et al., 2001; Filadelfo et al., 2009). The associated bathymetric and operational conditions were used to identify five "Bahamas Factors" (England 2007; and Chapter 1) that were likely to be associated with beaked whale strandings.

These same conditions are present at AUTEC, SCORE and PMRF. Stranding networks and formal reporting standards have been in place at these facilities since 2000. While this does not preclude an unreported MFAS related death at sea or stranding in a remote location (Faerber and Baird, 2010), it does reduce the likelihood of such an incident going unreported. However, no beaked whale mass stranding has been reported at any of these facilities.

In addition to the risk of stranding, behavioural reactions of beaked whales to MFAS operations and CEEs have been documented. The bioenergetics model developed in Chapter 4 and 5 suggests that repeated behavioural responses associated with MFAS operations may result in changes in calf survival and the probability of giving birth. Claridge (2013) reported a significant difference in the ratio of dependent calves to adult females (CA ratio) between AUTEC and a nearby, undisturbed population at Abaco. This difference could be duplicated using the bioenergetics model, as discussed in Chapter 5, which predicted a negative population growth rate at AUTEC. If this is the case, it suggests that MFAS operations at AUTEC may

have a “negative impact” on the population, as defined by the MMPA. Long-term monitoring of the abundance and demographic rates for the *Md* population on AUTEC is therefore desirable, in order to determine if repeated MFAS exposure is having this predicted impact.

This dissertation has described the development and application of tools that can contribute to such monitoring. In addition to measuring abundance over multiple temporal scales, the tools also provide a means of assessing the probability of a behavioural response (such as lost foraging dives or displacement) to MFAS exposure and for exploring the potential effect of any behavioural changes on energy intake, calf survival and reproductive success. The challenge is to place these tools in a framework that provides a level of long-term monitoring sufficient to detect population-level effects in a timely manner.

6.3 Results summary

6.3.1 Passive Acoustic Abundance Estimation

The initial question raised for monitoring is how best to estimate the number of animals present on a range. The extensive arrays of hydrophones on navy ranges, coupled with the development of passive acoustic tools for the detection and classification of *Md* echolocation clicks (Jarvis, 2012; Jarvis et al., 2014), has informed the development of the dive counting algorithm described in Chapter 2 (Moretti et al., 2010). Chapter 2 demonstrated how two years of data from the AUTEC hydrophone array could be used to estimate the number of animals present on the range over multiple temporal scales. Correction factors for the probability of detection and the false alarm rate were calculated by comparing a manual review of the number of *Md* groups extracted from the data with the number detected using semi-automated tools. These semi-automated methods can be used to provide estimates of abundance in the future. However, care

must be taken to ensure that the correction factors are routinely recalculated, to capture variability and assure sample independence.

Given the AUTEC range infrastructure, data can be collected on a near-continual basis. This means estimates can be examined on time scales ranging from hours to years. By comparison, estimates derived from visual data, using techniques such as capture-recapture or line-transect surveys, require extensive field efforts, because beaked whales are extremely hard to sight. For example, Claridge (2013) had to pool data across six years to estimate the number of animals at AUTEC using capture-recapture analysis. There were on average only four encounters with *Md* during approximately 30 days of field effort per year. By comparison, upwards of 100 group vocal periods (GVPs), each representing a foraging dive by a group of *Md*, are detected during a typical day at AUTEC.

6.3.2 A Risk Function for MFAS-mediated Behavioural Disturbance

GVP detections can also be combined with AUTEC operational data and passive acoustic detection of MFAS transmissions to investigate *Md* temporal and spatial distribution, and foraging before, during and after operations using MFAS. These data were used to estimate the parameters of the risk function documented in Chapter 3 and the bioenergetics model described in Chapter 5.

In addition to permits for operations on its ranges, the U.S. Navy must also seek permits for operation in un-instrumented training areas, where direct measurement of the effect of MFAS on cetaceans is extremely difficult. To meet this environmental obligation, an effects model is used to estimate the number of behavioural "takes" of animals, as defined by the U.S. Marine Mammal Protection Act. Estimating behavioural takes is carried out using a risk function that

maps the root-mean-squared receive level (RL) of MFAS to the probability of a behavioural reaction (Spigel, 2013). Chapter 3 described the derivation of an *Md* behavioural risk function, the first to be derived from actual MFAS operations (Moretti et al., 2014). A parametric equation that quantifies this relationship was developed that predicts the probability of an animal foregoing a deep foraging dive as a function of MFAS RL. The results indicate a 0.5 probability of foraging disruption at an RL of 150 dB re µPa. Based on a PMRF case study, this falls between the 140 dB re µPa step function used for the last approved Navy Ranges Environmental Impact Statement (2008) and the 165 dB re µPa Feller function that had been used prior to 2008. It is important to note that the risk function models response as a continuous function of RL, rather than using a simple threshold value. For regulation purposes, it is important to use the whole curve, as recommended by the National Academies of Sciences, Engineering, and Medicine (2017). In addition, the method described in Chapter 3 provides a means of analysing both future data and the effect of different MFAS sources. It also makes it possible to include the effects of additional covariates, such as distance to the source.

6.3.3 Using a Bioenergetics Approach to Investigate the Potential Long-term Effects of Repeated MFAS Exposure

Chapter 4 and 5 presented an adaptation of a bioenergetics model for long-finned pilot whales (*Globicephala melas*) developed by Hin et al. (in press). The model was parameterized for *Md* and used to investigate changes in demographic rates as a function of resource density with and without MFAS disturbance. One thousand simulated females were followed throughout their lifetimes from weaning. Body condition was defined as the ratio of reserve tissue mass (which is probably mostly lipid) to total mass. Both females and their calves were assumed to be at risk of death from starvation if their body condition fell below a threshold level, based on the lowest body condition values observed in harvested pilot whales. Energy intake depended on body

condition, body size and the density of resources (defined in terms of the maximum amount of assimilated energy an animal could acquire in one day). The energetic costs of maintenance, growth, pregnancy and lactation were modelled separately. The model outputs indicated that young females are likely to more susceptible to adverse effects from reduced resource density or disturbance, because the total amount of reserves they can carry is less than for older animals. Energy demands are greatest during the first half of lactation when females must supply all of the calf's energy requirements. Minimum body condition for both females and their calves typically occurred during this time.

With a resource density of 1.32 $MJ \cdot m^{-3}$, it was possible to duplicate the CA ratio of 0.52 reported by Claridge (2013) for the undisturbed population at Abaco. If daily energy assimilation is reduced, either as a result of lower resource density or effects of disturbance on foraging, there is a decline in body condition, especially during late gestation and lactation. This affects milk production and can lead to lower calf survival especially during the first year of lactation, when the calf is totally dependent on its mother. The time the female requires to rebuild her body condition at the end of lactation is also extended. This leads to a delay in pregnancy, a reduction in the overall probability of giving birth and a longer inter-calf interval. Taken together, these changes can result in a negative population growth rate. If resource density was reduced to 1.22 $MJ \cdot m^{-3}$, it was possible to duplicate the lower CA ratio of 0.21 observed by Claridge (2013) at AUTEC.

To investigate the effect of MFAS disturbance, a probability of disturbance vector that encompassed every day of a female's life from weaning to death was derived from passive acoustic data and operational logs provided by AUTEC for 2012. The start and stop time of each MFAS operation was identified. For each operation, the probability of displacement from the

range was estimated from the ratio of the number of GVPs detected during MFAS operations to the number detected in the absence of MFAS operations in the preceding period. It was assumed that the MFAS operations the animal was exposed to in 2012 were representative of yearly operations throughout its life. With a resource density of 1.32 $MJ \cdot m^{-3}$, the measured MFAS pattern of disturbance and with an assumed effect on energy assimilation of 0.5 for every day that a female was disturbed, the predicted CA ratio also approximated that observed by Claridge (2013) at AUTEC.

Although it is known that animals move in response to operations at AUTEC (Joyce et al., in press; McCarthy et al., 2011; Tyack et al., 2011), it is not clear what effect such movement has on energy intake. Joyce et al. (in press) observed that satellite tagged *Md* resumed deep diving within 12 hours of being displaced from AUTEC by MFAS operations, which supports the assumption of a 50% reduction in energy assimilation

Both observational data (Claridge, 2013, 2006) and satellite tag data (Joyce et al., in press) suggest that animals found in the Tongue of the Ocean (TOTO) represent a discrete population. However, the effect of disturbance depends heavily on the proportion of time these animals spend on the range. AUTEC operations are generally isolated on the range, so MFAS operations are unlikely to affect *Md* that are outside the range borders. Unfortunately, there is currently no information on the percent of time *Md* in the TOTO population spend on AUTEC, although a more detailed analysis of data from satellite tagged animals may provide this in the future.

There are processes other than energy assimilation that could contribute to the difference in the CA ratios observed between Abaco and AUTEC. For example, there is a higher prevalence of cookie cutter shark bites on animals at AUTEC (D. Claridge personal communication). The

effect of such bites on a young calf could be significant. Differences in disease exposure could also help explain the differences. At this time, the results from the bioenergetics model are instructive but not definitive, though they strongly suggest that there is a requirement for systematic population monitoring.

6.3.4 A Comparison of Results from the Bioenergetics Model and Expert Elicitation.

Predictions from the bioenergetic model of the effects of varying levels of disturbance on calf survival and the probability of giving birth were also compared to those obtained via an expert elicitation (Booth et al., 2015). The model predictions of the relationship between the probability of giving birth and the number of days of disturbance fell roughly within the lower quartile of expert predictions if the resource density was 1.45 $MJ.m^{-3}$. This corresponded to favourable environmental conditions that allowed animals to compensate for the effect of lost foraging opportunities on subsequent days. In a less favourable environment, with a resource density of 1.32 $MJ \cdot m^{-3}$, the relationship between the probability of giving birth and the number of days of disturbance also fell within the first quartile of the expert predictions with up to 22 days of disturbance, but this probability fell to zero with 25 days of disturbance. This was because animals were unable to accumulate sufficient reserves to breed successfully at this level of disturbance. The relationship between calf survival and the number of days of disturbance in both favourable and less favourable environments matched the median expert opinion quite closely for levels of disturbance up to about 40 days of disturbance. However, calf survival in the bioenergetics model declined to zero at higher levels of disturbance, because no calves were predicted to be born at these levels. In contrast, the experts generally predicted that disturbance would only reduce calf survival by 50%, even at the highest levels. However, they were not asked to consider the possibility that there was an interaction between the effects of disturbance

on the two vital rates. At 1.45 MJ·m^{-3} survival suffered little decrease with up to 50 days of disturbance at which point it decreased to zero by 55 days of disturbance. By contrast, the median value predicted by the experts hit an asymptotic limit of a roughly 0.5 effect on survival after approximately 260 days of disturbance.

The experts were effectively asked to consider calf survival and the probability of giving birth as independent processes. However, within the bioenergetic model, they are tightly coupled, therefore, the bioenergetics model provides the opportunity to investigate such dependencies in detail. Providing experts with access to the outputs from models of this kind could inform the elicitation processes, thus helping the experts to explore such interrelationships.

6.4 Planning for Long-term Monitoring

The report of the National Academy of Sciences (NAS) Committee on the Cumulative Effects of Stressors on Marine Mammals (National Academies of Sciences, Engineering, and Medicine, 2017) considered the effect of anthropogenic stressors on animal populations and reviewed approaches to understanding their cumulative effect. They concluded that, in many cases, such effects are unknown and can be unpredictable, and stated that there is a "pressing need for early detection of population declines" (National Academies of Sciences, Engineering, and Medicine, 2017). The Committee also suggested that comparisons with a reference population can be informative, but that variability must be considered. For *Md* at AUTEC, the Abaco population provides such a potential reference population.

The Committee also explicitly recommended that "Responsible agencies should develop relatively inexpensive surveillance systems that can provide early detection of major changes in population status and health". Cumulative effects can potentially cause a major decline over a

relatively short period. For instance, if the AUTEC population is already under stress, changes to any one of a number of factors such as prey availability, MFAS operations, or inter-specific competition, could result in a decline in the population. The tools described in this dissertation can contribute to the detection of such changes and potentially serve as an "early warning" system. Certainly, the Navy hydrophone arrays were not "inexpensive" to install, but they exist and are available for monitoring. By leveraging these existing systems, cost-effective passive acoustic methods can be applied.

There are cautions within the NAS Committee's recommendations. Defining a population and the area over which it ranges can be difficult. Clearly, the effect of foraging disruption is dependent on the home range of the animals as well as the temporal and spatial distribution of prey within their range. Claridge (2013) suggested that *Md* at AUTEC and Abaco represent distinct populations. The local canyon bathymetry is likely to restrict the range of each population, which supports this contention. If the animals that use the AUTEC range remain within the TOTO they can only move to the North or to the South as the range occupies the width of the TOTO.

One of the aims of the monitoring programme described here is to detect any population level changes and to determine what drives those changes. However, a resource-limited population may exhibit signs of stress that may be difficult to distinguish from the effects of MFAS exposure. In addition, natural variation within the populations must be accounted for.

Claridge (2013) identified demographic differences between the AUTEC and Abaco populations. To reach the demographic levels reported by Claridge, the bioenergetics suggests a growth rate (≈0.98) that would result in a population in decline. Yet, AUTEC has been in operation since the

late 1960s and beaked whales have been routinely detected using passive acoustics and sighted since 2003. It could also be that the population is being supplemented by immigration from another population, outside the TOTO, although this would have to involve the movement of non-breeding animals to account for the observed demographic structure.

By incorporating tags into the monitoring programme at AUTEC it may be possible to better quantify the animals' range as well as the effect of MFAS operations on foraging success. Fleishman et al. (2016) laid out the steps required to design a monitoring programme with this in mind. They are: developing a theory of change, estimating the magnitude of effect, selecting the monitoring response variable and specifying the temporal sequence of monitoring.

For *Md* at AUTEC, it is hypothesized that repeated disruption of foraging dives results in a reduction in energy intake that affects individual health and could reduce a female's probability of giving birth and calf survival. If the animals in the TOTO do represent a discrete population, it is likely a large proportion of that population will be exposed to most MFAS signals. This means the magnitude of effect will be felt across the entire population.

Perhaps the simplest response variable is animal abundance, which can be estimated directly with passive acoustic monitoring. However, there is a danger that by the time there is a measurable change in abundance, it may be too late to adjust the management strategy (National Academies of Sciences, Engineering, and Medicine, 2017), and therefore the temporal sequence of monitoring must be chosen to allow sufficient time to detect changes. The AUTEC hydrophones are cabled to shore, thus any delays in accessing data can, in theory, be minimized. Consequently, passive acoustic monitoring using the AUTEC infrastructure provides an excellent opportunity for the early detection of any change in population size.

Other potential indicators of change should not be ignored. While it is unlikely they can be used to detect abrupt changes in abundance, they can inform the decision-making process and help in the evaluation of short-term changes. For instance, individual health (as measured by body condition) may affect the probability of giving birth, calf survival or the time to weaning, and this will be reflected in the CA ratio. So, the CA ratio and body condition can both provide potential additional response variables. The CA ratio can be measured through observational studies, and it may be possible to measure body condition using photogrammetry or tag-based (Angliss et al., 1995; Best and Rüther, 1992; J.W. Durban et al., 2015; Perryman and Lynn, 2002) measurements (Aoki et al., 2011; Biuw et al., 2003; Miller et al., 2016). Data on individual health could also inform the bioenergetics model.

6.5 Passive Acoustic vs. Visual Methods

To estimate *Md* density and abundance using passive acoustics, data must be collected across the entire hydrophone array. However, such monitoring would not provide information on the demographic characteristics of the population, or on demographic rates such as migration, the probability of giving birth and calf survival. If the range of the population is substantially larger than that monitored by the hydrophones, a decline in the population may not be evident if the monitored area is preferred habitat (Thomas, 1996). In such a case, the overall population may be in decline, but the number within the preferred habitat may remain the same until total population size is below the maximum number of animals the preferred habitat can accommodate.

Passive acoustic abundance estimates based on click or dive counting both assume that cues are produced at a constant rate. In the case of click counting, it is assumed that the mean number of

clicks produced per unit of time remains constant, unless further auxiliary data are gathered to check this assumption. Dive counting assumes the mean dive rate and group size remain constant over time. Changes in factors such as prey distribution or size could affect the dive rate or the click rate. A change in the total clicks produced per day, whether on a per dive basis or as a result of a change in the total number of dives per day, will lead to a change in the abundance estimate, even if there has been no change in actual abundance (or could mask a real change in abundance if one occurs). A change in the number of dives made per day or the number of individuals in a group will affect the dive counting estimate in a similar fashion. These estimation methods also assume a consistent probability of detection and false positive rate, both of which could be affected by environmental changes, especially changes to the number of other species whose calls interfere with *Md* click detection.

Visual methods have successfully been used to estimate some of these variables and parameters, including group size, mean dive rate, demographic rates, and population range (Claridge, 2013). Photo-ID and line transect data have been used to produce abundance estimates for AUTEC (Claridge, 2013, 2006), and, because they rely on different assumptions, these estimates can be used to cross-validate those from passive acoustics methods. For example, capture-recapture estimates from photo-ID data assume all animals are equally detectable (or that all relevant variables affecting detectability are known and collected), while line transect surveys assume that availability and perception biases are zero or are known.

Observers collecting photo-ID data have also been able to gather faecal and biopsy samples which were used to investigate whether the animals observed in the TOTO represent a distinct population (Claridge, 2013). While not definitive, they do suggest a difference in food sources.

Potentially, they could also be used to determine stress levels and reproductive status (St Aubin et al., 1996; Thomson and Geraci, 1986).

The major challenge with visual observations is data collection because *Md* are hard to detect and photograph at sea. Even at AUTEC, where passive acoustics have been used to direct observers to areas where vocalizing animals are present, finding these animals has proved difficult. On-water observations require calm sea conditions that are rare, given the prevailing winds in the Bahamas. A preliminary review of the 3-dimensional animal tracks show that animals come to the surface up to 1.5 km from where they were first detected acoustically (Dolan et al., 2019). Unless the sea is calm, the probability the animals will be successfully sighted is low (Claridge, 2013).

Visual data collection requires that personnel remain in the field for extended time periods waiting for the range to become available and for suitable sea-state conditions. For example, as part of a study on AUTEC in June-July 2017, a team of observers was in the field for 30 days. During this time, they were only able to spend 1.5 days on-water. No *Md* were sighted on these days. Claridge (2013) used data collected on 184 days over a six-year period from 2005 to 2010 to estimate abundance and demographic rates. However, only 90 of these days were actually spent on the water, and only 60 days provided sea-state conditions below Beaufort 3; on just 10 days was the sea-state below Beaufort 3 for the entire day (D. Claridge personal communication). What this meant in practical terms was that a field season of roughly 30 days communication yielded less than 4 days of data. However, these limited data provided the estimates of the age and sex structure of the Abaco and AUTEC populations that were used in this study. Estimates of migration rates, and adult survival were also produced, though the model for immigration provided "very little information" (Claridge, 2013).

6.6 Evaluation for Long-term Monitoring

The last of the steps suggested by Fleishman et al. (2016) is to determine the temporal sequence of monitoring. To inform both the required rate and efficacy of monitoring a simple power analysis was conducted for obtaining abundance through passive acoustic and visual monitoring.

The power of a time series of abundance estimates obtained using passive acoustic methods depends on the precision and accuracy of the cue rates and their multipliers. For the dive counting methods presented in Chapter 2, these were the probability of detection (P), the rate of false positives (c), dive rate (r), and group size (s). Estimates of P and c were derived through a manual review of passive acoustic data, and they could be re-estimated on a regular basis. This is more problematic for the estimates of r and s, which are derived from tag and sighting data respectively.

The uncertainty associated with these parameter estimates is also important in determining the power of any time series to detect change. The coefficient of variation (CV) of 25% for the monthly dive counting estimates presented in Chapter 2 was calculated by combining the estimated CVs for $\hat{r}$ (0.055), $\hat{s}$ (0.106), $\widehat{P}$ (0.027) and $\hat{c}$ (0.223). The overall CV was driven primarily by the CVs for c and r. Reducing the CV on r will require additional at-sea data collection. However, the CV on c could be improved by additional sampling of passive acoustic data.

A power analysis (Steidl and Thomas, 2001) was conducted using the NOAA Trends software (Gerrodette, 1991, 1987) to estimate the number of months of passive acoustic analysis required to detect annual log-linear population decreases of 3% and 5% with a power of 0.8 and a Type 1 error rate (α-level) of 0.05 using a 2-tailed hypothesis test of trend. It assumed that passive

acoustic data are sampled to achieve a constant CV of 14.1% on the abundance estimates. It also assumed that process error is not a factor and that the individual parameter estimates are independent. With these assumptions, an overall decline of approximately 19% is required if it is to be detected with a power of 0.8. This would require approximately 60 months of estimates for a 3% annual decline, and 42 months for a 5% decline (Figure 6.3).

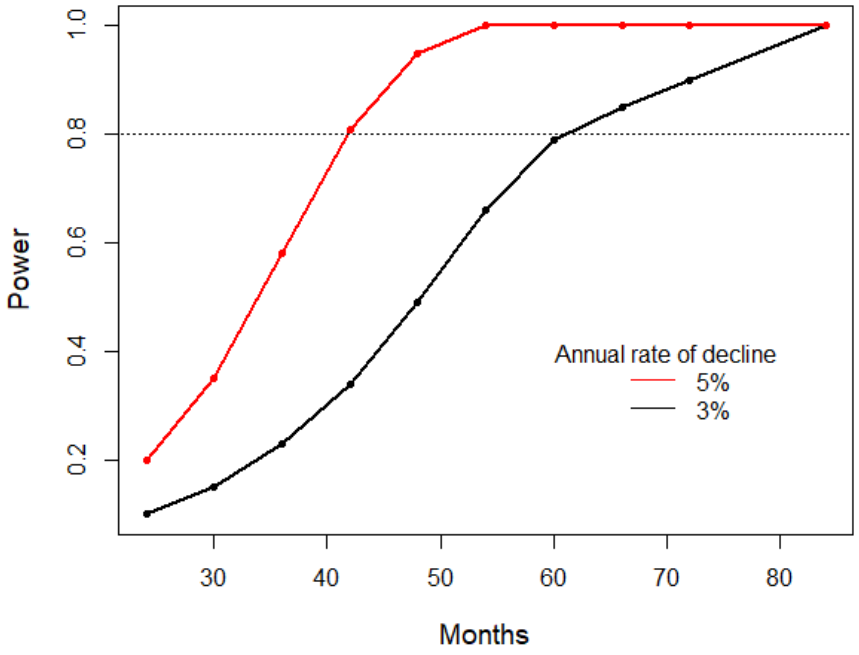

Figure 6. 3 Power of detecting a decline in abundance as a function of the number of months of passive acoustic analysis for an annual rate of decline of 3% (black) and 5% (red).

As noted above, photo-ID and line transect data can also be used to estimate population size, demographic characteristics and the demographic rates that drive population change (Matthiopoulos, 2011). A simple analysis was also conducted to investigate the power of a time series of abundance estimates based on the capture-recapture method presented in Claridge (2013) to detect a 5% annual decline in abundance with a power of 0.8 and Type 1 error rate of 0.05 (Figure 6.4). As with the estimate for passive acoustic monitoring, sample independence

and a constant CV were assumed and no account was made for process variation (Thomas et al., 2008).

Claridge (2013) analysed six years of photo-ID data and reported an abundance of 42 animals at AUTEC (75% HPDI = 32-55). Each year's effort consisted of approximately 30 field days. The HPDI reported was converted to a CV of 24%, assuming the abundance estimate followed a log-normal distribution (see Buckland et al. 1993, pages 88-89). Assuming one independent estimate every 6 years with CV of 24%, it would take over 30 years to detect a decline with a power of 0.8. Assuming that CV decreases with the square root of sampling effort, then with 60 field days per year, it would still require approximately 25 years of data collection. Estimates could be produced more often than each six years (or a trend model included as part of the capture-recapture modelling), but they would no longer be independent, and hence the above conclusions would be unlikely to change substantially.

The analysis suggests that visual observations are unlikely to provide an "early warning" of population change. These observational data are extremely important, but they require a long-term investment.

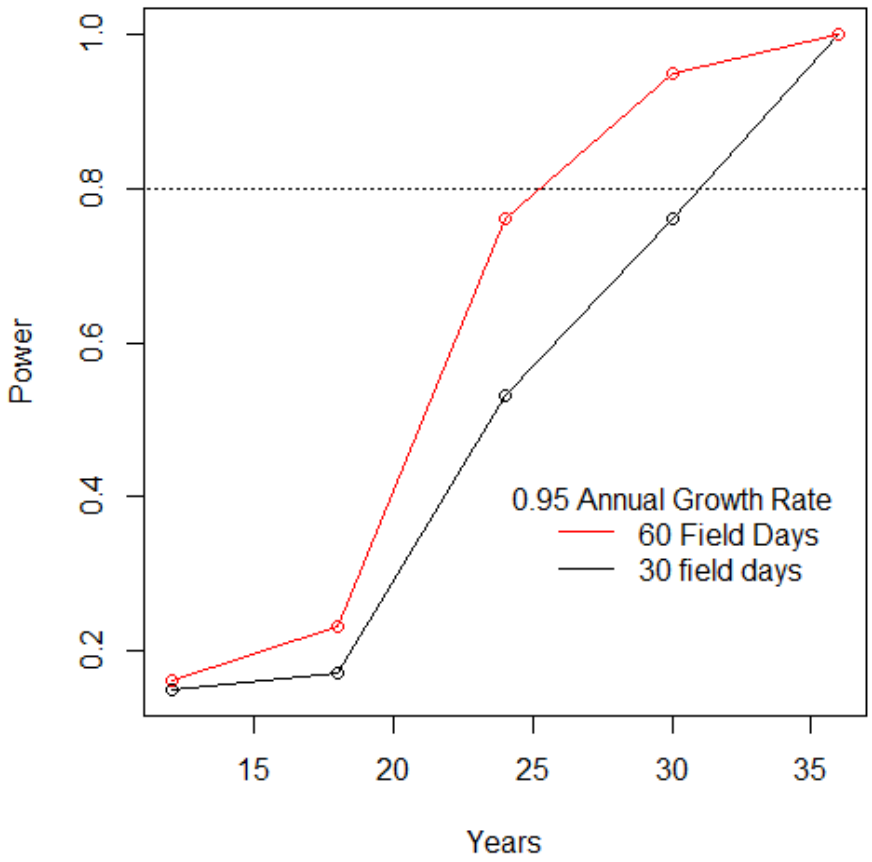

Figure 6.4 The power of mark-recapture estimates to detect a -5% annual decline in abundance as a function of the number of years of visual observation, assuming 30 days (black) and 60 days (red) in the field per year assuming six-year measurement periods.

Historically, monitoring teams have remained at AUTEC waiting for "good weather" days. However, it may be possible to react to weather forecasts with as little as three days' notice, thus reducing costs and increasing the number of days on which data could be collected for the same observer effort. This strategy was implemented at AUTEC in 2018 and is being evaluated.

The analysis of the observer-based data was only possible because of the availability of a comparable data set collected at Abaco. The bioenergetics model results were predicated on setting the model initial conditions to match the Abaco CA ratio. Abaco provides a comparative site that is MFAS-free with a population that is presumably in "good status" (National

Academies of Sciences, Engineering, and Medicine, 2017). Thus, the monitoring plan should include a parallel monitoring effort at Abaco that can provide a comparable number of *Md* encounter days, with the caution that further site-specific comparisons should be considered. These include measurement of prey types, density, and distribution, and an assessment of the density of predators, which could be important in determining the CA ratio and calf survival.

Therefore, a plan for long-term monitoring programme at AUTEC should include the following elements:

1. Monitor abundance on a monthly basis with continuous collection of passive acoustics data.
2. Record days when MFAS including source type, range rate and stop and start time of sonar bouts.
3. A minimum of 30 days of visual observations at AUTEC and Abaco to collect information for estimating demographic characteristics and demographic rates.

Assuming cue rates are stable, simply monitoring the number of GVPs detected would provide insight into population trends. However, this assumes cue stability is well understood. Monthly abundance estimates would also provide a measure of temporal variation in abundance, an essential component when measuring short term changes (Thomas, 1996).

At AUTEC, with any measured change, the initial focus would be on MFAS operations. Therefore, an independent measure of MFAS transmissions is critically important. Passive acoustic monitoring also provides a direct measure of the spatial and temporal variation of MFAS transmissions. It is equally important not to overlook environmental stressors, such as

prey and predator density, that could also affect the population. To date, predator density has not been considered, although an analysis of shark bite scars could provide an index of cookie cutter shark activity.

Visual observations will provide critical data on demographic rates (such as calf survival and fertility), demographic characteristics (such as the CA ratio) and basic biological parameters (such as time to weaning). Such measurements should also be continued at Abaco to provide a comparison to an undisturbed reference population.

6.7 Potential Future Studies

6.7.1 Improved Passive Acoustic Density Estimation

Jorge (2017) developed a method for estimating the number of animals per *Md* group using data collected at AUTEC. This method could be integrated into dive counting density estimation and used in addition to the visual estimate of mean group size. This could offer multiple advantages. First, if the group size changes with season or year, the algorithm dynamically adapts. Second, knowledge of changes in group size over time could provide additional insight into population structural changes. Third, the group size potentially could be used to help track groups across successive foraging dives. Tracking groups over the range could provide additional data including dive rate. If a long-term record of dive rate can be maintained, it could signal changes in the type, distribution, and concentration of prey.

6.7.2 Inter-click Interval (ICI)

Md clicks are currently only used to detect deep foraging dives. However, a change in the inter-click interval (ICI) could also indicate a change in foraging behaviour and potential prey. The first step in post-processing of echolocation click detections is to form click trains on each

hydrophone for each detection type reported. From *Md* click trains, the ICI is reported, so tracking mean ICI may be possible, recognizing that pauses between clicks and missed clicks influence the estimates. Recording tags can be used to provide baseline information and measure the uncertainty in the passive acoustic estimates by measuring the basic cue rates (dives, clicks) and their associated variability (Shaffer et al., 2013) on the animals with a high degree of certainty. These measurements can then be directly compared to the measurements made on the surrounding hydrophones.

For click counting algorithms, the click detection rate per hydrophone is estimated based a comparison with the mean number of clicks produced over a GVP as measured on a recording tag. By measuring the ICI and the start and GVP start and stop time, an estimate of the clicks per dive can be produced. Such long-term estimates could provide insight into the stability of the click rate used for click counting.

6.7.3 Bioenergetics Model Expansion

The bioenergetics model presented in Chapter 4 provides a tool to investigate the effect of MFAS disturbance on key population parameters including the probability of giving birth and calf survival.

An expanded collection of tag data would inform the development of a more realistic understanding of animal movement and the range of the population. The model is driven by the effect of reduced energy intake, so recording tags data could be used to measure the number of buzzes as a proxy for prey capture attempts; a more direct measure of the effect of displacement on feeding success and thus energy intake. The current level of disturbance was calculated in terms of dives "lost" as inferred from passive acoustic measurements and used to estimate lost

energy intake. However, these data provide information only when animals are vocalizing on-range, so the estimate of effect in terms of calories lost was a "best" estimate. Directly recording dives via tags around operations will provide a direct measurement of dive behaviour that can be used as a proxy for their foraging behaviour.

Development of a prototype *Md* buzz-detector has been completed (Jarvis, in preparation). The rapid increase in click rate is believed to signal a prey capture attempt. By measuring the rate of buzz detections, it may be possible to estimate the foraging success of animals on-range over time. This potentially could be used to dynamically adjust caloric intake based on a direct measure of prey capture attempts.

6.7.4 Prey Mapping

To date, the density and distribution of potential *Md* prey at both sites are largely unknown, although results from a 2015 prey mapping survey conducted at both AUTEC and Abaco are being analysed. Preliminary results, based on data collected over a two-week period, point to differences in the size and distribution of prey at the two sites (K. Benoit-Bird, personal communication).

Expanded mapping of the spatial and temporal distribution of prey at Abaco and AUTEC could provide insights into the observed differences in *Md* population structure between the two sites. As prey data become available, they can be used to inform changes in potential habitats. This is particularly important if animals move off the AUTEC hydrophone array. Multiple research programmes are beginning to explore the distribution of deep prey (Benoit-Bird, 2014; Benoit-Bird et al., 2016; Hazen et al., 2011). However, this is challenging because of the extreme depths at which *Md* forage.

Two methods have been postulated: using an unmanned autonomous vehicle (AUV); and inferring prey density using data from AUTEC bottom-mounted bidirectional nodes. The entire AUTEC range, and areas north and south, along with the Abaco study area were surveyed (Benoit-Bird, 2014; Benoit-Bird et al., 2016). Data from this pilot project should provide an initial estimate of the distribution, relative sizes, and patchiness of prey at both sites for the two weeks of the survey. However, nothing is known about temporal variation in prey distribution and abundance.

The second postulated method is the use of AUTEC bidirectional nodes as potential echo-sounders. The AUTEC array contains nodes with listening hydrophones, and also nodes that can both transmit and receive signals. The latter nodes are used for transmission of communication signals and are capable of transiting an arbitrary waveform in the 8-11 kHz frequency band on command from shore. Signal reflections from prey could be monitored on the receive-hydrophone on the same node. Potentially, this would allow the prey field over the entire range to be assessed on temporal scales of hours to years, thus providing long-term measurements of changes in prey distribution. The nodes could be programmed to ping from the bottom and listen to returns from prey higher in the water column. While the depth, and frequency dependent size resolution would be limited, the potential spatial and time scales are unprecedented. If successful, a 1,200 km^2 area could be mapped simultaneously at a user-defined sampling interval for the life of the range.

6.8 Conclusions

This dissertation presents results from over eight years of applied research into the effect of MFAS on *Md*. The displacement of animals exposed to MFAS has been widely reported and is

now generally accepted (D'Amico et al., 2009; Filadelfo et al., 2009; McCarthy et al., 2011; Moretti et al., 2010, 2014; Tyack et al., 2011). The tools described herein enable the long-term estimation of *Md* abundance. The behavioural risk function analysis provided a parametric equation based on *in situ* operational data that maps the probability of behavioural disruption to an MFAS RL that can inform *Md* take estimates in areas outside the TOTO. The prototype bioenergetic model allows the investigation of the effect of MFAS disruption of foraging dives, and its long-term effect on such factors as females' probability of giving birth, calf survival, and the population growth rate.

Claridge (2013) was the first to suggest that repeated MFAS exposure potentially resulted in a population level effect. Her study was also the first to establish the presence of two separate *Md* populations, one presumably MFAS disturbed (AUTEC) and one undisturbed (Abaco), and to compare the results from the disturbed to the undisturbed population. Results from her study were used to cross-validate the passive acoustic density estimate and to establish a baseline for the bioenergetics model. The measured disturbance was then added to the model.

The bioenergetics model produced a CA ratio for an undisturbed population of that approximates that reported by Claridge for Abaco and suggests the level of MFAS disturbance measured at AUTEC could lead to the differences in demographic values reported.

As previously discussed, drivers other than MFAS exposure could be responsible for the inter-site differences. Initial measurements of the prey fields have indicated differences between the two sites. A lower habitat quality at AUTEC could lead to higher calf mortality. However, a low-quality habitat will amplify the population effect of disturbance. It may be that the measured difference between sites is caused by such a combination of factors. For example,

perhaps repeated displacement causes animals to be more frequently exposed to predators. Typically, the very young are the most susceptible. A reduction of young would directly lower the CA ratio while, as reported by Claridge (2013), the ratio of calves to juveniles between sites would remain approximately the same.

If MFAS disruption at AUTEC does affect individuals' health, a measurable difference in body condition between individuals at the AUTEC and Abaco populations may be observable via photogrammetry or tag-based buoyancy estimates. However, body condition of all adult females varies with their life history stage (i.e. whether they are pregnant, lactating or neither). Data on body condition would, therefore, have to be augmented with information on whether or not the individual was pregnant or accompanied by a dependent calf. It may be possible to discern a female's state through a combination of hormone analysis of biopsy or faecal samples, combined with visual observation and photogrammetry.

"Sonar sensitive" beaked whales are widely distributed around the globe. Both Blainville's and Cuvier's beaked whales have been the predominant species in MFAS-related stranding events. However, with the proliferation of quiet diesel-electric submarines, training with MFAS is increasingly a critical component of anti-submarine warfare. As with most human activities, the challenge is to reduce the environmental effects of this training (Moretti, 2012). To minimize the risk of dispersed populations, reducing the exposed area and concentrating the use of MFAS systems in specified ranges may reduce the overall impact of such training events. While no direct evidence exists, animals that frequent MFAS active areas such as AUTEC may habituate to MFAS operations. Relegating MFAS use to ranges while monitoring for concerning population level changes may offer a reasonable means of minimizing environmental effects while meeting the U.S. Navy's very real need to train with MFAS. However, to make informed

decisions, the long-term effect of past and future exposure must be understood. The bioenergetic model suggest MFAS behavioural disruption could lead to a negative growth rate that if it exists, should be measurable using the methods discussed in this thesis. This work strongly suggests ongoing monitoring for population-level changes should be a priority. Given the unique resources available at AUTEC, along with the comparative Abaco site, it is hoped the tools developed and data collected here will aid reasoned decision making both now and into the future.

6.9 Contributions

The analysis presented in this chapter was conducted by the author.

Karin Dolan assisted in extracting data from 3-dimensional *Md* passive acoustic tracks at AUTEC to estimate the distance animals travel from depth to the surface.

7.0 References

Aguilar de Soto, N., Madsen, P.T., Tyack, P., Arranz, P., Marrero, J., Fais, A., Revelli, E., Johnson, M., 2012. No shallow talk: Cryptic strategy in the vocal communication of Blainville's beaked whales. Marine Mammal Science 28, E75–E92.

Ainslie, M.A., 2010. Principles of sonar performance modelling. Springer, Chinchester, UK.

Andrew, R.K., Howe, B.M., Mercer, J.A., Dzieciuch, M.A., 2002. Ocean ambient sound: comparing the 1960s with the 1990s for a receiver off the California coast. Acoustics Research Letters Online 3, 65–70.

Angliss, R.P., Rugh, D.J., Withrow, D.E., Hobbs, R.C., 1995. Evaluations of aerial photogrammetric length measurements of the Bering-Chukchi-Beaufort Seas stock of bowhead whales (*Balaena mysticetus*). Report of the international Whaling Commission 45, 313–324.

Antunes, R., Kvadsheim, P.H., Lam, F.P.A., Tyack, P.L., Thomas, L., Wensveen, P.J., Miller, P.J.O., 2014. High thresholds for avoidance of sonar by free-ranging long-finned pilot whales (*Globicephala melas*). Marine Pollution Bulletin 83, 165–180.

Aoki, K., Watanabe, Y.Y., Crocker, D.E., Robinson, P.W., Biuw, M., Costa, D.P., Miyazaki, N., Fedak, M.A., Miller, P.J., 2011. Northern elephant seals adjust gliding and stroking patterns with changes in buoyancy: validation of at-sea metrics of body density. Journal of Experimental Biology 214, 2973–2987.

Aristotle, 1965. Aristotle Historia Animalium: Books I-III, Translation by Peck A. L. Harvard University Press.

Arranz, P., Aguilar de Soto, N., Madsen, P.T., Brito, A., Bordes, F., Johnson, M.P., 2011. Following a Foraging Fish-Finder: Diel Habitat Use of Blainville's Beaked Whales Revealed by Echolocation. PLOS ONE 6, e28353.

Atlantic Fleet Training and Testing Final Environmental Impact Statement/Overseas Environmental Impact Statement, 2013.

Au, W.W.L., 1993. The Sonar of Dolphins. Springer-Verlag New York, Inc., New York, NY.

Au, W.W.L., Herzing, D.L., 2003. Echolocation signals of wild Atlantic spotted dolphin (*Stenella frontalis*). The Journal of the Acoustical Society of America 113, 598–604.

Babisch, W., 2014. Updated exposure-response relationship between road traffic noise and coronary heart diseases: A meta-analysis. Noise and Health 16, 1–9.

Baggenstoss, P.M., 2011a. Separation of sperm whale click-trains for multipath rejection. The Journal of the Acoustical Society of America 129, 3598–3609.

Baggenstoss, P.M., 2011b. An algorithm for the localization of multiple interfering sperm whales using multi-sensor time difference of arrival. The Journal of the Acoustical Society of America 130, 102–112.

Baggenstoss, P.M., 2008. Joint localization and separation of sperm whale clicks. Canadian Acoustics 36, 125–131.

Baird, R.W., Webster, D.L., McSweeney, D.J., Ligon, A.D., Schorr, G.S., Barlow, J., 2006. Diving behaviour of Cuvier's (*Ziphius cavirostris*) and Blainville's (*Mesoplodon densirostris*) beaked whales in Hawai'i. Canadian Journal of Zoology 84, 1120–1128.

Baird, R.W., Webster, D.L., Schorr, G.S., McSweeney, D.J., Barlow, J., 2008. Diel variation in beaked whale diving behavior. Marine Mammal Science 24, 630–642.

Balcomb, K.C., Claridge, D.E., 2001. A mass stranding of cetaceans caused by naval sonar in the Bahamas. Bahamas Journal of Science 8, 1–8.

Barlow, J., 1999. Trackline detection probability for long-diving whales, in: Marine Mammal Survey and Assessment Methods, Garner, G. W., Amstrup, S. C., Lakke, J. L., Manly, B. F., McDonald, L. L., Robertson, D. G. (Eds). Presented at the Symposium on Surveys, Status & Trends of Marine Mammal Populations, Balkema Press, Rotterdam, Seattle, WA, USA, pp. 209–221.

Barlow, J., Calambokidis, J., Falcone, E.A., Baker, C.S., Burdin, A.M., Clapham, P.J., Ford, J.K.B., Gabriele, C.M., LeDuc, R., Mattila, D.K., 2011. Humpback whale abundance in the North Pacific estimated by photographic capture-recapture with bias correction from simulation studies. Marine Mammal Science 27, 793–818.

Barlow, J., Gisiner, R., 2006. Mitigating, monitoring and assessing the effects of anthropogenic sound on beaked whales. Journal of Cetacean Research and Management 7, 239–249.

Basner, M., Babisch, W., Davis, A., Brink, M., Clark, C., Janssen, S., Stansfeld, S., 2014. Auditory and non-auditory effects of noise on health. The Lancet 383, 1325–1332.

Baumann-Pickering, S., Roch, M.A., Brownell Jr, R.L., Simonis, A.E., McDonald, M.A., Solsona-Berga, A., Oleson, E.M., Wiggins, S.M., Hildebrand, J.A., 2014. Spatio-temporal patterns of beaked whale echolocation signals in the North Pacific. PLoS ONE 9, e86072.

Baumann-Pickering, S., Simonis, A.E., Solsona Berga, A., Merkens, K.P.B., Oleson, E.M., Roch, M.A., Wiggins, S.M., Rankin, S., Yack, T.M., others, 2013. Species-specific beaked whale echolocation signals. The Journal of the Acoustical Society of America 134, 2293–2301.

Bayne, E.M., Habib, L., Boutin, S., 2008. Impacts of chronic anthropogenic noise from energy-sector activity on abundance of songbirds in the boreal forest. Conservation Biology 22, 1186–1193.

Beale, C.M., Monaghan, P., 2004. Behavioural responses to human disturbance: a matter of choice? Animal Behaviour 68, 1065–1069.

Benjaminsen, T., Christensen, I., 1979. The Natural History of the Bottlenose Whale, *Hyperoodon ampullatus*, in: Winn H.E., Olla B.L. (Eds) Behavior of Marine Animals. Cetceans. Plenum Press, New York, pp. 143–164.

Benoit-Bird, K.J., 2014. Deep-diving autonomous underwater vehicle provides insights into scattering layer dynamics. The Journal of the Acoustical Society of America 135, 2154–2154.

Benoit-Bird, K.J., Southall, B.L., Moline, M.A.A.., 2016. Predator-guided sampling reveals biotic structure in the bathypelagic. Proceedings of the Royal Society B: Biological Sciences 283, 20152457.

Bernaldo de Quirós, Y., Fernandez, A., Baird, R.W., Brownell, R.L., Aguilar deSoto, N., Allen, D., Arbelo, M., Arregui, M., Costidis, A., Fahlman, A., Frantzis, A., Gulland, F.M.D., Iñíguez, M., Johnson, M., Komnenou, A., Koopman, H., Pabst, D.A., Roe, W.D., Sierra, E., Tejedor, M., Schorr, G., 2019. Advances in research on the impacts of anti-submarine sonar on beaked whales. Proceedings of the Royal Society B: Biological Sciences 286, 20182533.

Best, P.B., Rüther, H., 1992. Aerial photogrammetry of southern right whales, *Eubalaena australis*. Journal of Zoology 228, 595–614.

Biuw, M., McConnell, B., Bradshaw, C.J., Burton, H., Fedak, M., 2003. Blubber and buoyancy: monitoring the body condition of free-ranging seals using simple dive characteristics. Journal of Experimental Biology 206, 3405–3423.

Blackstock, S.A., Fayton, J.O., Hulton, P.H., Moll, T., 2018. Quantifying Acoustic Impacts on Marine Mammals and Sea Turtles: Methods and Analytical Approach for Phase III Training and Testing (Technicl Report No. TR08281). Naval Undersea Warfare Center, Newport, RI.

Blackwell, S.B., Nations, C.S., McDonald, T.L., Greene Jr, C.R., Thode, A.M., Guerra, M., Michael Macrander, A., 2013. Effects of airgun sounds on bowhead whale calling rates in the Alaskan Beaufort Sea. Marine Mammal Science 29, E342–E365.

Bloch, D., 1993. Age and growth parameters of the long-finned pilot whale off the Faroe Islands. Report of the International Whaling Commission Special Issue 14, 163–207.

Booth, C.G., Donovan, C., Plunkett, R., Harwood, J., 2015. PCoD Lite - Using an Interim PCoD Protocol to Assess the Effects of Disturbance Associated with US Navy Exercises on Marine Mammal Populations: Interim Report. Report Code SMRUM-ONR-2015-004, Submitted to The Office of Naval Research –Marine Mammal & Biology Program.

Brandt, M.J., Diederichs, A., Betke, K., Nehls, G., 2011. Responses of harbour porpoises to pile driving at the Horns Rev II offshore wind farm in the Danish North Sea. Marine Ecology Progress Series 421, 205–216.

Brodie Jr., E.D., Formanowicz Jr., D.R., Brodie III, E.D., 1991. Predator avoidance and antipredator mechanisms: distinct pathways to survival. Ethology Ecology & Evolution 3, 73–77.

Brown, A.L., 1990. Measuring the effect of aircraft noise on sea birds. Environment International 16, 587–592.

Buck, J.R., Tyack, P.L., 2000. Response of gray whales to low-frequency sounds. The Journal of the Acoustical Society of America 107, 2774–2774.

Buckland, S.T., 2006. Point-transect surveys for songbirds: robust methodologies. The Auk 123, 345–357.

Buxton, R.T., McKenna, M.F., Mennitt, D., Fristrup, K., Crooks, K., Angeloni, L., Wittemyer, G., 2017. Noise pollution is pervasive in U.S. protected areas. Science 356, 531–533.

Buzzas, C., 2016. Natural Resources Defense Council, Inc. v. Pritzker. Public Land and Resources Law Review 0, Article 8.

Carrillo, M., Pérez-Vallazza, C., Álvarez-Vázquez, R., 2010. Cetacean diversity and distribution off Tenerife (Canary Islands). Marine Biodiversity Records 3, E97.

Castellote, M., Clark, C.W., Lammers, M.O., 2012. Acoustic and behavioural changes by fin whales (*Balaenoptera physalus*) in response to shipping and airgun noise. Biological Conservation 147, 115–122.

Castellote, M., Llorens, C., 2016. Review of the Effects of Offshore Seismic Surveys in Cetaceans: Are Mass Strandings a Possibility?, In: Popper A., Hawkins A. (eds) The Effects of Noise on Aquatic Life II. Advances in Experimental Medicine and Biology. Springer New York.

Cato, D.H., Noad, M.J., Dunlop, R.A., McCauley, R.D., Gales, N.J., Kent, C.P.S., Kniest, H., Paton, D., Jenner, K.C.S., Noad, J., 2013. A study of the behavioural response of whales to the noise of seismic air guns: Design, methods and progress. Acoustics Australia 41, 88–97.

Charif, R.A., Mellinger, D.K., Dunsmore, K.L., Fristrup, K.M., Clark, C.W., 2002. Estimated source levels of fin whale (*Balaenoptera physalus*) vocalizations: Adjustments for surface interference. Marine Mammal Science 18, 81–98.

Chepesiuk, R., 2005. Decibel hell: the effects of living in a noisy world. Environ Health Perspect 113, A34–A41.

Claridge, D., Dunn, C., 2017. Compare Reproductive Success and Social Structure of Beaked Whales (No. Contract No.: N66604-16-P-2161). Naval Undersea Warfare Center, Newport, RI.

Claridge, D.E., 2013. Population ecology of Blainville's beaked whales (*Mesoplodon densirostris*) (PhD Dissertation). University of St Andrews.

Claridge, D.E., 2006. Fine-scale distribution and habitat selection of beaked whales (MSc Thesis). University of Aberdeen.

Clark, C.W., Ellison, W.T., Southall, B.L., Hatch, L., Van Parijs, S.M., Frankel, A., Ponirakis, D., 2009. Acoustic masking in marine ecosystems: intuitions, analysis, and implication. Marine Ecology Progress Series 395, 201–222.

Clemen, R.T., Winkler, R.L., 1999. Combining probability distributions from experts in risk analysis. Risk Analysis 19, 187–203.

Coleman, R., Salmon, N.A., Hawkins, S., 2003. Sub-dispersive human disturbance of foraging oystercatchers *Haematopus ostralegus*. Ardea 91, 263–268.

Collins, M.D., 1993a. The adiabatic mode parabolic equation. The Journal of the Acoustical Society of America 94, 2269–2278.

Collins, M.D., 1993b. An energy-conserving parabolic equation for elastic media. The Journal of the Acoustical Society of America 94, 975–982.

Collins, M.D., 1992. A self-starter for the parabolic equation method. The Journal of the Acoustical Society of America 92, 2069–2074.

Collins, M.D., 1989. A higher-order parabolic equation for wave propagation in an ocean overlying an elastic bottom. The Journal of the Acoustical Society of America 86, 1459–1464.

Commander U. S. Pacific Fleet, 2003. Report on the results of the inquiry into allegations of marine mammal impacts surrounding the use of active sonar by USS Shoup (DDG 86) in the Haro Strait on or about 5 May 2003.

Cox, T.M., Ragen, T.J., Read, A.J., Vos, E., Baird, R.W., Balcomb, K., Barlow, J., Caldwell, J., Cranford, T., Crum, L., 2006. Understanding the impacts of anthropogenic sound on beaked whales. Journal of Cetacean Restoration Management 7, 177–187.

Curé, C., Isojunno, S., Visser, F., Wensveen, P.J., Sivle, L.D., Kvadsheim, P.H., Lam, F.A., Miller, P.J.O., 2016. Biological significance of sperm whale responses to sonar: comparison with anti-predator responses. Endangered Species Research 31, 89–102.

Curé, C., Sivle, L., Visser, F., Wensveen, P., Isojunno, S., Harris, C., Kvadsheim, P., Lam, F., Miller, P., 2015. Predator sound playbacks reveal strong avoidance responses in a fight strategist baleen whale. Marine Ecology Progress Series 526, 267–282.

Dähne, M., Gilles, A., Lucke, K., Peschko, V., Adler, S., Krügel, K., Sundermeyer, J., Siebert, U., 2013. Effects of pile-driving on harbour porpoises (*Phocoena phocoena*) at the first offshore wind farm in Germany. Environmental Research Letters 8, 025002.

Dalebout, M.L., Steel, D., Baker, C.S., Charleston, M., 2008. Phylogeny of the Beaked Whale Genus Mesoplodon (Ziphiidae: Cetacea) Revealed by Nuclear Introns: Implications for the Evolution of Male Tusks. Systematic Biology 57, 857–875.

D'Amico, A., Bergamasco, A., Zanasca, P., Carniel, S., Nacini, E., Portunato, N., Teloni, V., Mori, C., Barbanti, R., 2003. Qualitative correlation of marine mammals with physical and biological parameters in the Ligurian Sea. IEEE Journal of Oceanic Engineering 28, 29–43.

D'Amico, A., Gisiner, R.C., Ketten, D.R., Hammock, J.A., Johnson, C., Tyack, P.L., Mead, J., 2009. Beaked whale strandings and naval exercises. Aquatic Mammals 35, 452–472.

D'Amico, A., Verboom, W.C., 1998. Summary record and report of the SACLANTCEN Bioacoustics Panel. La Spezia, Italy.

Danil, K., St. Leger, J., 2011. Seabird and dolphin mortality associated with underwater detonation exercises. Marine Technology Society Journal 45, 89–95.

David, J.A., 2006. Likely sensitivity of bottlenose dolphins to pile-driving noise. Water and Environment Journal 20, 48–54.

De Roos, A.M., Galic, N., 2009. How resource competition shapes individual life history for nonplastic growth: ungulates in seasonal food environments. Ecology 90, 945–960.

Debich, A.J., Baumann-Pickering, S., Širović, A., Hildebrand, J.A., Alldredge, A.L., Gottlieb, R.S., Herbert, S.T., Johnson, S.C., Rice, A.C., Roche, L.K., 2015. Passive Acoustic Monitoring for Marine Mammals in the SOCAL Naval Training Area Dec 2012-Jan 2014. Scripps Institution of Oceanography, Marine Physical Laboratory, La Jolla, CA.

DeRuiter, S.L., Southall, B.L., Calambokidis, J., Zimmer, W.M.X., Sadykova, D., Falcone, E.A., Friedlaender, A.S., Joseph, J.E., Moretti, D., Schorr, G.S., Thomas, L., Tyack, P.L., 2013. First direct measurements of behavioural responses by Cuvier's beaked whales to mid-frequency active sonar. Biology Letters 9, 0130223.

DiMarzio, N., Jones, B., Moretti, D., Oedekoven, C., 2018. Marine Mammal Monitoring on Navy Ranges (M3R) on the Southern California Offshore Range (SOAR) and the Pacific Missile Range Facility (PMRF) 2017. Naval Undersea Warfare Center, Newport, RI.

Dolan, K., Marques, T., Moretti, D., Claridge, D., Dunn, C., Benoit-Bird, K., 2019. Seeing the unobservable: Acoustic tracking reveals deep foraging behaviour and coordination in groups of Blainville's beaked whales. in preparation.

Duncan, A.C., 2017. Airgun arrays for marine seismic surveys-physics and directional characteristics, Proceedings of Acoustics, 19-2 November, Perth, Australia.

Dunlop, R.A., Noad, M.J., McCauley, R.D., Kniest, E., Slade, R., Paton, D., Cato, D.H., 2017a. The behavioural response of migrating humpback whales to a full seismic airgun array. Proceedings of the Royal Society B: Biological Sciences 284, 20171901.

Dunlop, R.A., Noad, M.J., McCauley, R.D., Scott-Hayward, L., Kniest, E., Slade, R., Paton, D., Cato, D.H., 2017b. Determining the behavioural dose–response relationship of marine mammals to air gun noise and source proximity. Journal of Experimental Biology 220, 2878–2886.

Durban, J. W., Fearnbach, H., Barrett-Lennard, L.G., Perryman, W.L., Leroi, D.J., 2015. Photogrammetry of killer whales using a small hexacopter launched at sea. Journal of Unmanned Vehicle Systems 3, 131–135.

Durban, J.W., Fearnbach, H., Barrett-Lennard, L.G., Perryman, W.L., Leroi, D.J., 2015. Photogrammetry of killer whales using a small hexacopter launched at sea. J. Unmanned Veh. Sys. 3, 131–135. https://doi.org/10.1139/juvs-2015-0020

Ellison, W., Stein, P., 1999. SURTASS LFA high frequency marine mammal monitoring (HF/M3) sonar : system description and test & evaluation (U.S. Navy Contract N66604-98-D-5725). Marine Acoustics , Inc.

Ellison, W.T., Southall, B.L., Clark, C.W., Frankel, A.S., 2012. A New Context-Based Approach to Assess Marine Mammal Behavioral Responses to Anthropogenic Sounds. Conservation Biology 26, 21–28.

England, G.R., 2007. National Defense Exemption from Requirements of the Marine Mammal Protection Act for Certain Sonar or Improved Extended Echo Ranging Sonobuoys. US Secretary of the Navy.

England, G.R., Evans, D., Lautenbacher, C., Morrissey-Livingstone, S., Hogarth, W., Johnson, H. T., 2001. Joint interim report Bahamas marine mammal stranding event of 15-16 March 2000. US Department of Commerce, US Secretary of the Navy.

EPA Risk Assessment Forum, 2012. Benchmark dose technical guidance. U.S. Environmental Protection Agency, Washington, DC.

Faerber, M.M., Baird, R.W., 2010. Does a lack of observed beaked whale strandings in military exercise areas mean no impacts have occurred? A comparison of stranding and detection probabilities in the Canary and main Hawaiian Islands. Marine Mammal Science 26, 602–613.

Falcone, E.A., Schorr, G.S., Douglas, A.B., Calambokidis, J., Henderson, E., McKenna, M.F., Hildebrand, J., Moretti, D., 2009. Sighting characteristics and photo-identification of Cuvier's beaked whales (*Ziphius cavirostris*) near San Clemente Island, California: a key area for beaked whales and the military? Marine Biology 156, 2631–2640.

Falcone, E.A., Schorr, G.S., Watwood, S.L., DeRuiter, S.L., Zerbini, A.N., Andrews, R.D., Morrissey, R.P., Moretti, D.J., 2017. Diving behaviour of Cuvier's beaked whales exposed to two types of military sonar. Royal Society Open Science 4, 170629.

Farmer, N.A., Noren, D.P., Fougères, E.M., Machernis, A., Baker, W., K.V., 2018. Resilience of the endangered sperm whale *Physeter macrocephalus* to foraging disturbance in the Gulf of Mexico, USA: A bioenergetic approach. Marine Ecology Progress Series 589, 241–261.

Fernández, A., Edwards, J.F., Rodriguez, F., De Los Monteros, A.E., Herraez, P., Castro, P., Jaber, J.R., Martin, V., Arbelo, M., 2005. "Gas and fat embolic syndrome" involving a mass stranding of beaked whales (family Ziphiidae) exposed to anthropogenic sonar signals. Veterinary Pathology 42, 446–457.

Fernández-Juricic, E., Tellería, J.L., 2000. Effects of Human Disturbance on Spatial and Temporal Feeding Patterns of Blackbird *Turdus merula* in Urban Parks in Madrid Spain. Bird Study 47, 13–21.

Fields, M.J., Sand, R.S., 1993. Factors Affecting Calf Crop. CRC Press, Boca Raton, FL.

Filadelfo, R., Mintz, J., Michlovich, E., D'Amico, A., Tyack, P.L., Ketten, D.R., 2009. Correlating military sonar use with beaked whale mass strandings: what do the historical data show? Aquatic Mammals 35, 435–444.

Finneran, J., J., Houser, D.S., 2006. Comparison of in-air evoked potential and underwater behavioral hearing thresholds in four bottlenose dolphins (*Tursiops truncatus*). The Journal of the Acoustical Society of America 119, 3181–3192.

Finneran, J., Jenkins, A.K., 2012. Criteria and Thresholds for Navy Acoustic Effects Analysis Technical Report. SPAWAR Marine Mammal Program., San Diego, CA.

Finneran, J.J., Carder, D.A., Schlundt, C.E., Ridgway, S.H., 2005. Temporary threshold shift in bottlenose dolphins (*Tursiops truncatus*) exposed to mid-frequency tones). The Journal of the Acoustical Society of America 118, 2696–2705.

Finneran, J.J., Schlundt, C.E., 2010. Frequency-dependent and longitudinal changes in noise-induced hearing loss in a bottlenose dolphin (*Tursiops truncatus*). The Journal of the Acoustical Society of America 128, 567–570.

Fleishman, E., Costa, D.P., Harwood, J., Kraus, S., Moretti, D., New, L.F., Schick, R.S., Schwarz, L.K., Simmons, S.E., Thomas, L., Wells, R.S., 2016. Monitoring population-level responses of marine mammals to human activities. Marine Mammal Science 32, 1004–1021.

Francis, C.D., Ortega, C.P., Cruz, A., 2009. Noise pollution changes avian communities and species interactions. Current Biology 19, 1415–1419.

Franssen, E., van Wiechen, C., Nagelkerke, N., Lebret, E., 2004. Aircraft noise around a large international airport and its impact on general health and medication use. Occupational and Environmental Medicine 61, 405–413.

Frid, A., Dill, L., 2002. Human-caused disturbance stimuli as a form of predation risk. Conservation Ecology 6, p16.

Fristrup, K.M., Hatch, L.T., Clark, C.W., 2003. Variation in humpback whale (*Megaptera novaeangliae*) song length in relation to low-frequency sound broadcasts. The Journal of the Acoustical Society of America 113, 3411–3424.

Gerrodette, T., 1991. Models for power of detecting trends: a reply to Link and Hatfield. Ecology 72, 1889–1892.

Gerrodette, T., 1987. A power analysis for detecting trends. Ecology 68, 1364–1372.

Giddings, T.E., 2008. RIMPAC-08 Planning and Support and OAML Certification (No. N00014- 08- M– 0007). Metron Inc, Reston, VA.

Gill, J.A., Norris, K., Sutherland, W.J., 2001. Why behavioural responses may not reflect the population consequences of human disturbance. Biological Conservation 97, 265–268.

Gillespie, D., Dunn, C., Gordon, J., Claridge, D., Embling, C., Boyd, I., 2009. Field recordings of Gervais' beaked whales *Mesoplodon europaeus* from the Bahamas. The Journal of the Acoustical Society of America 125, 3428–3433.

Goldbogen, J.A., Southall, B.L., DeRuiter, S.L., Calambokidis, J., Friedlaender, A.S., Hazen, E.L., Falcone, E.A., Schorr, G.S., Douglas, A., Moretti, D.J., Kyburg, C., McKenna, M.F., Tyack, P., L., 2013. Blue whales respond to simulated mid-frequency military sonar. Proceedings of the Royal Society B: Biological Sciences 280.

Gormley, A.M., Dawson, S.M., Dawson, S.M., Slooten, E., Bräger, S., 2005. Capture-recapture estimates of Hector's dolphin abundance at Banks Peninsula, New Zealand. Marine Mammal Science 21, 204–216.

Götz, T., Janik, V.M., 2011. Repeated elicitation of the acoustic startle reflex leads to sensitisation in subsequent avoidance behaviour and induces fear conditioning. BMC Neuroscience 12:30, 1–12.

Gowans, S., Whitehead, H., Arch, J.K., Hooker, S.K., 2000. Population size and residency patterns of northern bottlenose whales (*Hyperoodon ampullatus*) using the Gully, Nova Scotia. Journal of Cetacean Research and Management 2, 201–210.

Gowans, S., Whitehead, H., Hooker, S.K., 2001. Social organization in northern bottlenose whales, *Hyperoodon ampullatus*: not driven by deep-water foraging? Animal Behaviour 62, 369–377.

Grace, J., 2008. Diesel-Electric Submarines, the US Navy's Latest Annoyance. National Defense Magazine 1–6.

Habib, L., Bayne, E.M., Boutin, S., 2007. Chronic industrial noise affects pairing success and age structure of ovenbirds, *Seiurus aurocapilla*. Journal of Applied Ecology 44, 176–184.

Harris, C., Thomas, L., Falcone, E., Hildebrand, J., Houser, D., Kvadsheim, P., Lam, F., Miller, P.J.O., Moretti, D., Read, A., Slabbekoorn, H., Southall, B., Tyack, P., Wartzok, D., Janik, V.M., 2018. Marine mammals and sonar: Dose-response studies, the risk-disturbance hypothesis and the role of exposure context. Journal of Applied Ecology 55, 396–404.

Harris, D.V., 2012. Estimating whale abundance using sparse hydrophone arrays (PhD Dissertation). University of St Andrews.

Harris, R.E., Miller, G.W., Richardson, W.J., 2001. Seal responses to airgun sounds during summer seismic surveys in the Alaskan Beaufort Sea. Marine Mammal Science 17, 795–812.

Hatch, L., Clark, C., Merrick, R., Van Parijs, S., Ponirakis, D., Schwehr, K., Thompson, M., Wiley, D., 2008. Characterizing the Relative Contributions of Large Vessels to Total Ocean Noise Fields: A Case Study Using the Gerry E. Studds Stellwagen Bank National Marine Sanctuary. Environmental Management 42, 735–752.

Hazen, E.L., Nowacek, D.P., St. Laurent, L., Halpin, P.N., Moretti, D.J., 2011. The relationship among oceanography, prey fields, and beaked whale foraging habitat in the Tongue of the Ocean. PloS ONE 6, e19269.

Heath, B., Wyatt, R., 2014. Sound Source Verification to Assess Marine Mammal Impact Drift Buoy, Towed Array Solutions. Sea Technology 55, 47–50.

Heyning, J.E., 1984. Functional morphology involved in intraspecific fighting of the beaked whale, *Mesoplodon carlhubbsi*. Canadian Journal of Zoology 62, 1645–1654.

Hildebrand, J.A., 2009. Anthropogenic and natural sources of ambient noise in the ocean. Marine Ecology Progress Series 395, 5–20.

Hildebrand, J.A., Baumann-Pickering, S., Frasier, K.E., Trickey, J.S., Merkens, K.P., Wiggins, S.M., McDonald, M.A., Garrison, L.P., Harris, D., Marques, T.A., Thomas, L., 2015. Passive acoustic monitoring of beaked whale densities in the Gulf of Mexico. Scientific Reports 5, 16343.

Hin, V., Harwood, J., M. de Roos, A., in press. Bio-energetic modeling of medium-sized cetaceans shows high sensitivity to disturbance in seasons of low resource supply. Ecological Applications.

Hooker, S.K., Baird, R.W., Fahlman, A., 2009. Could beaked whales get the bends?: Effect of diving behaviour and physiology on modelled gas exchange for three species: *Ziphius cavirostris, Mesoplodon densirostris and Hyperoodon ampullatus*. Respiratory Physiology & Neurobiology 167, 235–246.

Hooker, S.K., Iverson, S.J., Ostrom, P., Smith, S.C., 2001. Diet of northern bottlenose whales inferred from fatty-acid and stable-isotope analyses of biopsy samples. Canadian Journal of Zoology 79, 1442–1454.

Houser, D.S., Dankiewicz, L.A., Stockard, T.K., Ponganis, P.J., 2008. Ultrasound inspection for intravascular bubbles in a repetitively diving dolphin. Bioacoustics 17, 310–312.

Houser, D.S., Finneran, J.J., 2006. A comparison of underwater hearing sensitivity in bottlenose dolphins (*Tursiops truncatus*) determined by electrophysiological and behavioral methods. The Journal of the Acoustical Society of America 120, 1713–1722.

Houser, D.S., Martin, S.W., Finneran, J.J., 2013. Exposure amplitude and repetition affect bottlenose dolphin behavioral responses to simulated mid-frequency sonar signals. Journal of Experimental Marine Biology and Ecology 443, 123–133.

Howland, H.C., 1974. Optimal strategies for predator avoidance: the relative importance of speed and manoeuvrability. Journal of Theoretical Biology 47, 333–350.

International Program on Chemical Safety (IPCS), 2009. Principles for modelling dose-response for the risk of assesment of chemicals (Environmental Health Criteria No. 239). United Nations Environment Programme, the International Labour Organization and the World Health Organization.

Ising, H., Kruppa, B., 2004. Health effects caused by noise: Evidence in the literature from the past 25 years. Noise and Health 6, 5–13.

Jarvis, S., in preparation. Using a field of bottom-mounted hydrophones to estimate beaked whale prey capture events.

Jarvis, S.M., 2012. A novel method for multi-Class classification using support vector machines (PhD Dissertation). University of Massachusetts, Dartmouth, MA.

Jarvis, S.M., DiMarzio, N., Morrissey, R., Moretti, D., 2008. A novel multi-class support vector machine classifier for automated classification of beaked whales and other small odontocetes. Canadian Acoustics 36, 34–40.

Jarvis, S.M., Morrissey, R.P., Moretti, D.J., DiMarzio, N.A., Shaffer, J.A., 2014. Marine Mammal Monitoring on Navy Ranges (M3R): A toolset for automated detection, localization, and monitoring of marine mammals in open ocean environments. Marine Technology Society Journal 48, 5–20.

Jepson, P.D., Arbelo, M., Deaville, R., Patterson, I.A.P., Castro, P., Baker, J.R., Degollada, E., Ross, H.M., Herráez, P., Pocknell, A.M., Rodríguez, F., Howie, F.E., Espinosa, A., Reid, R.J., Jaber, J.R., Martin, V., Cunningham, A.A., Fernández, A., 2003. Gas-bubble lesions in stranded cetaceans. Nature 425, 575–576.

Jewell, R., Thomas, L., Harris, C.M., Kaschner, K., Wiff, R., Hammond, P., Quick, N., 2012. Global analysis of cetacean line-transect surveys: detecting trends in cetacean density. Marine Ecology Progress Series 453, 227–240.

Johnson, M., Madsen, P.T., Zimmer, W.M.X., Aguilar de Soto, N., Tyack, P.L., 2006a. Foraging Blainville's beaked whales (*Mesoplodon densirostris*) produce distinct click types matched to different phases of echolocation. Journal of Experimental Biology 209, 5038–5050.

Johnson, M., Madsen, P.T., Zimmer, W.M.X., De Soto, N.A., Tyack, P.L., 2006b. Foraging Blainville's beaked whales (Mesoplodon densirostris) produce distinct click types matched to different phases of echolocation. Journal of Experimental Biology 209, 5038–5050.

Johnson, M.P., Hickmott, L.S., Aguilar de Soto, N., Madsen, P.T., 2008. Echolocation behaviour adapted to prey in foraging Blainville's beaked whale (*Mesoplodon densirostris*). Proceedings of the Royal Society of London B: Biological Sciences 275, 133–139.

Johnson, M.P., Madsen, P.T., Zimmer, W.M.X., Aguilar de Soto, N., Tyack, P.L., 2004. Beaked whales echolocate on prey. Proceedings of the Royal Society B: Biological Sciences 271, S383–S386.

Johnson, M.P., Tyack, P.L., 2003. A digital acoustic recording tag for measuring the response of wild marine mammals to sound. IEEE Journal of Oceanic Engineering 28, 3–12.

Jones, B.A., Stanton, T.K., Lavery, A.C., Johnson, M.P., Madsen, P.T., Tyack, P.L., 2008. Classification of broadband echoes from prey of a foraging Blainville's beaked whale. The Journal of the Acoustical Society of America 123, 1753–1762.

Jorge, P., 2017. Applying Generalized Linear Models to Estimate Group Size and Improve Blainville's Beaked Whale Abundance Estimation (MSc Thesis). Universidade de Lisboa.

Joyce, T.W., Durban, J.W., Claridge, D.E., Dunn, C.A., Hickmott, L.S., Fearnbach, H., Moretti, D., Dolan, K., in press. Behavioral responses of satellite-tagged Blainville's beaked whales (*Mesoplodon densirostris*) to mid-frequency active sonar. Marine Mammal Science.

Kaschner, K., Quick, N.J., Jewell, R., Williams, R., Harris, C.M., 2012. Global coverage of cetacean line-transect surveys: status quo, data gaps and future challenges. PLoS ONE 7, e44075.

Kastelein, R.A., Gransier, R., Hoek, L., Olthuis, J., 2012. Temporary threshold shifts and recovery in a harbor porpoise (*Phocoena phocoena*) after octave-band noise at 4 kHz. The Journal of the Acoustical Society of America 132, 3525–3537.

Kasuya, T., 1997. Life history of Baird's beaked whales off the pacific coast of Japan. Report of the International Whaling Commission 47, 969–979.

Kasuya, T., 1977. Age determination and growth of the Baird's beaked whale with a comment on the fetal growth rate. The Scientific Reports of the Whales Research Institute 29, 1–20.

Keller, C.A., Garrison, L., Baumstark, L.I.R., Ward-Geiger, L.I., Hines, E., 2012. Application of a habitat model to define calving habitat of the North Atlantic right whale in the southeastern United States. Endangered Species Research 18, 73–87.

Ketten, D.R., 2014. Sonars and strandings: Are beaked Whales the Aquatic Acoustic Canary? Acoustics Today 10, 46–56.

Ketten, D.R., 1995. Estimates of blast injury and acoustic trauma zones for marine mammals from underwater explosions, in: Sensory Systems of Aquatic Mammals. De Spil Publishers, Woerden, The Netherlands, pp. 391–407.

Ketten, D.R., Lien, J., Todd, S., 1993. Blast injury in humpback whale ears: evidence and implications. The Journal of the Acoustical Society of America 94, 1849–1850.

King, S.L., Schick, R.S., Donovan, C., Booth, C.G., Burgman, M., Thomas, L., Harwood, J., 2015. An interim framework for assessing the population consequences of disturbance. Methods in Ecology and Evolution 6, 1150–1158.

Knol, A.B., Slottje, P., van der Sluijs, J.P., Lebret, E., 2010. The use of expert elicitation in environmental health impact assessment: a seven step procedure. Environmental Health 9, 1–19.

Koblitz, J.C., Adamiak, M.G., Carlström, J., Thomas, L., Carlén, I., Teilmann, J., Tregenza, N., Wennerberg, D., Kyhn, L., Svegaard, S., Koza, R., Kosecka, M., Pawliczka, I., Tiberi Ljungqvist, C., Brundiers, K., Wright, A., Mikkelsen, L., Tougaard, J., Loisa, O., Galatius, A., Jüssi, I., Benke, H., 2014. Large-scale static acoustic survey of a low-density population—Estimating the abundance of the Baltic Sea harbor porpoise. The Journal of the Acoustical Society of America 136, 2248–2248.

Kooijman, S.A.L.M., 2010. Dynamic Energy Budget Theory for Metabolic Organisation. Third Edition. Cambridge University Press, Cambridge, UK.

Küsel, E.T., Mellinger, D.K., Thomas, L., Marques, T.A., Moretti, D., Ward, J., 2011. Cetacean population density estimation from single fixed sensors using passive acoustics. The Journal of the Acoustical Society of America 129, 3610–3622.

Kyhn, L.A., Tougaard, J., Thomas, L., Duve, L.R., Stenback, J., Amundin, M., Desportes, G., Teilmann, J., 2012. From echolocation clicks to animal density—Acoustic sampling of harbor porpoises with static dataloggers. The Journal of the Acoustical Society of America 131, 550–560.

Lercher, P., Evans, G., Meis, M., 2003. Ambient noise and cognitive processes among primary schoolchildren. Environment and Behavior 35, 725–735.

Lockyer, C., 1993. Seasonal changes in body fat condition of northeast Atlantic pilot whales, and their biological significance. Report of the International Whaling Commission Special Issue 14, 205–324.

Luo, J., Siemers, B.M., Koselj, K., 2015. How anthropogenic noise affects foraging. Global Change Biology 21, 3278–3289.

Lurton, X., DeRuiter, S., 2011. Sound radiation of seafloor-mapping echosounders in the water column, in relation to the risks posed to marine mammals. The International Hydrographic Review 6, 7–17.

Lusseau, D., Higham, J.E.S., 2004. Managing the impacts of dolphin-based tourism through the definition of critical habitats: the case of bottlenose dolphins (*Tursiops spp.*) in Doubtful Sound, New Zealand. Tourism Management 25, 657–667.

MacLeod, C.D., Santos, M.B., Pierce, G.J., 2003. Review of Data on Diets of Beaked Whales: Evidence of Niche Separation and Geographic Segregation. Journal of the Marine Biological Association of the UK 83, 651–665.

Madsen, P.T., Johnson, M., Aguilar de Soto, N., Zimmer, W.M.X., Tyack, P., 2005. Biosonar performance of foraging beaked whales (*Mesoplodon densirostris*). Journal of Experimental Biology 208, 181–194.

Madsen, P.T., Kerr, I., Payne, R., 2004. Echolocation clicks of two free-ranging, oceanic delphinids with different food preferences: false killer whales *Pseudorca crassidens* and Risso's dolphins *Grampus griseus*. Journal of Experimental Biology 207, 1811–1823.

Madsen, P.T., Wahlberg, M., Tougaard, J., Lucke, K., Tyack, P., 2006. Wind turbine underwater noise and marine mammals: implications of current knowledge and data needs. Marine Ecology Progress Series 309, 279–295.

Malme, C.I., Miles, P.R., Clark, C.W., Tyack, P., Bird, J.E., 1984. Investigations of the potential effects of underwater noise from petroleum-industry activities on migrating gray-whale behavior. Phase 2: January 1984 migration (The U.S. Department of Energy's Office of Scientific and Technical Information No. Report: PB-86-218377/XAB; BBN-5586). Bolt, Beranek and Newman, Inc., Cambridge, MA.

Manzano-Roth, R., Henderson, E.E., Martin, S.W., Martin, C., Matsuyama, B.M., 2016. Impacts of U.S. Navy training events on Blainville's beaked whale (*Mesoplodon densirostris*) foraging dives in Hawaiian waters. Aquatic Mammals 42, 507–518.

Marques, T., Munger, L., Thomas, L., Wiggins, S., Hildebrand, J., 2011. Estimating North Pacific right whale *Eubalaena japonica* density using passive acoustic cue counting. Endangered Species Research 13, 163–172.

Marques, T.A., Thomas, L., Martin, S.W., Mellinger, D.K., Ward, J.A., Moretti, D.J., Harris, D., Tyack, P.L., 2013. Estimating animal population density using passive acoustics. Biological Reviews 88, 287–309.

Marques, T.A., Thomas, L., Ward, J., DiMarzio, N., Tyack, P.L., 2009. Estimating cetacean population density using fixed passive acoustic sensors: an example with Blainville's beaked whales. The Journal of the Acoustical Society of America 125, 1982–1994.

Martin, A.R., Rothery, P., 1993. Reproductive parameters of female long-finned pilot whales (*Globicephala melas*) around the Faroe Islands. Report of the International Whaling Commission, Special Issue 14, 263–304.

Martin, K.E., Benmouyal, G., Adamiak, M.G., Begovic, M., Burnett, R.O., Carr, K.R., Cobb, A., Kusters, J.A., Horowitz, S.H., Jensen, G.R., others, 1998. IEEE standard for synchrophasors for power systems. IEEE Transactions on Power Delivery 13, 73–77.

Martin, S.W., Marques, T.A., Thomas, L., Morrissey, R.P., Jarvis, S., DiMarzio, N., Moretti, D., Mellinger, D.K., 2013. Estimating minke whale (*Balaenoptera acutorostrata*) boing sound density using passive acoustic sensors. Marine Mammal Science 29, 142–158.

Matthiopoulos, J., 2011. How to be a quantitative ecologist: the'A to R'of green mathematics and statistics. John Wiley & Sons.

Mattsson, A., Parkes, G., Hedgeland, D., 2012. Svein Vaage Broadband Air Gun Study, in: Popper, A.N., Hawkins, A. (Eds.), The Effects of Noise on Aquatic Life, Advances in Experimental Medicine and Biology. Springer, New York, NY, pp. 469–471.

McCann, C., 1963. Occurrence of Blainville's beaked whale [*Mesoplodon densirostris* (Blainville)] in the Indian Ocean. Journal of the Bombay Natural History Society 60, 727–731.

McCarthy, E., Moretti, D., Thomas, L., DiMarzio, N., Morrissey, R., Jarvis, S., Ward, J., Izzi, A., Dilley, A., 2011. Changes in spatial and temporal distribution and vocal behavior of Blainville's beaked whales (*Mesoplodon densirostris*) during multi-ship exercises with mid-frequency sonar. Marine Mammal Science 27, E206–E226.

McClure, C.J., Ware, H.E., Carlisle, J., Kaltenecker, G., Barber, J.R., 2013. An experimental investigation into the effects of traffic noise on distributions of birds: avoiding the phantom road. Proceedings of the Royal Society of London B: Biological Sciences 280.

McDonald, .M A., Fox, C.G., 1999. Passive acoustic methods applied to fin whale population density estimation. The Journal of the Acoustical Society of America 105, 2643–2651.

McDonald, M.A., Hildebrand, J.A., Wiggins, S.M., 2006. Increases in deep ocean ambient noise in the Northeast Pacific west of San Nicolas Island, California. The Journal of the Acoustical Society of America 120, 711–718.

McDonald, M.A., Hildebrand, J.A., Wiggins, S.M., Ross, D., 2008. A 50 Year comparison of ambient ocean noise near San Clemente Island: A bathymetrically complex coastal region off Southern California. The Journal of the Acoustical Society of America 124, 1985–1992.

McHuron, E., Costa, D., Schwarz, L., Mangel, M., 2017. A behavioral framework for assessing the population consequences of anthropogenic disturbance on pinnipeds. Methods in Ecology and Evolution 8, 552–560.

McHuron, E.A., Schwarz, L.K., Costa, D.P., Mangel, M., 2018. A state-dependent model for assessing the population consequences of disturbance on income-breeding mammals. Ecological Modelling 385, 133–144.

McSweeney, D.J., Baird, R.W., Mahaffy, S.D., 2007. Site fidelity, associations, and movements of Cuvier's (*Ziphius cavirostris*) and Blainville's (*Mesoplodon densirostris*) beaked whales off the island of Hawai 'i. Marine Mammal Science 23, 666–687.

Mead, J.G., 1989. Beaked whales of the genus Mesoplodon, in: Ridgeway, S.H., Harrison, R. (Eds.), Handbook of Marine Mammals. Academic Press, London, U.K., pp. 349–430.

Mead, J.G., 1984. Survey of reproductive data for the beaked whales (Ziphiidae). Report of the International Whaling Commission (Special Issue 6) 6, 91–96.

Mellinger, D.K., Küsel, E.T., Harris, D., Thomas, L., Matias, L., 2014. Estimating singing fin whale population density using frequency band energy. The Journal of the Acoustical Society of America 136, 2275–2275.

Mesnick, S., Ralls, K., 2018. Sexual Dimorphism, in: Perrin, W.F., Würsig, B., Thewissen, J.G.M. (Eds.), Encyclopedia of Marine Mammals (Third Edition). Academic Press, Burlington, MA, pp. 848–853.

Miller, P., Antunes, R., Alves, C., Wensveen, P., Kvadsheim, P., Kleivane, L., Norland, N., Lam, F., van IJsselmuide, S., Visser, F., Tyack, P., 2011. The 3S experiments: studying the behavioural effects of naval sonar on killer whales (*Orcinus orca*), sperm whales (*Physeter macrocephalus*), and long-finned pilot whales (*Globicephala melas*) in Norwegian waters. (No. Tech. Rept. SOI-2011-001). Scottish Oceans Institute., St. Andrews, U.K.

Miller, P., Narazaki, T., Isojunno, S., Aoki, K., Smout, S., Sato, K., 2016. Body density and diving gas volume of the northern bottlenose whale (*Hyperoodon ampullatus*). J Exp Biol 219, 2458–2468.

Miller, P.J., Antunes, R.N., Wensveen, P.J., Samarra, F.I., Catarina Alves, A., Tyack, P.L., Kvadsheim, P.H., Kleivane, L., Lam, F.A., Ainslie, M.A., 2014. Dose-response relationships for the onset of avoidance of sonar by free-ranging killer whales. The Journal of the Acoustical Society of America 135, 975–993.

Miller, P.J., Kvadsheim, P.H., Wensveen, P.J., Antunes, R., Alves, A.C., Visser, F., Kleivane, L., Tyack, P., L., Sivle, L.D., 2012. The severity of behavioral changes observed during experimental exposures of killer (*Orcinus orca*), long-finned pilot (*Globicephala melas*), and sperm (*Physeter macrocephalus*) whales to naval sonar. Aquatic Mammals 38, 362–401.

Miller, P.J.J., Johnson, M.P., Madsen, P.T., Biassoni, N., Quero, M., Tyack, P.L., 2009. Using at-sea experiments to study the effects of airguns on the foraging behavior of sperm whales in the Gulf of Mexico. Deep Sea Research Part I: Oceanographic Research Papers 56, 1168–1181.

Miller, P.J.O., Kvadsheim, P.H., Lam, F.P.A., Tyack, P.L., Curé, C., DeRuiter, S.L., Kleivane, L., Sivle, L.D., van IJsselmuide, S.P., Visser, F., Wensveen, P.J., von Benda-Beckmann, A.M., López, L.M., Narazaki, T., Hooker, S.K., 2015. First indications that northern bottlenose whales are sensitive to behavioural disturbance from anthropogenic noise. Royal Society Open Science 2.

Møhl, B., Wahlberg, M., Madsen, P.T., Miller, L.A., Surlykke, A., 2000. Sperm whale clicks: Directionality and source level revisited. The Journal of the Acoustical Society of America 107, 638–648.

Moore, J.E., Barlow, J.P., 2013. Declining Abundance of Beaked Whales (Family Ziphiidae) in the California Current Large Marine Ecosystem. PLoS ONE 8, e52770.

Moretti, D., 2012. Science on whales, submarines, and conservation meets the news. Conservation Biology 26, 379–381.

Moretti, D., Marques, T.A., Thomas, L., DiMarzio, N., Dilley, A., Morrissey, R., McCarthy, E., Ward, J., Jarvis, S., 2010. A dive counting density estimation method for Blainville's beaked whale (*Mesoplodon densirostris*) using a bottom-mounted hydrophone field as applied to a Mid-Frequency Active (MFA) sonar operation. Applied Acoustics 71, 1036–1042.

Moretti, D., Thomas, L., Marques, T., Harwood, J., Dilley, A., Neales, B., Shaffer, J., McCarthy, E., New, L., Jarvis, S., Morrissey, R., 2014. A Risk Function for Behavioral Disruption of Blainville's Beaked Whales (*Mesoplodon densirostris*) from Mid-Frequency Active Sonar. PLoS ONE 9, e85064.

Morrell, S., Taylor, R., Lyle, D., 2008. A review of health effects of aircraft noise. Australian and New Zealand Journal of Public Health 21, 221–236.

Morrison, S.A., Winston, C., Watson, T., 1999. Fundamental flaws of Social regulation: The case of airplane noise. The Journal of Law and Economics 42, 723–744.

Münzel, T., Gori, T., Babisch, W., Basner, M., 2014. Cardiovascular effects of environmental noise exposure. European Heart Journal 35, 829–836.

Nabe-Nielsen, J., Sibly, R.M., Tougaard, J., Teilmann, J., Sveegaard, S., 2014. Effects of noise and by-catch on a Danish harbour porpoise population. Ecological Modelling 272, 242–251.

National Academies of Sciences, Engineering, and Medicine, 2017. Approaches to Understanding the Cumulative Effects of Stressors on Marine Mammals. Washington, DC: The National Academies Press.

New, L.F., Clark, J.S., Costa, D.P., Fleishman, E., Hindell, M.A., Klanjšček, T., Lusseau, D., Kraus, S., McMahon, C.R., Robinson, P.W., 2014. Using short-term measures of behaviour to estimate long-term fitness of southern elephant seals. Marine Ecology Progress Series 496, 99–108.

New, L.F., Moretti, D.J., Hooker, S.K., Costa, D.P., Simmons, S.E., 2013. Using energetic models to investigate the survival and reproduction of beaked whales (family Ziphiidae). PLoS ONE 8, e68725.

Nowacek, D.P., Johnson, M.P., Tyack, P.L., 2004. North Atlantic right whales (*Eubalaena glacialis*) ignore ships but respond to alerting stimuli. Proceedings of the Royal Society of London B: Biological Sciences 271, 227–231.

O'Hagan, A., Buck, C.E., Daneshkhah, A., Eiser, J.R., Garthwaite, P.H., Jenkinson, D.J., Oakley, J.E., Rakow, T., 2006. Uncertain Judgements: Eliciting Expert Probabilities. John Wiley & Sons, West Sussex, England.

Olesiuk, P.F., Nichol, L.M., Sowden, M.J., Ford, J.K.B., 2002. Effect of the sound generated by an acoustic harassment device on the relative abundance and distribution of harbor porpoises (*Phocoena phocoena*) in Retreat Passage, British Columbia. Marine Mammal Science 18, 843–862.

Parks, S.E., Clark, C.W., Tyack, P.L., 2007. Short- and long-term changes in right whale calling behavior: The potential effects of noise on acoustic communication. The Journal of the Acoustical Society of America 122, 3725–3731.

Parks, S.E., Searby, A., Celerier, A., Johnson, M.P., Nowacek, D.P., Tyack, P.L., 2011. Sound production behavior of individual North Atlantic right whales: implications for passive acoustic monitoring. Endangered Species Research 15, 63–76.

Payne, R., Webb, D., 1971. Orientation by means of long range acoustic signaling in baleen whales. Annals of the New York Academy of Sciences 188, 110–141.

Perrin, W.F., Myrick, A.C., 1980. Age determination of toothed whales and sirenians, Reports of the International Whaling Commission, Special Issue 3. International Whaling Commission, Cambridge, UK.

Perrin, W.F., Würsig, B., Thewissen, J.G.M. (Eds.), 2009. Encyclopedia of Marine Mammals. Academic Press, San Diego, CA.

Perryman, W.L., Lynn, M.S., 2002. Evaluation of nutritive condition and reproductive status of migrating gray whales (*Eschrichtius robustus*) based on analysis of photogrammetric data. Journal of Cetacean Research and Management 4, 155–164.

Perveen, R., Kishor, N., Mohanty, S.R., 2014. Off-shore wind farm development: Present status and challenges. Renewable and Sustainable Energy Reviews 29, 780–792.

Pirotta, E., Booth, C.G., Costa, D.P., Fleishman, E., Kraus, S.D., Lusseau, D., Moretti, D., New, L.F., Schick, R.S., Schwarz, L.K., Simons, S.E., Thomas, L., Tyack, P.L., Weise, M.J., Wells, R.S., Harwood, J.H., 2018. Understanding the population consequences of disturbance. Ecology and Evolution 8, 9934–9946.

Pirotta, E., Mangel, M., Costa, D.P., Mate, B., Goldbogen, J.A., Palacios, D.M., Hückstädt, L.A., McHuron, E.A., Schwarz, L., New, L., 2017. A Dynamic State Model of Migratory Behavior and Physiology to Assess the Consequences of Environmental Variation and Anthropogenic Disturbance on Marine Vertebrates. The American Naturalist 191, E40–E56.

Pirotta, E., Milor, R., Quick, N., Moretti, D., Di Marzio, N., Tyack, P., Boyd, I., Hastie, G., 2012. Vessel noise affects beaked whale behavior: results of a dedicated acoustic response study. PLoS ONE 7, e42535.

Pitman, R., 2008. Mesoplodont whales (*Mesoplodon spp.*), in: Encyclopaedia of Marine Mammals. Academic Press, p. 721.

Pitman, R.L., 2002. Mesoplodont whales, in: Perrin, W.F., Würsig, B., Thewissen, J.G.M. (Eds.), Encyclopedia of Marine Mammals. Academic Press, Burlington, MA, pp. 738–742.

Powell, L.A., 2007. Approximating variance of demographic parameters using the delta method: a reference for avian biologists. The Condor 109, 949–954.

Quick, N., Scott-Hayward, L., Sadykova, D., Nowacek, D., Read, A., 2016. Effects of a scientific echo sounder on the behavior of short-finned pilot whales (*Globicephala macrorhynchus*). Canadian Journal of Fisheries and Aquatic Sciences 74, 716–726.

Ralph, C.J., Scott, J.M. (Eds.), 1981. Estimating Numbers of Terrestrial Birds, Studies in Avian Biology No. 6. Cooper Ornithological Society, Lawrence, Kansas.

Reijnen, R., Foppen, R., Braak, C.T., Thissen, J., 1995. The effects of car traffic on breeding bird populations in woodland. III. Reduction of density in relation to the proximity of main roads. Journal of Applied Ecology 32, 187–202.

Richardson, W.J., Miller, G.W., Greene, C.R., 1999. Displacement of migrating bowhead whales by sounds from seismic surveys in shallow waters of the Beaufort Sea. The Journal of the Acoustical Society of America 106, 2281–2281.

Rolland, R.M., Parks, S.E., Hunt, K.E., Castellote, M., Corkeron, P.J., Nowacek, D.P., Wasser, S.K., Kraus, S.D., 2012. Evidence that ship noise increases stress in right whales. Proceedings of the Royal Society B: Biological Sciences 279, 2363–2368.

Rolt, K.D., 1994. The Fessenden oscillator: History, electroacoustic model, and performance estimate. The Journal of the Acoustical Society of America 95, 2832–2832.

Rommel, S.A., Costidis, A.M., Fernandez, A., Jepson, P.D., Pabst, D.A., McLellan, W.A., Houser, D.S., Cranford, T.W., Van Helden, A.L., Allen, D.M., others, 2005. Elements of beaked whale anatomy and diving physiology and some hypothetical causes of sonar-related stranding. Journal of Cetacean Research and Management 7, 189–209.

Ross, G.J., Best, P. B., Mead, J. G., 1988. A review of the colour patterns and their ontogenetic variation in beaked whales (Ziphiidae, Cetacea). International Whaling Commission (SC40/SM6).

Schlundt, C.E., Finneran, J.J., Carder, D.A., Ridgway, S.H., 2000. Temporary shift in masked hearing thresholds of bottlenose dolphins, *Tursiops truncatus*, and white whales, *Delphinapterus leucas*, after exposure to intense tones. The Journal of the Acoustical Society of America 107, 3496–3508.

Schorr, G.S., Falcone, E.A., Moretti, D.J., Andrews, R.D., 2014. First long-term behavioral records from Cuvier's beaked whales (*Ziphius cavirostris*) reveal record-breaking dives. PLoS One 9, e92633.

Senzaki, M., Yamaura, Y., Francis, C.D., Nakamura, F., 2016. Traffic noise reduces foraging efficiency in wild owls. Scientific Reports 6, 30602.

Shaffer, J., Moretti, D., Jarvis, S., Tyack, P., Johnson, M., 2013. Effective beam pattern of the Blainville's beaked whale (*Mesoplodon densirostris*) and implications for passive acoustic monitoring. The Journal of the Acoustical Society of America 133, 1770–1784.

Shaffer, J.A., Baggenstoss, P., Claridge, D., Dunn, C., Marques, T., Thomas, L., 2015. Beaked Whale Group Deep Dive Behavior from Passive Acoustic Monitoring. Naval Undersea

Warfare Center Newport United States, https://apps.dtic.mil/dtic/tr/fulltext/u2/1014305.pdf.

Shannon, G., McKenna, M.F., Angeloni, L.M., Crooks, K.R., Fristrup, K.M., Brown, E., Warner, K.A., Nelson, M.D., White, C., Briggs, J., McFarland, S., Wittemyer, G., 2016. A synthesis of two decades of research documenting the effects of noise on wildlife. Biological Reviews 91, 982–1005.

Sivle, L.D., Kvadsheim, P.H., Fahlman, A., Lam, F.P., A., Tyack, P.L., Miller, P.J.O., 2012. Changes in dive behavior during naval sonar exposure in killer whales, long-finned pilot whales, and sperm whales. Frontiers in Physiology 3, 1–12.

Slabbekoorn, H., Bouton, N., van Opzeeland, I., Coers, A., ten Cate, C., Popper, A.N., 2010. A noisy spring: the impact of globally rising underwater sound levels on fish. Trends in Ecology & Evolution 25, 419–427.

Southall, B.L., Benoit-Bird, K.J., Moline, M.A., Moretti, D.J., 2019. Quantifying deep-sea predator–prey dynamics: Implications of biological heterogeneity for beaked whale conservation. Journal of Applied Ecology 00:1-10.

Southall, B.L., Bowles, A.E., Ellison, W.T., Finneran, J.J., Gentry, R.L., Greene Jr, C.R., Kastak, D., Ketten, D.R., Miller, J.H., Nachtigall, P.E., 2007. Structure of the noise exposure criteria. Aquatic mammals 33, 427–434.

Southall, B.L., Moretti, D.J., Abraham, B., Calambokidis, J., DeRuiter, S.L., Tyack, P.L., 2012. Marine mammal behavioral response studies in southern California: advances in technology and experimental methods. Marine Technology Society Journal 46, 48–59.

Southall, B.L., Rowles, T., Gulland, F., Baird, R.W., Jepson, P.D., 2013. Final report of the Independent Scientific Review Panel investigating potential contributing factors to a

2008 mass stranding of melon-headed whales (*Peponocephala electra*) in Antsohihy, Madagascar. Independent Scientific Review Panel.

Speirs-Bridge, A., Fidler, F., McBride, M., Flander, L., Cumming, G., Burgman, M., 2010. Reducing overconfidence in the interval judgments of experts. Risk Analysis: An International Journal 30, 512–523.

Spigel, E., 2013. Determination of Acoustic Effects on Marine Mammals and Sea Turtles for the Mariana Islands Training and Testing Environmental Impact Statement/Overseas Environmental Impact Statement, NUWC-NPT Technical Report. Naval Undersea Warfare Center, Newport, RI.

St Aubin, D.J., Ridgway, S.H., Wells, R.S., Rhinehart, H., 1996. Dolphin thyroid and adrenal hormones: circulating levels in wild and semidomesticated *Tursiops truncatus*, and influence of sex, age, and season. Marine Mammal Science 12, 1–13.

Stansfeld, S., Matheson, M.P., 2003. Noise pollution: non-auditory effects on health. British Medical Bulletin 68, 243–257.

Steidl, R.J., Thomas, L., 2001. Power Analysis and experimental design, in: Scheiner, S.M., Gurevitch, J. (Eds.), Design and Analysis of Ecological Experiments. Oxford University Press, pp. 14–36.

Stewart, B.S., Clapham, P.J., Powell, J.A., Reeves, R.R., 2002. National Audubon Society Guide to Marine Mammals of the World, 1st ed. Knopf, New York.

Stimpert, A.K., DeRuiter, S.L., Southall, B.L., Moretti, D.J., Falcone, E.A., Goldbogen, J.A., Friedlaender, A., Schorr, G.S., Calambokidis, J., 2014. Acoustic and foraging behavior of a Baird's beaked whale, *Berardius bairdii*, exposed to simulated sonar. Scientific Reports 4, 7031. https://doi.org/DOI: 10.1038/srep07031

Tarnopolsky, A., Watkins, G., Hand, D.J., 1980. Aircraft noise and mental health: I. Prevalence of individual symptoms. Psychological Medicine 10, 683–698.

Thomas, L., 1996. Monitoring long-term population change: Why are there so many analysis methods? Ecology 77, 49–58.

Thomas, L., Burnham, K.P., Buckland, S.T., 2008. Temporal inferences from distance sample surveys, in: Buckland, S.T., Anderson, D.R., Borchers, D.L., Thomas, L. (Eds.), Advanced Distance Sampling. Oxford Universtiy Press.

Thomson, C.A., Geraci, J.R., 1986. Cortisol, aldosterone, and leucocytes in the stress response of bottlenose dolphins, *Tursiops truncatus*. Canadian Journal of Fisheries and Aquatic Sciences 43, 1010–1016.

Tougaard, J., Carstensen, J., Teilmann, J., Skov, H., Rasmussen, P., 2009. Pile driving zone of responsiveness extends beyond 20 km for harbor porpoises (*Phocoena phocoena* (L.)). The Journal of the Acoustical Society of America 126, 11–14.

Tyack, P.L., Johnson, M., Aquilar-Soto, N., Sturlese, A., Madsen, P.T., 2006. Extreme diving of beaked whales. Journal of Experimental Biology 209, 4238–4253.

Tyack, P.L., Zimmer, W.M.X., Moretti, D.J., Southall, B.L., Claridge, D.E., Durban, J.W., Clark, C.W., D'Amico, A., DiMarzio, N.A., Jarvis, S., McCarthy, E., Morrissey, R., Ward, J., Boyd, I.L., 2011. Beaked Whales Respond to Simulated and Actual Navy Sonar. PLoS ONE 6, e17009.

Urick, R.J., 1996. Principles of Underwater Sound 3rd Edition, 3rd ed. Peninsula Publishing, Los Altos, CA.

U.S. Fleet Forces Command, 2008. Atlantic Fleet active sonar training environmental impact statement/ overseas environmental impact statement. United States Department of the Navy, Norfolk, VA.

Villegas-Amtmann, S., Schwarz, L.K., Sumich, J.L., Costa, D.P., 2015. A bioenergetics model to evaluate demographic consequences of disturbance in marine mammals applied to gray whales. Ecosphere 6, 1–19.

Vincent, H.T., 2001. Models, algorithms, and measurements for underwater acoustic positioning (PhD Dissertation). University of Rhode Island.

Vires, G., 2011. Echosounder effects on beaked whales in the Tongue of the Ocean, Bahamas (Master's Thesis). Duke University.

Ward, J.A., Thomas, L., Jarvis, S., DiMarzio, N., Moretti, D., Marques, T.A., Dunn, C., C laridge, D., Hartvig, E., Tyack, P., 2012. Passive acoustic density estimation of sperm whales in the Tongue of the Ocean, Bahamas. Marine Mammal Science 28, E444–E455.

Warren, L.R., 1988. Hull-mounted sonar/ship design evolution and transition to low-frequency applications. IEEE Journal of Oceanic Engineering 13, 296–298.

Watkins, W.A., Tyack, P., Moore, K.E., Bird, J.E., 1987. The 20-Hz signals of finback whales (*Balaenoptera physalus*). The Journal of the Acoustical Society of America 82, 1901–1912.

Weinberg, H., Keenan, R.E., 1996. Gaussian ray bundles for modeling high-frequency propagation loss under shallow-water conditions. The Journal of the Acoustical Society of America 100, 1421–1431.

Welch, C., 2016. Mysterious New Whale Species Discovered in Alaska [WWW Document]. National Geographic News. URL https://news.nationalgeographic.com/2016/07/new-whale-species/

Whitehead, H., 2013. Trends in cetacean abundance in the Gully submarine canyon, 1988–2011, highlight a 21% per year increase in Sowerby's beaked whales (*Mesoplodon bidens*). Canadian Journal of Zoology 91, 141–148.

Whitehead, H., Gowans, S., Faucher, A., Mccarrey, S.W., 1997. Population Analysis of Northern Bottlenose Whales in the Gully. Marine Mammal Science 13, 173–185.

Wiggins, S.M., McDonald, M.A., Munger, L.M., Moore, S.E., Hildebrand, J.A., 2004. Waveguide propagation allows range estimates for North Pacific right whales in the Bering Sea. Canadian Acoustics 32, 146–154.

Williams, R., Erbe, C., Ashe, E., Beerman, E., Smith, J., 2014. Severity of killer whale behavioral responses to ship noise: A dose–response study. Marine Pollution Bulletin 79, 254–260.

Williams, R., Wright, A.J., Ashe, E., Blight, L.K., Bruintjes, R., Canessa, R., Clark, C.W., Cullis-Suzuki, S., Dakin, D.T., Erbe, C., Hammond, P.S., Merchant, N.D., O'Hara, P.D., Purser, J., Radford, A.N., Simpson, S.D., Thomas, L., Wale, M.A., 2015. Impacts of anthropogenic noise on marine life: Publication patterns, new discoveries, and future directions in research and management. Ocean & Coastal Management 115, 17–24.

Wood, S.N., 2017. Generalized Additive Models: An Introduction with R, 2nd ed. CRC press, New York, NY.

Wright, A.J., Soto, N.A., Baldwin, A.L., Bateson, M., Beale, C.M., Clark, C., Deak, T., Edwards, E.F., Fernández, A., Godinho, A., Hatch, L.T., Kakuschke, A., Lusseau, D., Martineau,

D., Romero, M.L., Weilgart, L.S., Wintle, B.A., Notarbartolo-di-Sciara, G., Martin, V., 2007. Do Marine Mammals Experience Stress Related to Anthropogenic Noise? International Journal of Comparative Psychology 20, 274–316.

Yack, T.M., Barlow, J., Roch, M.A., Klinck, H., Martin, S., Mellinger, D.K., Gillespie, D., 2010. Comparison of beaked whale detection algorithms. Applied Acoustics 71, 1043–1049.

Zimmer, W.M.X., Harwood, J., Tyack, P.L., Johnson, M.P., Madsen, P.T., 2008. Passive acoustic detection of deep-diving beaked whales. The Journal of the Acoustical Society of America 124, 2823–2832.

Zimmer, W.M.X., Johnson, M.P., Madsen, P.T., Tyack, P.L., 2005. Echolocation clicks of free-ranging Cuvier's beaked whales (*Ziphius cavirostris*). The Journal of the Acoustical Society of America 117, 3919–3927.

Zimmer, W.M.X., Tyack, P.L., 2007. Repetitive shallow dives pose decompression risk in deep-diving beaked whales. Marine Mammal Science 23, 888–925.